UCLouvain
Louvain Institute of Biomolecular Science and Technology (LIBST)
Unité de Physiologie Moléculaire (FYMO)

The *Saccharomyces cerevisiae* Golgi Gdt1 protein is a Ca^{2+}-Mn^{2+}/H^{+} exchanger and its abundance is regulated by Ca^{2+} and Mn^{2+}

Thèse présentée par Antoine DESCHAMPS en vue de l'obtention du grade de docteur en sciences

Promoteur	Prof. Pierre Morsomme
Président du jury	Prof. Michel Ghislain
Membres du jury	Prof. Bruno André
	Prof. Marc Boutry
	Prof. Sakari Kellokumpu
	Prof. Patrice Soumillion

Février 2022

REMERCIEMENTS

J'ai atterri en FYMO en 2011 pour mon mémoire. Et nous voici en 2022, à clôturer ma thèse. Autrement dit, pour un étudiant "de passage", j'aurai séjourné un bon bout de temps entre les murs du 3e étage du Carnoy… Bien sûr, il y a eu quelques interruptions, pour stage et voyage à l'étranger, et je n'ai pas vraiment eu un parcours de thèse linéaire. Mais ce qui est sûr, si je suis resté si longtemps, c'est que je me suis trouvé dans un environnement où je me sentais bien ! Et ça tient pour beaucoup aux personnes qui m'ont entourées, co-doctorants, profs, post-docs, support technique et administratif, étudiants, etc.

A l'interface de tout ce beau monde, le cytosquelette qui maintient l'intégrité de la cellule, ce sont les chercheurs permanents. Après avoir commencé sous une co-promotion de Pierre Morsomme et Patrice Soumillion, quelques "aléas" de début de thèse (assortis d'un changement de sujet de recherche) ont fait en sorte que je continue uniquement chez Pierre.

Les années qui ont suivi m'ont alors permis de développer cette relation avec beaucoup de bonheur (j'espère partagé ;-)). Merci Pierre pour la bienveillance et l'atmosphère agréable que tu entretiens au sein de ton équipe. Je pense que tu as parfaitement saisi que c'est grâce à cette ambiance agréable que chacun peut se développer en toute sérénité, et ainsi contribuer au mieux au travail d'équipe. Merci aussi pour la confiance dont tu nous témoignes régulièrement, en nous permettant de développer nos idées, en nous laissant assez libres de faire la planification expérimentale de nos recherches, en nous proposant de participer à divers congrès et activités d'échange scientifique. Merci aussi pour ta disponibilité au quotidien (ta porte est rarement fermée, parfois légèrement entrouverte, mais le plus souvent grande ouverte !). Lorsqu'on a besoin de discuter, que ce soit de nos derniers résultats d'expérience, bons comme mauvais, mais aussi de nos doutes face aux difficultés de la recherche, ou plus légèrement de nos activités de vacances, récoltes de pommes, blessures lors de la pratique d'un sport, etc., on sait qu'on peut entrer dans ton bureau.

Avec les autres chercheurs permanents de FYMO, et plus globalement du LIBST, la collaboration, plutôt que la compétition, est mise au cœur de l'organisation des équipes. Pourvu que cette valeur soit encore longtemps entretenue par tous !

Merci aussi aux membres de de mon jury de thèse, les Prof. Marc Boutry, Bruno André, Sakari Kellokumpu, Patrice Soumillion et Michel Ghislain, pour le temps que vous avez consacré pour la lecture et la critique constructive de

ma thèse. L'intérêt que vous avez ainsi témoigné pour mon travail est vraiment gratifiant et donne du sens à ce travail de recherche de longue haleine.

Ensuite, en début de voie sécrétoire, au réticulum endoplasmique, les bases solides pour débuter les projets de recherche sont maintenues en place par une valeureuse équipe de support technique, logistique et administratif ! Merci Anne-Marie, Michèle, Monique, Marie-Christine, Dany, Marie-Eve, Régeanne, Adeline, Joseph, Ben, Hervé, Cyril, pour tous les services rendus au bénéfice de tous en FYMO ! Sans cela, le labo tournerait sans doute très vite en un fameux bazar... Merci pour votre implication et la volonté affichée pour trouver toute sorte de solutions lorsqu'un jeune (ou plus si jeune) chercheur fait face à une question. Merci aussi, même si le Covid ne permet plus de le voir autant ces derniers temps, pour votre chouette implication dans toute une série d'activités annexes, mais ô combien importantes (préparation d'un drink, d'un hot-dog, d'un vélo folklo, d'un festin pâtés-boudins, soutien à Saint-Nicolas, et j'en passe) !

Les projets en cours de construction atterrissent ensuite à l'appareil de Golgi. Lieu hautement symbolique dans mon projet de thèse, c'est là que les projets sont modifiés, modelés, parfois déconstruits puis rebâtis, lentement affinés et contrôlés encore, avant d'être libérés pour continuer leur route dans la cellule. Doctorants et post-docs sont les premiers acteurs de ces transformations et de ce minutieux travail, à observer les résultats, les interpréter, et imaginer de nouvelles manières de les travailler. J'ai eu le bonheur de partager la route avec cette joyeuse équipée pendant de belles années, en côtoyant 2 (ou 3, voire 4) générations de doctorants !

Merci à Didier, Anne-So et Jennifer pour votre accueil au sein de l'équipe et votre soutien pour les épreuves FRIA, au début de ma thèse. C'est sûrement en partie à cause de vous que je me suis dirigé vers Gdt1p au moment de me réorienter vers un nouveau projet de thèse ;-) Merci à Palani aussi, post-doc sur le projet Gdt1p, discret (moins après 2-3 Chimay bleues :D), mais toujours d'une grande gentillesse.

Merci Anne-So pour la belle collaboration qu'on a eue et tous les chouettes moments partagés. Voisins de bureau, de paillasse, actifs ensemble pour rassembler les indices quant à la fonction de Gdt1p sur notre "tableau d'enquête", mais aussi pour découvrir Boston, préparer un vélo folklo ou ajouter un panier de course, organiser un drink ou un badminton d'équipe, discuter de nos chansons du moment ou échanger les derniers ragots du labo !

Merci ensuite à Jérôme, mon compagnon d'infortune en début de thèse (bien que la fortune ait été meilleure pour toi au FRIA, mais je ne t'en veux pas ;-)), toujours prompt à me présenter comme "celui qui a fait le tour du monde à vélo". J'ai d'ailleurs tout essayé pour te faire attraper le virus (du vélo, entendons-nous bien), depuis le fait de remplir ensemble tous les créneaux libres sur le vélo folklo le jeudi matin (et il y en a beaucoup, des créneaux libres, à ce moment-là des 24h !), à venir à vélo à Wavre de grand matin pour faire ensuite le trajet jusqu'à LLN (bref, pour moi, un aller-retour LLN-Wavre), et jusqu'à s'essayer au tandem ensemble au retour d'une journée vélo. Mais je pense que rien n'y a fait... :D

Merci bien sûr à Louise et Jiri ! Arrivés après moi sur le projet Gdt1p, et repartis avant... (quand je vous disais que je suis resté longtemps) Le duo enjoué de "l'autre bureau" a vraiment bien fonctionné, mais attention à ne pas se trouver dans les parages en période d'orage :D Merci pour les passionnantes discussions, le plus souvent autour d'un thé (pour moi, un café !), à analyser les résultats dans tous les sens, à essayer de voir comment faire coller les choses. Et puis, merci pour votre enthousiasme à chacun dans toutes les activités sociales d'équipe, d'unité et d'institut. Votre dynamisme fût précieux pour entretenir et créer tous ces chouettes moments. Merci aussi Louise pour ton exemple d'efficacité, ce fût une source d'inspiration pour moi ! Thank you, Jiri, for your never-ending questioning about the operation of the biological systems we analyze, it is also inspiring to see so much passion about science! Merci également à Henri-François, que je joins aisément aux deux larrons précédents, pour ta grande implication dans tous les projets de recherche de l'équipe, et ta disponibilité pour aider et contribuer à l'avancement de chacun. Ton apport à toutes les discussions, avec ton expertise d'autres techniques que celles auxquelles nous étions familiers, d'un autre organisme modèle, fût (et est toujours) précieux pour beaucoup de nous. J'ai beaucoup apprécié de partager le même bureau pendant ces années, et de pouvoir discuter si souvent de questions scientifiques. En ce sens, tu as grandement contribué à développer mon sens critique. Merci aussi pour les notes de musique, c'est un beau souvenir qui restera pour moi ;-) A tous les trois, qui êtes toujours engagés dans la recherche académique, je vous souhaite beaucoup de bonheur dans ce boulot passionnant. Que vous gardiez le feu sacré pour la recherche fondamentale !

Merci aussi à FTB, mon comparse de fin de thèse, avec qui on partage les affres de la rédaction... Grâce à toi, en plus d'avoir découvert pas mal de bons morceaux, j'ai bien amélioré mes compétences en "image processing". Et désolé pour l'aération excessive du bureau (déjà bien avant Covid), mais c'était pour t'aider à renforcer ton immunité ;-) Courage pour la fin, la ligne d'arrivée est à portée de vue !

Merci enfin à toute la "nouvelle génération" (plus si nouvelle que ça d'ailleurs, certains sont déjà presque au bout de leur thèse), Benjamin, Camille, Alex, Guillemette, Quentin, vous insufflez un vent de fraîcheur dans l'équipe ! Vive les Monday cakes, les nanodisques, les cellules d'insectes, les surfaces nanostructurées, etc. Merci à chacun pour votre bonne humeur et pour la merveilleuse ambiance que vous mettez dans l'équipe. C'est un vrai plaisir de voir votre cohésion, à partager autant la joie des bons résultats de l'un ou de l'autre, que la déception en cas de raté. Et merci d'accepter encore les vieux comme moi à se joindre à la fête :D Je vous souhaite beaucoup de réussite dans votre projet de recherche, et que cette période de thèse vous permette d'imaginer aussi votre voie future, quelle qu'elle soit ;-)

Et puis, merci également à tous les doctorants et post-docs de FYMO avec lesquels j'ai partagé beaucoup de beaux moments. Tim, Laurie, Seb, Sylvain, Jahed, Xavier, Bruna, Max, Hajar, Kaushal, Pawel, Aga, François, Nico, Mathieu, et beaucoup d'autres ! Quelle belle ambiance lors des nombreuses activités ensemble, drinks, pasta party, weekends, soirées jeux, barbecues, foot, soirées pizza, 24h vélo, quinzaine, etc. Et quelle chouette atmosphère au quotidien dans les couloirs du labo !

Après avoir transité par le Golgi, les protéines sont emmenées dans les complexes réseaux exo- et endocytiques. Les arrivées et départs sont fréquents dans les labos de recherche, où mémorants et stagiaires transitent et se croisent (et certains se retrouvent parfois finalement recyclés au Golgi ;-)). J'ai eu le plaisir de travailler avec beaucoup d'étudiants au sein du labo. Merci à chacun et chacune, Sophie, Marie-Lise, Catherine, Guillemette, Quentin, Félicie, Andréa, pour votre implication dans votre projet de recherche ! Vous voir au quotidien évoluer, vous questionner, prendre confiance en vous, donne pour moi un vrai sens à la mission d'encadrement et de guidance de ces mémoires. A votre tour de transmettre aux suivants et d'essaimer, en FYMO et ailleurs.

Et puis, venus de l'extérieur de la cellule, l'endocytose mène jusqu'à la vacuole bon nombre protéines et composés variés. Là, ils sont digérés, compostés, dégradés. Mais ça, c'est la version péjorative de cet organite. En fait, on peut plutôt voir la vacuole comme la "ressourcerie" de la cellule. Pour moi, cette ressourcerie prend l'image de la famille et des amis, sur qui j'ai toujours pu compter. Bien que je puisse parfois sembler imperturbable et insensible au stress, lors des épreuves des études et du doctorat, le soutien et l'amour de mes proches m'a été essentiel pour surmonter toutes les difficultés. Merci à chacun pour votre présence. Bien sûr, je vous aime !

Enfin, je ne pourrais pas terminer mon tour de la cellule sans parler des mitochondries. Je ne l'ai pas encore évoqué jusqu'à présent, mais j'ai énormément apprécié mon travail d'assistant. Là où la recherche vous fait parfois passer par des hauts et des bas, des questionnements intenses sur le sens de vos journées, l'enseignement m'a fourni l'énergie pour me faire fonctionner. C'est sans doute grâce à ce bel équilibre entre un projet de recherche à long terme et les TPs et séances de labo à court terme, que j'ai pu surmonter les écueils et persévérer pour arriver au terme de ma thèse. Un grand merci à toutes les personnes avec lesquelles j'ai travaillé à ces tâches d'enseignement. Bernadette, Ramazan, Ricky, Samuel, Sharon, Marine et quelques autres à Woluwé, la chouette ambiance de travail (et les gâteaux ! :D) a largement contrebalancé la longueur des trajets. Belle continuation à tous ! Et ici à LLN, Madeleine, Sebastian, Damien, et bien sûr Joseph, ce fût un réel plaisir de travailler de concert pour donner les séances de labo, les adapter, les ajuster, et trouver la meilleure formule pour donner aux étudiants le goût de la biochimie et de la biologie moléculaire !

A tous les étudiants, vous êtes l'avenir !

Antoine

ABSTRACT

The Golgi apparatus is a major hub for post-translational modifications and for protein sorting. Accordingly, the preservation of Golgi structure and functionalities are everlasting tasks. It is ensured by mechanisms involving the control of luminal chemical composition and of lipid bilayer thickness, and is supported by structural and transport machineries at the cytosolic side of Golgi cisternae. Failings of those mechanisms usually lead to various cellular troubles, including glycosylation defects.

In 2012, some congenital disorders of glycosylation were related to mutations of TMEM165 protein in human. As this protein was not characterized at that time, we started in our laboratory the study of Gdt1p, the *Saccharomyces cerevisiae* ortholog of TMEM165. It was demonstrated that Gdt1p is a Golgi-localized transmembrane protein able to transport Ca^{2+} and Mn^{2+} cations. Furthermore, *GDT1* deletion is also characterized by Golgi trafficking defects and glycosylation troubles. The predicted topology of the protein matches with the usual topology of exchangers.

In this study, we investigated two elements of Gdt1p physiological function, its transport mechanism and its regulation. Starting from the assumption that Gdt1p could exchange H^+ ions against Ca^{2+} and Mn^{2+} cations across the Golgi membrane, we developed measurement strategies to assess it. A heterologous expression system using *Lactococcus lactis* was set up for direct H^+ transport assay and a Golgi-localized pH sensor was developed for *in vivo* measurements in *S. cerevisiae*. Thanks to them, Gdt1p-mediated H^+ transport activity was demonstrated. Then, we looked at Gdt1p regulation. We observed that Gdt1p is rapidly downregulated as a response to extracellular Mn^{2+} addition and that regulation occurs both at transcriptional and post-translational levels. The fast and efficient retrieval of Gdt1p from the Golgi membrane to be sorted to the vacuole probably occurs trough a novel degradation pathway.

TABLE OF CONTENT

LIST OF FIGURES

ABBREVIATIONS

ALP	Alkaline phosphatase
A. thaliana	*Arabidopsis thaliana*
ATP	Adenosine triphosphate
BAPTA	1,2-bis(*o*-aminophenoxy)ethane-*N,N,N′,N′*-tetraacetic acid
BCA	Bicinchoninic acid
BSA	Bovine serum albumin
CDG	Congenital disorder of glycosylation
CHX	Cycloheximide
COG	Conserved-oligomeric Golgi complex
CPY	Carboxypeptidase Y
CPS	Carboxypeptidase S
DMSO	Dimethyl sulfoxide
DTT	Dithiothreitol
EE	Early endosomes
EGAD	Endosomes and Golgi associated degradation
EGTA	Ethylene glycol-bis(β-aminoethyl ether)-*N,N,N′,N′*-tetraacetic acid
ER	Endoplasmic reticulum
ERAD	Endoplasmic reticulum associated degradation
ESCRT	Endosomal sorting complexes required for transport
FM4-64	*N*-(3-Triethylammoniumpropyl)-4-(6-(4-(Diethylamino) Phenyl)Hexatrienyl)Pyridinium Dibromide
FRET	Förster Resonance Energy Transfer
GAP	GFP-Aequorin protein
GAP1	GFP-Aequorin Protein 1
GFP	Green fluorescent protein
GOMED	Golgi membrane-associated degradation
HA	Hemagglutinin
ICP-AES	Inductively coupled plasma – atomic emission spectroscopy
ICP-MS	Inductively coupled plasma – mass spectrometry
kDa	kiloDalton
L. lactis	*Lactococcus lactis*
MES	2-(*N*-morpholino)ethanesulfonic acid

MVB	Multivesicular bodies
OD_{600}	Optical density at 600 nm
PBS	Phosphate-buffered saline
PCR	Polymerase chain reaction
PMSF	Phenylmethylsulfonyl fluoride
PSII	Photosystem II
rpm	Rotation per minute
RT-qPCR	Reverse transcriptase – quantitative PCR
S. cerevisiae	*Saccharomyces cerevisiae*
SD	Synthetic defined medium
SDS-PAGE	Sodium dodecyl sulfate – polyacrylamide gel electrophoresis
sfpHluorin	superfolder pHluorin
SNARE	Soluble NSF attachment protein receptor
TCA	Trichloroacetic acid
TGN	*trans*-Golgi network
TMD	Transmembrane domain
Tris	Tris(hydroxymethyl)aminomethane
UPF0016	Unknown protein family 0016
V-ATPase	Vacuolar ATPase
VPS	Vacuolar protein sorting
YD	Yeast extract - dextrose medium
WT	Wild type

NOMENCLATURE

For clarity, here is the nomenclature used for genes and proteins in this manuscript:

Gene:	*GDT1, TMEM165*
Deleted gene:	*gdt1Δ* or *GDT1* deletion, *TMEM165* deletion
Protein:	Gdt1p, TMEM165

PUBLICATIONS

The most noteworthy observations performed during this thesis are related in two scientific publications:

Deschamps, A., A. S. Colinet, O. Zimmermannova, H. Sychrova and P. Morsomme (2020). "A new pH sensor localized in the Golgi apparatus of *Saccharomyces cerevisiae* reveals unexpected roles of Vph1p and Stv1p isoforms." Sci Rep **10**(1): 1881.

Deschamps, A., L. Thines, A. S. Colinet, P. Morsomme. "Exchange of H^+ for Ca^{2+} and Mn^{2+} mediated by Gdt1p and its involvement in Golgi pH regulation." *Paper in preparation*.

Besides, I also contributed to the elaboration of other research papers and of one review:

Demaegd, D., A. S. Colinet, A. Deschamps and P. Morsomme (2014). "Molecular evolution of a novel family of putative calcium transporters." PLoS One **9**(6): e100851.

Colinet, A. S., P. Sengottaiyan, A. Deschamps, M. L. Colsoul, L. Thines, D. Demaegd, M. C. Duchene, F. Foulquier, P. Hols and P. Morsomme (2016). "Yeast Gdt1 is a Golgi-localized calcium transporter required for stress-induced calcium signaling and protein glycosylation." Sci Rep **6**: 24282.

Colinet, A. S., L. Thines, A. Deschamps, G. Flemal, D. Demaegd and P. Morsomme (2017). "Acidic and uncharged polar residues in the consensus motifs of the yeast Ca2+ transporter Gdt1p are required for calcium transport." Cell Microbiol **19**(7).

Thines, L., A. Deschamps, P. Sengottaiyan, O. Savel, J. Stribny and P. Morsomme (2018). "The yeast protein Gdt1p transports Mn(2+) ions and thereby regulates manganese homeostasis in the Golgi." J Biol Chem **293**(21): 8048-8055.

Thines, L., A. Deschamps, J. Stribny and P. Morsomme (2019). "Yeast as a Tool for Deeper Understanding of Human Manganese-Related Diseases." Genes (Basel) **10**(7).

Stribny, J., L. Thines, A. Deschamps, P. Goffin and P. Morsomme (2020). "The human Golgi protein TMEM165 transports calcium and manganese in yeast and bacterial cells." J Biol Chem **295**(12): 3865-3874.

FOREWORD

The general aim of our research is to decipher the physiological role(s) of a poorly characterized protein family named UPF0016 (Unknown Protein Family 0016), recently renamed *GDT1 family* in protein databases. The interest of studying this protein family first pops up when the human ortholog of the family, *TMEM165*, was identified as the genetic cause of a rare inherited disease (1). *GDT1* orthologs are found in all kingdoms of life and have been relatively well conserved throughout evolution if we consider their predicted topology and the signature sequence of the protein (2). In our lab, the commonly used working model is the yeast *Saccharomyces cerevisiae*. Even though yeast and mammals can appear very different, their intracellular organization is strikingly similar. Therefore, for clarity and concision of the manuscript, I focused the literature review mainly on yeast physiology. When appropriate, comparison with human physiology will be made.

PART I

SETTING UP THE CONTEXT

« No cellular organelle has been the subject of as many, as long-lasting, or as diverse polemics as the Golgi apparatus. »

William Gordon Whaley

CHAPTER 1

FUNCTIONS AND HOMEOSTASIS OF THE GOLGI APPARATUS

1. The Golgi apparatus, a hub of the cell

a. Eukaryotic cells possess a complex endomembrane system

Eukaryotic cells are characterized by an intracellular organization into several subcellular compartments (Figure 1). Those compartments, called organelles, are dedicated to different cellular functions. The spatial segregation of different biological roles within those organelles is a great opportunity, since the diversification of physical properties and of chemical composition allows the acquisition of novel and more specialized biological functions. Additionally, such a segregation is a good way for cells to increase their fitness by taking advantage of organellar characteristics to optimize metabolic processes.

By the end of the 19th century, Camillo Golgi, an Italian medical doctor, described a particular arrangement of internal reticulated membranes having a croissant shape, close to the nucleus and the centrosome, and that were strongly stained by iron nitrate (3). A few years later, this particular arrangement was renamed "Golgi apparatus". We will simply denominate it as "Golgi" in this manuscript. For a long time, a controversy about the real existence of this cellular compartment has been ongoing, as some microscopists were thinking that this observation was the result of a staining artifact. It is only in the 1950s, when electron microscopy emerged, that the real existence of the Golgi was definitely confirmed. Here, we should also

stress that in *Saccharomyces cerevisiae*, the Golgi does not have the appearance of a croissant shaped membrane stacking but rather appears as individual vesicles spread across the cytosol (4).

In cells, the Golgi does not stand totally isolated but is part of a large endomembrane system encompassing different organelles. When looking from the inside to the periphery of the cell, the endomembrane system starts with the nuclear envelope, encloses endoplasmic reticulum, Golgi, *trans*-Golgi network (TGN), exo- and endocytic pathways, multi-vesicular bodies (MVB), vacuoles (or lysosomes in human) and finishes to the plasma membrane. In *S. cerevisiae*, recent work suggests that early endosomes (EE) do not exist on their own but rather are one with the TGN (5, 6). This endomembrane system is strongly interconnected by the continuous flow of vesicles that emerge from, and end up in, the different compartments (Figure 1). Vesicular fluxes are coordinated by a vast tubular network and numerous organellar contact sites also take part in the interconnexion of the endomembrane system.

b. The Golgi stands in a central position of the secretory pathway

The secretory pathway can be considered as a "functional unit" of the endomembrane system. It plays major roles for the production, the trafficking, the secretion, the recycling and the degradation of most secreted proteins and proteins exposed to the extracellular environment. In addition, proteins that are retained in the membranes or in the lumen of the endomembrane system are also produced and processed by the same machinery. Together, about one third of all proteins are synthesized, matured and conveyed by the secretory pathway (7, 8). Even though there are some specificities according to the organism, the global organization of the endomembrane system is relatively well conserved in all eukaryotes. The protein production starts at the rough endoplasmic reticulum, where ribosomes translate the genetic instructions. Synchronously to their synthesis, proteins are translocated into the lumen – or integrated into the membrane for membrane proteins – of this organelle by the so called translocon. Then, most of these synthesized proteins transit through the Golgi before reaching their final destination, mostly the plasma membrane, the extracellular space, or the vacuole/lysosome. Certain proteins are also retained in the endoplasmic reticulum, or specifically addressed to the nuclear envelope, to the Golgi, or to the endosomes.

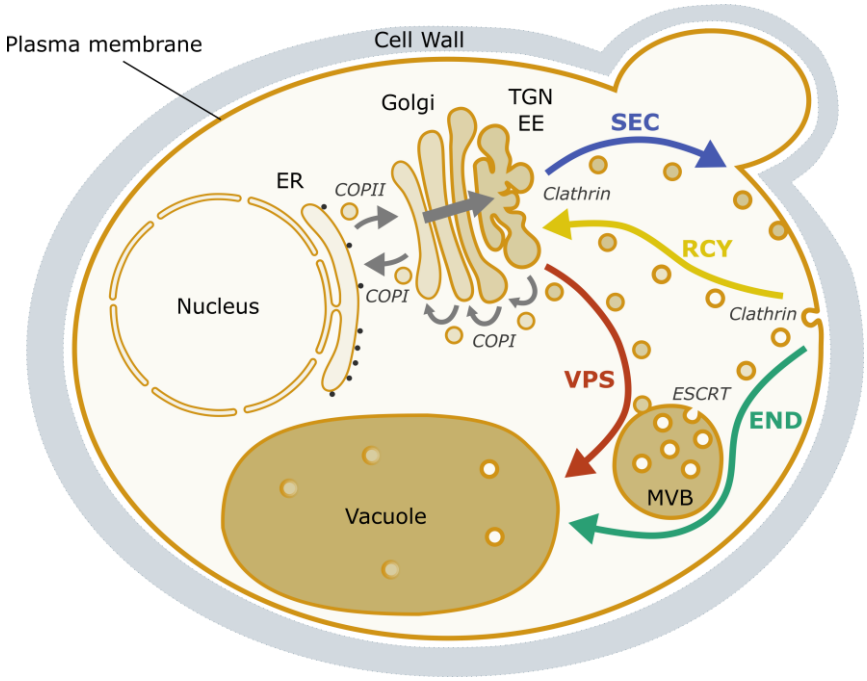

Figure 1. Endomembrane system of the budding yeast cell.
The different organelles are strongly interconnected by a continuous flow of vesicles. In the early secretory pathway, the path is more or less linear from the *ER* to the TGN via the Golgi stacks/compartments (even though fluxes occur in both directions). COPII and COPI coated vesicles traffic in the anterograde or retrograde direction, respectively. Then, exocytic vesicles follow the secretory pathway (SEC) while vacuolar proteins enter the vacuolar protein sorting pathway (VPS). Eventually, some plasma membrane proteins and extracellular compounds are internalized through endocytosis (END). After being internalized, some cargoes are recycled (RCY) back to the TGN to avoid degradation, and others are sent to the vacuole via the multi-vesicular bodies (MVB). This degradation route possibly involves a passage via the TGN/EE before cargoes reach the MVB (5, 9). At the MVB membrane, ESCRT complexes perform internalization of vesicles into the MVB lumen. The clathrin coat proteins act at several places to shape vesicles of the exocytic and endocytic networks. Figure inspired from (10). Note that the Golgi is here, and in following figures, represented as a membrane stack to simplify the identification of this organelle in schemes, even though it does not have this morphology in budding yeast.

c. Processing activity and shunting station are the two main functions of the Golgi

During their trafficking across the Golgi, many proteins are post-translationally modified as a result of the action of a set of Golgi-resident proteins. Those modifications are essential for proteins to get their final structure and therefore to meet their function, or to protect them from subsequent degradation. Those modifications can consist of the processing of the amino acid sequence itself, thanks to the activity of endopeptidases,

for example to cleave the signal peptide or to remove the auto-inhibitory region of proteases once they have reached their final location (11, 12), or it can occur via the addition of a set of chemical adducts, such as lipids or sugars. Some of those post-translational modifications permanently stay on the proteins after being added, while others are transient and serve as regulators or signaling during the protein life-span. Secretory and vacuolar proteins encounter several checkpoints during their journey through the secretory pathway and it is only if correctly folded and with all required attributes that they should be routed to their final destination (13).

In order to continuously organize the protein composition of the Golgi, an intense trafficking activity is required. This has two concomitant functions, to keep Golgi-resident enzymes and the appropriate lipids at the right position of the Golgi and, simultaneously, to transport secretory and vacuolar proteins forward in the secretory pathway. Historically, two models were proposed for the organization of the Golgi complex. A vesicular transport model where each compartment or each stack is "stable" and distinct from others, with resident enzymes, and in which cargo proteins and lipids are brought from upstream compartments and then actively removed to be sent to downstream compartments. And a maturation model where cargo proteins and lipids stay in the "same" compartment that step by step acquires the biochemical characteristics of downstream compartments thanks to the retrograde transport that brings processing enzymes from more mature compartments (14, 15). This is made possible by the continuous creation of new *cis*-Golgi cisternae that arise from the merge of vesicles coming from the ER. Despite the fact that, on some aspects, it is difficult to reconciliate the two models (16, 17), the maturation model has been supported by direct observations in yeast (4, 18) and is nowadays widely accepted (19, 20).

The anterograde and retrograde trafficking tasks are ensured by a large number of cytosolic proteins that act from the cytosolic side of the early secretory pathway. COPII coated vesicles mediate anterograde transport from the ER to the *cis*-Golgi, while COPI coated vesicles take over retrograde transport from the Golgi to the ER as well as the retrograde transport in between Golgi cisternae (Figure 1). Those coat complexes are then assisted by tethering factors and SNAREs for the tethering and the fusion of those vesicles at their target site (21-23). Eventually, proteins that should be sent forward, to the exocytic or endocytic networks, are sorted in the TGN. The sorting mechanisms are diversified according to the destination and the fate of the cargo. The most common Golgi to vacuole trafficking pathways are presented in *Box 1*. The specific question of the degradation routes of Golgi-resident proteins will be more deeply discussed latter on in this manuscript, when Gdt1p degradation will be assessed (Part III, Chapter 3).

BOX 1: Main Golgi to vacuole trafficking routes.

In the *trans*-Golgi and the TGN, secretory and vacuolar proteins are sorted by various mechanisms, as reviewed in Lujan *et al.* (13). Sorting can result from inherent physicochemical properties of the proteins and of the surrounding lipid bilayer, leading to TMD length-based partitioning, to protein aggregation mechanisms, or to partitioning based on membrane lipid composition. Alternatively, dedicated cytosolic proteins are involved in the recognition and the sorting of membrane proteins at the late Golgi. Finally, receptor mediated sorting is required for soluble luminal proteins. Once sorted, proteins are engaged in appropriate trafficking pathways.

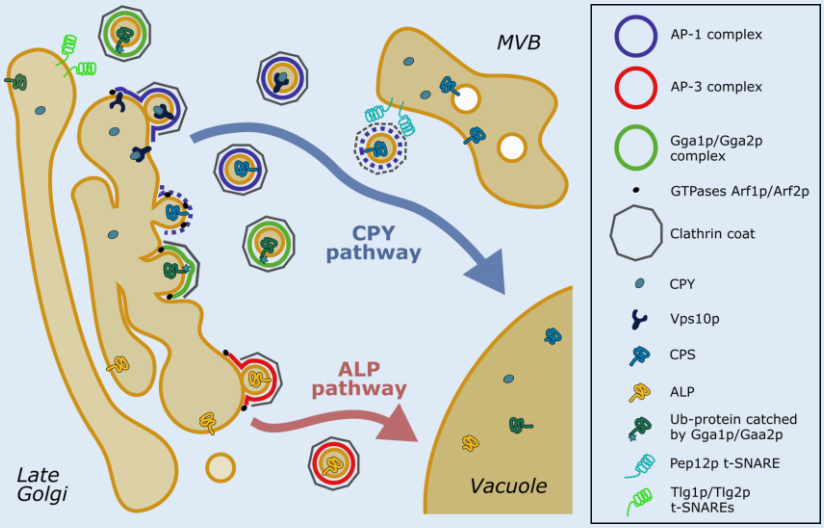

Figure 2. Golgi exit routes usually involve clathrin coat, clathrin adaptors and GTPases activity.
The main trafficking pathways conveying vacuolar proteins from the Golgi to the vacuole are depicted. Proteins can either traffic directly from the TGN to the vacuole via the ALP pathway, or have an intermediate step in the MVB. More details are found in the main text. Figure inspired from (10) and (13).

Basically, there are two main trafficking routes from the Golgi to the vacuole. In yeast, many vacuolar proteases are following the canonical vacuolar protein sorting (VPS) / carboxypeptidase Y (CPY) pathway (24, 25). This pathway involves the formation of clathrin coat vesicles, which is assisted by the AP-1 adaptor complex that recognizes target proteins. Once proteins are sorted at the TGN and incorporated in appropriate vesicles, they are sent towards the MVB where AP-1 and clathrin depolymerize. CPY, that is a soluble protease, necessitates the Vps10 receptor to be recognized and appropriately sorted in this pathway (26). Vacuolar membrane proteins, like the carboxypeptidase S (CPS), does not necessitate such receptor to follow the

CPY pathway. Besides, a second important Golgi to vacuole trafficking route has been characterized. Named alternate pathway / alkaline phosphatase (ALP) pathway, it also necessitates clathrin coat and is coordinated by the AP-3 adaptor complex (27, 28). If CPY pathway or ALP pathway is deficient, vacuolar proteins can sometimes take advantage of the remaining Golgi to vacuole trafficking route to reach their destination (29, 30). Especially, the possible interconnexions in between the different trafficking routes are not fully disentangled.

In support to those trafficking pathways, a set of adaptors and GTPases are also important for the sorting of proteins in the late Golgi and for their incorporation in clathrin-coated vesicles. Gga1p and Gga2p are Golgi-localized clathrin adaptors able to recognize ubiquitylated substrates (31-33). Syntaxins/t-SNAREs are also involved in the trafficking routes by triggering the fusion of vesicles to their target site. Hence, Tlg1p and Tlg2p are localized in late Golgi compartments and early endosomes, while Pep12p is located in late endosomes and MVB and involved in the CPY pathway (34). More recently, the role of the TGN as a recycling compartment was also further studied (5). Ubiquitin signaling mediated by several ubiquitin ligases and adaptor proteins is often involved in such recycling processes. (9, 35, 36).

2. Characteristics and determinants of Golgi luminal content and membrane composition

Now, we know that the Golgi is a hub for most of the secreted and organellar proteins. There, a big flow of all those proteins continuously run through and, at the same time, extremely well-ordered sequential modifications have to be completed. To maintain the organization of such a crowded organelle is a challenge for all eukaryotic cells. Hence, various biomolecular mechanisms satisfy the organization requirements necessary to keep efficient and accurate this transformation factory. Among the means used by eukaryotic cells, pH control and gradual acidification is a hallmark and a guide for Golgi organization. Lipid bilayer thickness and its fitting with transmembrane spans of proteins is probably another tool that cells are using to keep their Golgi well organized, in combination with the specific lipidic composition of its membrane (Figure 3).

a. Gradual acidification is a hallmark of the secretory pathway

The predominant biochemical characteristic of the secretory pathway is its step by step acidification (Figure 3). While the endoplasmic reticulum has an internal pH almost neutral and close to the cytosolic pH, exocytic vesicles and vacuoles are strongly acidic. In yeast, pH values of 7.3 in the cytosol (37), 7.1 for ER lumen (38), mildly acidic in TGN/prevacuolar compartments (39), and 5.6-6.2 for the vacuole (37, 40, 41) were previously reported (Figure 6). While the endomembrane system is a moving system, with lots of vesicles that are constantly budding or fusing at the different stages of the secretory pathway, this gradual acidification is essential to make the different compartments functionally specific compared to up- and downstream organelles.

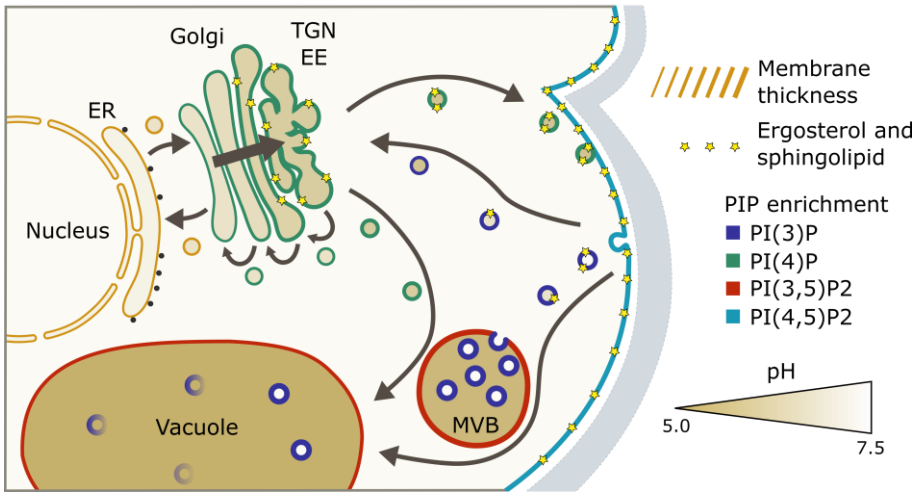

Figure 3. Organelles of the endomembrane system exhibit differences of membrane composition and internal pH values.
The internal pH becomes more and more acidic alongside the secretory pathway, with the pH of the ER that is close to 7.0, and exocytic vesicles with a pH <5.5. Regarding endocytic vesicles, they initially exhibit the pH of the extracellular medium, but then acidification also occurs, in early endosomes, MVB and vacuole to reach a value close to 5.0. In parallel, membrane thickness increases from the ER to the plasma membrane, according to the gradual ergosterol and sphingolipid enrichment. Finally, phosphoinositides (PIP) are also enriched specifically at one or another location. Altogether, those parameters drive membrane protein localization and control enzymatic activity in the lumen of organelles.

i. An acidic luminal pH supports Golgi functions

Acidic pH within organelles has a key role to assure the biological functions they have to encounter. In the lumen of the Golgi, a slightly acidic pH is a prerequisite to properly perform post-translational modifications, as many glycosylation enzymes have an optimal pH for activity. It also plays roles in protein sorting and for the maintenance of the Golgi structure. Upstream and downstream in the secretory pathway, specific pH values are crucial to sustain many functions, such as retrieval of luminal HDEL tagged proteins by the Erd2p receptor (42, 43), formation of glycosylation enzymes homomers and heteromers in the ER and the Golgi (44, 45), sorting of lysosomal mannose-6-phosphate containing acid hydrolases in higher eukaryotes (46), zymogen activation and proteolytic activity in the vacuole (47), dissociation of ligands from receptors after endocytosis (48), storage of Ca^{2+} and other compounds in the vacuole (49), or for global maintenance of intracellular pH (50, 51). Given the continuous flow of vesicles of different pH alongside the Golgi, a robust operating system is mandatory to control Golgi pH.

ii. The master regulator of secretory pathway acidification is the V-ATPase

The most important player devoted to secretory pathway acidification is the vacuolar H^+-ATPase (V-ATPase). This proton pump is evolutionary and structurally related to the family of F_1F_0 ATP synthases (52), but its role is diametrically opposite. Under physiological conditions, its function is not to synthetize ATP by using a proton gradient, but rather to generate such a gradient by consuming ATP. Despite its name might suggest that V-ATPases are specifically vacuolar proteins, they are also the main proton pump localized all along the secretory pathway. The V-ATPase is a large complex composed of 14 subunits that are organized in two specific domains. The V_0 domain contains 6 subunits and is membrane embedded. This domain performs proton translocation across phospholipidic membranes. The V_1 domain, composed of 8 subunits, is a soluble complex travelling from the cytosol to the membrane in order to form a fully assembled V-ATPase complex with proton pumping activity. When bound to V_0, V_1 domain operates ATP hydrolysis and transfers the energy thus generated to the integral membrane V_0 domain through a rotational motion (Figure 4).

The activity of the V-ATPase is regulated via the reversible assembly or disassembly of V_1 with V_0 domain. Especially, glucose deprivation leads to 70% V-ATPase dissociation within 5 minutes. On the contrary, restoration of glucose availability induces fast reassembly of full V-ATPase complexes (53). This process, extensively studied in *Saccharomyces cerevisiae*, has also been

observed in higher eukaryotes (54). The dissociation upon glucose deprivation is thought to be important to save ATP. V-ATPase localization specifies its behavior regarding glucose-dependent association/dissociation, as vacuolar complexes are more prone to dissociation than V-ATPase complexes at other locations of the secretory pathway (55, 56). It suggests that Golgi and prevacuolar compartments need continuously operable or activable V-ATPase complexes, whatever the extracellular glucose abundance. The constant presence of such a proton pump could be essential to maintain the correct organization of the secretory pathway by preserving a proper pH gradient.

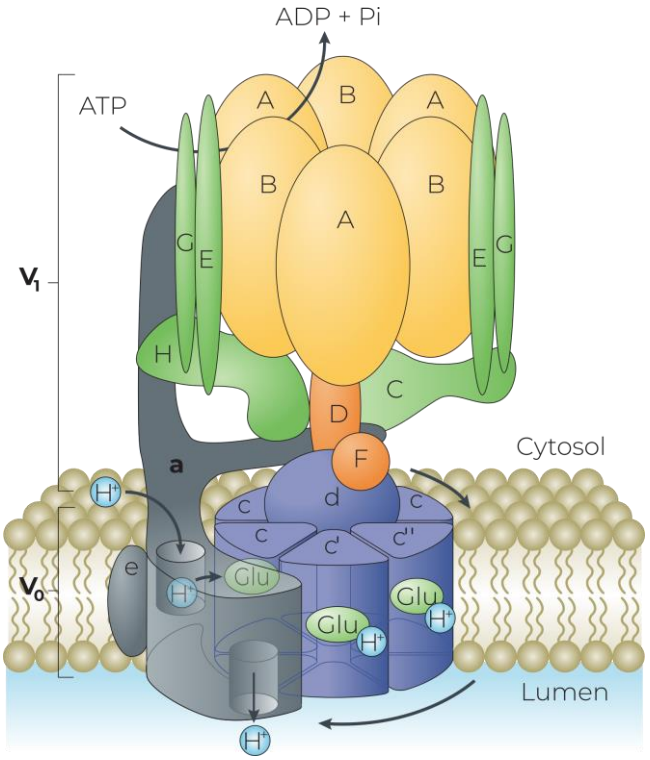

Figure 4. V-ATPase structure and H⁺ translocation mechanism.
The V-ATPase is composed of fourteen subunits, organized in two distinct domains, a membrane embedded V0 domain and a peripheral soluble V1 domain. The V1 domain performs ATP hydrolysis and transfers energy with a circular motion to the V0 that translocates H^+ across the membrane. The subunit *a* connects the two domains and catch H^+ at the cytosolic side of the membrane to transfer it to a glutamate of the subunit *c*. After the movement has completed a full rotation, H^+ is transferred in a second hemi-channel of the subunit *a* and is finally released at the luminal side of the membrane. In *S. cerevisiae*, the subunit *a* is the only that exists in two different isoforms, Vph1p and Stv1p. Adapted from (57).

BOX 2. V-ATPase subunit *a* isoforms for fine-tuned regulation.

In *Saccharomyces cerevisiae*, all V-ATPase subunits exist in a single isoform, except for the subunit *a* of the V_0 domain, which has two isoforms, *VPH1* (Vacuolar pH) and *STV1* (Similar To VPH1). This subunit drives H^+ ions via a hemi-channel from the cytosolic side of the membrane to a glutamate buried in the core proteolipid ring of the V_0 transmembrane domain and then transfers them to the luminal side via a second hemi-channel (58, 59) (Figure 4). In addition, subunit *a* also targets V-ATPases to the appropriate place in the cell. The Vph1p isoform goes to vacuolar membrane (60), while Stv1p isoform locates at Golgi and endosomal membranes (61). It is also to be noted that Stv1p-containing complexes are 10 to 20 times less abundant than Vph1p-containing complexes (61) and that Stv1p-containing complexes hydrolyze ATP less efficiently than Vph1p ones (55). While the proton transfer is mediated by the carboxy terminal transmembrane part of the protein, the targeting information is contained in its amino terminal cytosolic domain (62). When overexpressed, *STV1* complements the absence of *VPH1* and Stv1p is then also detected at the vacuolar membrane (61).

In human cells, several isoforms stand for 6 out of the 14 subunits and are sometimes expressed in specific tissues (renal, neural, endothelial, osteoclasts, testis, lung, epididymis, or ubiquitous). Although the roles of the different human isoforms are not completely understood, it probably contributes to specialize the properties of the V-ATPase to those different tissues (57). For subunit *a*, the *a3* and *a4* isoforms peculiarly target the V-ATPase to the plasma membrane of osteoclasts or to the apical membrane of renal intercalated cells and epididymal clear cells, respectively (63-65).

How the gradual acidification is controlled by a unique pump remains enigmatic. One hypothesis is that the gradual increase of H^+-ATPases abundance alongside the secretory pathway generates such a gradual acidification. Pump abundance may be controlled by its "retention time" that could differ from one place of the secretory pathway to another. Alternatively, or complementary, the V-ATPase activity could be regulated alongside the secretory pathway. Eventually, other proton transporters could also play a role in the regulation of the secretory pathway acidification. However, it is worth noting that V-ATPases are essential in higher eukaryotes. In yeast, V-ATPase is dispensable if cells are grown in media with low extracellular pH (< 5.5), presumably because luminal acidification could occur via the internalization of some extracellular medium. Accordingly, endocytosis becomes essential in strains deleted for the V-ATPase (66, 67).

iii. Counterions conductivity and proton leak channel balance Golgi pH

When pumping protons from the cytosol to the Golgi lumen, the V-ATPase creates a positive inside membrane potential (50, 68). In order to sustain proton pumping activity, cells have to mitigate the amplitude of this membrane potential. This presumably occurs through the transport of other ions, either via the intake of Cl^- anions or via the efflux of K^+ cations (50). The Golgi pH Regulator (GPHR) anion channel takes over Cl^- transit at the Golgi in animal cells (69) and the chloride/proton exchanger Gef1p could sustain similar function in *medial*-Golgi, *trans*-Golgi and pre-vacuolar compartments in yeast cells (70-72). Regarding alkali cations transport, several hypothetical transporters could ensure this function, such as Nhx1p, an endosomal Na^+-K^+/H^+ exchanger related to human Na^+/H^+ exchanger (NHE) family (73). Kha1p is another candidate for K^+/H^+ exchange in the Golgi (Figure 6) (74, 75). Several of those studies highlighted that counterion transport is required to achieve the luminal acidic pH in organelles by enabling V-ATPase H^+ transport without limitation, but that this counterion conductivity does not directly control the luminal pH as the addition of different K^+ or Cl^- ionophores does not permit a more pronounced acidification of the Golgi lumen.

Therefore, another mechanism that controls the pH value in lumen of organelles is its inherent H^+ permeability. A predicted but still unidentified *"proton leak channel"* is probably assuming this task. Especially, it appears that proton permeability decreases from early to late secretory pathway (76) indicating that the proton leak parameters could determine the resting luminal pH alongside the secretory pathway (Figure 5). Among the candidates for such a proton leak, NHE family members could maybe fulfill this function even though its mode of action remains elusive (51). Besides, the human SLC4A2 hydrogen carbonate/chloride exchanger has been recently described as controlling the resting Golgi pH, which is inversely correlated to its expression level (77). The imported HCO_3^- would react with H^+ to form carbonic acid that can then dissociate into CO_2 and H_2O and exit the Golgi under those chemical forms. The *S. cerevisiae* homolog of *SLC4A2*, named *BOR1*, is a putative plasma membrane boron exporter (78), but its transport activity has not been directly demonstrated to date. Hence, Bor1p-mediated HCO_3^- transport could be assessed, as it is also an interesting candidate for such proton leak function.

Generally speaking, the proton leak pathway and the V-ATPase proton pump have to work properly in order to generate the desired acidity alongside the secretory pathway, but at the same time, they should be constrained when it

is relevant to avoid futile cycles of H^+ influx and efflux across the Golgi membrane.

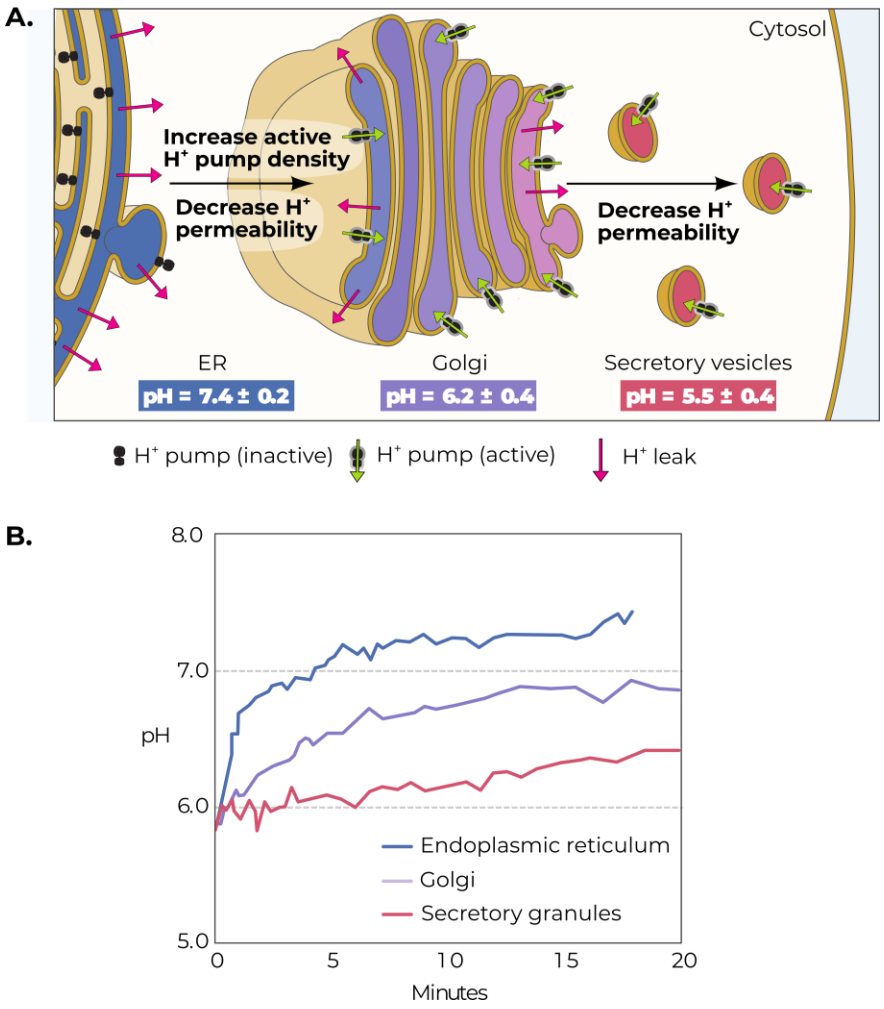

Figure 5. The pH of the secretory pathway results from an equilibrium of H^+ loading and H^+ leak.
A. Model of proton pumping and proton leakage established from the known pH values and pH leakages alongside the secretory pathway. There is a gradual increase in the density of active H^+ pump and a gradual decrease of H^+ leakage due to inherent lipid membrane properties and/or to the presence of dedicated proton leak channels. **B.** Determination of the rate of proton leakage from various compartments, when proton loading is inhibited by bafilomycin. The lumen of each individual compartment was artificially acidified to pH 6.0 prior to measurement. Figure adapted from (50).

b. A set of pumps and exchangers control the luminal Golgi chemical composition

Beside pH homeostasis, the luminal concentration of other chemicals has to be carefully kept up by the cell. Of course, substrates that are consumed by metabolic reactions in the Golgi have to be loaded into it. Notably, a set of solute carriers from the SLC35 family imports activated sugars, usually mono- or diphosphate-nucleotide sugars, into the Golgi lumen in exchange for the corresponding monophosphate-nucleotide devoid of monosaccharide (79). Inorganic phosphate, that is produced during the elongation of polysaccharides, is a "waste" of Golgi metabolism and is recycled back to the cytosol through Erd1p (80).

Next to its post-translational functions, the secretory pathway has also a detoxification role. Actually, some compounds are transferred from the cytosol to the Golgi lumen and will finally end up in the extracellular medium or in the vacuole by passively following the flux of material and vesicles in the anterograde direction. For example, Ca^{2+}, Mn^{2+}, and even Cd^{2+} cations are presumably extruded out of the cell thanks to Pmr1p protein (81, 82). In addition to the detoxification purpose, Ca^{2+} and Mn^{2+} Golgi loading via Pmr1p is also essential to sustain glycosylation and sorting activities of the Golgi (83, 84). Indirectly, other transporters located upstream or downstream in the secretory pathway are also expected to act on Golgi Mn^{2+} and Ca^{2+} content via the vesicular trafficking. Among those, Spf1p (also denominated as Cod1p) is thought to pump Ca^{2+} and possibly Mn^{2+} towards the ER lumen (85-87), while Atx2p and Smf2p are presumably extruding Mn^{2+} out of some late Golgi or post-Golgi compartments (Figure 6) (88, 89).

Lately, Gdt1p was also shown to be involved in Ca^{2+} and Mn^{2+} detoxification, in complement to Pmr1p (90-92). The exact role of Gdt1p and its transport mechanism are not fully understood yet. It will be thoroughly discussed later on in this manuscript.

Finally, the concentrations of other cations, like K^{+}, Na^{+}, Zn^{2+}, Mg^{2+}, Fe^{2+} or Cu^{+}, are also controlled in the secretory pathway by a set of transporters, as reviewed by Cyert and Philpott (93).

c. Membrane composition and role of phosphoinositides

Lipid bilayers are defining the borders of cellular compartments, in between cytosol and extracellular space, and in between organelle lumen and cytosol. Even though they are basically constituted of the same compounds – *i.e.* glycerophospholipids, sphingolipids and ergosterol (or cholesterol in animal

cells) –, their relative amounts vary and are specific for each membrane. The peculiarities of each membrane are important to specialize them, in particular to guide the subcellular localization of transmembrane and anchored proteins.

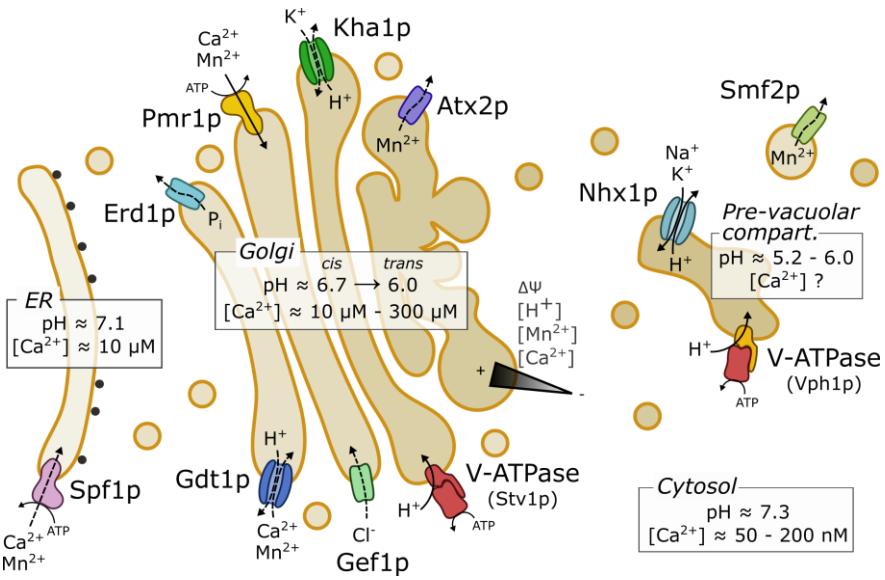

Figure 6. Golgi ion homeostasis is controlled by a set of dedicated transporters. Several membrane proteins import different ions to the secretory pathway lumen. Transport is energized by ATP hydrolysis for ATPases or by the concentration gradient of another chemical for exchangers. Additionally, some membrane proteins passively allow chemicals to travel from the more to the less concentrated side of the membrane. The well-established transport activities are represented with solid lines, the still elusive transports are represented with dashed lines. As a result, the concentrations of H^+, Ca^{2+} and Mn^{2+} are higher in the Golgi lumen than in the cytosol and there is a positive luminal membrane potential. The pH and the $[Ca^{2+}]$ in the different compartments are indicated. More details about the nature of the different transporters is given in the main text. Note that carriers from the SLC35 family are not indicated on the scheme, but they could also participate in pH regulation.

Among the characteristics of lipid bilayers, membrane thickness is a parameter that is adjusted from one membrane to another. The length of acyl chains, their saturation level, the nature of head groups and the relative amount of ergosterol dictate membrane thickness. Therefore, sphingolipid – that, in yeast, are usually constituted of particularly long acyl chains – and ergosterol enrichment in the plasma membrane, compared to the early secretory pathway membranes, increases membrane thickness (Figure 3)

(94). Such ergosterol enrichment presumably also intensifies lateral compaction of acyl chains, reducing acyl chain mobility, which participates in membrane thickening and increases impermeability of the plasma membrane (95). Particularly, unlike synthesis of other major membrane lipids – sterols and glycerophospholipids – that mainly occurs in the ER, sphingolipid synthesis starts in the ER by the production of ceramide and continues in the Golgi by the addition of the sugar head group (96). In yeast, this later step is partly performed by the Golgi-localized inositol phosphorylceramide synthase Aur1p (97, 98). The *trans*-Golgi is a sorting place for lipids, possibly via an exclusion mechanism from the highly curved COPI vesicles mediating Golgi retrograde transport, making it a place of steep transition in membrane thickness (95). Membrane thickness is driving membrane proteins shipment, as hydrophobic mismatch of proteins with too long transmembrane domains (TMD) in the ER membrane provokes their clustering and their probable exit out of the ER (99, 100). Consequently, the length of transmembrane domains contains in average 5 more amino acids for plasma membrane localized proteins than for early secretory pathway retained proteins (101-103). Considering Golgi resident membrane proteins, it was shown that an appropriate transmembrane length is required to retain the sialyl-transferase in Golgi membranes, while the shortening of TMD of plasma membrane proteins delocalize them to the Golgi apparatus (104). TMD length is then one of the sorting signals and is supported by other segregation mechanisms, such as interactions with specific receptors or clustering and oligomerization with other membrane proteins.

Phosphoinositides – or phosphatidylinositol phosphate (PIP) lipids – are specific phospholipids, mainly present in the cytosolic leaflet of membranes, that serve as membrane anchored signals. They derive from the phosphatidylinositol, a glycerophospholipid containing a *myo*-inositol group – a carboxylic sugar that is synthesized from glucose 6-phosphate – at its polar extremity. Phosphatidylinositol can be differentially and reversibly phosphorylated by several kinases and phosphatases on the hydroxyl groups in position 3, 4 and 5 of the *myo*-inositol function, giving rise to PI(4)P, PI(3,5)P_2, PI(4,5)P_2, etc. (105). At the plasma membrane, PI(4,5)P_2 can be hydrolyzed by a phospholipase, generating diacylglycerol and IP_3, a soluble secondary messenger. In the secretory pathway, PIPs play essential roles for vesicle trafficking and for Golgi functions (106). Vps34, a phosphatidylinositol 3-kinase, is required for protein transport from the Golgi to the vacuole (107, 108), while Pik1, a phosphatidylinositol 4-kinase, is involved in the generation of exocytic vesicles from the *trans*-Golgi (109, 110). Globally, PI(4)P is enriched at the Golgi and in secretory vesicles, PI(3)P in early endosomes and in MVB, and PI(3,5)P_2 at the vacuolar membrane (Figure 3) (105).

3. A story of egg or chicken: Is it chemical gradients or protein localization that orchestrates Golgi organization?

The Golgi exhibits a complex organization and is constantly remodelled to maintain its functionality. From the *cis*- to the *trans*-Golgi, membrane thickness increases and membrane permeability diminishes, pH decreases, PIPs composition varies, and Ca^{2+} and Mn^{2+} concentrations are rising. Those parameters govern Golgi operations but, at the same time, they are themselves controlled by the activity of a set of Golgi resident enzymes. Now, the interesting point is that enzymes retention in the Golgi usually depends on the existence of the aforementioned gradients. This statement can even be extended to the organization of the endomembrane system as a whole.

Luminal pH guides protein localization in the secretory pathway …

At first, the luminal pH drives the localization of many proteins in the secretory pathway through different mechanisms. HDEL/KDEL tagged proteins are recycled from the Golgi to the ER by their dedicated receptor in a pH-dependent manner. The affinity of the receptor for the HDEL/KDEL target sequence is enhanced at lower pH, therefore binding it in the *cis*-Golgi lumen, and weakens at higher pH, therefore releasing the cargo once in the ER lumen (42, 43). Many type-II integral membrane proteins involved in the glycosylation process are also shipped at their appropriate localization in a pH-dependent manner (44, 45, 111, 112). Protein sorting in the TGN also depends on the pH, because V-ATPase deficiency or inhibition leads to mistargeting of plasma membrane and Golgi proteins to the vacuole, like the plasma membrane H^+-ATPase Pma1p or the late Golgi Kex2p endoprotease (113) – the last one being also dependent on Ca^{2+} to ensure its activity (114) –, while it concomitantly affects the targeting of vacuolar proteins (115).

… while V-ATPase activity is regulated by membrane composition …

Secondly, the activity of the V-ATPase is itself regulated by the Golgi organization. For example, phospholipid flippases activity and ergosterol synthesis regulate V-ATPase activity (116). Next to this, the specific enrichment of some phosphoinositides (PIPs) drives V-ATPase localization and activity. Actually, subunit *a* isoforms localization depends on PIPs, since Stv1p N-terminal cytosolic tail interacts with PI(4)P (117) and that $PI(3,5)P_2$ activates V-ATPase assembly and activity by interacting with Vph1p (118, 119). As a consequence, the pH gradient alongside the secretory pathway is dependent on PIPs regulation. Additionally, PIPs are also involved in

vesicular trafficking in the secretory pathway. For example, TRPML1 endolysosomal Ca^{2+} channel in animal cells and the homologous Yvc1p vacuolar Ca^{2+} channel in yeast are both activated by $PI(3,5)P_2$ (120). Ca^{2+} release acts on vesicular trafficking, presumably because it activates vesicular fission and fusion events mediated by the SNARE protein family (121, 122). It is likely that other transporters involved in Golgi pH and ionic concentration regulation are also regulated by PIPs and by membrane composition.

... and that membrane composition depends on enzymatic activity

Finally, membrane composition is also controlled by the presence of the appropriate metabolic enzymes in the Golgi apparatus and in surrounding organelles. For example, sphingolipid synthesis is finished by a Golgi resident enzyme, Aur1p, in correlation with a lengthening of transmembrane domains of Golgi resident proteins from the *trans*-Golgi compared to *cis*- and *medial*-Golgi resident proteins (97). Considering PI(4)P, that is enriched in the Golgi, its concentration is synchronously lowered in *cis*- and *medial*-Golgi through the action of the integral membrane phosphoinositide phosphatase Sac1p in a mechanism assisted with Vps74p, the yeast ortholog of human GOLPH3. This activity is crucial to maintain *medial*-Golgi resident proteins at their correct place (123). Next to it, PI(4)P is also sensitive to pH, at its cytosolic side, via the protonation or deprotonation of its head group. This chemical modification affects the binding of PI(4)P effector proteins and regulates cargo sorting (124). Remarkably, cytosolic pH is itself dependent on the activity of H^+ pumps, mainly the plasma membrane localized Pma1p and the V-ATPase that is active at the Golgi membrane (41).

Additional regulation mechanisms are also involved

The Golgi organization is also supported by a set of proteins and complexes dedicated to this task, like t-SNAREs and v-SNAREs, Golgins, COGs, the TRAPP complex and others, reviewed in (13, 125-127). Of course, those proteins should also be localized at appropriate site to ensure their function (128, 129). Moreover, it was shown that the cooperation and the interactions in between those different actors participate in Golgi organization (130). To date, the complete mechanisms driving Golgi organization are far from being well-understood and lots remain to be discovered about them (13, 23).

Altogether, those observations raise the question of who is the real Golgi orchestra leader? Maybe there is not a single leading mechanism and one can speculate that it is the coordinated and balanced actions of the different

regulators of Golgi, *i.e.* lipid bilayer composition, membrane transporters localization and activity, and luminal and cytosolic ionic concentrations, that together maintain a functional Golgi organization. The appearance and the evolution of the endomembrane system is a beautiful example of cellular biology complexity and efficacy.

CHAPTER 2

GLYCOSYLATION OF PROTEINS LARGELY TAKES PLACE IN THE EARLY SECRETORY PATHWAY

1. General aspects about glycosylation

The addition and the elongation of oligosaccharides on proteins and lipids, a process called glycosylation, is the most substantial modification that takes place in the Golgi. Regarding protein glycosylation, saccharide polymers are most commonly added either on the hydroxyl group of the side-chains of serines and threonines, or on the nitrogen of the amide function of asparagine side-chains, and are referred to as O- and N-glycosylation, respectively.

Protein glycosylation plays many different roles for living organisms, as reviewed in (131). It is a barcode for cells to recognize their "mates" from "strangers", it serves cellular adhesion and migration, or it protects lysosomal/vacuolar-resident proteins from degradation. Glycosylation also serves as a benchmark to control protein trafficking alongside the secretory pathway (132). Finally, by exerting intra- and inter-molecular interactions, it affects the folding and the shape of proteins. Hence, glycosylation is usually necessary for glycoproteins to ensure their biological function. In eukaryotes, the glycosylation procedure has taken advantage of the intracellular compartmentalization. Therefore, it substantially differs in prokaryotes.

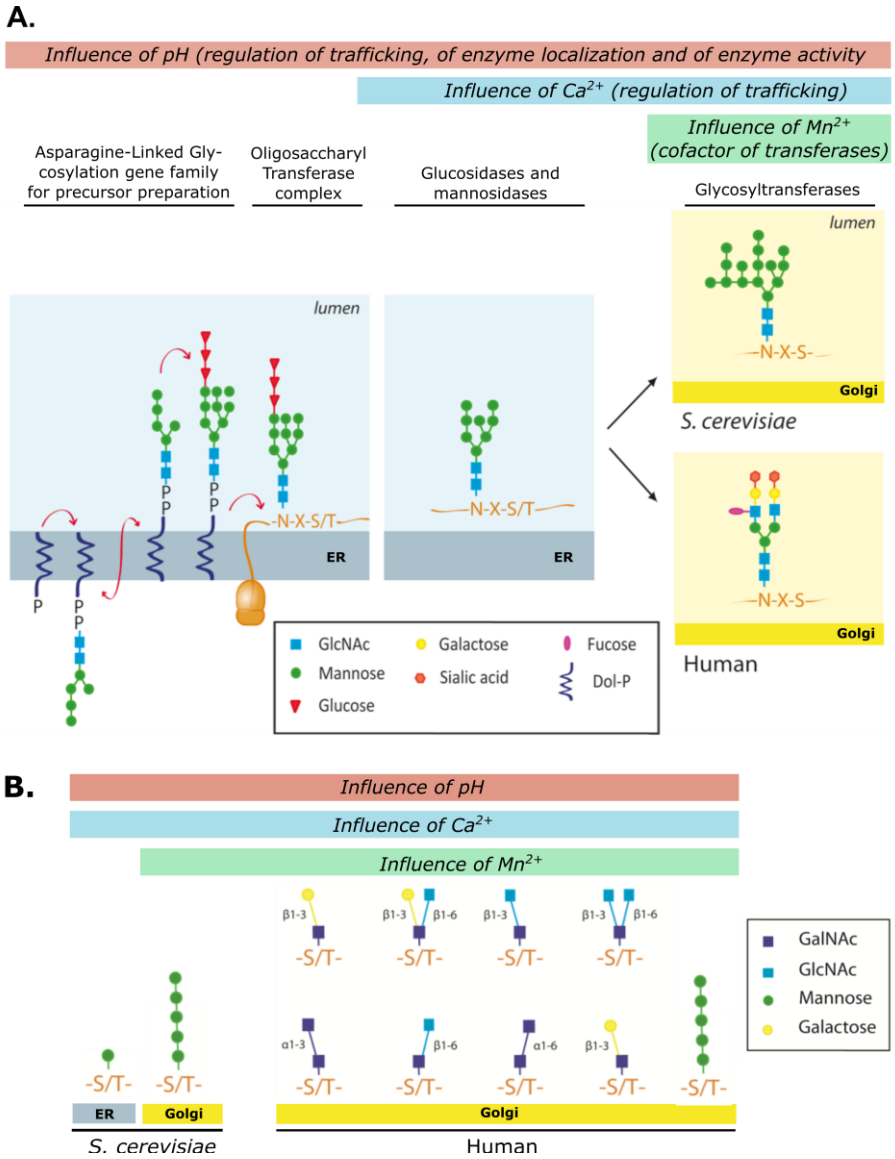

Figure 7. Overview of the N- and O-glycosylation processes.
A. N-glycosylation is initiated at the ER by the production of a precursor, which is then transferred on the amide function of asparagines belonging to the N-X-S/T consensus sequence. After trimming of glucoses and of a few mannoses by dedicated hydrolases, the protein exits the ER and glycan elongation is pursued in the Golgi lumen. In yeast, high mannose structures are produced. In human, more complex glycan structures are often assembled. **B.** In *S. cerevisiae*, O-mannosylation is the only O-glycosylated form. It is initiated in the ER by the addition of the first mannose residue and then glycan elongation is pursued in the Golgi lumen. In human, mucine type O-glycosylation is the most common O-glycoform. It takes place only in the Golgi lumen and always consists of the initial addition of a GalNAc, followed by a diversity of monosaccharide adducts. It should be noted that high mannose N-glycosylation and O-mannosylation also take place in human

cells. The glycosylation process is performed in an optimal manner if luminal pH optimally sustains enzymatic activity, if Ca^{2+}-dependent vesicular trafficking operates properly and if Mn^{2+} availability is sufficient to play its role as cofactor for a set of glycosyltransferases. Figure adapted from (133).

a. N-linked glycosylation

N-glycosylation is initiated by the production of lipid-linked oligosaccharides at the ER membrane by a set of *ALG* proteins (Asparagine-Linked Glycosylation). Then, the glycan precursor is transferred by the *OST* complex (Oligo-Saccharyl Transferase complex) to some asparagine residues belonging to the N-X-S/T consensus sequence in nascent proteins. The local structural conformation of the acceptor protein has to be sufficiently flexible to accept the transfer of the oligosaccharide precursor. Hence, its transfer is not favoured in secondary structures of proteins such as α helices or β sheets and the majority of N-glycosylation sites are found in loops (134). Next, the oligosaccharide is trimmed by several glucosidases and mannosidases. Once trimming completed, the protein exits the ER and reaches the Golgi where terminal glycosylation occurs by the addition of mannoses in *S. cerevisiae*, or by a variety of sugars in mammals (Figure 7A).

b. O-linked glycosylation

Regarding protein O-glycosylation, there is more substantial differences in between yeast and human. In *S. cerevisiae*, O-glycosylation starts in the ER by the addition of a first mannose residue mediated by *PMT* proteins (Protein O-Mannosyl Transferase). Elongation is then pursued in the Golgi lumen by the action of α-1,2- and α-1,3-mannosyl transferases (135) and the final product is usually a linear glycan of up to 5 mannose residues (136), although longer structures have been described. In human, O-mannosylation coexists with other O-glycosylation subtypes. The most common is the mucin type O-glycosylation, which is initiated by the linkage of a N-acetylgalactosamine (GalNAc) on the target protein sequence. Mucin type O-glycosylation occurs specifically in the Golgi on fully folded proteins. Height different core structures emerge from the addition of galactose, mannose and/or N-acetylglucosamine (GlcNAc) to the initial GalNAc, followed by further elongation with the addition of 1 to 10 additional monosaccharides, including fucoses, sialic acids or GlcNAc (Figure 7B) (137).

2. The glycosylation process is like a funambulist in the Golgi apparatus

While the amino acid sequence of a protein is strictly defined, glycosylation structures are by nature heterogenous parts in glycoproteins. From one glycosylation site to another within a single protein, or for the corresponding glycosylation site into two identical proteins, glycosylation structures will differ from one site to another (136, 138, 139). As an explanation, the local protein sequence was shown to influence the outcome of each glycosylation site (140). Indeed, according to the local folding, the glycan under synthesis will be more or less easily available to glycosylation enzymes. Next to local protein sequence, and even though the Golgi flux is strongly controlled, the transit speed of the growing glycosylation adducts through the Golgi apparatus influences the glycosylation outcome. In the secretory pathway, glycan synthesis is dynamic and exhibits a competitive process of different glycosylation enzymes for the same substrates. As a result, each glycosylation site of each protein is represented as a pool of different glycan assemblies, with usually one (or a few) major product, and a large set of minor products (138). The heterogeneity of glycosylation products does probably represent an evolutive advantage, because it allows cells to increase their glycoproteome diversity in an enormous way.

Nevertheless, the conditions allowing glycosylation enzymes to fully work must be fulfilled in order to perform glycosylation as efficiently as possible. Especially, an optimal organization of the glycosylation enzymes alongside the different stacks of the Golgi is crucial. Accordingly, failures in Golgi organization and trafficking or pH dysregulations lead to glycosylation abnormalities (44, 141-143).

3. Disorders of glycosylation can be induced by various genetic causes

a. CDGs are an expanding family of inherited diseases

As the glycosylation of proteins has so many roles for cellular and organism maintenance and because it has been estimated that 20% to 50% of all proteins are modified by glycosylation (144-146), troubles in the procedure of glycosylation, when not lethal, will generally lead to various and often severe symptoms (147). Together, all genetic mutations causing glycosylation troubles are designated as *Congenital Disorders of Glycosylation* (CDGs). The first diagnosis of glycosylation disorder was established in 1980 (148) but its underlying genetic cause was identified only in 1995 (149). Twenty years after the first CDG diagnosis, there were nine different known causes of CDGs (150) and, nowadays, 137 genes have been related to glycosylation disorders (151). This number is expected to continue to increase, since 2% of all expressed proteins in animals are involved, directly or indirectly, in the glycosylation process (144). Therefore, many different genetic mutations can cause glycosylation deficiencies. Next to enzymes directly involved in the addition of monosaccharides to the growing oligosaccharides, many other enzymes, involved in the production and the transport of the activated sugars or implicated in secretory pathway organization and homeostasis, are also frequent causes of glycosylation disorders. For examples, seven out of the eight human COG subunits (Conserved Oligomeric Golgi), involved in the intra-Golgi vesicular trafficking, or different mutations of the V-ATPase and their accessory proteins, have been identified as causing CDGs (151).

b. Golgi ion homeostasis dysregulation impairs glycosylation

Here, we will focus on ion homeostasis in view of our protein of interest – Gdt1p – that is presumably involved in cation transport across the Golgi membrane. As stated in the previous chapter, the intraluminal ionic content is involved in the maintenance of the Golgi organization and is devoted to ensure its functions. Consequently, and accordingly, the glycosylation process is also regulated by several ions in different ways (Figure 7).

The Mn^{2+} cation serves as a cofactor for a set of glycosyltransferases of the "*A folding group*", by orienting two catalytic aspartate and glutamate and by stabilizing the lipid-pyrophosphate leaving group (152, 153). As an example in human, binding of Mn^{2+} to the β-1,4-galactosyltransferase is necessary to produce efficient catalytic activity (154). Therefore, it is not surprising that Mn^{2+} homeostasis impairment in the Golgi causes glycosylation disorders. Accordingly, SLC39A8-CDG patients – that are deficient in cellular Mn^{2+}

intake at the plasma membrane – exhibit glycosylation troubles because of Mn^{2+} deprivation in the Golgi lumen (Park, 2015). A similar observation is drawn with the yeast *PMR1* gene, because deletion of this Golgi Ca^{2+}-Mn^{2+} ATPase triggers glycosylation defects that can be counteracted by the addition of extra Mn^{2+} (83, 84).

The Ca^{2+} cation, while probably not a preferential cofactor of enzymes involved in glycosylation, plays multiple roles for Golgi organization. Especially, Ca^{2+} is known to be important for vesicles budding and fusion and is therefore essential to ensure secretory pathway functionality (155, 156). Particularly, Ca^{2+} is an inducer of SNAREs activity (157). Strikingly, Ca^{2+} supplementation is able to partially restore the glycosylation defects observed in the *pmr1Δ* strain (84, 158). It has been suggested that Ca^{2+} supplementation in yeast, by fastening the Golgi trafficking, helps to sustain the Golgi lumen with Mn^{2+} through retrograde – and possibly also anterograde – trafficking (89). Next to that, Ca^{2+} ions, as divalent cations, could maybe replace and/or compete with Mn^{2+} at its binding site in glycosyltransferases, therefore affecting glycosylation.

Regarding pH, it was previously pointed out that it has a big influence on the Golgi organization. Especially, the gradual acidification of the secretory pathway is involved in the formation of homomers and heteromers of the glycosylation enzymes, both in yeast and in higher eukaryotes (159). The formation of such complexes, along with the "kin recognition" hypothesis (160), is probably important to ensure the correct targeting and retention of glycosyltransferases to the Golgi. Moreover, it is thought that the formation of those complexes regulates the activity of the glycosyltransferases. This may reflect substrate channeling through the complexes (159). Furthermore, it is well-known that enzymes have by hitherto an optimal pH for their activity, through the appropriate protonation or deprotonation of all acido-basic chemical function of amino acid lateral chains.

Therefore, perturbations of the Golgi pH often lead to glycosylation impairments or to other cellular dysregulations, such as cancers, degenerative disorders, and even to an increased sensitivity to some viral infections (161). Accordingly, mutations in several V-ATPase subunits have been identified as causing glycosylation impairments (162, 163), while alterations of NHE7 Na^+/H^+ antiporter or of Cl^- transporters also promote the appearance of degenerative diseases, probably due to Golgi pH dysregulation (161). In yeast, Golgi pH alkalization arising in *vma* mutants similarly causes glycosylation defects (164).

c. Mutations of *TMEM165* cause glycosylation disorders

In 2012, some mutations in the *TMEM165* human gene were identified as causing glycosylation disorders to five patients with CDG phenotype (1). *TMEM165* belongs to the Uncharacterized Protein Family 0016 (UPF0016). UPF0016 members are found in all kingdoms of life and have been relatively well conserved during evolution, because most organisms, from yeast to human, but also plants and many bacteria and archaea, possess at least one gene belonging to UPF0016 (2). This conservation points out that the biological functions of UPF0016 are greatly beneficial to their host organisms, regardless the biological and ecological context in which they live. Recently, the UPF0016 family was renamed *GDT1 family* in protein databases in reference to the yeast UPF0016 ortholog, GDT1, which is the most characterized to date and the model member for the whole family.

TMEM165-CDG patients display N-glycans hypo-sialylation and hypo-galactosylation (1). In a sixth patient identified in 2015, it was also pointed out that the glycosylation defects are not constant during life, but rather varies during at least several weeks after birth (165). A deep analysis performed by mass spectrometry underlined that N-glycosylation galactosylation is strongly affected, N-acetylglucosaminylation is moderately impaired and sialylation is relatively slightly contrived in TMEM165 depleted HeLa and HEK cells (166), while O-glycosylation displays undersialylation when looking at the serum of one *TMEM165-CDG* patient (167). In addition, the reduction of *TMEM165* expression in zebrafish embryos also leads to N-glycosylation deficiencies, indicating a conserved role for *TMEM165* members in animals (168). Eventually, oral galactose supplementation was tested as a treatment and it led to the partial restauration of N-glycosylation defects for some *TMEM165-CDG* patients (169).

In 2012, when *TMEM165* was linked to glycosylation functions, this protein was not at all characterized and the underlying biochemical explanation for the phenotype observed in *TMEM165-CDG* patients was not really understood. Therefore, extensive studies were conducted to try to uncover the physiological roles of TMEM165. In our lab, the yeast ortholog Gdt1p is commonly used as a model protein to gain insights into *GDT1* family functions.

CHAPTER 3

ON THE WAY TO UNCOVER THE PHYSIOLOGICAL ROLES OF GDT1P

1. TMEM165 and Gdt1p share common functions in Golgi Ca^{2+}, Mn^{2+}, and pH homeostasis

Not very surprisingly, when TMEM165 localization was assessed, it was discovered that the protein mostly stands at the Golgi membrane (170). In the yeast *Saccharomyces cerevisiae*, the place of residence of Gdt1p is also the Golgi, more specifically the *cis*- and *medial*-Golgi (90). In parallel to human glycosylation disorders related to *TMEM165* deficiency, *GDT1* deletion also leads to glycosylation defects in yeast, specifically when cells are grown with the addition of 50 to 500 mM Ca^{2+} in the extracellular medium (91). Furthermore, the deletion of *GDT1* results in hypersensitivity of the *pmr1Δ/gdt1Δ* strain to 400 mM extracellular Ca^{2+} and to the chelating agent EGTA (ethylene glycol tetraacetic acid), while *TMEM165* deficient cells display lysosomal pH dysregulation, which becomes most of the time more acidic (90). Recently, it was also shown that the Golgi pH is more acidic in cells depleted for TMEM165 (171). In yeast, the influence of *GDT1* on pH homeostasis was tested by performing phenotypical measurements of different strains combining *GDT1* and V-ATPase subunits deletions. It was observed that *GDT1* deletion partially counteracts *stv1Δ* BAPTA sensitivity (80), the BAPTA (1,2-bis(*o*-aminophenoxy)ethane-*N,N,N',N'*-tetra-aceticacid) being a Ca^{2+}-specific chelator. Interestingly, supplementation of the extracellular medium with extra Mn^{2+} restores N-glycosylation, both for *TMEM165* affected human cells and in the *gdt1Δ* yeast strain (91, 172).

In early studies about *TMEM165* and *GDT1*, the conservation of function among the *GDT1* family was assessed. Especially, *GDT1* and *TMEM165* share a strong sequence conservation (32% sequence identity, 52% sequence similarity), except for their N-terminus extension, which is 55 amino acids longer in the human protein, and could be dedicated to regulatory functions specific to human cells (2). However, the high conservation of the core part of the sequence suggests a possible conservation of function across evolution. Experimentally, the complementation of the growth defect of the *gdt1Δ* strain on high extracellular Ca^{2+} and high extracellular Mn^{2+} by *TMEM165* strengthens the idea that the functions of TMEM165 and Gdt1p have been conserved during evolution (Figure 8) (173, 174). Though, it has to be noted that the complementation goes better with TMEM165 protein variants devoid of the non-conserved N-terminal part of the sequence. Since this N-terminal extension possibly plays regulatory roles, its presence could inhibit TMEM165 protein activity or perturb TMEM165 folding when heterologously expressed in yeast. Altogether, the study of Gdt1p function will hopefully bring valuable information to understand TMEM165 implication in CDG.

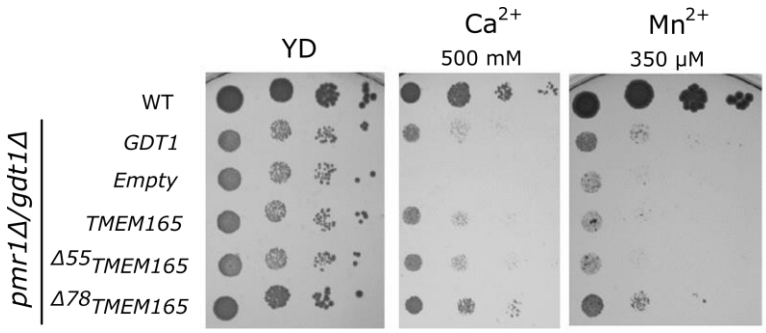

Figure 8. Human *TMEM165* and *S. cerevisiae GDT1* genes play similar functions for Ca^{2+} and Mn^{2+} detoxification.
The *pmr1Δ/gdt1Δ* strain is sensitive to medium supplementation with Ca^{2+} and Mn^{2+} cations. The expression of *GDT1* from plasmid improves growth compared to cells bearing an empty plasmid. Similarly, *TMEM165* expression also improves the growth. Strikingly, deletion of the N-terminal extension of *TMEM165* (Δ55 and Δ78) further improves resistance. Modified from (174).

2. TMEM165 and Gdt1p possess topological features of secondary transporters

In silico analysis predicted that TMEM165 and Gdt1p are membrane proteins composed of six transmembrane spans. They are evolutionary emanating from the duplication and the fusion of an original sequence coding for a smaller protein with only three predicted transmembrane spans. The two resulting transmembrane clusters have an opposite orientation in the membrane and are connected by a large loop enriched with acidic amino acids. Also, the protein contains a putative signal sequence at its N-terminus, presumably for its recognition by the Signal Recognition Particle complex and for its subsequent insertion in the ER membrane.

By looking more closely at the amino acid sequence, it appears that the *GDT1* family is characterized by a signature sequence – E-x-G-D-(KR)-(TS), where x represents any hydrophobic amino acid – that locates in the predicted 1st and 4th trans-membrane spans of the protein (Figure 9A) (2). The presence of such a sequence, enriched in charged and hydrophilic amino acids, suggests a function of the protein related to the transport of polar molecules across hydrophobic membranes. The antiparallel topology of the protein and the concomitant presence and the high conservation of two copies of such a characteristic motif in two distinct predicted transmembrane spans points out a transport mechanism that could involve an exchange of substrates, as observed for the Ca^{2+}/cation antiporter (CaCA) superfamily (175, 176). The aspartate and glutamate residues could be important for the neutralization of the positive charges of cations such as Ca^{2+} and Mn^{2+}, reducing the energy barrier that ions have to overcome to cross a hydrophobic membrane. Other hydrophilic residues in the vicinity of the predicted pore, such as Ser, Thr, Lys and Arg, would provide a hydrophilic microenvironment all along the cation's road.

Recently, a predicted tridimensional structure of Gdt1p was generated by the AlphaFold software, a tool using artificial intelligence to computationally draw protein structures from raw amino acid sequences (177). Although this prediction has to be considered with caution, it is interesting to note that Gdt1p predicted structure generated by this computational method is in accordance with the structural organization that was anticipated from previous analysis of the peculiarities of Gdt1p sequence (Figure 9B). In addition to previous features, this model predicts a bending in α helixes of TMs 1 and 4. This bending takes place around a glycine residue that belongs to the signature sequence. The side chain of glycine, which contains a single H, allows large latitude in the variation of the phi and psy dihedral angles and therefore large conformational changes during protein activity.

Such a bending in transmembrane domains is regularly observed in cation antiporters, such as the H^+/Ca^{2+} exchanger from *Archaeoglobus fulgidus* or the Na^+/Ca^{2+} exchanger from *Methanococcus jannaschii* (176, 178).

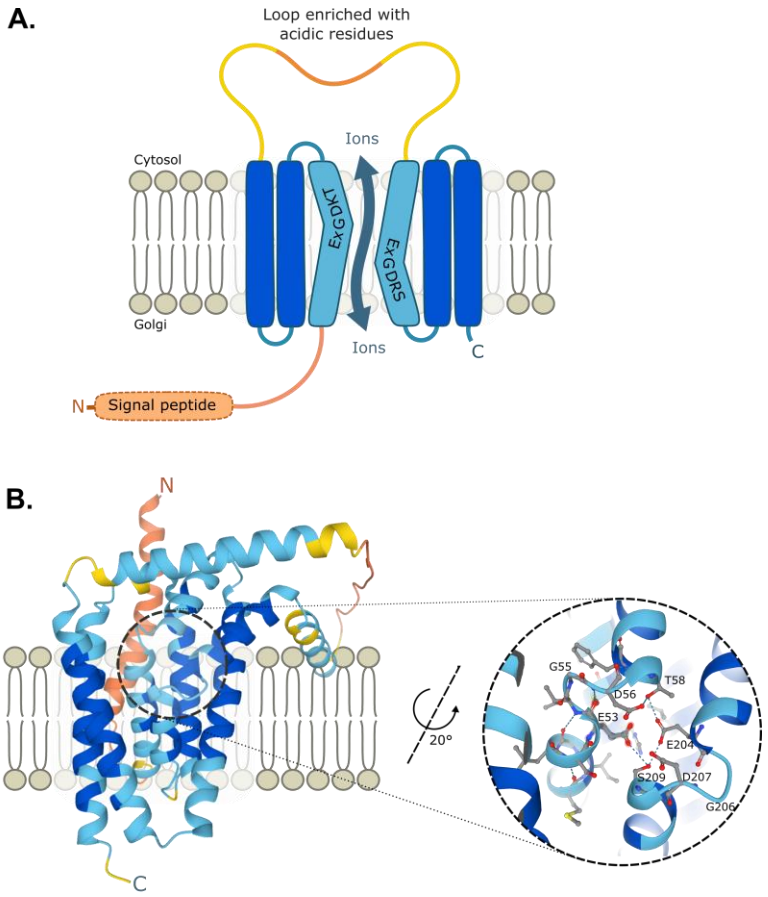

Figure 9. Predicted Gdt1p structure and putative hydrophilic pore.
Gdt1p probably possesses a 23 N-ter signal peptide and two sets of three transmembrane spans oriented with an opposite orientation in the membrane, that are connected by a large hydrophilic loop enriched with acidic amino acids. In TMDs 1 and 4, a conserved E-x-G-D-(KR)-(TS) motif putatively forms a hydrophilic pore for the transfer of hydrophilic molecules. **A.** Planar projection of the expected topology (173). **B.** Predicted tridimensional structure generated by the AlphaFold algorithm (Uniprot P38301) and zoom on the putative central pore of the proteins, with highlighted hydrophilic amino acids that could mediate cation transport (177). The color code of the tridimensional prediction represents the confidence of the prediction, with dark blue being very highly confident, light blue moderately confident, yellow lowly confident and orange very lowly confident. For ease of viewing, the planar projection is roughly represented with identical colors.

3. *GDT1* orthologs fulfil different functions related to Mn^{2+}, Ca^{2+} or pH regulation

Apart from the studies of human *TMEM165* and yeast *GDT1*, a growing number of research groups are working on the deciphering of *GDT1* family members functions in various organisms, as reviewed by Thines *et al.* (179).

In plant cells, several *GDT1* paralogs usually coexist. The CMT1/BICAT2 protein from *Arabidopsis thaliana* resides in the inner membrane of the chloroplast and was shown to be important for Mn^{2+} supply of the chloroplast (180, 181), while PAM71/CCHA1 is another *A. thaliana GDT1* family member, which is located in the thylakoid membrane, that is also crucial for the proper supplying of the thylakoids with Mn^{2+} (182, 183). There, Mn^{2+} is part of a Mn_4CaO_5 cluster in the oxygen-evolving complex of the Photosystem II that oxidizes water molecules into O_2, releasing H^+ and mediating electron transfer in the thylakoid membrane. In addition to its role in Mn^{2+} supply of the chloroplast, CMT1/BICAT2 role in lightness - darkness responsive Ca^{2+} signaling of the chloroplast has also been demonstrated (184). Plausible H^+ transport was also highlighted, because *PAM71/CCHA1* deletion in *A. thaliana* affects its cytosolic pH, makes the plant more sensitive to external pH variations and alters pH gradient across the thylakoid membrane (182, 183).

In bacteria and in cyanobacteria, MneA from *Vibrio cholerae* and SynPAM71 from *Synechocystis* prevent Mn^{2+} toxic accumulation in the cytosol (185-187). SynPAM71 also supports Mn^{2+} transport across thylakoid membrane to ensure photosystem activity in cyanobacteria (185, 186).

Finally, in several organisms, such as the protist parasite *Trypanosoma cruzi*, model mice, or plant, Golgi localized *GDT1* orthologs have been examined and their function for Mn^{2+} or Ca^{2+} homeostasis was systematically pointed out, either for glycosylation, or for lactation (188-192). Moreover, several *GDT1* orthologs were expressed in the *gdt1Δ* yeast strain and assessed for Ca^{2+} sensitivity: the full-length *Candida albicans* ortholog *CaGDT1*, the full-length *Zea mays* ssp *Mexicana* L *ZmmCCHA1*, as well as truncated versions of *A. thaliana* orthologs *PAM71* and *CMT1*. They all confer an increase resistance to high extracellular Ca^{2+} to the *gdt1Δ* strain, suggesting a conserved function for Ca^{2+} homeostasis (184, 193, 194).

4. Study of Gdt1p transport activity, physiological roles and regulation

a. Measurements of Ca^{2+} and Mn^{2+} transport across biological membranes

As Gdt1p is predicted to be a cation transporter, measurements were set up in our lab to confirm it via a direct transport assay. Gdt1p was efficiently expressed in *Lactococcus lactis* bacterial membrane and intracellular Ca^{2+} and Mn^{2+} measurements were performed by incorporating Fura-2 into the cells (Figure 10). Fura-2 is an aminopolycarboxilic acid that displays variable fluorescent properties when binding those cations. Thanks to this system, it was demonstrated that Gdt1p conveys Ca^{2+} and Mn^{2+} cations through biological membranes, but not Mg^{2+}, neither other common physiological cations such as Na^{+}, K^{+}, Cu^{2+}, or Ni^{2+} (91, 92). Furthermore, competition uptake assays revealed that Ca^{2+} import is reduced when Mn^{2+} is concomitantly added in the extracellular medium and vice versa. This extra measurement indicates that the transport of the two cations probably occurs in the same direction (92). Nevertheless, based on phenotypical assays in yeast and in human, it was sometimes suggested that Gdt1p and TMEM165 could import Mn^{2+} in the Golgi in exchange for Ca^{2+} cations (195, 196).

b. Effects of *GDT1* up- and downregulation on cellular Ca^{2+} and Mn^{2+} homeostasis

In order to understand the physiological roles of Gdt1p, many experiments were also conducted in its original host organism, *S. cerevisiae*. As already mentioned previously, the Golgi membrane possesses a relatively well characterized Ca^{2+}/Mn^{2+} P-type ATPase, Pmr1p. The role of this pump is to fill the Golgi lumen with those cations in order to sustain Golgi functions and to avoid toxic accumulation in the cytosol. In a *pmr1Δ* strain, cells undergo glycosylation defects, protein trafficking alterations and they become more sensitive to high extracellular Ca^{2+} (84). Strikingly, those phenotypes also characterize the *gdt1Δ* strain, and some effects are even additive in the double *pmr1Δ/gdt1Δ* strain (90, 173).

When looking at the global homeostasis of those cations, it was observed that the deletion of either *PMR1* or *GDT1* causes an accumulation of Ca^{2+} and Mn^{2+} into the cell (91, 92). The suspected reason is that, when cells cannot account on the secretory detoxification way, they boost their vacuolar detoxification functions, therefore increasing their total intracellular amount. The calmodulin-calcineurin system monitors the cytosolic Ca^{2+} concentration. When there is excessive cytosolic Ca^{2+}, the Crz1 transcription factor is activated and triggers the expression of a vacuolar Ca^{2+} transporter,

Pmc1p (197, 198). A similar regulation mechanism could maybe drive Mn^{2+} accumulation in the vacuole when *PMR1* and/or *GDT1* are defective (199).

The Ca^{2+} cation is a well-known secondary signal transducer that is involved in a series of intracellular signaling pathways (200). In yeast, transient Ca^{2+} increases occur after osmotic shocks, cold stress, alkaline stress, exposure to pheromones, or, for glucose-starved cells, in response to newly available fermentable carbon sources. In normal conditions, the cytosolic Ca^{2+} concentration is maintained at a very low level, between 50 and 200 nM (201). In organelles, the $[Ca^{2+}]$ is 10^2-10^3 times more concentrated (the free Ca^{2+} concentration is estimated at 10 µM in the ER, 10 to 300 µM in the Golgi lumen, and 30 µM in the vacuole (202-204)) (Figure 6). When cells aim to produce cytosolic $[Ca^{2+}]$ increase, they can allow Ca^{2+} to enter from the extracellular medium and/or from internal Ca^{2+} stores. On the contrary to animals where sarco-/endoplasmic reticulum is the usual Ca^{2+} storage place, the vacuole, being at the same time larger than other organelles and containing large amounts of bound Ca^{2+} (203), is the main Ca^{2+} stock for yeast cells. Therefore, in many cases, Ca^{2+} exits the vacuole through Yvc1p, a stretch-activable Ca^{2+} channel (205).

If Gdt1p is effectively loading the Golgi with Ca^{2+}, its deletion could affect the shape and the intensity of the transient cytosolic Ca^{2+} increases. Hence, $[Ca^{2+}]_{cytosol}$ was monitored by several research groups, including ours, following various stress applications. While *PMR1* or *SPF1/COD1* deletion generally increases the intensity of the Ca^{2+} pulses because of the elevated $[Ca^{2+}]_{vacuole}$, the concomitant deletion of *PMR1* and *GDT1* or *SPF1* and *GDT1* unexpectedly does not cause a synergistic effect on the cytosolic Ca^{2+} elevation after a saline stress or after a glucose pulse (87, 91). On the contrary, *GDT1* overexpression in the *pmr1Δ* strain increases the intensity of the Ca^{2+} pulse compared to the *pmr1Δ/gdt1Δ* strain (91, 206). Furthermore, in a similar way as the deletion of plasma membrane Ca^{2+} importers or as the deletion of vacuolar Ca^{2+} sequestrators, *GDT1* deletion even decreases the height of the Ca^{2+} pulse release in glucose-starved cells following a Ca^{2+} pulse, compared to the *WT* strain, (87). It suggests that, compared to Pmr1p and Spf1p, Gdt1p does not contributes much to Ca^{2+} storage in the secretory pathway. Nevertheless, in some specific conditions, it still appears that Gdt1p pump Ca^{2+} towards the Golgi lumen. It is especially the case when looking at Ca^{2+} dissipation of some TECC (Transient Elevation of Ca^{2+} Concentration, observed after the addition of fresh glucose to starved cells), when cells are grown in a medium at pH 5.0 (207).

Manganese displays roles in the redox control of cells. Among other mechanisms, it binds Sod2p, a superoxide dismutase located in the mitochondria, to protect cells against oxidative stress. Mn^{2+}-dependent

Sod2p activity can be monitored by an *in vitro* assay and is a direct indication of cytosolic Mn^{2+} loading. When *SMF2* is deleted, cytosolic Mn^{2+} decreases and Sod2p activity is reduced (88). On the contrary, *PMR1* deletion causes an increase of cytosolic Mn^{2+} and an activation of Sod2p activity (88). Similarly, *GDT1* deletion activates Sod2p activity (92). It suggests a concomitant action of Pmr1p and Gdt1p for Mn^{2+} cytosolic extrusion to the Golgi lumen.

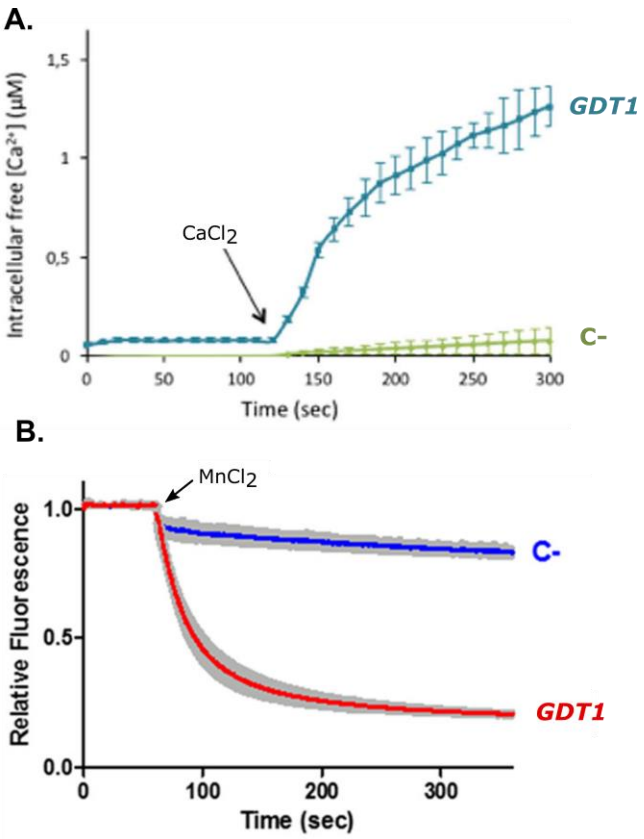

Figure 10. Gdt1p transports Ca^{2+} and Mn^{2+} cations across biological membranes. Gdt1p was expressed in *L. lactis* to test its ability to convey cations across a lipid bilayer. **A.** When compared to a negative control, *i.e.* cells that do not express Gdt1p, the intracellular [Ca^{2+}] increases faster in Gdt1p expressing cells after addition of $CaCl_2$ in the extracellular medium, suggesting that the influx of Ca^{2+} is facilitated by Gdt1p. **B.** The intracellular [Mn^{2+}] is estimated from the quenching by Mn^{2+} of an internalized fluorescent sensor, Fura-2. Similarly, Gdt1p expression increases Mn^{2+} influx into bacteria as compared to the negative control. Adapted from (91, 92).

c. At the Golgi, Gdt1p influences enzymatic activity and protein trafficking

The impact of *GDT1* deletion on Golgi functions should be looked into details to deeper understand Gdt1p roles. Post-translational modifications or trafficking could both be affected by pH, Ca^{2+} or Mn^{2+}, and those two Golgi biological functions are strongly interconnected. Hence, it could be difficult to discriminate and to elucidate what is the exact role of Gdt1p. Therefore, deep and cautious studies are required.

The carboxypeptidase Y (CPY) usually follows the vacuolar protein sorting pathway to reach the vacuole lumen. In classical YD growth medium, if *PMR1* is deleted, trafficking is affected and some CPY proteins are missorted, eventually ending up in the extracellular medium. Noteworthy, the additional deletion of *GDT1* dismisses CPY trafficking defects. On the contrary, *GDT1* overexpression increases trafficking defects. If the medium is supplemented with 400 mM Ca^{2+}, the trend is opposite, no more defect is observed in the *pmr1Δ* strain but trafficking defects come out in the *pmr1Δ/gdt1Δ* strain (Figure 11A) (173).

CPY is also N-glycosylated during its transit through the ER and the Golgi. Glycosylation defects characterize the *pmr1Δ* strain. Interestingly, growth medium supplementation with 500 mM Ca^{2+} corrects glycosylation in the *pmr1Δ* strain and induces glycosylation defects to *gdt1Δ* cells. The addition of 500 µM of Mn^{2+} restores glycosylation in every case. Regarding O-glycosylation, the case study of Gas1p – a N- and O-glycosylated surface protein – is interesting. The glycosylation defects are quite similar as the ones observed for CPY, except that manganese alone cannot restore all glycosylation defects, while the concomitant addition of 500 µM $MnCl_2$ and 500 mM $CaCl_2$ do so (Figure 11B) (91).

The availability of inactive or selective Gdt1p mutants for Ca^{2+} or Mn^{2+} transport would be extremely beneficial to gain more insights into Gdt1p physiological functions. Several mutagenesis performed in our research group highlighted that the conserved motifs are important for Gdt1p activity, either when assessed by phenotypical assay on Ca^{2+} supplemented media with *S. cerevisiae*, or when direct transport activity was performed in bacteria (206, 208). Strikingly, a totally inactive transporter has never been obtained, according to transport assays performed in *L. lactis* (208).

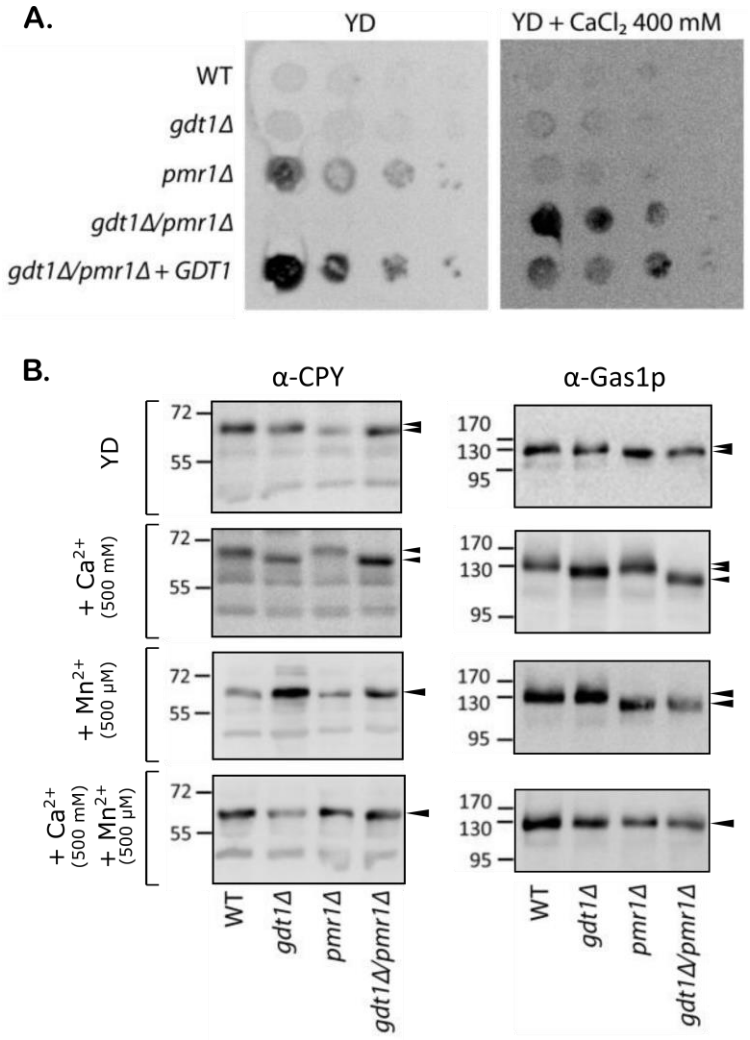

Figure 11. Gdt1p sustains Golgi functions in a Ca^{2+}-dependent manner.
A. CPY vacuolar protease is mistargeted to the extracellular medium when trafficking troubles occur, as detected by *western blotting* with α-CPY antibodies. The extracellular protein content was passively bound to nitrocellulose membranes by a 24-hours contact incubation with the cells growing on indicated media. While overexpression of *GDT1* in the *pmr1Δ* strain increases trafficking defects in YD medium, *GDT1* deletion in the *pmr1Δ* strain induces trafficking defects when cells are cultivated with 400 mM $CaCl_2$.
B. Glycosylation defects are detected thanks to migration shifts of the N-glycosylated CPY protein and of the N- and O-glycosylated Gas1p protein. In the *pmr1Δ* strain, glycosylation defects are corrected by the addition of Ca^{2+}. On the contrary, glycosylation defects appear in the *gdt1Δ* strain when grown with extra Ca^{2+}. Mn^{2+} supplementation is able to restore glycosylation in most cases, except for O-glycosylation of Gas1p that requires Mn^{2+} and Ca^{2+} complementation. Reference protein markers are indicated (kDa). Figure adapted from (173) and (91).

d. Gdt1p abundance is regulated, for which purpose?

Gdt1p and Pmr1p do highly colocalize in yeast cells (90) and they presumably have complementary function for Ca^{2+} and Mn^{2+} pumping towards the Golgi lumen (92, 173). In human cells, the spatial proximity of TMEM165 and SPCA1 – the functional homolog of Pmr1p – is also important, as stated by proximity ligation assay (209). Therefore, could the deletion of one of those genes induces an upregulation of the other one, and vice versa?

Strikingly, it was rather observed that the deletion of *PMR1* decreases Gdt1p cellular abundance (Figure 12A). Again, in human, SPCA1 knock-out is causing TMEM165 downregulation (209). Otherwise, *GDT1* deletion does not affect Pmr1p abundance (91). The biological relevance of Gdt1p decrease is not clear to date, but rather raises additional questions regarding the physiological functions of Gdt1p. Especially, it suggests that Gdt1p and Pmr1p could have opposite effects on the relative concentrations of Ca^{2+} and Mn^{2+} at both sides of the Golgi membrane. It should also be noted that a co-immunoprecipitation trial performed in our laboratory could not uncover Gdt1p - Pmr1p physical interaction.

Interestingly, it was observed that Gdt1p reduction of abundance no longer occurs when vacuolar degradation is defective, in the *pep4Δ* strain. Besides, Ca^{2+} supplementation partly restores Gdt1p abundance, with the calcineurin that could be involved in this process (Figure 12A) (133).

Curiously, it was also discovered that the addition of 1 to 5 mM of $MnCl_2$ in the extracellular medium, which constitutes a large excess relative to usual Mn^{2+} availability, induces a fast and pronounced degradation of Gdt1p (Figure 12B). Similarly, TMEM165 is also rapidly degraded to the lysosome after the addition of 500 µM $MnCl_2$ in the culture medium (Figure 12C). TMEM165 sensitivity to Mn^{2+} starts even from 25 µM Mn^{2+} when the exposure is performed for 36 hours (210). The lower threshold inducing protein degradation in human cells makes sense since pluricellular organisms maintain epithelial barriers and enjoy detoxification mechanisms at the organism level that avoid too important fluctuations of the extracellular fluid composition, while unicellular organisms have to face stresses at an individual level. Therefore, yeast cells can probably cope with higher extracellular Mn^{2+} thanks to additional detoxification mechanisms. Still, it is remarkable that the sensitivity to Mn^{2+} of Gdt1p and TMEM165 is observed in these two so divergent organisms. This points out that it is a crucial regulation mechanism for cells to cope with Golgi localized *GDT1* family members when facing unexpected Mn^{2+} supply.

This degradation phenomenon and its underlying mechanism is one of the biological questions I will address in my thesis. It will therefore be extensively discussed latter on in the manuscript.

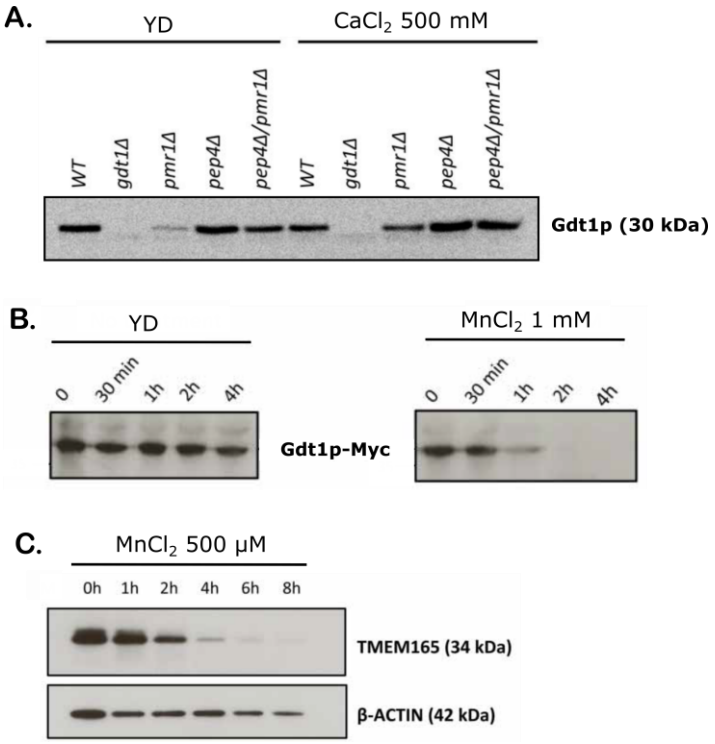

Figure 12. Gdt1p and TMEM165 abundances are regulated by Ca^{2+} and Mn^{2+}.
A. Gdt1p is less abundant in the *pmr1Δ* strain. This decrease of abundance is reverted in the *pmr1Δ/pep4Δ* strain, where vacuolar degradation is impaired. Moreover, Gdt1p decrease in abundance is also counterfeited by Ca^{2+} addition in the growth medium. **B.** Gdt1p is actively degraded after addition of Mn^{2+} in the extracellular medium. **C.** In human cells, TMEM165 is also sensitive to Mn^{2+} exposure. Figure adapted from (133) and (210).

PART II

AIM OF THE STUDY

Biological context

As stated in the introduction, Gdt1p – and its human ortholog TMEM165 – are Golgi localized transporters, possibly exchangers. To date, their exact role in cellular physiology is not clear yet and their influence on glycosylation is not precisely understood. While Ca^{2+} and Mn^{2+} Gdt1p-mediated transport activities have been demonstrated thanks to a heterologous expression tool, the transport determinants, *i.e.* driving force, direction of transport, activation and regulation, remain enigmatic. Though, several experiments suggested that Ca^{2+} and Mn^{2+} cations could be carried out from the cytosol to the Golgi lumen, against their concentration gradient. Besides, it was also highlighted that the pH homeostasis could be affected by GDT1 family members. Henceforth, the pH gradient could serve as the driving force to induce Ca^{2+} and Mn^{2+} transport.

In order to make a step forward in the understanding of the physiological functions and of the regulatory mechanisms of Gdt1p, it is crucial to acquire accurate *in vivo* data in its native host organism.

Objectives

My PhD thesis covers <u>two biological questions</u>:

a. Does Gdt1p convey H^+ ions during the transport of Ca^{2+} and Mn^{2+} cations through the Golgi membrane?

b. What is the pathway for Gdt1p degradation upon Mn^{2+} exposure?

I will try to unravel those questions thanks to <u>three working strategies</u>:

1st strategy

To develop probes for *in vivo* Ca^{2+}, Mn^{2+} and pH measurements in the Golgi lumen.

The main challenge resides in the adaptation of available methodologies to make them suitable to the expected concentrations of *S. cerevisiae* Golgi lumen. For Ca^{2+} and pH measurements, we will take advantage of sensors available for *in vivo* monitoring in other organisms and other yeast organelles. For Mn^{2+} quantification, we will develop strategies to evaluate its quantity within the Golgi.

2nd strategy

To perform pH measurements in order to assess the hypothesis that Gdt1p exchanges H^+ ions against Ca^{2+} and Mn^{2+} cations.

To do so, we will use *L. lactis* as a heterologous expression system for direct H^+ transport measurements, as already performed in our laboratory for Ca^{2+} and Mn^{2+} transport assays. In addition, by taking advantage of sensors dedicated to *in vivo* cytosol or Golgi monitoring in *S. cerevisiae*, either already available or developed in this research project, we aim at deciphering *in vivo* Gdt1p direction of transport.

3rd strategy

To enquire about the regulation of Gdt1p abundance.

Preliminary data and literature review indicate that both TMEM165 and Gdt1p could be regulated via a degradation mechanism induced by the addition of Mn^{2+} in the culture medium. However, the exact process involved in Gdt1p degradation is not unraveled and the physiological explanation for this downregulation is not clear yet. We will question them in this thesis by performing Gdt1p degradation assays in a selected set of strains involved in Ca^{2+} and Mn^{2+} homeostasis, or involved in trafficking and degradation pathways.

PART III

TOOLS AND STRATEGIES TO STUDY GDT1P PHYSIOLOGICAL FUNCTIONS

This third part of the manuscript gathers the most relevant results obtained during my thesis. It will be presented in three chapters, since distinct biological hypotheses are questioned in the frame of this research. Also, given that several students performed their master thesis under my co-supervision with Prof. Morsomme and that their subject were often directly connected to my research topics, some of the data they acquired will be integrated into this thesis. When this is the case, it will be explicitly stated.

The two first chapters, concerning the development of Golgi-localized probes for *in vivo* monitoring of several parameters such as pH or [Ca^{2+}], and questioning the putative exchange of H^+ against Ca^{2+} and Mn^{2+} mediated by Gdt1p, have been relatively well completed. Therefore, they have been or are currently in process of publication. In this manuscript, in addition to the published data, a set of additional trials and measurements are also displayed.

The third chapter, which addresses the regulation modes of Gdt1p, represents a more exploratory topic. Indeed, even though many of the known protein degradation routes are assessed in my thesis, it seems that Gdt1p is degraded in an unconventional way – or that we failed to identify a known way –. Therefore, our data lead us to develop other research methodologies for future uncovering of Gdt1p degradation route.

« The heart of science is measurement. »

Erik Brynjolfsson

CHAPTER 1

TARGETING OF PROBES FOR *IN VIVO* GOLGI [CA^{2+}] AND PH MONITORING IN *S. CEREVISIAE*

1. Preliminary trials with various Ca^{2+} sensors

Results presented in this subchapter were obtained by Guillaume Poncelet, a Master student who initiated this research project before I jumped into the lab, Sophie Sluysmans, who worked under my supervision, and myself.

a. Why are intraluminal Ca^{2+} measurements important for Gdt1p function elucidation?

For the purpose of gene function elucidation, the deletion of the gene from the genome, when not lethal, is often the first way to get relevant information, by looking for example at phenotypic traits. With *S. cerevisiae*, chromosome modifications are easy because *S. cerevisiae* commonly executes homologous recombination. Moreover, the possibility to grow haploid cells is an extra advantage for the generation of deletion strains.

Hence, the EUROFAN II systematic deletion project (211) generated a collection of about 5,000 *S. cerevisiae* deleted strains, from its 6,000 genes.

However, gene deletion often conducts to the activation of compensatory mechanisms. It is illustrated by *PMR1* deletion. When cells cannot account on this transporter to expel excessive cytosolic Ca^{2+} or Mn^{2+}, they stimulate their sequestration within the vacuole (81). Accordingly, cytosolic Ca^{2+} peaks, a stress response commonly resulting from vacuolar Ca^{2+} release, are higher in the *pmr1Δ* strain than in the *WT* strain. In cases where metabolic and regulatory modifications induced by a gene deletion are not sufficiently deciphered, data interpretation is sometimes misleading. When cytosolic [Ca^{2+}] was measured for the *gdt1Δ* strain thanks to the well-established bioluminescent aequorin probe, a series of assumptions were usually necessary to interpret the observed data (91, 207). Sometimes, a satisfying interpretation was not even obtained. Indeed, many cellular processes are implicated in the regulation of cytosolic Ca^{2+} and one does not know how *GDT1* deletion affects all of them.

Henceforth, we aim at measuring the luminal Golgi Ca^{2+} concentration, where data interpretation should be less influenced by the many mechanisms of cellular Ca^{2+} control than when looking at cytosolic [Ca^{2+}]. Since no valuable methodology was available for yeast Golgi Ca^{2+} monitoring at the beginning of this research project, we decided to take advantage of Ca^{2+} sensors used in other biological contexts (212) and to try to translate their use to *S. cerevisiae* Golgi.

b. Available probes for *in vivo* Ca^{2+} measurements

Hundreds of papers describe many various Ca^{2+} probes (213, 214). They have different properties in terms of affinity (K_d), brightness and quantic yield, reading mode (bioluminescence, fluorescence intensity, ratiometric fluorescent read-out), spectral characteristics, chemical properties (hydrophilic, hydrophobic), availability of modified forms (e.g. acetoxymethyl esterified forms for intracellular loading), resistance to photobleaching, etc. According to the application, one or another sensor can be more suitable for measurement (215). Generally speaking, two main strategies can be used for *in vivo* measurements. The first one consists of the use of chemical sensors that have to be loaded or internalized by the cell prior to measurement. The second one takes advantage of genetically encoded probes that are directly produced by the cell itself. Chemical probes are usually organic molecules able to bind Ca^{2+}, thereby modulating their spectral properties. They can either be injected into cells thanks to adapted

needles, or enter cells by crossing lipid bilayer thanks to their inherent hydrophobic properties, or even be internalized by endocytosis. The main drawback of those methodologies is that it is pretty difficult to get a well-defined compartmentalization. Since the Golgi in *S. cerevisiae* consists of small circular-shaped compartments spread across the cytosol, it would be very though to measure specifically and exclusively the luminal Golgi Ca^{2+} concentration by using those probes. Therefore, we will rather opt for genetically encoded Ca^{2+} probes (214), that can be directed more precisely to the Golgi lumen.

Ca^{2+} has the ability to be recognized by simple protein folds in a quite specific manner, with carboxyl and carbonyl groups that usually coordinates the Ca^{2+} cation (216). The most common and the best studied Ca^{2+}-binding domain in proteins is the EF-hand motif (200, 217). Upon binding to Ca^{2+}, changes in protein conformation are susceptible to modify enzymatic properties or spectral read-out.

i. Aequorin, the most widely used bioluminescent Ca^{2+}-sensor

This photoprotein of 22 kDa is naturally associated with the *Green Fluorescent Protein* (GFP) in the jellyfish *Aequorea victoria*, from which both have been isolated (218). Aequorin is able to oxidize coelenterazine into coelenteramide in an excited state. The excited coelenteramide then relaxes its energy by emitting a photon. This reaction requires oxygen as a substrate and needs binding of Ca^{2+} to the protein for the catalysis to occur (Figure 13A) (219, 220). Having no ortholog in most organisms, the aequorin usually does not interfere with any physiological function when heterologously expressed. Finally, bioluminescence is a peculiar capability and, therefore, there is usually no interference with endogenous emitted signal, on the contrary to fluorescence emission. Up to now, the aequorin has been cited in almost two thousand scientific papers and it is obviously an attractive option for intracellular Ca^{2+} measurements (221).

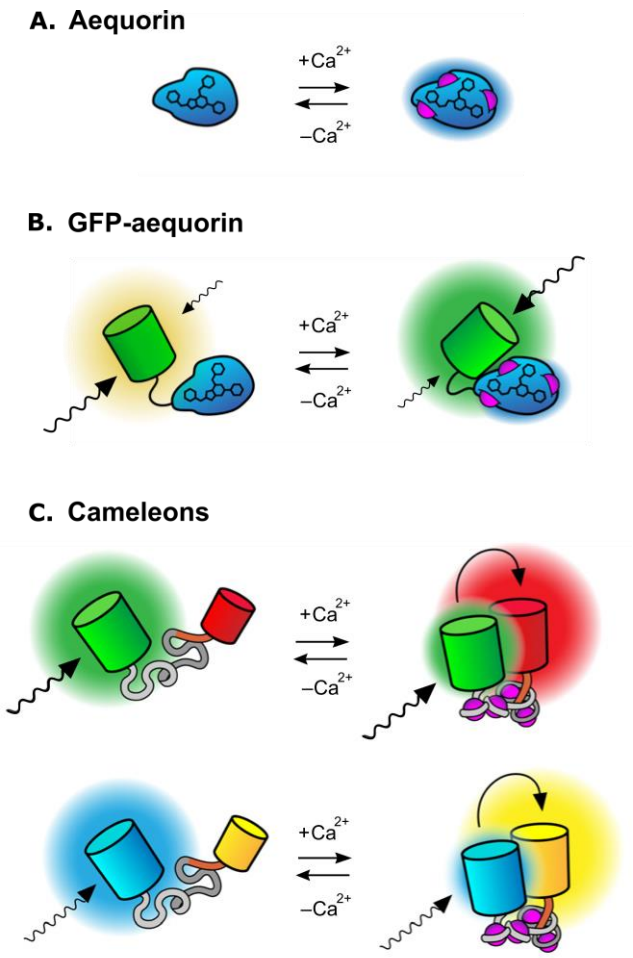

Figure 13. Selected genetically-encoded Ca2+ sensors for yeast Golgi monitoring. **A.** Chemiluminescent protein aequorin. This photoprotein does not require incident light excitation, but rather consumes a substrate, the coelenterazine compound, to produce photons. The light emission is dependent on Ca^{2+} binding by the protein. For quantitative measurements, a final discharge of the luminescence is performed by saturating all aequorin proteins with Ca^{2+}. **B.** GFP-Aequorin protein (GAP) is a fluorescent sensor that takes advantage of the Ca^{2+}-binding properties of the aequorin moiety and of the fluorescent properties of the GFP. Usable in a ratiometric manner, the binding of Ca^{2+} to the aequorin moiety changes protein conformation and the sensibility of the two excitation peaks of the GFP, at 403 and 470 nm (wavy lines). The emission is systematically recorded at the same wavelength of 510 nm. **C.** Cameleons are *Förster Resonance Energy Transfer* (FRET)-based Ca^{2+} indicators. Upon binding of Ca^{2+} by the M13 calmodulin-binding peptide, the two fluorophores get closer, allowing FRET to occur. Colors denote the availability of sensors with various spectral properties. Figure adapted from (214).

ii. Calmodulin-based fluorescent Ca^{2+}-sensors

The calmodulin (CaM) is by far the most abundant and the best characterized protein implying EF-hands. This cytosolic protein is highly conserved and almost universally used for Ca^{2+} signaling. In terms of structure, two EF-hand pairs are separated by a flexible helical linker (217). Upon binding to Ca^{2+}, the conformation of the linker region is modified. Consequently, hydrophobic surfaces at both extremities of the protein will be exposed to the environment and became available for interactions with other proteins (217, 222).

Researchers have taken advantage of this Ca^{2+}-related conformational change to design various fluorescent Ca^{2+} probes. For example, Cameleon probes commonly consist of chimeric proteins composed of *Blue Fluorescent Protein* (BFP) - CaM - M13 peptide - GFP (223), where M13 is a CaM-binding peptide that derives from skeletal muscle myosin light chain kinase (224). When CaM binds four Ca^{2+} ions, its conformation changes. In consequence, M13 peptide and CaM will curl around each other, bringing closer the two GFP variants (225). This rapprochement of the two fluorescent proteins generates *Förster Resonance Energy Transfer* (FRET) that serves as the read-out for Ca^{2+} measurement (Figure 13C).

iii. GAP, a GFP-Aequorin fusion for Ca^{2+}-measurement

As stated previously, the aequorin is a well-known bioluminescent Ca^{2+}-binding protein. To perform imaging, fluorescent sensors are more appropriate because they emit a bulk of photons during the course of one experiment. Quite recently, a research group combined the Ca^{2+} binding properties of aequorin with the fluorescent property of the GFP, by designing a Ca^{2+} probe denominated as *GFP-Aequorin Protein* (GAP) (226). The C-terminus of a specific GFP variant (Q80R, F99S, M153T, V163A) is fused via a 16 amino acids linker to the N-extremity of the apoaequorin. It generates a ratiometric fluorescent Ca^{2+} sensor with a high dynamic range. Depending on $[Ca^{2+}]$, the two excitation peaks of 403 and 470 nm are distinctively active, while the emission occurs at a single wavelength of 510 nm (Figure 13B). It does not necessitate reconstitution with the coelenterazine cofactor, and is temperature-, Mg^{2+}- and pH-insensitive (in the range of pH 6.2 to 8.2).

c. Fusion with the transmembrane domain of type II membrane proteins is a good way to target proteins to the Golgi lumen

i. Localization to the Golgi can be obtained

Proteins are precisely localized within one or another organelle thanks to various targeting signals and retention mechanisms. We took advantage from the efficient retention mechanisms of Golgi-localized proteins to address sensors to the *cis*- and *medial*-Golgi apparatus, where Gdt1p does localize. To this end, we fused different aequorin variants or GAP1 – a low affinity variant of the GAP sensor, with K_d = 12 µM (226) – to the N-terminal part of Mnn2p, an alpha-1,2-mannosyltransferase located in the early Golgi (227). The N-terminal region we used consists of the 36 first amino acids of Mnn2p and contains the cytosolic extension of the protein, its sole transmembrane span (TMD, *transmembrane domain*) and a few luminal amino acids, and are an efficient and sufficient retention signal to target proteins to the Golgi (228). A Gly_3-HA-Gly_3 linker was inserted to connect the two parts of the chimeric protein and serves as a spacer to avoid noxious interactions of the probe with the phospholipidic membrane (Figure 14).

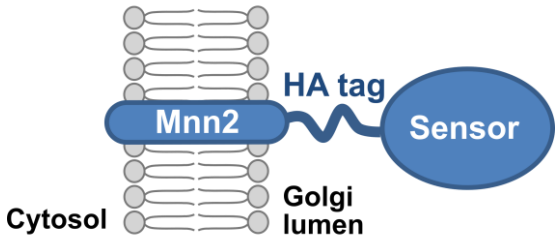

Figure 14. Targeting strategy for new Golgi-localized probes in *S. cerevisiae*.
In order to send probes within the Golgi lumen, chimeric proteins were constituted of the 36 first amino acids of Mnn2p, a type-II transmembrane Golgi-resident mannosyltransferase, connected to the sensor sequence via a Gly_3–hemagglutinin(HA)–Gly_3 linker.

By using this targeting strategy, the chimeric proteins seem correctly targeted to the secretory pathway. Nevertheless, the use of a strong expression system, with constructs under the control of the pTPI promoter on the centromeric pRS315 plasmid, generally leads to mislocalization of the probe. We commonly observed some signal that does not correspond to the commonly described Golgi shape in *S. cerevisiae*, and that could indicate some protein retention in the ER (Figure 15A) or some mistargeting to vacuoles. In order to avoid this, we tested presumably weaker promoters, pSNA2 and pGDT1. When expressed under the promoter of *GDT1* – pGDT1 – we finally obtained a quite well-defined localization of our probes, in small circular compartments looking like Golgi compartments. When assessed by immunofluorescence microscopy, the Mnn2-HA-Aequorin chimeric protein almost completely colocalizes with the Golgi localized Gdt1p (Figure 15B). When looking at protein segregation by subcellular fractionation on sucrose gradient, there is some overlay of Mnn2-HA-Aequorin with Gdt1p (Figure 15C). Similarly, Mnn2-HA-GAP1 also co-fractionates partly with Gdt1p (Figure 15D). Even tough, there is a noticeable shift of the Ca^{2+} probes towards more dense fractions of the gradient, that could correspond to ER or intermediate compartments in between ER and Golgi, as indicated by the profile of the ER marker Ost1p. CPY was used as a vacuolar marker in this experiment.

ii. When fused with Mnn2p transmembrane span, probe topology is adequate and uniform

Next to subcellular localization, it is also of critical importance that the probe faces the Golgi lumen, and not the cytosol. Mnn2p possesses a single transmembrane domain and a large soluble region and exerts its catalytic activity in the lumen of the secretory pathway. It is suspected that the single TMD and the surrounding amino acids sequence drives protein retention at the Golgi membrane and dictates protein insertion within the membrane with a specific topology. Accordingly, the addition of a soluble protein after the predicted TMD of Mnn2p should lead to the same orientation for the chimeric proteins as for the native Mnn2p. However, the construction of chimera sometimes causes unexpected protein behaviors. Therefore, we decided to control protein topology by developing a protease resistance/degradation assay.

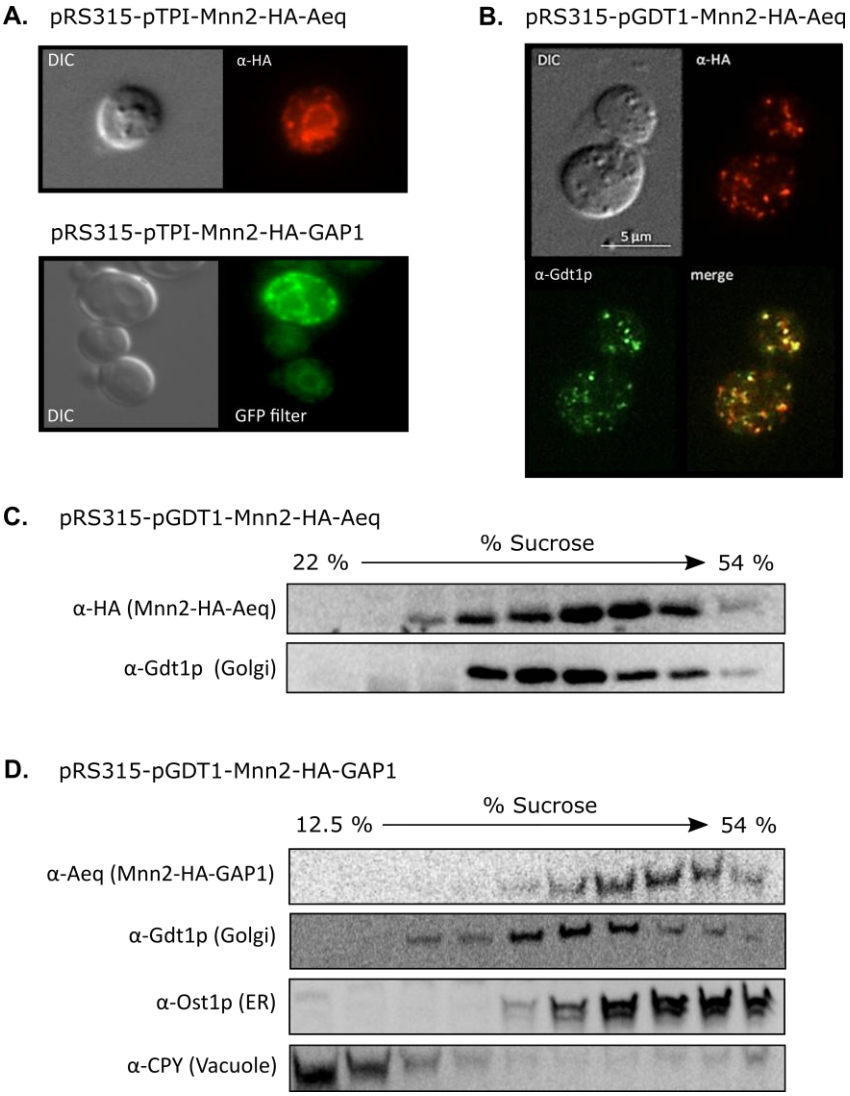

Figure 15. Use of the mild pGDT1 promoter, compared to the stronger pTPI promoter, improves targeting to the Golgi of Ca^{2+} probes fused to the N-terminal part of Mnn2p.

A. Localization of Golgi-targeted Ca^{2+} sensors when expressed under the control of the strong constitutive pTPI promoter. For immunofluorescence detection of Mnn2-HA-Aequorin, α-HA rat primary antibodies and Alexa Fluor 546-conjugated anti-rat IgG antibodies were used. For fluorescence microscopy imaging of Mnn2-HA-GAP1 (GFP-Aequorin Protein 1), a GFP filter was used. DIC is represented. **B.** Localization of the Golgi-targeted Mnn2-HA-Aequorin when expressed under the control of the weak pGDT1 promoter. Immunofluorescence detection of the chimeric protein thanks to α-HA rat primary antibodies and Alexa Fluor 546-conjugated anti-rat IgG antibodies were used. Anti-Gdt1p rabbit primary antibodies and Alexa Fluor 488-conjugated anti-rabbit IgG were used for Golgi outlining. DIC and merge are also presented. **C.** *and* **D.** Localization of

Mnn2-HA-Aequorin and Mnn2-HA-GAP1 expressed under the control of pGDT1 were also assessed by subcellular fractionation on sucrose gradient. The constructs were detected by α-HA or α-Aequorin antibodies, and α-Gdt1p, α-Ost1p and α-CPY were used as references for Golgi, ER and vacuole detection, respectively. Subcellular fractionation was performed on a discontinuous sucrose gradient, ranging from 12.5 to 54 %. Experiments with the aequorin were performed by Guillaume Poncelet and experiments with GAP1 were performed by Sophie Sluysmans.

Golgi vesicles were collected after the procedure of subcellular fractionation on sucrose gradient, as stated in the previous part. Then, Golgi vesicles were incubated with trypsin, a serine protease that cuts proteins and peptides mainly at the carboxyl side of arginine and lysine residues. If the globular soluble part of the sensor locates in the Golgi lumen, it should be protected from proteolytic degradation, while cytosolic facing proteins should be digested. As controls, samples not submitted to trypsin, incubated concomitantly with trypsin and a detergent – Triton X-100 – to solubilize Golgi membrane, or with the supplemental addition of a trypsin inhibitor, were also analyzed. Remarkably, the aequorin is protected from degradation when incubated with trypsin, as the intensity of the signal detected by *western blotting* is close to the one of the two positives controls, and that protein degradation is almost complete in the negative control where detergent is added (Figure 16). Note that I also used the same procedure to assess Gdt1p topology. Thanks to this assay, we were able to confirm the assumption that the largest soluble loop of Gdt1p, positioned in between TMDs 3 and 4, is facing the cytosol (Figure 9 *and* Figure 18D) (2).

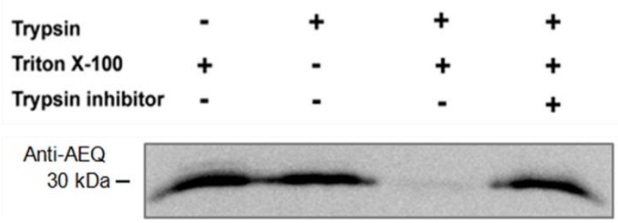

Figure 16. Golgi-localized aequorin fused to the transmembrane span of Mnn2p is oriented towards the Golgi lumen.
WT cells transformed with pRS315-pGDT1-MNN2(1-36)-Gly_3-HA-Gly_3-AEQ-tCYC1 were collected and subcellular fractionation was performed. Golgi-enriched fractions were then submitted to trypsin digestion (0.01 mg/ml trypsin, 30 min at 25°C), with or without detergent addition (1% Triton X-100, final concentration). In the absence of detergent (Lane 2), the large soluble sensor part of the chimeric proteins is protected against digestion, as deciphered by *western blotting* analysis with α-AEQ antibodies. As controls, a sample was loaded without trypsin treatment (Lane 1), a sample was simultaneously confronted to Triton X-100 and trypsin in order to solubilize the Golgi membranes and to render all proteins accessible for digestion (Lane 3) and a last sample was simultaneously submitted to trypsin, Triton X-100 and several trypsin inhibitors (Lane 4).

Such an assay was also further developed latter on in this research project, to assess the topology of other Golgi-targeted probes. It confirmed that the use of the first 36 amino acids of Mnn2p is a suitable targeting sequence to localize probes in the Golgi lumen (Figure 18D).

d. In our hands, monitoring of the Golgi Ca^{2+} concentration could not be achieved

Despite strong efforts to obtain an operable Ca^{2+} sensor for Golgi measurements, we were never able to achieve this objective… There are major difficulties in such a probe design. At first, the Golgi Ca^{2+} concentration in *S. cerevisiae* is not known. From measurements in other organisms and in other organelles of yeast, we can estimate that it is situated in the micromolar range, probably in between 10 µM, that is the $[Ca^{2+}]_{ER}$ measured in *S. cerevisiae* (202), and 300 µM, the estimated upper level of $[Ca^{2+}]_{Golgi}$ in mammalian cells (204, 229). As Ca^{2+} sensors usually display a 1-2 order of magnitude dynamic range, we tested probes with various K_D, GAP1 – 12 µM (226), aequorin(D119A) – 260 µM (230), aequorin(N28L;D119A) – ~ 2 mM (231). Secondly, other physicochemical parameters could affect probe efficacy, such as pH, redox status, ionic strength, availability of chaperones for protein folding, concentration of other divalent cations, etc. The influence of those parameters on probe effectiveness *in vivo* is hard to evaluate. Finally, sensitivity is also a critical bottleneck. Indeed, when expressed at too high level, we commonly observed probes mislocalization, either some retention in the ER, or mistargeting to the vacuole. As a solution, we decreased the strength of protein expression. While it solved protein localization troubles, the cost is a lower signal over noise ratio and therefore difficulties to detect the specific fluorescent/luminescent signal exploitable for Ca^{2+} measurement.

Altogether, the generation of a suitable Ca^{2+} probe for *S. cerevisiae* Golgi measurements was not successful. Further effort should be performed to reach this objective.

2. A new pH sensor for the Golgi of *S. cerevisiae*

Data presented hereunder have been published. For consistency with other elements exhibited in this thesis, the introduction and discussion parts have been slightly adapted compared to the publication.

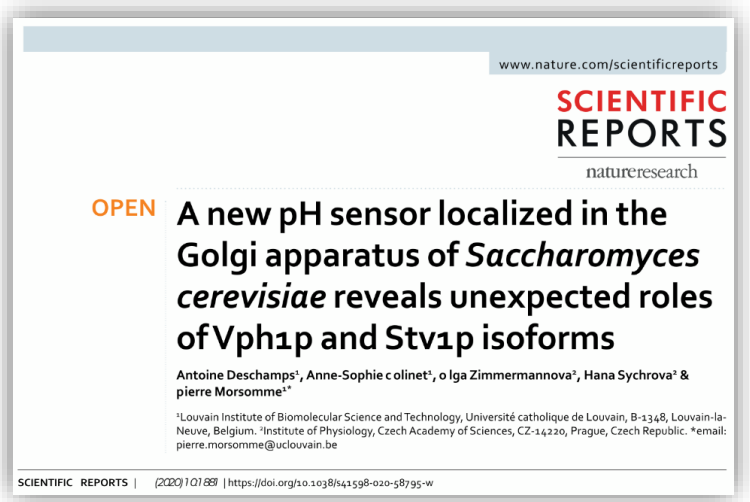

www.nature.com/scientificreports

SCIENTIFIC REPORTS

nature research

OPEN

A new pH sensor localized in the Golgi apparatus of *Saccharomyces cerevisiae* reveals unexpected roles of Vph1p and Stv1p isoforms

Antoine Deschamps[1], Anne-Sophie colinet[1], olga Zimmermannova[2], Hana Sychrova[2] & pierre Morsomme[1*]

[1]Louvain Institute of Biomolecular Science and Technology, Université catholique de Louvain, B-1348, Louvain-la-Neuve, Belgium. [2]Institute of Physiology, Czech Academy of Sciences, CZ-14220, Prague, Czech Republic. *email: pierre.morsomme@uclouvain.be

SCIENTIFIC REPORTS | (2020)10:1881 | https://doi.org/10.1038/s41598-020-58795-w

a. Why and how to measure pH in the organelles of the secretory pathway?

The pH gradient across biological membranes serves as the driving force for many secondary transporters. While at the plasma membranes the nature of this electrochemical gradient differs between the different kingdoms of life, the pH gradient is the main electrochemical gradient used in organelles of all eukaryotes by secondary transporters. Given the importance of pH homeostasis within the cell and particularly in the secretory pathway (reviewed in Casey *et al.* (232)), it is essential to possess appropriate tools to accurately measure this parameter *in vivo*. For the yeast *S. cerevisiae*, one probe is already available to measure the pH of the *trans*-Golgi network/endosomes lumen (39, 70) and the chemical probe BCECF is commonly used to measure the vacuolar pH (233). Recently, another sensor has been developed for pH measurements within the ER (38). However, there is no suitable sensor to precisely measure the early Golgi pH. Based on the pHluorin protein, a ratiometric pH probe derived from the GFP (234), we will take advantage of the targeting strategy we assessed with Ca^{2+} probes to develop a new Golgi-localized pH sensor in yeast.

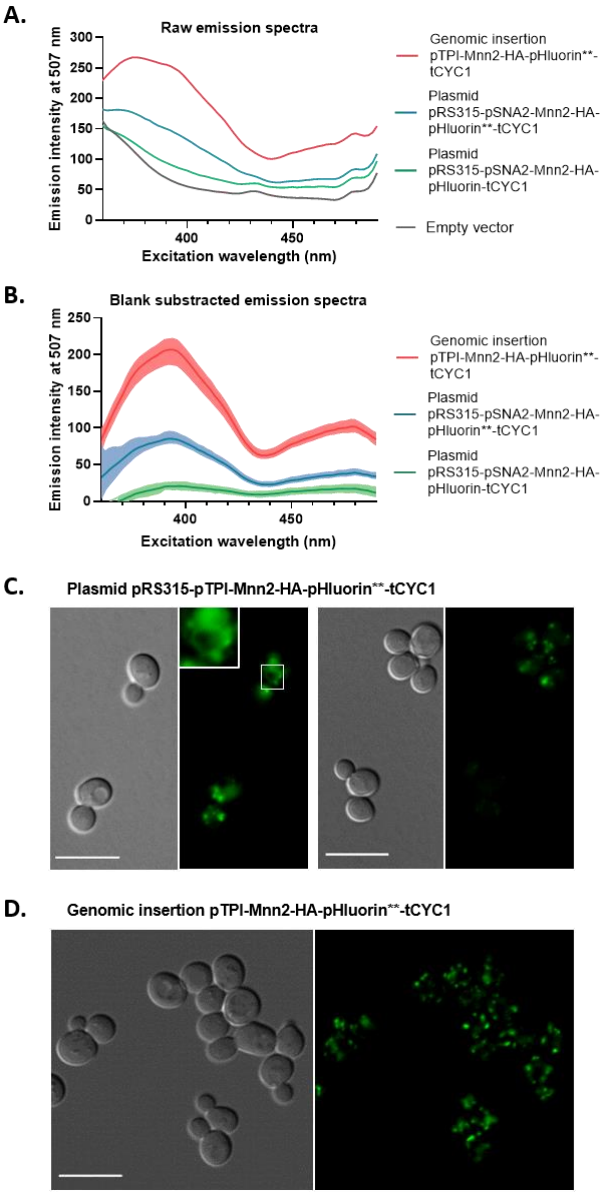

Figure 17. A pHluorin-based pH sensor targeted to the Golgi apparatus was designed and step by step optimized.

A. Adaptations to enhance the fluorescence intensity of the Golgi pH probe, as measured with a cell suspension adjusted to an identical optical density (OD_{600}) after two washings with fresh low fluorescent synthetic medium. All measurements were done with the BY4742 wild type background strain, transformed either with an empty plasmid (Empty vector, gray curve), with a plasmid containing the original pHluorin under the control of the weak pSNA2 promoter (pRS315-pSNA2-Mnn2-HA-pHluorin-tCYC1, green curve), with the same vector containing the pHluorin with two punctual mutations – F64L and M153R – (pRS315-pSNA2-Mnn2-HA-pHluorin**-tCYC1, blue curve), or with the genomic

insertion of the double mutated pHluorin under the control of the strong constitutive pTPI promoter (Genomic insertion pTPI-Mnn2-HA-pHluorin**-tCYC1, red curve). **B.** Blank subtracted spectra reveal the specific fluorescence of the probe. The fluorescent background of wild type cells transformed with an empty plasmid was subtracted to raw fluorescent spectra represented in part (A). *N* = 3. Means and ranges are represented. **C.** *and* **D.** Genomic integration improves homogeneity of the expression level of the protein of interest, compared to classical plasmid expression system. Fluorescence microscopy images of cells expressing Mnn2-HA-pHluorin** on a plasmid or inserted within the genome, both under the control of the pTPI promoter. Left: DIC; right: GFP filter. Scale bars = 10 μm.

b. Targeting of an improved pHluorin-based probe to the Golgi apparatus of *S. cerevisiae*

The first 36 amino acids of Mnn2p (228) have been linked to the N-terminus of the pHluorin via a HA tag which serves as a spacer to avoid noxious interactions of the pH probe with the phospholipidic membrane (Figure 14). Considering that the Golgi apparatus represents only a small fraction of the total cellular volume, the expression level of Golgi-localized proteins has to be maintained at a relatively low level to avoid mistargeting. Therefore, we expressed the construct on a pRS315 plasmid under the control of pSNA2, the mild constitutive promoter of the SNA2 gene (235). Unfortunately, the resulting fluorescence of our probe was very close to the fluorescence background (Figure 17A). Interestingly, several groups have identified punctual mutations that increase the brightness of the pHluorin with regards to the original version (236, 237). We inserted two of these mutations, F64L and M153R, respectively, to generate the Mnn2-HA-pHluorin** chimeric protein. This strategy enhanced the specific fluorescent signal of about three-fold (Figure 17A *and* B). Moreover, using a protease degradation assay, we observed that the mutated form of the pHluorin is much more resistant to protease degradation than the original version (*data not shown*), indicating that the stability of the protein could be increased thanks to these two mutations. According to Reifenrath *et al.* (38) who recently developed a pHluorin variant to measure the pH within the ER of *S. cerevisiae*, these mutations could facilitate the folding of the protein in the oxidative environment of the ER lumen.

By fluorescence microscopy, we could detect the probe in punctuated dots in many cells, which is the typical Golgi shape in *S. cerevisiae*. However, in some cells, the signal also exhibited the classical ER-like pattern, with a ring around the nucleus or alongside the cell periphery, or had the shape of vacuoles (Figure 17C). Given the heterogeneity of the signal, we inserted the construct within the *his3* locus of the genome, as it is known that genomic integration often homogenizes the expression level of a protein of interest from cell to

cell (238). This strategy highly improved the homogeneity of the localization (Figure 17D) and therefore the robustness of the next measurements, but the fluorescent level was still weak. Our last improvement consisted of changing the promoter to enhance the fluorescent signal. We replaced the pSNA2 promoter by a stronger constitutive promoter, namely pTPI. Compared to the plasmid expression system with pSNA2 promoter, these two last modifications increased the total fluorescent signal by a 2.5-fold, facilitating future pH determination (Figure 17A *and* B). For all the subsequent experiments in this study, we used the genome integrated pTPI-Mnn2-HA-pHluorin** strains. In addition, when doing fluorescence measurements, we always subtracted the fluorescence background, which stands for 20 to 30% of the total fluorescent signal, as measured with cells transformed with empty plasmid (Figure 17A).

c. The pH sensor localizes in the lumen of the *cis*- and *medial*-Golgi.

To further confirm that the probe is correctly localized at the Golgi apparatus, we carried out subcellular fractionations on sucrose gradient and performed co-localization fluorescence microscopy with Golgi and endosomal markers. The fractionation pattern of the Mnn2-HA-pHluorin** protein expressed from the genome under pTPI promoter perfectly fits the fractionation of the Golgi Ca^{2+}-Mn^{2+} ATPase Pmr1p. As Gdt1p and Pmr1p highly colocalize when analyzed by subcellular fractionation as well as by immunofluorescence microscopy (173, 206), we can conclude that the Mnn2-HA-pHluorin** pH sensor localizes in the same Golgi cisternae as Gdt1p. In contrast, the analysis of vacuolar, endoplasmic reticulum and plasma membrane markers demonstrate a distinct distribution profile for these organelles (Figure 18A). Then, Sed5p, Gos1p and Sec7p were respectively used as markers of the *cis*-, *medial*- and *trans*-Golgi for fluorescence microscopy. Note that those markers partly overlap during the maturation of the Golgi compartments (4). Endosomes detection relies on the endocytic marker FM4-64. We observed that the Mnn2-HA-pHluorin** construct mainly co-localizes with *cis*- and *medial*-Golgi markers and that a small fraction of the probe presumably also localizes further in the secretory pathway, within the *trans*-Golgi and the endosomes (Figure 18B). Quantification of the co-localization was performed on fixed cells using an object-based methodology (Figure 18C). For endosomal detection with FM4-64, the quantifications performed on fixed cells and with living cells gave very similar results (13.2% of co-localization with fixed cells, 13.3% of co-localization with living cells). Therefore, only the imaging with fixed cells is represented in Figure 18B. Overall, the two localization experiments endorse that the chimeric Mnn2-HA-pHluorin** protein localizes to the Golgi apparatus.

As a second step, we verified that the sensor is correctly oriented towards the lumen of the organelle, taking advantage of a protease degradation assay. After subcellular fractionation on sucrose gradient, Golgi-enriched fractions were incubated with proteinase K during 1 hour at 30°C (Figure 18D, 2nd lane). In parallel, an equivalent sample was incubated concomitantly with proteinase K and Triton X-100 to permeabilize the Golgi phospholipidic membrane (Figure 18D, 3rd lane). After the digestion was stopped with a mixture of protease inhibitors, these samples were analyzed by *western blotting*, compared together, as well as to the input (Figure 18D, 1st lane) and to a control of inhibitors efficiency (Figure 18D, 4th lane). Furthermore, Gdt1p cytosolic loop is completely degraded due to proteinase K proteolytic activity (Figure 18D, 2nd lane). Indubitably, the pHluorin is protected from proteinase K digestion by the Golgi lipid bilayer. Thereby, the sensor properly faces the Golgi lumen.

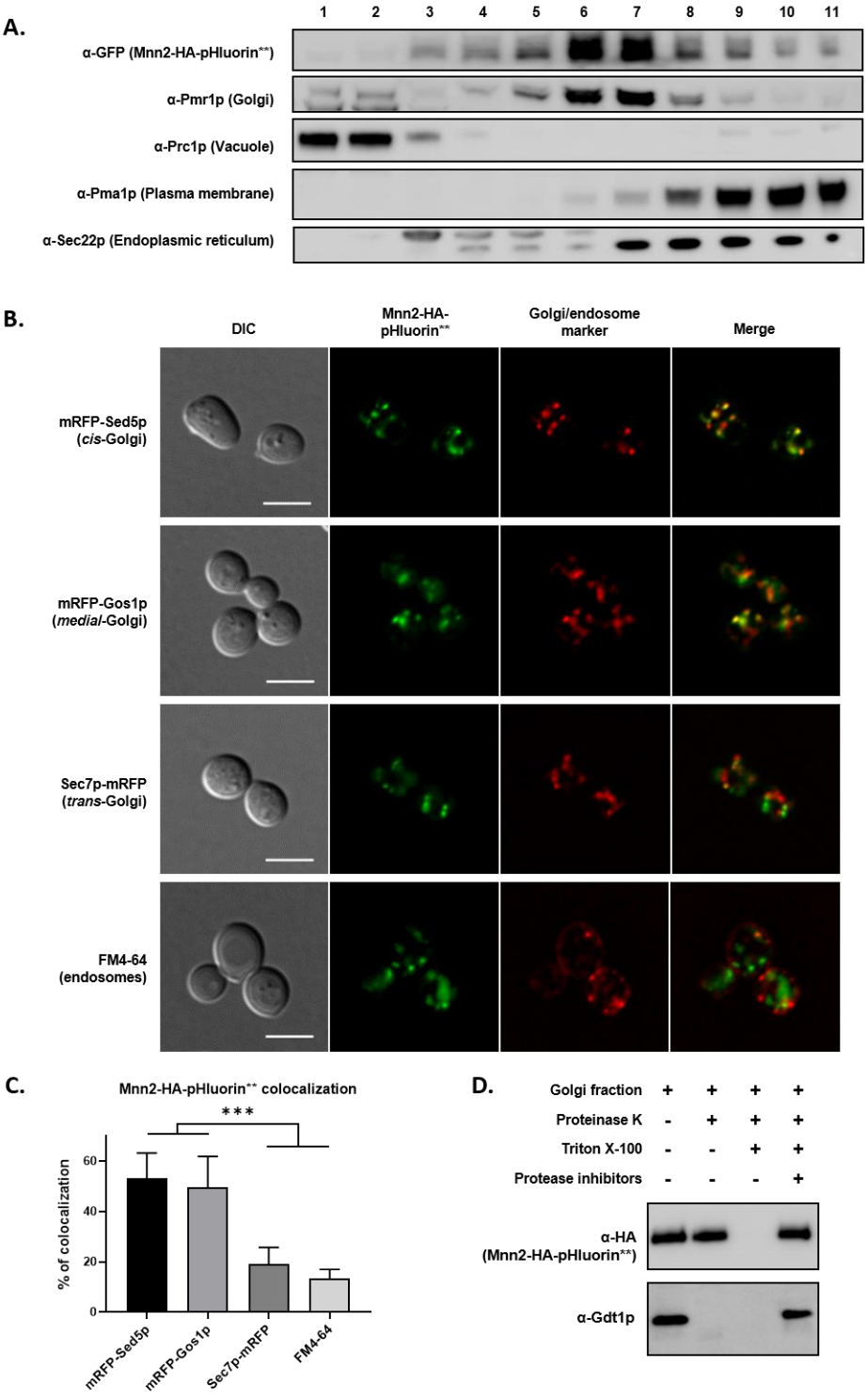
A.
1 2 3 4 5 6 7 8 9 10 11
α-GFP (Mnn2-HA-pHluorin**)
α-Pmr1p (Golgi)
α-Prc1p (Vacuole)
α-Pma1p (Plasma membrane)
α-Sec22p (Endoplasmic reticulum)
B.
DIC
Mnn2-HA-pHluorin**
Golgi/endosome marker
Merge
mRFP-Sed5p (cis-Golgi)
mRFP-Gos1p (medial-Golgi)
Sec7p-mRFP (trans-Golgi)
FM4-64 (endosomes)
C.
Mnn2-HA-pHluorin** colocalization
***
% of colocalization
0
20
40
60
mRFP-Sed5p
mRFP-Gos1p
Sec7p-mRFP
FM4-64
D.
Golgi fraction + + + +
Proteinase K - + + +
Triton X-100 - - + +
Protease inhibitors - - - +
α-HA (Mnn2-HA-pHluorin**)
α-Gdt1p

Figure 18. The pH sensor is localized in the *cis*- and *medial*-Golgi of *S. cerevisiae*.
A. According to subcellular fractionation, the Mnn2-HA-pHuorin** pH probe expressed from the genome under the control of the pTPI promoter co-fractionates with Golgi marker. Cells expressing the genome integrated Mnn2-HA-pHluorin** construct were fractionated on a discontinuous 12.5 – 54% sucrose gradient. After ultracentrifugation, the fractions were collected and numbered from the top of the gradient and were analyzed by *western blotting* using antibodies against the sensor (α-GFP) or against Pmr1p (Golgi apparatus), Pma1p (Plasma membrane), Sec22p (Endoplasmic reticulum), or Prc1p (Vacuole). **B.** The Mnn2-HA-pHluorin** protein, expressed similarly than in panel A, co-localizes mainly with *cis*- and *medial*-Golgi markers. Different Golgi markers were assessed by fluorescence microscopy – mRFP-Sed5p (*cis*-Golgi), mRFP-Gos1p (*medial*-Golgi), Sec7p-mRFP (*trans*-Golgi) – and FM4-64 chemical dye was used for endosomes detection. Representative images of cells imaged by DIC, with GFP filter, with RFP filter, and merge of the two fluorescent channels. **C.** Co-localization performed in (B.) was quantified as the number of Mnn2-HA-pHluorin** positive structures that co-localizes with these markers compared to the total number of Mnn2-HA-pHluorin** positive structures, using an object-based approach (N = 12 pictures, 31-38 cells per condition, except for FM4-64 for which n = 8 pictures, 101 cells). Scale bars = 5 µm. Means and 95% confidence intervals are shown. **D.** A topology assay attests that the probe is facing the lumen of the Golgi apparatus. Golgi-enriched fractions obtained by subcellular fractionation on sucrose gradient were submitted to 1 µg/ml proteinase K during 1 hour at 30 °C. The first lane is the positive control corresponding to the input; the second lane is the topology test, wherein the Golgi vesicles are incubated with proteinase K; the third lane is a negative control, the Golgi vesicles being incubated simultaneously with proteinase K and 1% Triton X-100 to permeabilize the phospholipidic membranes; the fourth lane corresponds to the negative control to which PMSF and a mix of protease inhibitors have been added. Anti-HA primary antibodies were used to detect the Mnn2-HA-pHluorin** construct. As a control, anti-Gdt1p antibodies detect the cytosolic loop of Gdt1p, which is degraded due to proteolytic activity.

d. *In vivo* calibration and determination of the Golgi pH.

The original pHluorin responds to the surrounding pH in a range from 5.5 to 8.0 (234). Despite the fact that the addition of the two mutations (F64L and M153R) separately does not strongly alter the pH-sensitive properties of the probe (236, 237), the combined addition of the two mutations could potentially distort the functionality of the sensor. Therefore, we performed an *in vivo* calibration of the probe by resuspending the cells in various pH buffers after permeabilization of both the plasma membrane and the Golgi membrane with 0.16% digitonin. By doing so, the blank corrected fluorescent spectra of the Mnn2-HA-pHluorin** protein perfectly responds to the surrounding pH, with opposite effects on the excitation at 400 or 480 nm when the pH fluctuates (Figure 19A). By using the fluorescent ratio of emission at 507 nm after excitation at 400 and 480 nm and plotting it versus pH, the calibration is obtained (Figure 19B). The sensor is therefore suitable for *in vivo* determination of the pH within the Golgi lumen.

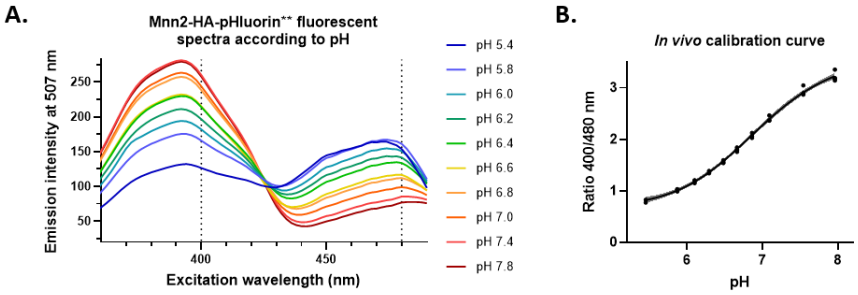

Figure 19. *In vivo* calibration of the Golgi-localized pH sensor.
A. *In vivo* calibration of the probe was performed. Cells expressing the sensor were permeabilized with 0.16% digitonin, followed by an incubation in citric acid – sodium hydrogen phosphate buffers at different pH, and their excitation spectra were measured with emission at 507 nm. The different excitation spectra of cells in pH buffers ranging from pH 5.4 to 7.8 are represented. **B.** Calibration curve of the pH versus 400/480 nm excitation ratio. A four-parameter logistical curve (sigmoidal curve) has been drawn through the experimental measurements. *N* = 3-4. Calibration curve is represented with 99% confidence interval.

Cytosolic and Golgi pH measurements were performed in parallel using a cytosolic pHluorin (239) and our newly developed Golgi-localized probe. As expected, the Golgi pH of cells in exponential phase is more acidic than the cytosolic pH, with a pH value of 6.65 ± 0.05 for the Golgi lumen, while the cytosolic pH is 7.27 ± 0.05 (Figure 20A *and* B). This is consistent with the expected Golgi pH value (232, 240) and with some measurements performed in other organisms, such as tobacco and *A. thaliana* plants (241, 242) and

mammalian cells (243, 244). This value for the Golgi pH is consistent with the gradual acidification of the secretory pathway. Indeed, endoplasmic reticulum pH and vacuolar pH of *S. cerevisiae* cells fed with glucose in exponential phase are equal to 7.1 and ≤ 6.0, respectively (38, 41, 116).

e. The V-ATPase is the main H^+-transporter of the early Golgi and Vph1p isoform has predominant activity compared to Stv1p isoform.

We measured the pH of the early Golgi in several strains deleted for different subunits of the V-ATPase. In the *vma13Δ* strain, Vma13p being the subunit H of the V-ATPase (245, 246), the Golgi lumen becomes near neutral (Figure 20A). Indeed, the V-ATPase has completely lost its activity in this strain. This result supports that the V-ATPase is the main proton pump in charge of the acidification of the secretory pathway. It also ensures that the pH sensor is functional and correctly oriented towards the Golgi lumen. Simultaneously, the cytosolic pH exhibits the opposite trend, being more acidic in the absence of a functional V-ATPase – as measured in the *vma13Δ* strain – than in the wild type strain (Figure 20B) (41).

In yeast, all the subunits of the V-ATPase have only one isoform, except for the subunit *a* of the V_0 domain, which exists as two isoforms. Vph1p mainly localizes in the vacuole, while Stv1p is found in V-ATPase complexes of the Golgi apparatus and of endosomes (60-62, 117). Using the new Golgi pH probe, we show that deletion of *STV1* only slightly increases the Golgi pH (Figure 20A). This corroborates phenotypic assays, protein sorting and glycosylation analysis performed previously (61, 164, 247). One explanation would be that the second isoform, Vph1p, that is several folds more expressed than Stv1p (61, 246), is sufficiently efficient to acidify the Golgi and the endosomes during its transit *en route* to the vacuole. In contrast, the deletion of *VPH1* strongly increases the Golgi pH compared to the wild type strain, almost to the same level as the *vma13Δ* strain (Figure 20A). It suggests that Vph1p plays a major role for the acidification of the Golgi apparatus and it contradicts the classical model of Stv1p being the main V-ATPase subunit *a* in the Golgi apparatus.

f. The V-ATPase moderates pH fluctuations in the Golgi during a glucose pulse.

It is well described that glucose availability influences the cytosolic pH (248-250). Especially, when cells are starved of glucose, the cytosolic pH decreases to a considerably lower value. Added back in the external medium, the glucose is transported into the cell, glycolysis is activated, ATP is produced and the proton pumps will extrude protons out of the cytosol (41, 251). As expected, when we monitored the cytosolic pH of glucose starved cells during glucose re-addition, we observed first a transient extra acidification – presumably due to glycolysis which produces protons – followed by an alkalization to return to a near neutral pH value. This trend occurs similarly in the wild type and in the *vma13Δ* strain (Figure 20D), except that the final pH is slightly more acidic in the *vma13Δ* strain, consistently with the steady-state pH measurements.

If we monitor the Golgi pH during the same process, the curve follows the same trend, first with a transient acidification that appears a few seconds after glucose addition, followed by a pH increase (Figure 20C). We should stress the point that the amplitude of pH increase is much lower in the Golgi than in the cytosol. In the wild type strain, the Golgi pH only varies of 0.2 pH unit, while it varies of more than 1.2 pH unit in the cytosol during the same glucose stress. It can be explained by the activity of the V-ATPase which pumps protons towards the Golgi lumen. Moreover, it has been previously described that the Golgi V-ATPase complexes do not undergo dissociation in response to glucose starvation, on the contrary to the vacuolar V-ATPase complexes (55). Accordingly, the Golgi pH is kept relatively stable and does not experience the same alkalization as the cytosolic pH after glucose re-addition. In comparison, the Golgi pH of *vma13Δ* varies of 0.6 pH unit, while the cytosolic pH of the same strain varies of about 1.0 pH unit.

Altogether, it shows that the Golgi pH is correlated to its cytosolic counterpart. This could be due to weak acids and/or to proton channels and proton exchangers. Noteworthy, the Golgi pH fluctuations are milder than the ones that occur in the surrounding cytosol, suggesting that there are mechanisms keeping the Golgi pH value in its optimal range. In addition, it confirms that the V-ATPase is essential to continuously maintain acidic the Golgi pH, because its absence makes the Golgi much more responsive to cytosolic pH variations.

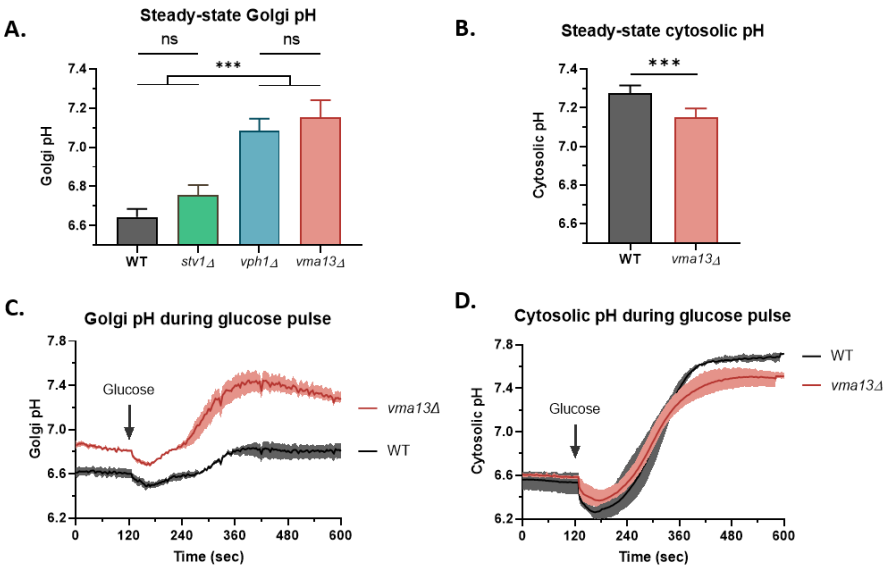

Figure 20. Golgi and cytosolic pH measurements at steady-state and during glucose pulse.

A. *and* **B.** Steady-state Golgi and cytosolic pH measurements of cells grown in synthetic medium buffered at pH 5.0 (50 mM MES (2-(*N*-morpholino)ethanesulfonic acid)). Cells were collected during exponential growth phase, resuspended in fresh medium and directly transferred into the fluorimeter for measurement. The fluorescent measurements were then converted into pH values thanks to *in vivo* pH calibration. *N* = 4-9. Means and 95% confidence intervals are represented. **C.** *and* **D.** Golgi and cytosolic pH measurements of cells starved of glucose, to which glucose is added back. Cells were collected during exponential growth phase, washed, resuspended into synthetic medium lacking glucose and incubated during 30 min on ice, as performed in another study (39). Cells were then incubated during 5 min at 28 °C prior to fluorescence measurement. After 120 sec of recording, glucose was added to the cell suspension at a final concentration of 2% and the measurement was prolonged up to 600 sec. The fluorescence was recorded with alternate excitation at 400 and 480 nm and the resultant fluorescent ratio was converted into pH value. *N* = 3 for Golgi pH measurements, *N* = 5 for cytosol pH measurements. Means and ranges are represented. Note that the synthetic growth media used in those experiments contain 0.9 mM Ca^{2+} and 2.7 µM Mn^{2+}.

3. Discussion

Adaptation of probes for the Golgi lumen is not so straightforward

In the secretory pathway, a large number of proteins are retained at their appropriate location thanks to a single transmembrane span. Even though the retention mechanisms are not fully understood, we can take advantage of this large pool of available targeting sequences to address proteins alongside the secretory pathway. In our hands, we could properly target different probes to the early Golgi lumen. Nonetheless, the correct localization was restricted to low expression systems. Indeed, when strongly expressed, we often faced mislocalization troubles, either because of ER retention of the constructs or due to escape of proteins towards the vacuole. Hence, the chimeric proteins had to be expressed with moderate and homogenous strength. The use of pGDT1 promoter in the centromeric yeast plasmids pRS315 or pRS416 generally led to expected localization, even though some protein retention within the ER does sometimes occur. Alternatively, the use of a stronger constitutive promoter, such as pTPI, combined to a genomic insertion of the construct, also commonly allowed for appropriate localization of the probes. Even though the preparation of strains with genomic modifications is more time-consuming, this latter strategy seems to us the best option to target probes in the yeast Golgi.

Historically, many sensors dedicated to *in vivo* measurements of biochemical parameters were developed for the cytosol. At the exception of some chemical sensors that can enter cells via incorporation in endosomes, or of hydrophobic molecules that will accumulate in lipid bilayers, the genetically encoded probes, as all soluble proteins, are easily produced in the cytosol of cells. Therefore, researchers have succeeded to obtain sensors to monitor pH, Ca^{2+}, Mg^{2+}, Zn^{2+}, Cl^{-}, IP_3, ATP, cAMP, nitric oxide, redox potential, molecular crowding, temperature, pressure and other parameters, in various organisms (252).

When sensors are intended to organellar measurements, they have to be adapted to the presumed parameters they will encounter in the lumen of the specified organelle. In particular, the Ca^{2+} concentration is much higher in the ER of animal cells and in the vacuole of yeast than in their cytosol. Regarding the Golgi lumen, its Ca^{2+} concentration is unclear. Therefore, we tried to adapt several Ca^{2+}-sensors with different Ca^{2+} affinities, such as different aequorin mutants or the GAP1 sensor, to perform measurements in the lumen of *S. cerevisiae* Golgi. Unfortunately, none of those attempts led to satisfying results. The reason for this is unclear. It could be that the folding of those probes within yeast ER is not optimal, maybe due to differences of biochemical properties and chaperones presence in between ER lumen and

cytosol, or that some biochemical parameters of the Golgi lumen – such as pH, ionic strength, or redox potential – does not allow for proper functioning of the sensors.

Regarding the monitoring of Golgi pH, by taking advantage of the pHluorin, a GFP variant that was suitably used for Golgi pH monitoring in other organisms (69, 141, 241, 243, 244, 253-255) or for pH monitoring in other organelles in yeast (38, 70, 73, 116), we succeeded to perform accurate pH measurements in *S. cerevisiae* Golgi. Notably, sensor brightness and/or folding was improved thanks to two point mutations (38, 236, 237) and a correct subcellular localization was obtained via the fusion with an appropriate targeting sequence and thanks to cell to cell equalization of probe expression via genomic integration (238). This newly available probe can now be extensively used to decipher what are the pH determinants in the early Golgi.

V-ATPase subunit a *isoforms display unexpected roles for Golgi acidification*

Using our newly developed Golgi probe, we observed that the Golgi pH is surprisingly much more affected by the deletion of *VPH1* than by the deletion of *STV1*. As Stv1p is commonly described as the subunit *a* isoform of the V-ATPase localized in the Golgi and the endomembrane system while Vph1p reaches the vacuolar membrane, the opposite trend was expected (61). Of course, Vph1p, which is more expressed than Stv1p (61), transits via the secretory pathway to reach the vacuole and transiently co-localizes with Stv1p (56) and it has been previously suggested that Vph1p could already form a functional V-ATPase involved in the acidification of the Golgi apparatus (39). Here, our data highlight that Vph1p is actually the main player for the acidification of the Golgi lumen while Stv1p plays only a minor role for H^+ pumping, at least when cells are exponentially growing. Hence, we can speculate that Stv1p could have more subtle roles at the Golgi, such as pH sensing, regulation of V-ATPase assembly, etc.

Golgi pH fluctuations are more constrained than cytosolic pH fluctuations

Another interesting observation is that, while the cytosolic pH is strongly affected by glucose availability, the Golgi pH is kept quite stable regardless glucose concentration in the external medium. Hence, the amplitude of pH changes is lower in the Golgi than in the cytosol, with an increase of 1 pH unit in the cytosol, while there is only 0.2 pH unit increase in the Golgi lumen (Figure 20C *and* D). This is probably due to H^+ transporters that keep the

Golgi acidic compared to the cytosol. Golgi pH maintenance is highly due to the presence of the V-ATPase, as Golgi pH fluctuations are 3-fold higher in the *vma13Δ* strain than in the *WT*.

It is known that vacuolar localized V-ATPase complexes undergo dissociation after glucose deprivation, while Golgi and endosomal Stv1p-containing V-ATPase complexes do not dissociate (55, 56, 62). Therefore, V-ATPase complexes specifically located in the Golgi apparatus could promptly pump protons towards the Golgi lumen after glucose re-addition. As a result, the secretory pathway functionalities would be very quickly recovered when cellular metabolism awakens. The direct *in vivo* measurement of Golgi pH was the best demonstration of this characteristic and it strengthens the fact that a robust Golgi pH control is critical for the cell.

« There are two possible outcomes:
If the result confirms the hypothesis, then you've made a measurement.
If the result is contrary to the hypothesis, then you've made a discovery. »

Enrico Fermi

CHAPTER 2

GDT1P TRANSPORTS H^+ IONS AND IS A STAKEHOLDER OF GOLGI PH HOMEOSTASIS

1. H^+ ions are realistic substrates of Gdt1p

Up to now, most of the studies related to the yeast Gdt1p and its orthologs have pointed out Ca^{2+} and/or Mn^{2+} transport activity or some implication in the homeostasis of those cations (179). In several papers, it was suggested that the transport of Ca^{2+} and Mn^{2+} could take place against their concentration gradient, and the influence of GDT1 family members on pH homeostasis has been highlighted in various biological contexts, in human, in yeast or in plants (80, 90, 171, 182, 183). However, in all aforementioned studies, the proton transport activity has never been directly recorded and one cannot exclude that those pH perturbations derive from other dysregulations, since the Ca^{2+} cation is a well-known secondary messenger and that Mn^{2+} cations serve as cofactor for various enzymes, in addition to play roles in redox regulation (200, 256, 257).

2. Development of a heterologous expression system for Gdt1p H^+ transport investigation

A heterologous expression system using *L. lactis* as a bacterial host was previously used in our laboratory to measure Ca^{2+} and Mn^{2+} influx mediated by Gdt1p (91, 92). Now, we took advantage of the same strategy to assess H^+ transport. Gdt1p was expressed in bacteria via an inducible expression system, *GDT1* gene being under the control of the nisin inducible promoter. To measure the intracellular pH, a genetically encoded superfolder-pHluorin variant named sfpHluorin (38) was concomitantly expressed in *L. lactis* using the same expression system. This sfpHluorin variant is the combination of the original pHluorin (234) with a superfolder GFP more prone to fluoresce in oxidizing environments than other GFP variants (258). Interestingly, the sfpHluorin contains two mutations (F64L and M153T) that are similar to the ones we selected (F64L and M153R) for the development of a Golgi-localized sensor for *S. cerevisiae*, as described in the first chapter of this section.

The expression level of both Gdt1 and sfpHluorin proteins was checked by *western blotting*, confirming that both were correctly expressed after nisin addition (Figure 21A). A noticeable observation is that sfpHluorin production is not equal when co-expressed with Gdt1p or when expressed alone in the control strain, especially in non-induced condition. The same statement is also true for Gdt1p production. Even if the exact reason for this is not clearly determined, we can speculate that the presence of an intergenic sequence in between the two coding sequences, by forming an "operon-like" system, could ease the binding or the release of ribosomes on the corresponding mRNA, and/or could affect the transcriptional regulation of the whole system.

Hopefully, it is not required to get the same sfpHluorin expression level in the different strains since pH values assessments are calculated in a ratiometric manner from the excitation spectra. *Per contra*, blank measurements were systematically recorded and subtracted in order to accurately infer the internal pH from deduced fluorescent spectra (Figure 21B). In such a way, the specific fluorescence excitation spectrum of sfpHluorin becomes clearly apparent and is cleaned from fluorescent background coming from molecules of the growth medium, prior to further calculation. In parallel, by doing an *in vivo* calibration with different pH buffers and H^+/K^+ nigericin ionophore to equilibrate internal with external pH, we made sure that the sensor properly responds to pH (Figure 21C *and* D).

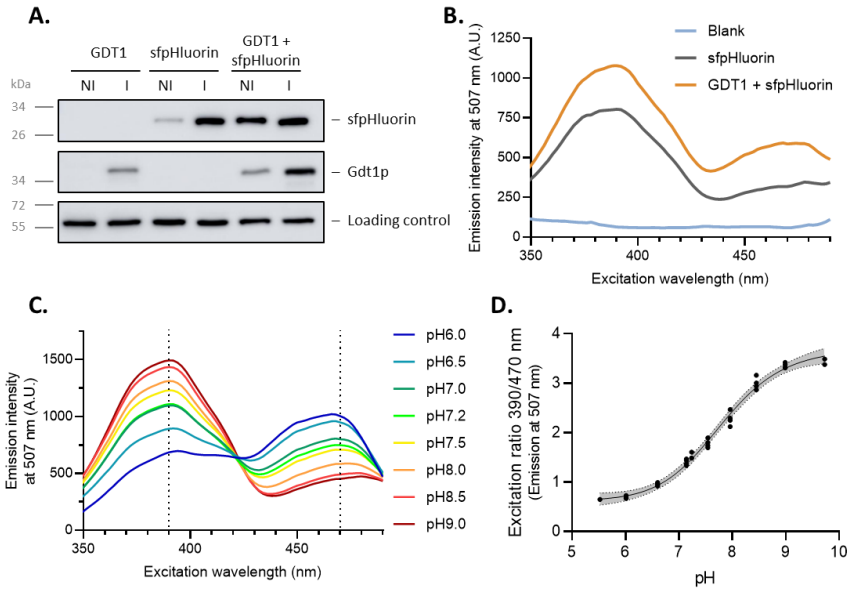

Figure 21. Setting up the parameters for intracellular pH measurements in *L. lactis* with sfpHluorin.

A. *L. lactis* cells are used as a tool to express Gdt1p at the membrane together with the sfpHluorin pH-sensor in the cytosol of the cell. Protein expression is induced by the addition of nisin for two hours in the culture medium. Comparison of non-induced (NI) and induced (I) cells expressing only GDT1, only sfpHluorin or both proteins (GDT1 + sfpHluorin). The sfpHluorin protein is detected by α-GFP antibodies, Gdt1p by α-Gdt1p antibodies and the loading control consists of an undetermined endogenous protein detected by α-Gdt1p antibodies. **B.** Excitation spectra of *L. lactis* cells not expressing the sfpHluorin (Blank), expressing the sfpHluorin alone (sfpHluorin), or together with GDT1 (GDT1 + sfpHluorin), after induction of the proteins of interest. The emission intensity is measured at 507 nm during excitation from 350 nm to 490 nm. For all further graphs, the blank was systematically measured and subtracted before pH calculations. **C.** Representative calibration experiment. Cells expressing the sfpHluorin were collected, washed twice and distributed in 2 ml microtubes. Cells harvested two hours after induction were washed, resuspended in different pH buffers, and nigericin was added at a final concentration of 0.5 µg/ml in order to permeabilize the membrane for H^+ and for K^+. Blank subtracted spectra are represented. The 390 and 470 nm excitation peaks (dashed lines) are highlighted, since they are used for ratio calculation and conversion into pH values. **D.** Calibration curve of the sfpHluorin expressed in *L. lactis*. Cells were treated similarly than in panel (C.). After blank subtraction (cells devoid of sfpHluorin), the 390/470 nm excitation ratio (with emission recorded at 507 nm) is plotted against pH. A 4-parameters sigmoidal curve is drawn through experimental data. N = 4, standard curve is represented with 99% confidence interval.

3. Gdt1p conveys H^+ against Ca^{2+} and Mn^{2+} cations through biological membranes

a. Gdt1p mediates H^+ transport across biological membranes

With this effective tool, *in vivo* internal pH measurements were then performed. The initial intracellular pH measured in *L. lactis* (Figure 22A *and* C) is coherent with pH values reported previously in the literature, which were in between 7.3 and 8.2 for various lactic acid bacteria and about 7.8 for *L. lactis* (259, 260). Strikingly, the intracellular pH is lower in Gdt1p-expressing cells than in control cells at the beginning of our experiments. As the washing buffer contains EGTA, there will probably be a *in to out* [Ca^{2+}] gradient. The intracellular [Ca^{2+}] is commonly estimated in between 100 and 300 nM in bacteria (261, 262) – but is possibly higher in Gdt1p-expressing cells (91) –, while the free extracellular [Ca^{2+}] is estimated at 0.7 nM in the washing solution (Maxchelator Ca-EGTA Calculator v1.2, parameters set at 28 °C, pH 7.4, ionic strength 0.2 N, 10 µM total Ca^{2+} - estimation based on ICP-AES measurements performed by Anne-Sophie Colinet in our lab –, 1 mM EGTA). Hence, if Gdt1p exchanges Ca^{2+} for H^+ ions, Ca^{2+} efflux will trigger the acidification of *L. lactis* cytosol prior to pH recordings. This is in line with our initial hypothesis.

After recording the basal pH during 60 seconds, 10 mM of NaOH was added in the extracellular medium and the intracellular pH was monitored for 4 additional minutes (Figure 22A). This addition creates a *in to out* [H^+] gradient and protons are inclined to exit the cell to equilibrate on either side of the membrane. Remarkably, the intracellular pH of cells expressing Gdt1p is modified in a higher amplitude and at a faster speed than control cells (Figure 22B). As the initial pH was not similar in *GDT1*-expressing cells and in control cells, we also conducted measurements in which we pre-treated control cells by the addition of 10 mM HCl in the extracellular medium. After 4 minutes incubation, the internal pH reaches the same value as *GDT1*-expressing cells. Then, the subsequent addition of NaOH (+ 20 mM to control cells, + 10 mM to *GDT1*-expressing cells) leads again to a faster alkalization in *GDT1*-expressing cells (Figure 22C).

In order to monitor putative protons influx, we also imposed an opposite gradient by the addition of HCl to *L. lactis* cell suspension and still recorded internal pH over time. At first, the decrease of the internal pH appears similar in control and *GDT1*-expressing cells (Figure 23A), but the quantification of pH decrease after HCl addition reveals a *GDT1* specific effect (Figure 23B). However, similarly to the previous experiment, after reaching the same initial pH in both strains by the addition of extracellular HCl, the subsequent

application of an identical acidic external pH – by adding a concentrated pH buffer at value 6.0 – highlights that *GDT1*-expressing cells convey protons more easily than control cells (Figure 23C). Together, those experiments are the first direct evidence that Gdt1p is able to transport protons through biological membranes.

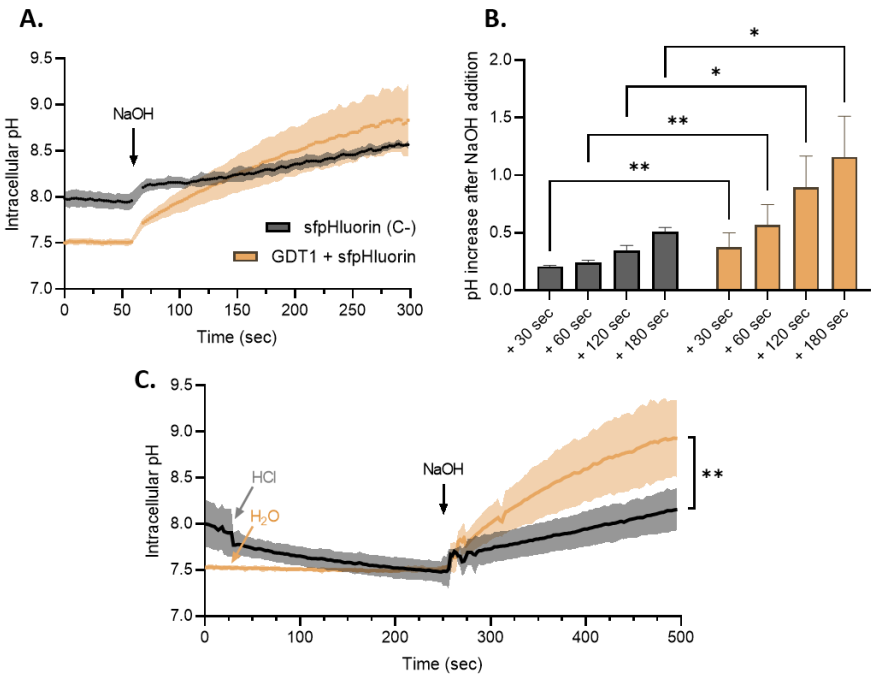

Figure 22. Gdt1p exports H^+ through the membrane of *L. lactis*.
L. lactis cells were grown in M17 broth with 1% glucose, exogenous protein expression was induced for two hours by the addition of nisin, an equal amount of cells was collected, and cells were washed with a buffered solution (100 mM KCl, 1 mM EGTA, 1 mM $MgCl_2$, 20 mM MOPS pH 7.4) before the beginning of pH recordings. **A.** Intracellular pH measurements over time of GDT1 expressing cells (GDT1 + sfpHluorin) and a negative control (sfpHluorin (C-)) after extracellular alkalization by the addition of sodium hydroxide (NaOH) at a concentration of 10 mM. This generates a H^+ gradient with lower external [H^+] compared to the intracellular [H^+]. Then, the internal pH was monitored during 4 additional minutes. N = 3 to 6, error bars represent SD. **B.** Quantification of pH increase at different time points (+ 30 sec, + 60 sec, + 120 sec, + 180 sec) compared to the pH recorded during the first 60 seconds of the measurement, prior to sodium hydroxide addition. N = 3 to 6, error bars represent SD. Mixed-effects model statistical analyses with multiple comparison via a Bonferroni test. **C.** In order to start from a similar internal pH for both strains, 10 mM of HCl was first added to the negative control (sfpHluorin (C-)). About four minutes later, alkalization of the extracellular medium was performed. NaOH was added to both cell populations, 10 mM was added to GDT1 + sfpHluorin expressing cells and 20 mM to the negative control, in order to neutralize the HCl and to reach the same final external pH. N = 5, error bars represent SD. The final value was statistically analyzed with an unpaired t-test.

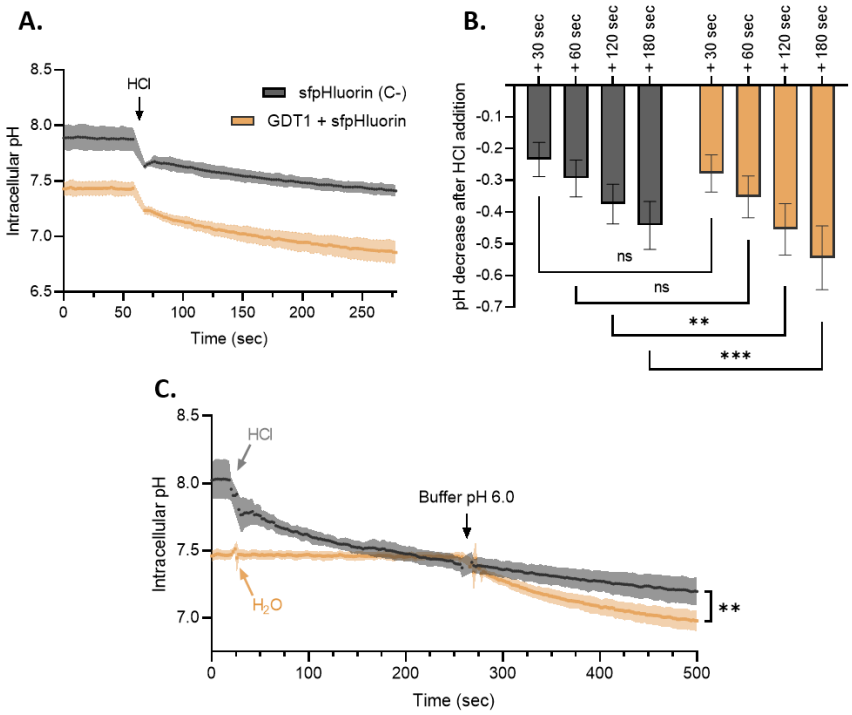

Figure 23. Gdt1p also imports H^+ through the membrane of *L. lactis*.
Same experimental procedure as in Figure 22, except that the extracellular medium was acidified during pH recording by the addition of HCl or MES buffer pH 6.0. **A.** Intracellular pH measurements over time of GDT1 expressing cells (GDT1 + sfpHluorin) and a negative control (sfpHluorin (C-)) after extracellular acidification by the addition of hydrochloride (HCl) at a concentration of 10 mM. This generates a H^+ gradient with higher external [H^+] compared to the intracellular [H^+]. Then, the internal pH was monitored during 4 additional minutes. N = 5 - 6, error bars represent SD. **B.** Quantification of pH decrease at different time points (+ 30 sec, + 60 sec, + 120 sec, + 180 sec) compared to the pH recorded during the first 60 seconds of the measurement, prior to HCl addition. N = 5 - 6, error bars represent SD. Mixed-effects model statistical analyses with multiple comparison via a Bonferroni test. **C.** In order to start from a similar internal pH for both strains, 10 mM HCl was first added to the negative control (sfpHluorin (C-)). About four minutes later, acidification of the extracellular medium was performed for both samples. The extracellular pH was set up at pH 6.0 by the addition of MES buffer at a final concentration of 50 mM. N = 6 - 7, error bars represent SD. The final value was statistically analyzed with an unpaired t-test.

b. The pH gradient influences Ca^{2+} and Mn^{2+} Gdt1p transport activity

As protons are thought to be the counterions of Ca^{2+} and Mn^{2+} during Gdt1p-mediated transport activity, a variation of the pH gradient across phospholipidic membrane should influence the transport of those two cations as observed for other H^+/Ca^{2+} antiporters (178, 263). Regarding Gdt1p, this assumption has already been assessed previously for Ca^{2+} (91).

Here, we highlight that both Ca^{2+} and Mn^{2+} transport activities are affected by the H^+ gradient. To do so, Ca^{2+} and Mn^{2+} import was measured thanks to Fura-2, as previously performed in our laboratory. Shortly, *L. lactis* cells were incubated with the esterified Fura-2-AM, which is able to cross membranes. Once into the cell, intracellular esterases will hydrolyze the ester function of the molecule resulting in a charged form of Fura-2 that is consequently trapped into the cell. Internal Ca^{2+} concentration is then measured in a ratiometric manner, with two excitation peaks at 340 and 380 nm that are inversely affected by the Ca^{2+} concentration. Mn^{2+} import into the cells can also be detected thanks to Fura-2 because its fluorescence is quenched by this cation. At 360 nm, the isosbestic point of the spectrum, the quenching by Mn^{2+} is independent from the Ca^{2+} concentration.

We performed Ca^{2+} and Mn^{2+} transport measurements with cells incubated in buffers at pH 6.8, 7.5 and 8.0. For both calcium and manganese, we observe that the higher the external pH, the more intense the cation import (Figure 24A *and* C). We can speculate that this is the direct consequence of the proton gradient that favors H^+ efflux when the external pH increases. Therefore, if Ca^{2+} and Mn^{2+} are transported in exchange for H^+, the influx of those cations would happen quicker when the efflux of H^+ is facilitated. Notably, in Ca^{2+} measurements, the initial slopes appear similar whatever the extracellular pH, while initial slopes differ in Mn^{2+} measurements. This maybe results from the different K_M of Gdt1p for the two cations (K_M for Ca^{2+} is 15.6 µM, K_M for Mn^{2+} is 83.2 µM (92)). Henceforth, Ca^{2+} transport could occur at maximum velocity when 25 µM $CaCl_2$ is added in the extracellular medium, while Mn^{2+} transport would occur at submaximal velocity. Nevertheless, the final intracellular Ca^{2+} and Mn^{2+} concentrations diverge according to the extracellular pH value, indicating that the thermodynamic equilibrium state depends on the pH gradient in a Gdt1p-dependent manner.

As controls, cells non-expressing Gdt1p were measured similarly. The basal transport activity recorded with those cells is not modified by changes of the external pH. Also, the addition of nigericin that dissipates the H^+ gradient across *L. lactis* membrane results in a similar transport activity in all assays whatever the external pH (Figure 24B *and* D). It confirms that the proton gradient itself is a parameter able to modulate Ca^{2+} and Mn^{2+} Gdt1p transport activity.

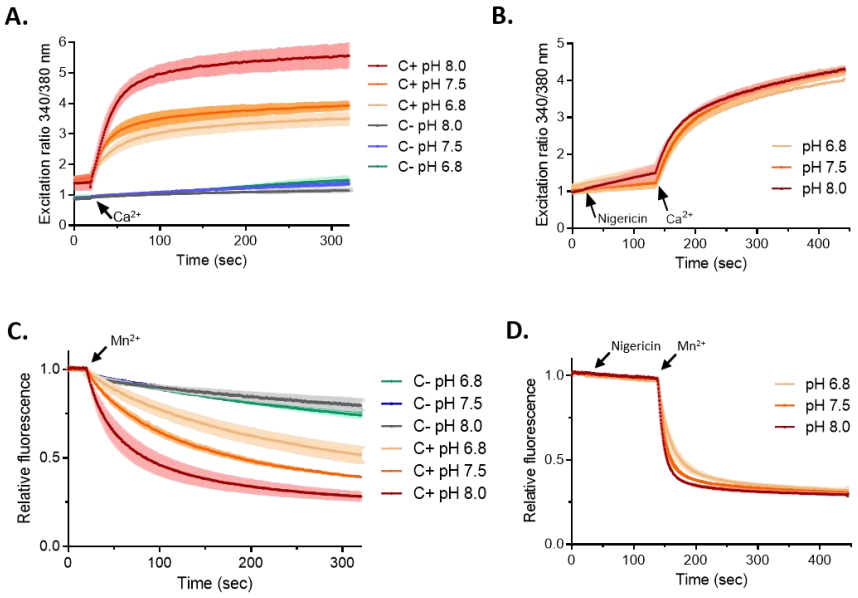

Figure 24. Ca^{2+} and Mn^{2+} Gdt1p-mediated influx is affected by the pH gradient.
L. lactis cells were grown, induced, and collected as in Figure 22. Then, cells were treated to incorporate Fura-2. Finally, they were washed twice with a washing buffer (100 mM KCl, 1 mM $MgCl_2$, 1 mM EGTA, 50 mM Tris at pH 6.8, 7.5 and 8.0) and finally resuspended in the corresponding buffer devoid of EGTA but previously passed through a calcium sponge resin to reduce as much as possible the free Ca^{2+} concentration. **A.** *and* **C.** Time-course Ca^{2+} and Mn^{2+} measurements of cells producing Gdt1p (C+) were performed at different extracellular pH, respectively pH 6.8, 7.5 and 8.0. Ca^{2+} influx is provoked by the addition of 25 µM $CaCl_2$ in the extracellular medium and is deduced from the calculation of the 340/380 nm excitation ratio, while 10 µM $MnCl_2$ is added to produce Mn^{2+} influx that is corroborated to quenching during excitation at 360 nm. The Fura-2 fluorescence emission is invariably recorded at 510 nm. A negative control (C-) is also performed with cells that do not express Gdt1p. N = 3, error bars represent SD. **B.** *and* **D.** To neutralize the pH gradient, H^+/K^+ nigericin ionophore is added to the cell suspension at a concentration of 0.5 µg/ml 2 minutes before the addition of Ca^{2+} or Mn^{2+} and the cation influx measurement is performed as previously. N = 3, error bars represent SD. Experiments presented in this figure were performed by Louise Thines.

c. Gdt1p operates as a Ca^{2+}-Mn^{2+}/H^+ exchanger

In a similar manner as in previous experiments, *L. lactis* cells were used for Gdt1p expression. Then, in order to straightforwardly measure Ca^{2+} or Mn^{2+} exchange with H^+, we measured the extracellular pH during Ca^{2+} and Mn^{2+} influx with a classical pH-meter. If there is some exchange activity, the entry of Ca^{2+} or Mn^{2+} should trigger an efflux of H^+ and therefore induce an acidification of the external medium. Because the internal pH is presumably highly buffered by a large number of weak acids and bases (264) and by several control mechanisms involving the sensing of internal pH and the activation of various H^+ pumps (240), the occurrence of internal pH changes needs quite strong driving forces, e.g. as performed in Figure 22 and Figure 23. Here, by resuspending the cells into a non-buffered solution, we facilitate the detection of external pH variations. By adding 20 mM $CaCl_2$ or 20 mM $MnCl_2$ in the extracellular medium, we first observe a pH drop that is similar for both strains (Figure 25A *and* B). This could be due to the Lewis acid properties of Ca^{2+} and Mn^{2+}, that will acidify the solution. After this initial pH drop, the external pH continues to decrease, but in a different manner for both strains. Indeed, the external pH decreases faster in cells expressing Gdt1p than in control cells (Figure 25A *and* B). This probably reflects the Ca^{2+}-Mn^{2+}/H^+ exchange activity mediated by Gdt1p.

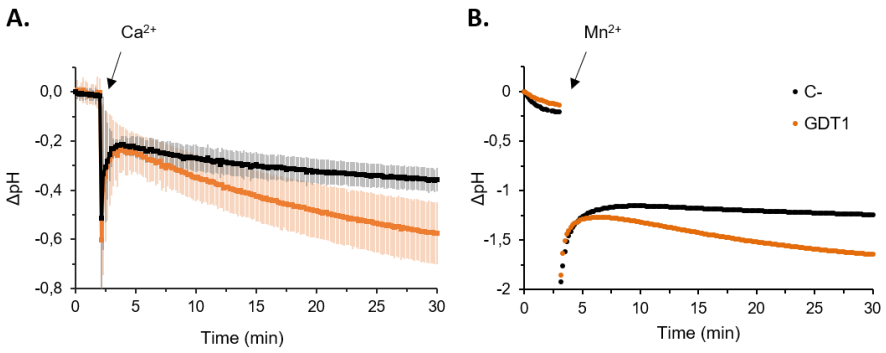

Figure 25. Exchange of H^+ against Ca^{2+} and Mn^{2+} cations is mediated by Gdt1p.
The extracellular pH of *L. lactis* cells expressing Gdt1p or transformed with an empty plasmid is recorded during the addition of Ca^{2+} or Mn^{2+} in the extracellular medium. Cells collected by centrifugation are washed with a low concentrated pH buffer (1 mM Tris pH 7.0). Then, the extracellular pH is recorded over time via a pH-meter. After recording the baseline for 2 minutes, **A.** 20 mM $CaCl_2$, or **B.** 20 mM $MnCl_2$ is added in the extracellular medium and the measurement is continued up to 30 minutes. Data are presented as normalized to the initial pH value of each curve that is set to zero, in order to underscore pH variations. When applicable, mean and SD are represented.

4. In *S. cerevisiae*, the impact of Gdt1p on Golgi pH homeostasis is revealed during pH fluctuations

a. Steady-state pH values are not substantially regulated by Gdt1p in *S. cerevisiae*

The previous measurements were performed in a heterologous expression system. It is remarkably suitable to measure direct transport activities, but it does not unveil the physiological function of Gdt1p in its natural environment. As a H^+ transporter localized at the Golgi membrane, Gdt1p could potentially affect both cytosolic and Golgi pH. Therefore, we monitored the pH in those two subcellular compartments via the expression of the original pHluorin (234) in the cytosol and thanks to the pHluorin variant targeted to the Golgi lumen that we developed during the first part of this thesis.

When cells are cultivated in synthetic medium and collected during exponential growth for direct pH measurement, the deletion of *GDT1* does not affect the cytosolic pH compared to the *WT* strain (Figure 26A). It is not totally unexpected, since many other transporters are operating H^+ import or export, from and to the cytosol (240). Accordingly, the alteration of one of the major pH regulators – the V-ATPase – by disrupting *VMA13*, leads to a slight acidification of the cytosol (Figure 26A). It was expected since less protons are extruded out of the cytosol in this strain.

Besides, Golgi pH measurements disclose that *GDT1* deletion does not substantially affect the luminal Golgi pH either (Figure 26B). It means that in normal conditions, Gdt1p Ca^{2+}-Mn^{2+}/H^+ exchange activity is not a predominant driver of Golgi luminal acidification. This role is probably mostly fulfilled by the V-ATPase alongside the secretory pathway acidification, since the Golgi pH becomes almost neutral in the *vma13Δ* strain (Figure 26B). Then, we wondered whether the inactivation of this H^+ pump could uncover Gdt1p activity. Both for cytosolic pH and for Golgi pH, the concomitant deletion of *GDT1* and *VMA13* does not change steady-state pH values compared to *VMA13* deletion alone (Figure 26A *and* B).

Eventually, Golgi pH measurements performed in various strains combining *GDT1* deletion with *PMR1*, *VCX1*, *STV1* or *VPH1* deletion did not further reveal the physiological role of Gdt1p for pH homeostasis (Annex 1). Altogether, those measurements indicate that the acidification of the Golgi lumen during exponential growth is not the main physiological role of Gdt1p.

b. During physiologic pH modifications, Gdt1p participates in the homeostasis of the Golgi pH

Traditionally, exchangers and symporters are described as having a high velocity, while pumps can produce larger concentration gradients, but in a slower fashion. Therefore, the co-existence in the same biological membrane of transporters with common substrates but different transport mechanisms makes sense, in order for cells to be able to rapidly transport a large amount of substrate at first, followed by a slower recovery of the resting state displaying expanded concentration gradients. Furthermore, secondary transporters and ATPases having different driving force, they can perform transport in different physiological status, which seems advantageous for cells to maintain homeostasis. For example, this system is well described with two yeast vacuolar Ca^{2+}-transporters, Pmc1p and Vcx1p (265).

Here, we hypothesize that Gdt1p could be important for cells to rapidly react during intracellular pH changes in complement to the predictably slower V-ATPase. A well-known procedure that triggers cytosolic pH fluctuations is the glucose deprivation – glucose addition process (53, 250). Cells deprived of carbon source slowly acidify the cytosol during 30-60 minutes. If glucose is added back to the growth media, it is rapidly imported into the cell and the glycolysis restarts. It provokes a transient additional acidification of the cytosol, possibly due to the production of H^+ by glycolysis, and then the increase of ATP concentration activates H^+-ATPases to pump protons outside of the cytosol. When performing such a process in the *gdt1Δ* strain and continuously recording the cytosolic pH, one could observe that the trend is very similar to the *WT* strain (Figure 26C). The only substantial change is a delay for *gdt1Δ* cells to recover their steady-state cytosolic pH, compared to the control strain (Figure 26D). This is possibly due to slight changes of the Ca^{2+} signalling occurring after glucose addition (266, 267).

By recording the Golgi pH during an identical procedure (Figure 26E), we observe curves with the same shape. Basically, fluctuations of the Golgi pH are a "copy-paste" of the cytosolic pH fluctuations. When comparing the Golgi pH fluctuations of *WT* and *gdt1Δ* strains, we observe that the Golgi pH reaches a higher value in the *gdt1Δ* strain than in the *WT* strain at the end of the recovery. This observation strongly suggests that Gdt1p participates in the pumping of protons towards the Golgi lumen, as does the V-ATPase, during those pH fluctuations.

Unexpectedly, when *GDT1* was deleted in the *vma13Δ* background, there was no significant change of Golgi pH fluctuations compared to the *VMA13* deletion alone (Annex 2). It may be that V-ATPase inactivation causes severe physiological disturbances and hence modifies the normal functionality of

the Golgi. Besides, we also looked at Golgi pH fluctuations in *vcx1Δ* and *vcx1Δgdt1Δ* strains. Vcx1p is a Ca^{2+}/H^{+} exchanger located at the vacuolar membrane and possesses several similarities with Gdt1p (207, 265, 268). Interestingly, the recovery takes a longer time in those strains than in the *WT*. Again, *GDT1* deletion is characterized by some further delay for pH recovery, and the pH value reached at the end of the measurement is higher when Gdt1p is not expressed (Annex 3).

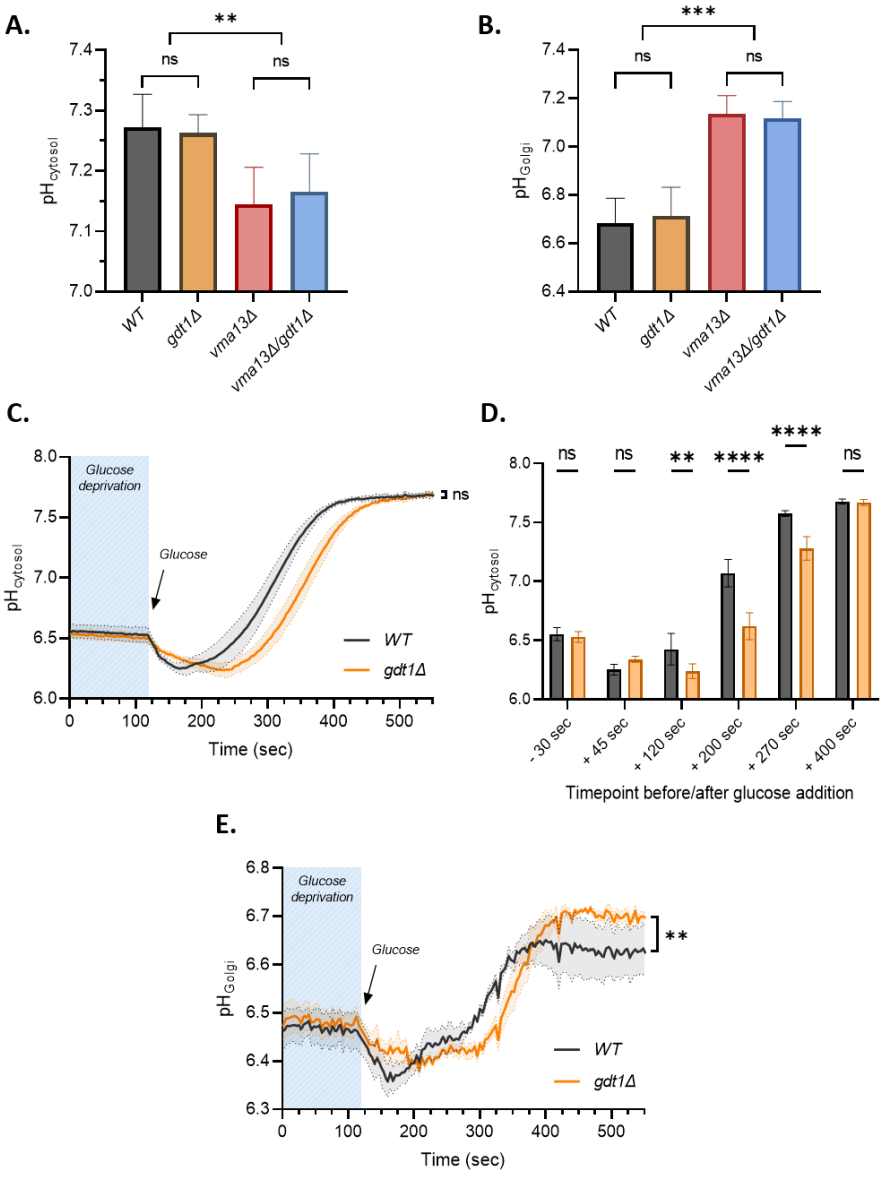

Figure 26. Gdt1p affects the Golgi pH during fluctuations.
A. *and* **B.** Cytosol and Golgi pH measurements in steady-state growth conditions. *WT*, *gdt1Δ*, *vma13Δ* and *vma13Δ/gdt1Δ* strains expressing cytosolic and Golgi pH probes were cultivated in synthetic media buffered at pH 5.0 (50 mM MES) and collected during mid-log phase for direct pH measurements. N = 7 to 14, error bars represent SD. Anova statistical analyses (Tukey test). **C.** Cytosol pH measurements during glucose deprivation / re-addition time-course assay. Cells were grown to mid-log phase in synthetic media buffered at pH 5.0 (50 mM MES), collected and washed 3 times in glucose deprived medium. After 30 minutes incubation on ice, cells were used for fluorescence measurement. The baseline was recorded during 2 minutes, then glucose was added to a final concentration of 2 % and the cytosolic pH was measured during 7 additional minutes. N = 3 for *gdt1Δ* strain and N = 7 for the *WT* strain. Means and SD are represented. The last point of the time-course measurement, at 550 sec, was considered for statistical analysis by a t-test. **D.** Quantification of cytosolic pH at different time points before (-30 sec) and after (+ 45 sec to + 400 sec) from the experiment presented in (C). Two-way Anova statistical analysis Anova (Bonferroni's multiple comparisons test). **E.** Golgi pH measurements performed during the same procedure as described in (C). N = 3, means and SD are represented. The last point of the time-course measurement, at 550 sec, was considered for statistical analysis by a t-test.

5. Discussion

Gdt1p H^+ transport activity demonstration is a key step for function elucidation

Thanks to *L. lactis* heterologous expression system, proton transport activity mediated by Gdt1p could be investigated. At first, the application of proton gradients across cytoplasmic membrane causes faster intracellular pH changes in GDT1-expressing cells than in control cells. Actually, the imposition of pH gradients in the two directions, *in to out* or *out to in*, both show an effect of Gdt1p expression on H^+ permeability. Moreover, the magnitude of proton transport seems comparable in both directions. At least two different reasons could explain it. If we consider unidirectional transport mediated by each individual protein, one explanation is that part of the protein is oriented with one topology and part with the opposite topology. However, membrane proteins usually display a preferential topology in accordance with the positive inside rule, both in prokaryotes and in eukaryotes (269). Gdt1p displays enrichment in lysines and arginines on one side of its predicted transmembrane domain and was therefore predicted to adopt one specific topology in the yeast Golgi membrane. This has been demonstrated in our lab by a protease degradation assay (2). Therefore, it would be surprising to get a relatively equal distribution of proteins with each topology in *L. lactis* cytoplasmic membrane. The second explanation is that Gdt1p could transport protons either in one or the other direction, according to the pH gradient that is applied across the membrane. Secondary transporters, as all enzymes, are catalyzers of biochemical reactions. Their role is to fasten the reaching of thermodynamic equilibrium, but they do not dictate the direction of it and they can theoretically operate in both ways. Of course, in biological systems, the direction of operability is usually driven by the concomitant concentration of substrates and products, or by the concentration of transported molecules at both sides of a biological membrane in the specific case of membrane channels and transporters. By using a heterologous expression system and by applying concentration gradients of the different transported molecules with a sufficient amplitude, we can here observe reversible transport activity of Gdt1p.

Though, the expression of an exogenous membrane protein could hypothetically increase the permeability of phospholipidic membranes for charged molecules, or could deregulate endogenous membrane transporters. Especially, since control cells already show inherent proton transport activity, this possibility is even more plausible. Therefore, we performed measurements with another methodology, where the transport activity of one substrate is modulated or initiated by the concentration gradient of its putative counterion. This is decisive to demonstrate Gdt1p

mediated proton transport activity. On one side, the larger the *in to out* proton gradient, the faster the Ca^{2+} or Mn^{2+} influx. On the other side, application of Ca^{2+} (or Mn^{2+}) *out to in* gradient induces protons efflux. Taken together, these data strongly suggest that Gdt1p conveys H^+ in exchange for Ca^{2+} and Mn^{2+} cations.

Gdt1p H^+ transport activity does not continually generate Golgi acidification

In order to clarify the physiological role of Gdt1p in its normal location, *i.e.* the Golgi membrane of *S. cerevisiae*, it is crucial to measure its activity in its native environment. Therefore, we measured the pH of the cytosol and of the Golgi lumen thanks to suitable pHluorin variants in various conditions. Curiously, *GDT1* deletion does not significantly impair physiological steady-state pH values, neither in the cytosol, nor in the Golgi. As there are other important pH regulators, such as the V-ATPase which is the main protein acting to acidify the secretory pathway (50, 270), Gdt1p is probably dispensable for Golgi acidification in favorable growth conditions.

However, when a quick response and a high rate of H^+ transport is required, the presence of a secondary transporter could be beneficial for the cell, since transport velocity of secondary transporters is usually higher than that of ATP-driven transporters. In yeast, pH homeostasis is intricate to glucose availability. When recording cytosol and Golgi pH during a glucose deprivation – re-addition experiment, it is striking that pH fluctuations in the Golgi mimics the fluctuations that occur in the cytosol. Still, some dedicated H^+ transporters have to maintain a relative acidity within the Golgi lumen, especially once glucose is again available. While the V-ATPase is predominant for Golgi acidification, Gdt1p participates in such a process. Especially, when the cytosolic pH increases steeply after glucose re-addition, the increase of the Golgi pH is rapidly restrained. The deletion of *GDT1* mitigates this restriction, since the final Golgi pH value attained in the *gdt1Δ* strain is significantly higher than the one of the *WT*.

« Le rassurant de l'équilibre, c'est que rien ne bouge. Le vrai de l'équilibre, c'est qu'il suffit d'un souffle pour tout faire bouger. »

Julien Gracq

CHAPTER 3

INVESTIGATION OF THE MECHANISMS REGULATING GDT1P ABUNDANCE

Some of the experiments presented hereafter were performed by Guillemette van Raemdonck and Quentin Lejeune. They both did their master thesis on research topics related to the regulation of Gdt1p, under my co-supervision with Prof. Morsomme. Where applicable, it will be explicitly mentioned.

1. The basis of protein degradation

Biological organisms live in continuously changing environment. Also, during their lifespan, organisms have to adapt their molecular composition to ensure all required functions. As proteins are the molecular machines that perform most of the biomolecular tasks of living organisms, cells developed various strategies to produce or activate proteins when appropriate, or, on the contrary, to inhibit or deactivate those molecular machines when necessary.

Regarding protein degradation, the first breakthrough in its comprehension arises when Christian De Duve and colleagues described the lysosome, a

particular organelle dedicated to the recycling and the storage of a large number of chemicals. The vacuole of yeasts and plants functionally corresponds to the lysosome of metazoans. The second well-known degradation machine is the proteasome. It is a huge protein complex composed of many subunits, and is mostly, but not solely, dedicated to the degradation of cytosolic proteins.

Thereupon, cells can trigger the degradation of proteins in several ways. At one extremity, autophagy is a bulk degradation process that collects large quantities of proteins and even entire organelles. At the other extremity, some degradation processes are extremely accurate in terms of specificity. For example, plasma membrane proteins, when intended for degradation, are usually specifically subjected to ubiquitylation. Then, they are specifically retrieved from the plasma membrane by endocytosis and later routed to the vacuole/lysosome. The degradation of plasma membrane proteins is of critical importance and has been substantially studied, because cells commonly face large changes of the extracellular chemical composition. In the cytosol, proteins intended for degradation are also commonly ubiquitinated before getting degraded by the proteasomal machinery. Newly synthetized proteins in the ER are controlled by a specific mechanism. If misfolded, proteins enter the *endoplasmic reticulum-associated protein degradation* (ERAD) process. In this procedure, selected proteins are retrotranslocated from the ER and sent to the proteasome. Eventually, the knowledge and the comprehension of degradation mechanisms implicated in the specific regulation of organelle resident proteins is much less extended.

2. Little is known about the degradation of Golgi proteins

Golgi-resident proteins abundance should also be controlled via some degradation processes. Standing in the center of the secretory pathway, where retrograde and anterograde fluxes interplay, they could potentially end up either at the proteasome, or in the vacuole. To date, little is known about it and no general model has been drawn regarding the control of Golgi-resident proteins. However, in recent years, a few research groups studied degradation routes for some proteins of the Golgi. Among the mechanisms, the *Golgi membrane-associated degradation* (GOMED) pathway performs Golgi degradation in a bulk manner, similarly to autophagy but independently of it (271). Regarding specific protein degradation, it was shown on one hand that protein oligomerization in the Golgi, by mimicking protein aggregation, induces its own trafficking to the vacuole/lysosome (272, 273). On the other hand, unfolded proteins in the Golgi can follow the ERAD pathway to be degraded (273), or a similar *endosome and Golgi-*

associated degradation (EGAD) pathway (274). Proteasomal degradation seems also involved in the global organization of the Golgi, in animal cells (275). Eventually, some ubiquitin ligases and a set of adaptors, such as the transmembrane ubiquitin ligase Tul1p (276) or the Golgi clathrin adaptors Gga1p and Gga2p (31, 277), are Golgi localized and could exert some role for the degradation of Golgi proteins, but their exact function is not clear yet. Altogether, many questions related to Golgi protein degradation remain unsolved.

3. Gdt1p is regulated by modifications of Ca^{2+} and Mn^{2+} distribution

As stated in the introduction, it was observed in our laboratory that Gdt1p abundance is reduced in a strain devoid of *PMR1*, the Ca^{2+}-Mn^{2+} ATPase of the Golgi apparatus. However, it is not clear whether Gdt1p could directly interact with Pmr1p in the Golgi, and therefore be potentially stabilized by such interaction, or if cation homeostasis dysregulation resulting from *PMR1* deletion causes Gdt1p decrease. Interestingly, Gdt1p abundance and glycosylation are both "corrected" by the addition of extra Ca^{2+} to the *pmr1Δ* strain.

a. Pmr1p selective mutants point out Mn^{2+} effect on Gdt1p control

Pmr1p has been extensively studied and some mutants of this protein with altered Ca^{2+} or Mn^{2+} transport activity were isolated. Hence, the *PMR1(D53A)* mutant displays reduced Ca^{2+} transport, *PMR1(Q783A)* reduced Mn^{2+} transport, and *PMR1(D778A)* is a fully inactive mutant as its ATPase activity has been lost (278-280). Therefore, we looked at Gdt1p abundance in strains expressing Pmr1p mutants. It is very clear that Gdt1p reduction of abundance specifically occurs when Pmr1p is unable to properly convey Mn^{2+} cations from the cytosol to the Golgi lumen (Figure 27A), as the abundance of Gdt1p is restored to the same level as in the *WT* strain when non-mutated *PMR1* or *PMR1(D53A)*, a mutant still able to convey Mn^{2+} but not Ca^{2+}, is expressed from a plasmid in the *pmr1Δ* strain. On the contrary, complementation of *pmr1Δ* with *PMR1(D778A)* and *PMR1(Q783A)* mutants, that are defective for Mn^{2+} transport, does not restore Gdt1p abundance to the *WT* level. Two hypotheses can be drawn from this observation. Either it is the increase of Mn^{2+} concentration in the cytosol that causes Gdt1p downregulation, or we could imagine that the deficiency of Golgi loading with Mn^{2+} causes Gdt1p decline. Mn^{2+} quantification in both compartments, cytosol and Golgi, would probably allow to disentangle the two explanations.

b. Mn^{2+} increase in the cytosol is associated with Gdt1p decline

It was previously highlighted that cytosolic [Mn^{2+}] is increased in the *pmr1Δ* mutant (88, 92). During her Master thesis, Guillemette van Raemdonck obtained data highlighting Mn^{2+} accumulation in the vacuole of the *pmr1Δ* strain. Furthermore, she showed that Mn^{2+} vacuolar overaccumulation specifically takes place for Mn^{2+}-deficient *PMR1* mutants. Pmr1p deficiency is probably triggering corrective mechanisms to reduce Mn^{2+} toxicity in the cytosol. Ccc1p, a vacuolar Mn^{2+} importer (281, 282), could be overexpressed or activated in such condition. On the contrary, Gdt1p is downregulated.

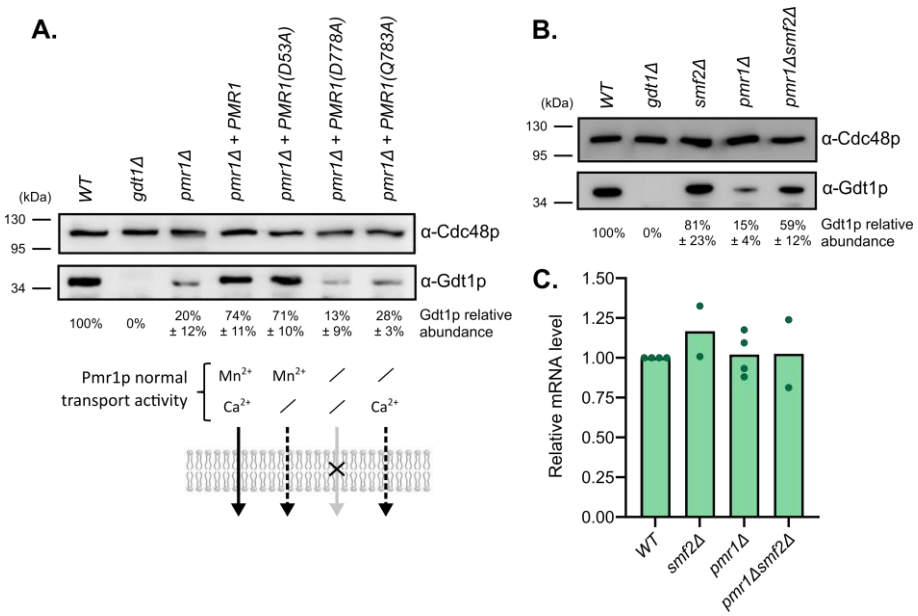

Figure 27. Gdt1p abundance is regulated by Mn^{2+} transporters.
Cells grown in YD to mid-log phase (OD_{600} ≈ 3.0) were collected and total protein extracts were analyzed by *western blotting*. The abundance of endogenous Gdt1p was analyzed in strains **A.** where *PMR1* is modified, either deleted or expressed with modified transport capacities from a pRS41N plasmid as expression system, or **B.** where *SMF2* and *PMR1* are deleted separately or simultaneously. For A. and B., representative experiments of 4 biological replicates are shown. Cdc48p is used as a loading control. Protein markers are indicated (kDa). Gdt1p relative abundance refers to Gdt1p signal in each strain compared to the signal in the *WT* strain, normalized by the signal of the loading control. Mean and SD are indicated. **C.** *GDT1* mRNA level in strains deleted for *PMR1*, *SMF2* or both is compared to the amount of *GDT1* mRNA in the *WT* strain, evaluated by RT-qPCR method. Data are presented as relative to the control strain. N = 2 to 4 independent biological experiments. The means and the individual values are presented, and each dot represents the mean of technical triplicates. RT-qPCR experiments were performed by Quentin Lejeune during his Master thesis.

Aside, *SMF2* deletion reduces import of Mn^{2+} from the extracellular medium (88). In this strain, total cellular manganese decreases by 5-fold and cytosolic [Mn^{2+}] is lower than in the *WT* strain (92), but Gdt1p abundance is not significantly modified (Figure 27B). Then, when *PMR1* and *SMF2* are conjointly deleted, the cellular manganese content increases compared to *smf2Δ* and reaches an intermediate level in between *WT* and *pmr1Δ* strains, as measured by *inductively-coupled plasma atomic emission spectrometry* (ICP-AES). In this double deleted strain, the cytosolic [Mn^{2+}] is sufficient to fully restore Sod2p activity (92). Those changes in the Mn^{2+} concentrations are corelated with Gdt1p abundance that increases in the *pmr1Δsmf2Δ* strain compared to *smf2Δ* (Figure 27B). This reinforces the assumption that cytosolic Mn^{2+} regulates Gdt1p abundance, even though we cannot definitely rule out the hypothesis that Golgi [Mn^{2+}] controls Gdt1p abundance.

c. Golgi Mn^{2+} determination is not an easy task

Compared to vacuolar Mn^{2+} quantification, Golgi Mn^{2+} determination is much more difficult to achieve. Guillemette van Raemdonck also tried to purify Golgi vesicles from various strains and to determine their Mn^{2+} content by ICP-AES, but the measurements were very close to the detection limit of the instrument. In addition, Golgi compartments purification was too much contaminated by other organelles to accurately determine $[Mn^{2+}]_{Golgi}$. Therefore, we can only speculate that $[Mn^{2+}]_{Golgi}$ is reduced when Pmr1p is ineffective for the transport of this cation. We do not know how *GDT1* up-/downregulation would affect the Golgi Mn^{2+} content.

d. Ca^{2+} supplementation synchronously restores Gdt1p abundance in the *pmr1Δ* strain, as well as glycosylation and growth speed

It was previously observed that the addition of Ca^{2+} in the extracellular medium of *pmr1Δ* cell culture counteracts the effect of *PMR1* deletion on Gdt1p cellular abundance (133). In parallel, glycosylation defects characterizing the *pmr1Δ* strain are also corrected by Ca^{2+} supplementation. Here, we looked closely at those two effects by adding rising amounts of $CaCl_2$ in growth media. Besides, we also recorded the growth speed of the *pmr1Δ* strain in those growth conditions. It is striking to observe that there is a coincident effect of Ca^{2+} supplementation on the three parameters (Figure 28A *and* B). We notice a gradual correction of Gdt1p abundance, glycosylation and growth speed after the addition of 2, 5 and 10 mM Ca^{2+}. From 10 to 50 mM Ca^{2+} supplementation, all three monitored parameters

display an optimum. At higher [Ca^{2+}], there is again growth slowdown, similar in *WT* and *pmr1Δ* strains. On the contrary to what we observe for the *pmr1Δ* strain, the *pmr1Δgdt1Δ* strain cannot account on Ca^{2+} supplementation to speed up growth (Figure 28B). Altogether, this suggests that Gdt1p affords fitness benefit to the cells in a Ca^{2+}-dependent manner.

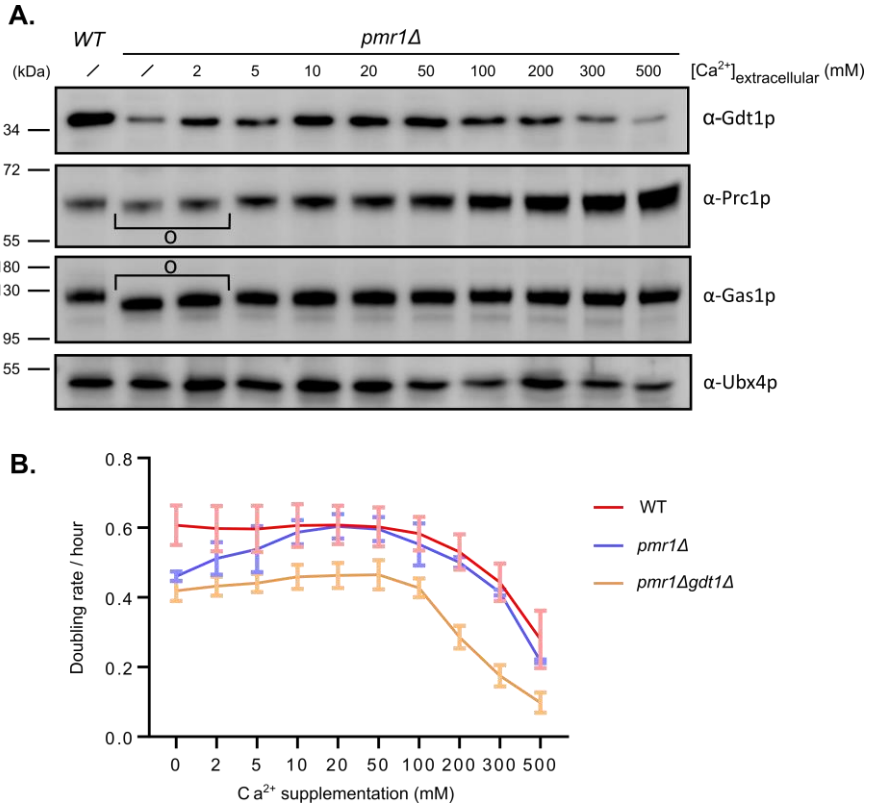

Figure 28. Mild Ca^{2+} supplementation improves growth, corrects glycosylation defects and increases Gdt1p abundance in the *pmr1Δ* strain.
A. Total protein extracts of the *WT* and the *pmr1Δ* strains, grown in normal YD medium ([Ca^{2+}] ≈ 0.75 mM) or in YD supplemented with increasing amounts of $CaCl_2$ and collected in mid-log phase (OD_{600} ≈ 3.0), were analyzed by *western blotting*. Endogenous Gdt1p abundance varies upon *PMR1* deletion and Ca^{2+} supplementation. Prc1p and Gas1p are also analyzed by *western blotting*. Mobility shifts, which are highlighted with an open circle, depict glycosylation troubles. Ubx4p serves as the loading control. Protein markers are indicated (kDa). **B.** The *WT*, *pmr1Δ* and *pmr1Δgdt1Δ* strains were grown in YD and YD supplemented with increasing Ca^{2+} concentrations. The number of doubling per hour is depicted. The higher this value, the faster cells divide. *N* = 3-4. Means and SD are represented.

4. Active targeting of Gdt1p to the vacuole occurs during high Mn^{2+} exposure

Next to Gdt1p downregulation when Pmr1p Mn^{2+} transport activity is altered, it was also noticed that Mn^{2+} addition in the extracellular medium causes Gdt1p and TMEM165 decreases (210). Those decreases happen in a relatively fast fashion, suggesting that an active degradation mechanism drives Gdt1p degradation. As degradation mechanisms of Golgi membrane proteins were rarely described, Gdt1p way of degradation is unknown and we will try to uncover via which process it takes place.

a. Extensive Gdt1p decrease is observed within 1 to 2 hours after Mn^{2+} application

We first aimed at confirming preliminary observation of Potelle *et al.* (210) by applying a similar Mn^{2+} addition to yeast cell suspension. Cells were grown to early/mid-log phase (OD_{600} ≈ 1.0-2.0) in classical YD medium, not supplemented with extra Mn^{2+}. In this medium, the [Mn^{2+}] is close to 5 µM (measurement of Anne-Sophie Colinet, by ICP-AES). Then, $MnCl_2$ was added in the culture medium at different concentrations and cells were collected 1 to 8 hours later. While the addition of 1 mM $MnCl_2$ does not cause Gdt1p decrease, as observed in a previous study (210), the addition of 5 mM $MnCl_2$, and even more consistently the addition of 10 mM $MnCl_2$, induces a rapid and acute Gdt1p drop (Figure 29A). It should also be noticed that 500 µM Mn^{2+} addition is sufficient to trigger Gdt1p degradation in the *pmr1Δ* strain (Figure 29D). This lower threshold probably results from a lower ability of yeast cells to deal with high cytosolic Mn^{2+} amounts when Pmr1p is not effective.

Interestingly, when looking at growth speed after $MnCl_2$ addition, it looks like cells go through an adaptation period. Especially under 10 mM Mn^{2+} treatment, growth speed decreases steeply during the second hour of Mn^{2+} treatment, but eventually recovers slightly afterwards (Figure 29B). To definitely affirm it, cell growth should be monitored more carefully.

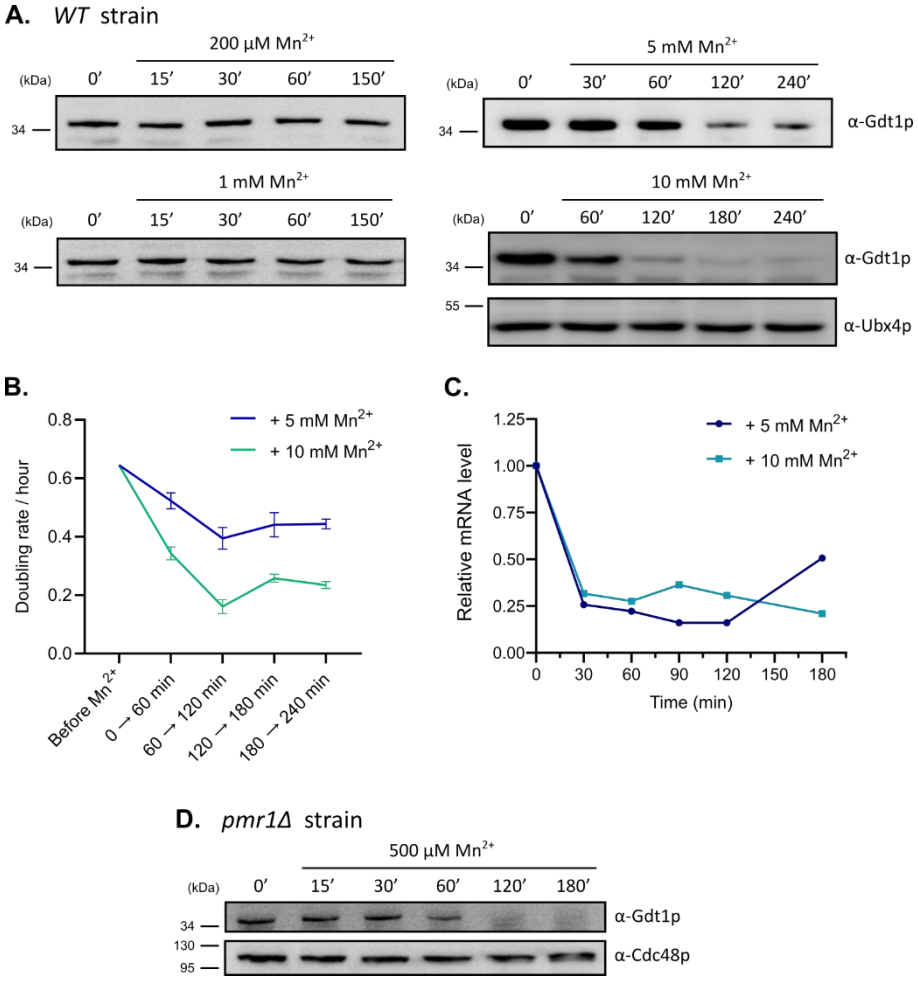

Figure 29. Gdt1p degradation upon Mn^{2+} exposure.
Cells were grown in YD medium to mid-log phase, $MnCl_2$ was added in the extracellular medium and cells were collected at different time points to analyze endogenous Gdt1p abundance by *western blotting*, *GDT1* mRNA level and growth speed. **A.** The *WT* strain was subjected to increasing amounts of Mn^{2+} to establish from which treshold does Gdt1p degradation occur. At least four biological replicates were performed with 5 and 10 mM $MnCl_2$ addition, from which one representative experiment is shown. **B.** The doubling rate of the *WT* strain is compared before and after the addition of 5 mM or 10 mM $MnCl_2$ in the extracellular medium. The number of doubling per hour is depicted. The higher the value, the faster cells divide. N = 13 to 23. Mean and SEM are represented. **C.** *GDT1* mRNA level is analyzed by RT-qPCR after Mn^{2+} addition in the extracellular medium of *WT* culture. Data are presented as relative to the initial time point (0 min). RT-qPCR experiments were performed by Quentin Lejeune during his Master thesis. **D.** As *pmr1Δ* strain is more sensitive to Mn^{2+} than the *WT*, it was subjected to a lower Mn^{2+} addition, 500 µM. Ubx4p and Cdc48p are used as loading controls. Protein markers are indicated (kDa).

b. Natural turnover of Gdt1p does not justify Mn^{2+}-dependent Gdt1p decrease

The decrease of Gdt1p abundance could result either from a diminution of its synthesis combined to the natural turnover of the protein, or from the activation of a specific degradation process triggering a fast decline of Gdt1p.

In the yeast genome database, Gdt1p half-life is reported, worth 3.1 hours [https://yeastgenome.org/locus/S000000391/protein], while the median protein half-life in budding yeast is 8.8 hours (283). This statement is based on a proteomic analysis, where the decay of proteins containing heavy isotopes was followed over time (283). As Gdt1p decrease is very pronounced in our experiments within two hours of Mn^{2+} exposure, the natural turnover alone is not sufficient to explain Gdt1p disappearance. To robustly confirm this, during his Master thesis, Quentin Lejeune experimentally recorded the natural turnover of Gdt1p upon cycloheximide treatment, an inhibitor of protein synthesis. He observed that, after the addition of cycloheximide, more than 5 hours are required to lose half of Gdt1p signal in *western blotting* (Figure 30).

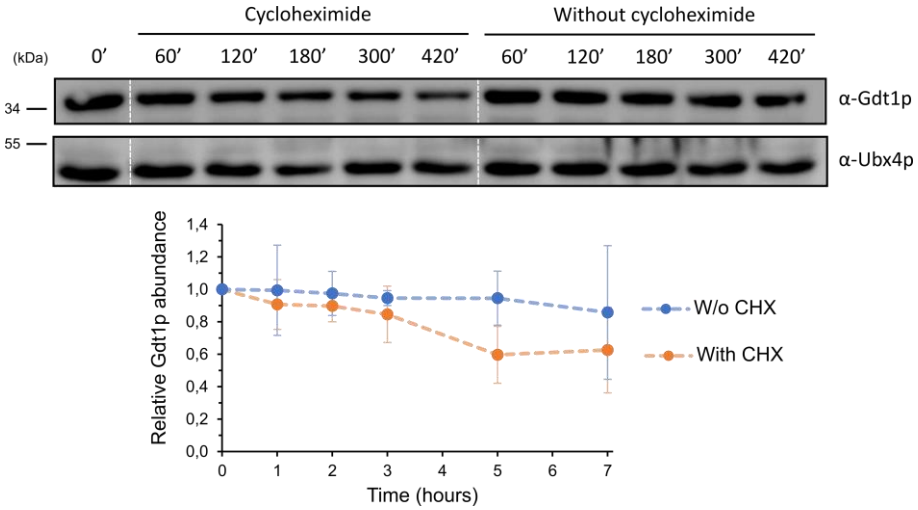

Figure 30. Gdt1p natural turnover indicates a half-life of about 5-7 hours.
After cycloheximide (CHX) was added to cell culture at a concentration of 100 µg/ml, endogenous Gdt1p decrease was followed by *western blotting*. This measurement serves as a read-out of Gdt1p half-life. Control with cells not treated with CHX was carried out in parallel. Ubx4p serves as the loading control and protein markers are indicated (kDa). Representative experiment of three biological replicates. The graph represents the relative Gdt1p abundance compared to the reference before CHX treatment (0'). For quantification, Gdt1p *western blot* intensity was normalized to the loading control intensity (α-Ubx4p). Experiments performed by Quentin Lejeune during his Master thesis.

In parallel, Quentin Lejeune also assessed the transcriptional regulation of *GDT1* by quantifying *GDT1* mRNA level in various *S. cerevisiae* deletant strains and upon Mn^{2+} addition. Interestingly, as Gdt1p protein abundance, *GDT1* mRNA level also decreases rapidly after Mn^{2+} addition, with a 70% decrease within 30 minutes (Figure 29C). However, decrease of Gdt1p abundance and of *GDT1* mRNA are not always correlated. For example, there is no apparent change of *GDT1* mRNA level in the *pmr1Δ* strain compared to the *WT* strain, while Gdt1p quantity is substantially lowered in this strain (Figure 27C).

c. Gdt1p is targeted to the vacuole for degradation

As Gdt1p seems actively degraded upon Mn^{2+} exposure, we aimed at identifying via which degradation process. In human cells, TMEM165 is presumably sent to the lysosome for degradation, as chloroquine treatment, which disorganizes the endo-lysosomal system (284), abolishes TMEM165 disappearance (210). In our hands, Gdt1p degradation is fully stopped in a *pep4Δ* strain that is characterized by inactive vacuolar proteases (12). Actually, no significant decrease of Gdt1p is observed, even after 4 hours (Figure 31A *and* B).

To go further, we constructed GFP-tagged versions of Gdt1p to track it by microscopy. As the N-terminal part of the protein is predicted to be cleaved, it is not a suitable place for GFP tagging. When we tried to tag Gdt1p at its C-ter, either into a plasmid expression system or by direct modification of the genome, we unfortunately never got the DNA construct of interest. The few popping clones were systematically mutated, like as the chimeric GDT1-GFP sequence was counterselected. Eventually, we achieved to tag Gdt1p with the GFP by inserting it in between amino acids 29 and 30 of Gdt1p, *i.e.* a few amino acids after the predicted signal peptide cleavage site, on the luminal side of the protein.

By tracking this Gdt1(1-29)-GFP-(30-280)Gdt1 construct before and after Mn^{2+} addition, the fluorescent pattern thoroughly changes. From small and focused dots typical of *S. cerevisiae* Golgi structures before Mn^{2+} addition, we end up after Mn^{2+} addition with large and blurred fluorescent compartments typical of the broad yeast vacuoles, where the GFP accumulates and remains relatively stable (Figure 31C).

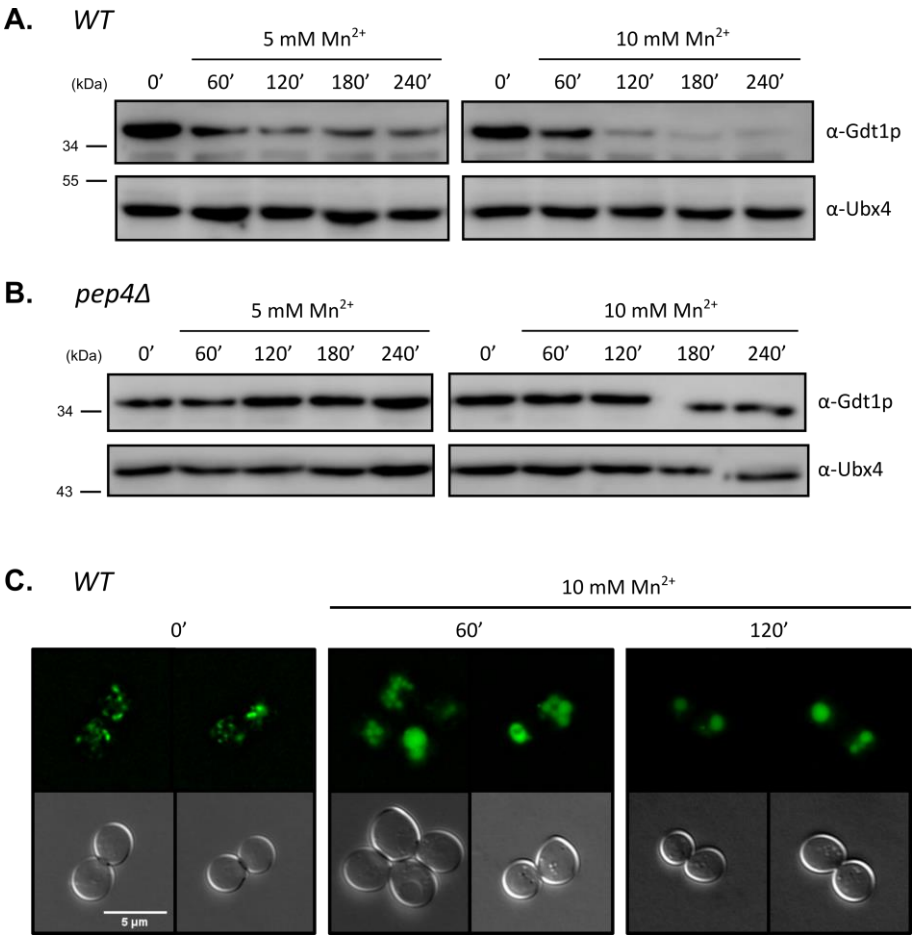

Figure 31. Vacuolar degradation is responsible for Gdt1p decrease after Mn^{2+} supplementation.

A. By exposing *WT* cells to 5 or 10 mM $MnCl_2$ for 0 to 240 minutes, endogenous Gdt1p abundance rapidly decreases. Representative *western blot* of at least three biological replicates. **B.** In the *pep4Δ* strain, no substantial decrease of endogenous Gdt1p is observed after $MnCl_2$ addition. Ubx4p is used as a loading control and protein markers are indicated (kDa). Representative *western blot* of at least three biological replicates. **C.** The *WT* strain transformed with pRS416-pTPI-GDT1(1-29)-GFP-(30-280)GDT1 plasmid is incubated with 10 mM $MnCl_2$ for up to 120 minutes. Cells are imaged by epifluorescence microscopy just before Mn^{2+} addition and after 60 or 120 minutes of Mn^{2+} exposure. Differential interference contrast (DIC) method is used to visualize cells shape and GFP signal depicts Gdt1p localization. Two representative images are shown for each condition.

d. Autophagy is not implicated in Mn^{2+}-dependent Gdt1p degradation

When living organisms are facing intense stresses, such as the large excess of Mn^{2+} we apply to yeast cells in our experiments, they have to significantly transform their metabolism and to remodel their defense mechanisms to overcome the stress. One could imagine that autophagy could be activated to broadly transform cellular proteome. Therefore, we tested two strains defective for autophagy, *atg1Δ* and *atg2Δ*, and applied again the usual Mn^{2+} addition. As Gdt1p disappears in those autophagy mutants as in the *WT* strain, it seems that autophagy is not involved in the process of Gdt1p degradation (Figure 32A *and* B). Alternatively, the GOMED (Golgi membrane-associated degradation) pathway, which is parallel to autophagy but independent of it, is a bulk degradation process of Golgi compartments (271) that could be responsible for Gdt1p disappearance. However, when monitoring the amount of other Golgi localized proteins, such as the Ca^{2+}/Mn^{2+}-ATPase Pmr1p or the integral membrane component of ER-derived COPII-coated vesicles Emp47p, during the same Mn^{2+} exposure, their abundance does not look affected (Figure 32C). Those results suggest that, rather than a bulk degradation of Golgi compartments, a quite specific degradation process probably extracts Gdt1p from the Golgi to send it to the vacuole for degradation.

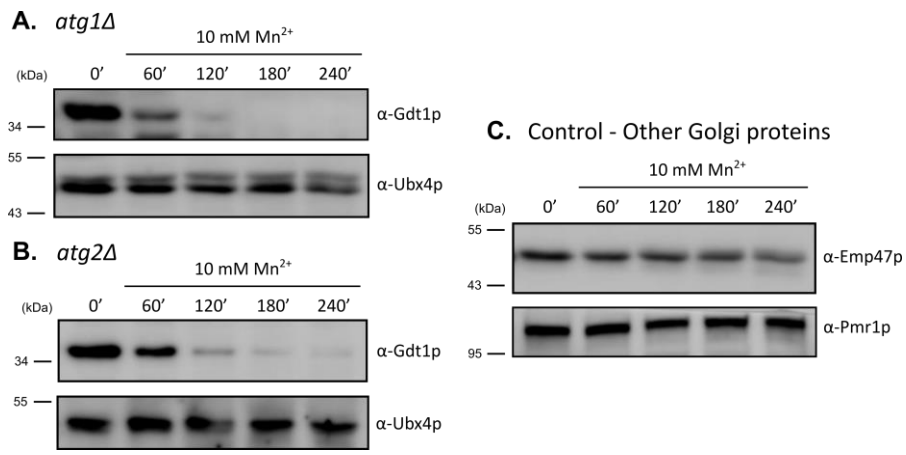

Figure 32. Autophagy does not cause Gdt1p degradation upon Mn^{2+} exposure.
A. *and* **B.** In a similar manner as in previous experiments, Gdt1p degradation was initiated by 10 mM $MnCl_2$ addition in the extracellular medium of exponentially growing cells. Total protein extracts from *atg1Δ* (A.) and *atg2Δ* (B.) cultures were collected every sixty minutes and analyzed by *western blotting*, and endogenous Gdt1p was analyzed. Ubx4p serves as a loading control. **C.** The abundance of two other Golgi localized proteins, Emp47p and Pmr1p, was also followed during the same experimental procedure. Representative *western blot* of at least two biological replicates (from *atg1Δ* and *gga2Δ* strains, where Gdt1p is normally degraded). Protein markers are indicated (kDa).

5. The degradation route of Gdt1p involves a transit via the MVB

Many proteins that are targeted to the vacuole transit via the multivesicular bodies. The vesicles coming from the endocytic route or from the TGN are recognized by a specific t-SNARE, Pep12p, which states at the membrane of this prevacuolar compartment (285, 286). MVB are characterized by a peculiar vesicular budding phenomenon, that goes from MVB membrane to MVB lumen. In this manner, some membrane proteins become internalized into the MVB lumen. Later on, when MVB fuse with vacuoles, internalized vesicles end up in the lumen of the vacuole and undergo degradation and proteolysis. Vesicular budding into MVB lumen is assisted by four *endosomal sorting complexes required for transport* (ESCRT) components that act successively, ESCRT-0, ESCRT-I, ESCRT-II and ESCRT-III (287).

Hence, we wondered whether Gdt1p reaches the vacuole via the MVB by analyzing its degradation in strains deleted either for *PEP12*, or for ESCRT subunits. Quite clearly, we observe that Gdt1p degradation requires Pep12p, as Gdt1p is stable when analyzed by *western blotting* in *pep12Δ* strain during Mn^{2+} treatment (Figure 33A). When looking by microscopy at Gdt1p localization, it appears that Gdt1p is retained in small vesicles looking like Golgi, endosomes, or other intermediate vesicles of the secretory pathway (Figure 33B). Colocalization experiments could specify it more precisely.

Elsewhere, in ESCRT mutants, Gdt1p degradation is not really abolished. Rather, in some ESCRT mutants there is remarkable appearance and accumulation of an intermediate degradation product of Gdt1p (Figure 33C). The accumulation of this product could result from the proteolytic activity of proteases in the lumen of prevacuolar compartment on few accessible positions. Indeed, Gdt1p possesses only short soluble loops at the luminal side of the membrane. Its main loop – that is recognized by our α-Gdt1p antibodies – is facing the cytosol (2) and would then be protected by the lipid bilayer. By microscopy, the Gdt1p-GFP chimeric proteins still largely reach the vacuole in *vps36Δ* and *vps24Δ* ESCRT mutants. However, we also notice the accumulation of fluorescent signal in peculiar prevacuolar compartments directly adjacent to vacuoles that are characteristic of class E *vps* mutants (288-290). In order to precisely identify vacuoles and their neighboring class E *vps* aberrant compartment, FM4-64 was used as a membrane marker. FM4-64 is a hydrophobic fluorescent compound that accumulates in lipidic membranes. If pulse-chased, FM4-64 first stains the peripheral plasma membrane, rapidly followed by endosomes staining, and finally ending with vacuolar staining. This is because of the endocytic route that brings material from the plasma membrane to the vacuolar membranes.

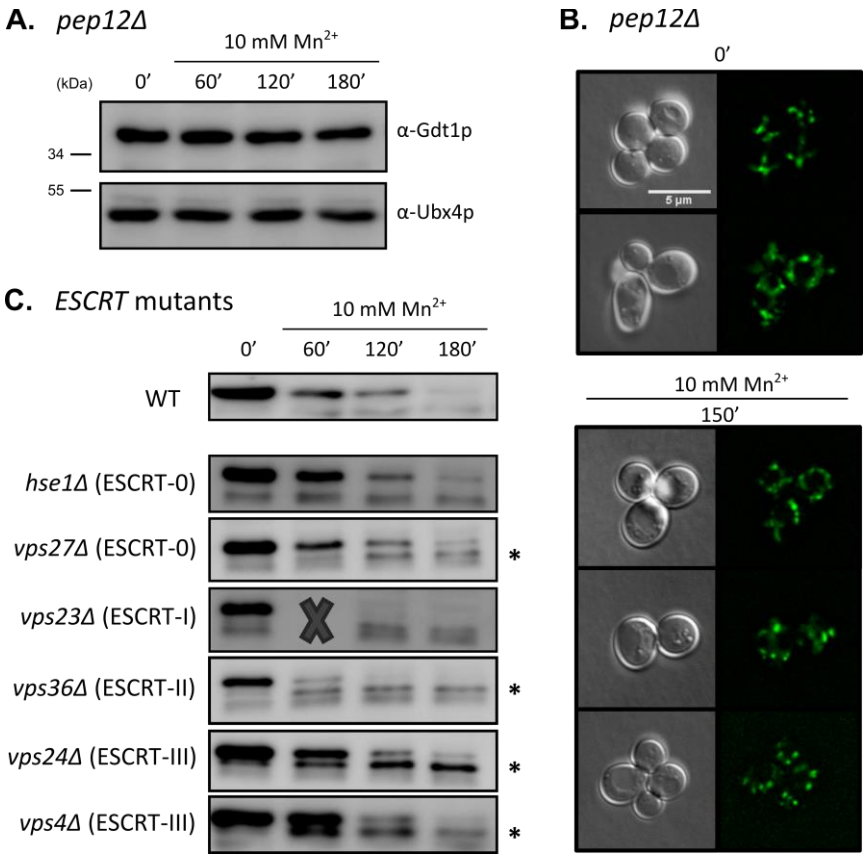

Figure 33. Gdt1p transits via the MVB before reaching the vacuole.
A. Exponentially growing *pep12Δ* cells are subjected to 10 mM $MnCl_2$ addition and cells were collected every sixty minutes. Endogenous Gdt1p was analyzed, Ubx4p serves as the loading control and protein markers are indicated (kDa). Representative *western blot* of two biological replicates. **B.** Gdt1(1-29)-GFP-(30-280)Gdt1 chimeric protein expressed from pRS416 plasmid under the control of pTPI promoter in the *pep12Δ* strain was viewed by microscopy, either prior to Mn^{2+} addition, or 150 minutes after the addition of 10 mM $MnCl_2$. GFP signal and corresponding DIC pictures are presented. Representative images are shown. **C.** Endogenous Gdt1p abundance was followed in various ESCRT mutants during high Mn^{2+} exposure, and compared to the *WT* strain. Indicated stars point out the accumulation of intermediate degradation products in some ESCRT mutants. **D.** Gdt1(1-29)-GFP-(30-280)Gdt1 expressed under pTPI promoter from pRS416 plasmid in *WT* and *vps24Δ* and *vps36Δ* ESCRT mutants was imaged prior and/or after 150 minutes incubation with 10 mM $MnCl_2$. In order to unambiguously detect vacuoles, FM4-64 was pulse-chased (15 min pulse, 2 washings, 30 min chase, temperature maintained at 30 °C). DIC, FM4-64, GFP and merge of both fluorescent channels are presented. Two representative images are shown for each condition. White arrows point out typical class E *vps* mutant phenotype.

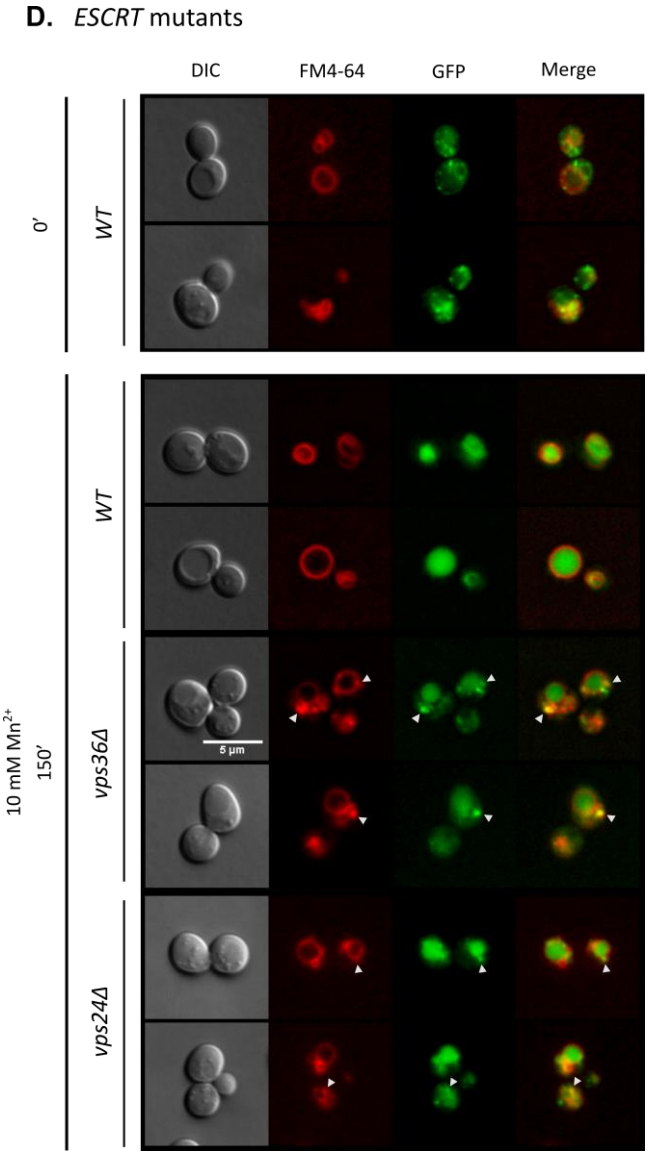

Figure 33 (*continued*).

Here, we applied a 15 minutes pulse followed by 30 minutes chase, while cells were continuously kept at 30 °C. Without Mn^{2+} addition, Gdt1p-GFP mostly appears in small vesicles that do not colocalize with the vacuoles. After 150 minutes of Mn^{2+} treatment, the GFP signal is almost exclusively detected into vacuoles in the *WT* strain. In *vps36Δ* and *vps24Δ* ESCRT mutants, the GFP signal stains vacuoles and "aberrant" class E compartments adjacent to vacuoles (Figure 33D).

6. Golgi exit of Gdt1p remains unknown

Gdt1p transits via the MVB *en route* to the vacuole to endure proteolysis. This is a well-known degradation pathway, which is usually followed by many plasma membrane proteins once they are endocytosed. However, the targeted degradation of membrane proteins from other compartments of the endomembrane system is less characterized.

Therefore, as no evident degradation mechanism is known for Golgi resident membrane proteins, we tested whether the most common trafficking routes from the Golgi to the vacuole could be responsible for Gdt1p degradation. AP-1 and AP-3 clathrin-associated complexes commonly drive proteins from the Golgi to vacuoles. In *apm1Δ, apm3Δ*, and *apm1Δapm3Δ* double deletant, where the mu subunit of AP-1 and AP-3 complexes are absent, Gdt1p degradation process is not altered when compared to its diminution in *WT* strain (Figure 34A *to* D). Alternatively, Gdt1p could transit via the plasma membrane before reaching the vacuole through endocytosis. However, no change of the degradation timing is observed in the *end3Δ* strain (Figure 34E).

The Golgi/TGN are also dedicated to protein recycling. Some plasma membrane proteins, after being endocytosed, can be retrieved from early endosomes and sent to the TGN for recycling instead of being targeted to the vacuole for degradation. This routing involves complex signaling mechanisms, where ubiquitin tagging is usually the key actor that differentiates proteins, hence specifying their fate.

Ubiquitylation is a multistep process. The E1 ubiquitin-activating enzyme prepares the ubiquitin moiety, which is next bound to E2 ubiquitin-conjugating enzymes and finally transferred to their targets by the action of E3 ubiquitin ligases (291). In yeast, several E3 ubiquitin ligases exist. Rsp5p is the main ubiquitin ligase involved in the endocytosis of plasma membrane proteins (292). It was also shown that Rsp5p can be implicated in the ubiquitylation of proteins at other stages of the secretory pathway (293, 294). Next to Rsp5p, Tul1p is the E3 ubiquitin ligase of the Dsc E3 ligase complex (276, 295). This complex regulates protein trafficking at the Golgi, as well as in endosomal network and at the vacuole membrane (296). Therefore, we wondered whether those ubiquitin ligases could be involved in Gdt1p degradation process.

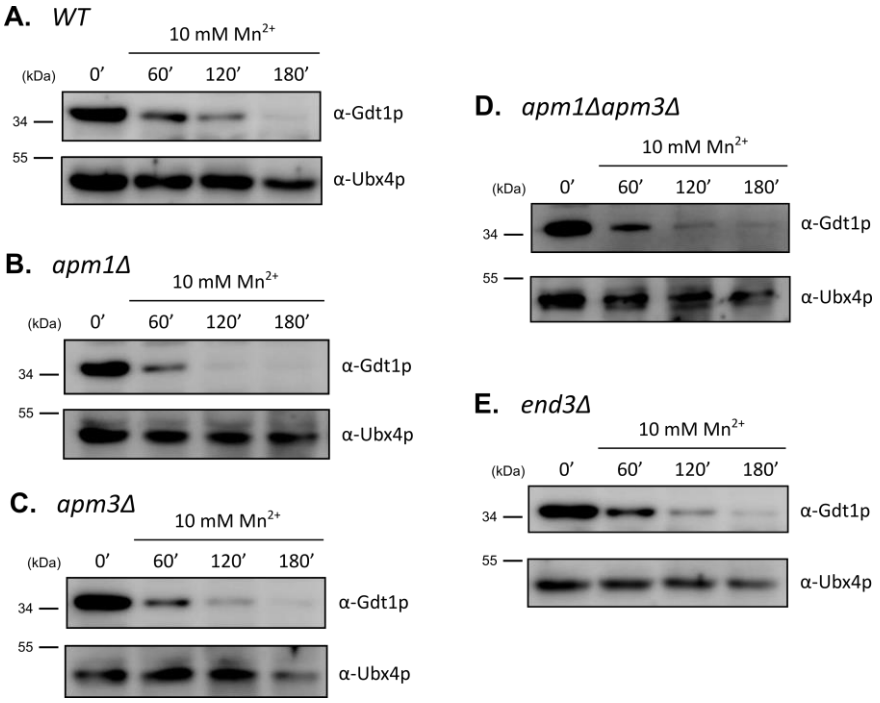

Figure 34. Gdt1p does not follow the classical clathrin-mediated Golgi to vacuole routes.
Degradation of endogenous Gdt1p upon Mn^{2+} exposure was assessed in several strains deficient for AP-1, AP-3 or endocytosis. **A.** As compared to a control, Gdt1p degradation after $MnCl_2$ addition occurs with a similar timing in **B.** *apm1Δ*, **C.** *apm3Δ*, **D.** *apm1Δapm3Δ* and **E.** *end3Δ* strains. Ubx4p is used as a loading control and protein markers (kDa) are indicated.

The deletion of *TUL1* does not change Gdt1p degradation dynamic (Figure 35C). In contrast, by using the *npi1-1* strain, where Rsp5p is weakly expressed (297), we can observe that Gdt1p degradation takes place slower than in the *WT* strain (Figure 35A, B, D *and* E). However, the faint degradation slowdown contrasts with the severe degradation arrest described in other studies where *npi1-1* strain revealed Rsp5p implication in the endocytosis of specific plasma membrane cargoes (298, 299). Therefore, we can speculate that the slower degradation in our experiments could result from indirect effect of *RSP5* downregulation rather than from a direct ubiquitylation activity on Gdt1p.

Finally, we looked at a large set of proteins possibly involved in Golgi to vacuole specific degradation process. None of the mutant strains we assessed had a significant impact on Gdt1p Mn^{2+}-triggered degradation (Annex 4). Here is the exhaustive list of tested mutants: *gga1Δ*, *gga2Δ*, *gga1Δgga2Δ*, that

are Golgi clathrin adaptors, and the *gga1Δapm1Δ* strain ; *ssh4Δ*, *ear1Δ*, *bsd2Δ*, *rcr1Δ*, *rcr2Δ*, *bul1Δ*, *bul2Δ*, *bul1Δbul2Δ* and *EN60* strain, which are strains deficient for Rsp5p adaptors bordering the Golgi, the endosomes/MVB or the plasma membrane, some of them being involved in the regulation of Smf1p and Smf2p Mn^{2+}-transporters (300-302), some others regulated by the calcineurin signaling pathway (303) ; *arf2Δ*, a GTPase involved in intra-Golgi trafficking ; *doa4Δ*, a deubiquitinase that is required for ubiquitin recycling in prevacuolar compartments ; *sna1Δsna2Δsna3Δsna4Δ*, which are involved in protein sorting and trafficking and could serve as Rsp5p adaptors.

In some of those strains, we can notice a slight slowdown of the degradation process – that could be confirmed by experimental repetitions –, but there was no strong phenotype. Hence, we cannot stand out Gdt1p interactors involved in Gdt1p retrieval from its usual place, the *cis*- and *medial*-Golgi, to be sent in a vacuolar degradation route.

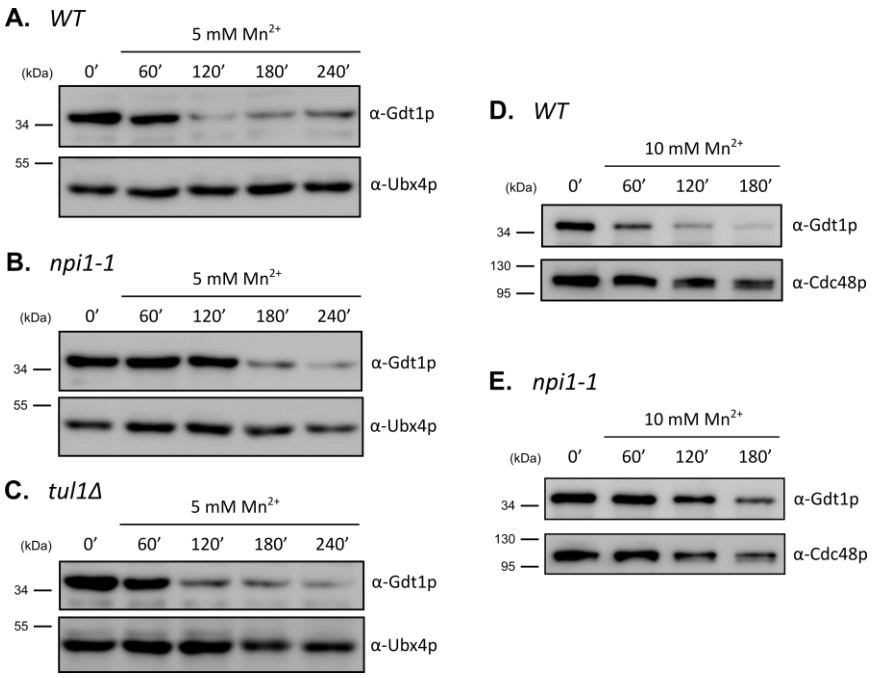

Figure 35. Ubiquitin ligases Rsp5p and Tul1p are not essential for Gdt1p degradation.
The degradation of endogenous Gdt1p following the addition of 5 or 10 mM Mn^{2+} is analyzed in **A.** *and* **D.** a control strain, **B.** *and* **E.** the *npi1-1* strain where Rsp5p is downregulated and **C.** the *tul1Δ* strain. Rsp5p downregulation causes Gdt1p delay of degradation of about 60 minutes. Ubx4p and Cdc48p are used as loading controls, and protein markers (kDa) are indicated. For the *npi1-1* strain, representative experiment of two biological replicates at each Mn^{2+} concentration.

7. Discussion

Effective regulatory mechanisms control Gdt1p abundance

When looking at Gdt1p regulation, it is particularly interesting to notice that Gdt1p abundance is regulated both at transcriptional and post-translational levels. Both regulatory mechanisms are controlled by Gdt1p substrates. Hence, when the Golgi-localized Pmr1p ATPase is deficient for Mn^{2+} transport, it causes a decrease of Gdt1p. On the contrary, Ca^{2+} supplementation boosts Gdt1p abundance. Pmr1p and Gdt1p were sometimes proposed to have complementary functions to fill the Golgi lumen with Ca^{2+} and Mn^{2+} cations (133, 208). However, Gdt1p decline when Pmr1p is absent rather suggests opposite – or at least distinct – physiological functions. Next to this, Gdt1p could be stabilized in the Golgi by some physical interaction with Pmr1p, as deletion of those genes display several similar phenotypes and that they considerably colocalize in Golgi compartments (90). Nonetheless, Gdt1p abundance is not simply correlated to Pmr1p presence/absence, therefore indicating that Gdt1p stability does not solely depend on Pmr1p presence in the Golgi membrane.

Eventually, extracellular Mn^{2+} excess triggers a rapid vacuolar Gdt1p degradation. A similar downregulation of the Smf1p plasma membrane Nramp metal transporter, which is degraded at the vacuole upon Mn^{2+} addition, has been described in the literature (304). Therefore, the simplest explanation is that cells proceed to Gd1p degradation to protect themselves from toxic manganese. However, this explanation is not fully satisfying because *gdt1Δ* cells are also more sensitive to Mn^{2+} and accumulate more manganese than the *WT* strain (92).

Anyway, as cells have maintained a similar degradation procedure for the human TMEM165 and the yeast Gdt1p in the course of evolution (210), this suggests that it is a crucial mechanism for cell survival. In yeast, Gdt1p degradation process is also accompanied by a restriction of its mRNA level. It avoids futile cycles of protein synthesis / protein degradation and constraints Gdt1p abundance at a low level.

Gdt1p regulation is correlated to healthy Golgi functions

In previous studies, the role of TMEM165 and Gdt1p for the glycosylation process has been extensively studied (91, 172, 195). In yeast, glycosylation troubles appear in the *gdt1Δ* strain exposed to high extracellular Ca^{2+}. On the contrary, Ca^{2+} supplementation corrects the glycosylation problems of the

pmr1Δ strain. Here, we observed that Ca^{2+} addition to *pmr1Δ* cells have a triple effect. It rectifies glycosylation, it increases Gdt1p abundance and it improves growth rate. It is difficult to know exactly what is the underlying explanation for the three above-mentioned elements. Yet, as Ca^{2+} addition does not improve growth of the *pmr1Δgdt1Δ* strain and induces glycosylation defects in the *gdt1Δ* strain, we can speculate that Gdt1p increase is necessary for the two others parameters to become optimal. Further research would be necessary to decipher the determinants of proper Golgi functioning.

The degradation route conveying Gdt1p from the Golgi to the vacuole is not completely identified

Our data quite clearly demonstrate that Gdt1p is actively sorted from the Golgi membrane to be sent to the vacuole lumen upon Mn^{2+} exposure. Membrane protein degradation process usually requires ubiquitylation, trafficking to MVB membrane, internalization into MVB lumen and finally release into the vacuole. ESCRT components seem indeed required to support an efficient degradation of Gdt1p. Especially with mutants of the ESCRT-II and ESCRT-III complexes, we also noticed the stabilization of a degradation product of Gdt1p. This indicates that at least a pool of the proteins remains stuck in the membrane of prevacuolar compartments. This also suggests that several ways could maybe be followed by Gdt1p for its degradation. As an alternative, Gdt1p could be deprived of its ability to be recognized by the ESCRT machinery. For example, it is known that ubiquitylation serves as a marker to enter in the ESCRT pathway (305). If some ubiquitylation of Gdt1p is mildly stable, it could lose it before being internalized into the MVB lumen and hence stay stuck at the MVB membrane.

Regarding a possible ubiquitylation step, we were unable to determine whether Gdt1p degradation accounts on such protein tagging. In proteomic analyses, Gdt1p ubiquitylation was observed (306, 307). However, after Mn^{2+} addition, we could not detect ubiquitylated Gdt1p (*data not shown* – experiments performed by Guillemette van Raemdonck during her Master thesis). Of course, protein ubiquitylation is often transient and the pool of target ubiquitylated protein can be quite faint compared to the total Gdt1p amount. Though, by using several ubiquitin ligases or ubiquitin ligase adaptors mutants, we could not establish whether Gdt1p ubiquitylation is controlling its degradation. The only noticeable observation is some slowdown of Gdt1p decline when the ubiquitin ligase Rsp5p is downregulated, but it could be caused by indirect effects.

Gdt1p exits the Golgi in an unknown manner

Protein trafficking in the Golgi has been extensively studied. Many routing complexes have been characterized and their main cargoes are known. However, those trafficking routes are mostly involved in the normal transport of proteins, solely transiting though the Golgi. Gdt1p usually stands in the Golgi membrane, but is rapidly retrieved from its location just after cells face elevated amounts of extracellular Mn^{2+}. Via which mechanism is Gdt1p taken out of the Golgi remains totally unknown. At least two hypotheses should be considered. Either Gdt1p is constantly recycled from late Golgi cisternae to early Golgi cisternae. This procedure could be turned off due to Mn^{2+} addition, leading to a loss of Gdt1p in the Golgi. Or there is an active mechanism that identifies Gdt1p in the Golgi, tags it or extracts it from its usual place to send it to the vacuole. In order to disentangle the two hypotheses and to try to identify new actors involved in Golgi proteins retention or retrieval, broader screening approaches should be developed.

PART IV

DISCUSSION AND FORMULATION OF NEW HYPOTHESES FROM OUR OBSERVATIONS

« Chaque fois que nous entendrons dire : de deux choses l'une, empressons-nous de penser que, de deux choses, c'est vraisemblablement une troisième. »

Jean Rostand

1. Discussion regarding Golgi pH control mechanisms

The gradual acidification of the secretory pathway lumen is critical to maintain its integrity and to encounter its metabolic functions. Despite the fact that this gradual acidification is a well-established fact, the molecular mechanisms controlling it are far from completely understood.

a. Role of the V-ATPase

More than two decades ago, the V-ATPase has been identified as the main proton pump in the secretory pathway (246). In various organisms, its implication for Golgi and TGN acidification has been directly recorded (161, 241). Here, we highlight that the V-ATPase is also essential for yeast Golgi acidification. This observation was expected. What was less expected is that Stv1p – the Golgi-localized isoform of the subunit *a* of V_0 domain – seems dispensable for Golgi acidification in rapidly growing cells, while *VPH1* deletion – the vacuolar isoform of the same subunit – causes Golgi acidification defects. Stv1p and Vph1p derive from a common ancestor gene that was probably able to fulfill V-ATPase roles both at the Golgi and in the vacuole (308), as it is also the case for some actual species that possess one single subunit *a* isoform (309). Therefore, Stv1p and Vph1p isoforms emergence during evolution probably gave a selective fitness advantage to actual budding yeast cells compared to their ancestor with a single subunit *a* isoform. Keeping Vph1p involved in the usual acidification of the secretory pathway maybe allowed Stv1p to take other more specialized roles, like pH sensing, membrane fusion or V-ATPase regulation (57, 310, 311).

Regarding Golgi organization, several research groups hypothesized that there is a lateral segregation of proteins along Golgi stacks, called "rapid partitioning model", where some zones are dedicated to post-translational modifications and other zones are devoted to the anterograde flux of cargo proteins or to the retrograde recycling of Golgi enzymes (13, 125). Besides, it was highlighted that the Golgi luminal pH drives protein oligomerization, which triggers protein trafficking (44, 45). Although in *S. cerevisiae,* peculiar Golgi morphology may hide such a lateral segregation, one could imagine

that Stv1p – and other subunit *a* isoforms in other eukaryotes – could be involved in the segregation of proteins alongside a single stack by performing acidification in subspecific areas of the Golgi. Alternatively, Stv1p could be required only in specific physiological conditions, for example when cells endure intense cytosolic pH changes, as it happens when there are modifications of the catabolized carbon source. The fact that Stv1p-containing complexes does not undergo dissociation during glucose depletion, while Vph1p-containing complexes do, supports this hypothesis (55, 62). Eventually, Stv1p could also compete with Vph1p to reduce V-ATPase activity in early Golgi compartments, but not/less in late-Golgi, therefore taking part in the implementation of the pH gradient from one Golgi cisternae to the next one.

b. Looking for a H^+ leak channel

Next to H^+ import to the Golgi lumen, putative "leak mechanisms" are expected to balance Golgi pH by allowing controlled H^+ efflux (50, 77, 141, 161). Though, the identity of such leak channel(s) is (are) not determined in yeast. The availability of tools for pH monitoring, as the one we developed in this work, could contribute to the discovery of the sought channel(s). Among the candidates in *S. cerevisiae*, we point out Gef1p, a putative Cl^-/H^+ exchanger (70), or Nhx1p and Kha1p, predicted Na^+/H^+ and K^+/H^+ exchangers (73, 74). Carrying out Golgi pH measurements in strains deficient for those proteins could answer whether they are or not implicated in Golgi pH control. Nevertheless, in our hands, Kha1p is not associated with a more acidic Golgi lumen (Annex 1), and Gef1p and Nhx1p are rather localized in the TGN or in endosomes than at the early Golgi. Henceforth, performing Golgi pH measurements in a yeast mutants' library represents an attractive manner to identify proteins required for Golgi pH balancing.

c. Control mechanisms to maintain Golgi relative acidity

Our measurements highlight that Golgi pH fluctuations are quite restrained compared to cytosolic pH fluctuations. In the cytosol, pH variations come from the production and the consumption of free H^+ ions by metabolic processes and from the influx and the efflux of acido-basic compounds. Those fluctuations are balanced by the action of specific H^+ transporters, mainly the plasma membrane H^+-ATPase Pma1p and the vacuolar V-ATPase (41). In the Golgi lumen, H^+ production can arise from the glycosylation process or from lactose production (80, 191). This metabolic outcome takes part to the needed acidification of the Golgi lumen but should be limited or counteracted to avoid any over-acidification. It presumably occurs thanks to the aforementioned H^+ leak way. Despite this, cytosolic pH changes clearly determine Golgi pH changes, as the shape of pH fluctuations were similar in

both compartments in our experiments. This thermodynamic equilibrium could result from the existence of membrane permeant weak acids and bases, such as ammonia or carbonic acid, or from the presence of secondary transporters in the Golgi membrane. Interestingly, lipid bilayer permeability decreases alongside the secretory pathway. It presumably results from membrane thickening, from the thinner ER membrane to the ticker plasma membrane (95, 312) but cells should also deal with the regulation of channels and secondary transporters involved in H^+ transport. In yeast, the identity of a putative Golgi H^+ leak channel has not been determined (161).

Hence, Gdt1p could operate as the leak channel researchers are looking for. This was already suggested by previous phenotypical assays (80). However, although straightforward, our measurements cannot resolve whether Gdt1p encounters the role of such H^+ leak channel.

Finally, our probe development strategy paves the road to the design of new pH probes. Actually, it would be worthwhile to complete *in vivo* pH recordings specifically in the *cis*-, *medial*- and *trans*-Golgi cisternae or in the TGN of *S. cerevisiae* to gain more insights into the gradual acidification of the secretory pathway.

2. On the way to Gdt1p physiological function elucidation

a. Gdt1p H^+/cation exchange activity could be reversed in accordance with contrasting concentration gradients

By using a bacterial heterologous expression as a tool for transport assays, we highlighted Gdt1p-mediated H^+ transport activity. Furthermore, several experiments underlined Ca^{2+}-Mn^{2+}/H^+ exchange. *In vivo* pH recordings in yeast also brought clues to elucidate Gdt1p physiological function at the Golgi.

According to our pH measurements and to anterior Ca^{2+} and Mn^{2+} phenotypical assays, we propose a model where Gdt1p usually transports Ca^{2+} and Mn^{2+} cations to the Golgi lumen by taking advantage of the H^+ gradient generated by the V-ATPase (Figure 36, left panel). In this situation, the role of Gdt1p is complementary to that of Pmr1p to extrude any excess of cytosolic Ca^{2+} and Mn^{2+} and to feed the secretory pathway with those cations (91, 92, 193, 195). Gdt1p has affinities for Ca^{2+} and Mn^{2+} cations (K_M = 15 µM for Ca^{2+}, 83 µM for Mn^{2+} (92)) that are lower than the ones of Pmr1p (K_M = 0.1 µM for Ca^{2+} (313), 0.02 µM for Mn^{2+} (280)), but is probably characterized by transport kinetic and mechanism that may be beneficial for the cell in some conditions, as we will discuss it hereunder.

The calcium being a cytosolic secondary messenger, it is essential that cells possess transporters able to rapidly cope with any increase of its cytosolic concentration to avoid messy signaling information. Besides, there are increasing evidences that Ca^{2+} is involved in the control of the vesicular trafficking (314, 315) by modulating SNAREs activity (121, 122, 157). Therefore, Gdt1p activity could be important for the proper regulation of Golgi vesicular trafficking thanks to rapid release or re-uptake of Ca^{2+} into the Golgi lumen. Hence, *gdt1Δ* cells exposed to high extracellular Ca^{2+} suffer from glycosylation defects that might result from trafficking defects. As a corollary, in the *pmr1Δ* strain, *GDT1* deletion or overexpression are characterized by trafficking defects in a Ca^{2+}-dependent manner (173). Hence, it is conceivable that local Ca^{2+} signaling events around Golgi compartments, that regulate intra-Golgi membrane trafficking (315), are disturbed when *GDT1* is deficient.

For its part, manganese is a well-known regulator of redox status within biological systems (257) but also serves as a cofactor for several glycosylation enzymes in the Golgi apparatus (316-318). If it is not loaded sufficiently in the Golgi lumen, it is a cause of glycosylation disorder (319). In favorable growth conditions, Gdt1p is maybe a partner of Pmr1p to provide their Mn^{2+} cofactor to glycosylation enzymes.

However, not only Gdt1p-mediated Ca^{2+} and Mn^{2+} transport could be impactful on Golgi homeostasis. Especially, the pH is a key parameter for most biochemical phenomena. Protonation or deprotonation of amino acids will directly affect the shape and therefore the functionality and the interactions of most proteins and pH decline from secretory pathway "origin", *i.e.* the ER, to "destination", *i.e.* exocytic vesicles and vacuoles, is important to maintain the organization of the secretory pathway (50, 320). Here, our data let us speculate that Gdt1p is able to use the transmembrane Ca^{2+} and Mn^{2+} gradient to convey protons from the cytosol to the Golgi lumen, in support to the V-ATPase, when cells are facing a rapid cytosolic pH increase (Figure 26C *and* 26E). Thanks to Gdt1p transport activity, the Golgi lumen does not experience a too intense pH increase and rather keeps some acidity in the Golgi lumen. Hence, we complete our model with a putative reverse transport activity (Figure 36, right panel). Of course, we have to be cautious in the interpretation of the measurements, as we do not know how all the transporters act during such pH fluctuations, and as we cannot monitor all the ionic gradients simultaneously. Nevertheless, our hypothesis is that the reverse activity of Gdt1p, by participating in the maintenance of an acidic Golgi luminal pH, could help preserving the Golgi structure and ensures a fast renaissance of Golgi metabolic functions by avoiding losses of

Golgi resident enzymes and mistargeting of incompletely modified cargoes. Accordingly, Gdt1p maybe provides some fitness advantage to its host cell.

Interestingly, in human cells, mutations or depletion of TMEM165 is associated with a more acidic steady-state luminal pH (90, 171). As this trend is opposite to the observations we performed in this study, it supports the hypothesis that GDT1 family members could perform transport of H^+ (and of Ca^{2+} and Mn^{2+}) in the two directions, according to the relative concentration gradients across the Golgi membrane.

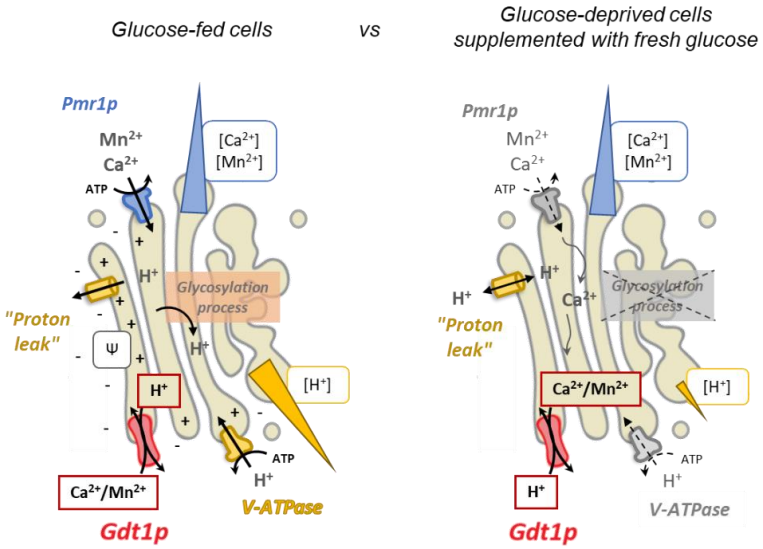

Figure 36. Model of reversible transport activity mediated by Gdt1p.
Left part: In favorable growth conditions, when cells are fed with glucose and that ATP is easily available, both the V-ATPase and Pmr1p are actively pumping protons and divalent cations from the cytosol to the Golgi lumen. It engenders a net gradient of Ca^{2+}, Mn^{2+} and H^+, as well as a positive inside membrane potential Ψ (50, 68). Moreover, the activity of glycosylation enzymes engenders a release of protons within the Golgi lumen and participates in its acidification (80). With the hypothesis that several H^+ ions are exchanged for a single Ca^{2+} or Mn^{2+} cation, Gdt1p would import Ca^{2+} and Mn^{2+} cations and export H^+ in an energetically favorable manner. In those conditions, Gdt1p supports Pmr1p in the loading of the Golgi lumen with Ca^{2+} and Mn^{2+}. Furthermore, the presumed H^+ leak system that participates in the efflux of H^+ out of the Golgi could get the assistance of Gdt1p for this purpose. **Right part:** During glucose deprivation, yeast cells get their cytosol acidified because the plasma membrane Pma1p H^+-ATPase and the secretory pathway/vacuolar V-ATPase are unable to export protons out of the cytosol. In parallel, the glycosylation process is shut down. As some passive equilibration mechanisms are still present, the Golgi to cytosol pH gradient and the membrane potential will decline until they are neutralized. When glucose is added back, the cytosolic pH increases rapidly (Figure 26C). As a result, Gdt1p could revert its transport activity to take advantage of the Ca^{2+} and Mn^{2+} gradients that are reminiscent from earlier period and/or regenerated by Pmr1p, to import protons from the cytosol to the Golgi lumen. Gdt1p would therefore participate in the maintenance of some acidity within the Golgi lumen.

b. Prediction of Gdt1p transport stoichiometry

As we postulated that Gdt1p can act as a Ca^{2+}-Mn^{2+}/H^{+} exchanger, the transport stoichiometry appears as an important question. By using the Gibbs equation, we can analyze the different possibilities from a thermodynamic point of view. Of course, all the parameters are not precisely known. Especially, little is known regarding the Mn^{2+} concentrations, both in the cytosol and in the Golgi lumen. Next, even if predicted as slightly positive inside, the Golgi membrane potential has never been recorded in yeast cells. Therefore, we will only consider Ca^{2+}/H^{+} exchange in the following calculations, and we will arbitrary assume a null membrane potential.

Gibbs equation: $\Delta G = 2.303\ R\ T \log(C_{Golgi}/C_{cytosol}) + Z\ F\ \Delta V$

Where: ΔG*: free-energy change (kJ/mol)*
R*: gas constant (kJ/(mol*K))*
T*: temperature (K)*
C_{Golgi}*: concentration of the considered ion in the Golgi*
$C_{cytosol}$*: concentration of the considered ion in the cytosol*
Z*: charge of the considered ion*
F*: Faraday's constant (kJ/(mol*K))*
ΔV*: membrane potential (V)*

For the transport to be thermodynamically favorable: $\Delta G = \Delta G_{Ca^{2+}} + x\ \Delta G_{H^{+}} \leq 0$
Where "x" represents the number of H^{+} ***ions exchanged for one*** Ca^{2+} ***cation***

At steady-state, considering that $pH_{cytosol} = 7.3$ *(Figure 26A) ;* $pH_{Golgi} = 6.7$ *(Figure 26B) ;* $[Ca^{2+}]_{cytosol} = 100$ *nM (Figure 6) ;* $[Ca^{2+}]_{Golgi} = 100\ \mu M$ *(Figure 6) ;* $\Delta V = 0$.

The Gibbs equation becomes:
$2.303\ R\ T \log (10^{-4}/10^{-7}) + Z\ F\ 0 \leq - x\ 2.303\ R\ T \log (10^{-7.3}/10^{-6.7}) + Z\ F\ 0$

Hence leading to: $x \geq 5$

Suggesting that the energy provided by the efflux of five H^{+} ions from the Golgi lumen to the cytosol would be required to import a single Ca^{2+} cation during steady-state growth. Again, as we had to arbitrary choose the $[Ca^{2+}]_{Golgi}$ and the Golgi membrane potential, such estimation has to be taken with caution.

During glucose pulse experiment, the pH gradient is reduced, but the Ca^{2+} gradient could be maintained, hence leading to feasible reverse transport activity.

c. As many membrane transporters, Gdt1p is regulated by its substrates

The transcriptional and the post-translational regulation of transporters by their own substrate is a usual loop control system. It is easy to understand for plasma membrane transporters since cells have to avoid overaccumulation of potentially toxic compounds (298) or, for fitness purposes, to favor preferential nutrients when available (297). If plasma membrane selectivity cannot adequately control the influx of chemicals, then transporters from intracellular compartments can sometimes compensate. Apart, extracellular fluid that is internalized by endocytosis finally ends up in the lumen of the endomembrane system, via the endocytic route, the recycling pathway, and the anterograde route. Consequently, organellar transporters should be controlled accordingly, either overexpressed or downregulated.

Here, we are the witnesses of Gdt1p regulation by two of its substrates, the Ca^{2+} and Mn^{2+} cations. Surprisingly, the addition of the two cations have an opposite effect on Gdt1p cellular abundance. While Ca^{2+} rather increases Gdt1p level, Mn^{2+} addition, from a certain concentration threshold, causes a fast drop of Gdt1p amount. As the two cations are expected to be transported by Gdt1p in the same direction, as stated from competition transport assays (92), it is difficult to draw a single model to explain the two opposite regulatory effects.

The most spectacular observation is the rapid targeting of Gdt1p to the vacuole upon high Mn^{2+} exposure. Gdt1p degradation is even combined with a transcriptional downregulation. The manganese transition metal, while essential for various cellular processes and helpful to neutralize reactive oxygen species (257), becomes very harmful at high concentration (321-323). Hence, cells probably evolved control mechanisms to avoid excessive cellular Mn^{2+} entry. Of course, Gdt1p resides in intracellular compartments. When there is high extracellular Mn^{2+}, we assume that $[Mn^{2+}]$ increases in the cytosol too. Pmr1p probably accentuates its pumping towards the Golgi lumen, as a detoxification mechanism. In parallel, the retrograde trafficking maybe brings extracellular Mn^{2+} into the Golgi lumen. If the Mn^{2+} concentration increases substantially in the Golgi lumen, one could imagine that the cell has to protect itself against putative Gdt1p-mediated Mn^{2+} leakage from the Golgi to the cytosol. To avoid an unconsidered Mn^{2+} influx towards the cytosol, yeast and human cells so actively kick off Gdt1p and TMEM165 out of their Golgi membrane. Nonetheless, only direct Golgi $[Mn^{2+}]$ quantification and *in vivo* Gdt1p-mediated Mn^{2+} transport measurements in yeast could undeniably prove this hypothesis.

Regarding Ca^{2+}-dependent Gdt1p regulation, the explanation is less straightforward. On one side, the increase of Gdt1p abundance upon Ca^{2+} addition in *pmr1Δ* cells could simply be a way for yeast cells to compensate for the loss of Pmr1p. However, as this increase of Gdt1p abundance upon Ca^{2+} addition is not observed in the *wild type* strain (133) and as Mn^{2+} addition engenders the opposite trend, this explanation is not completely satisfying. On the other side, it is suspected that Ca^{2+} supplementation, by fastening membrane fusion and fission events, increases the flux of vesicular trafficking, redistributes Mn^{2+} in the Golgi saccules and improves the glycosylation process (89). If Gdt1p is involved in membrane fusion or fission events via controlled Ca^{2+} influx or efflux from Golgi compartments, its overexpression in high Ca^{2+} feed conditions, by supporting a as performant as possible intra-Golgi trafficking, could represent a fitness advantage.

3. The degradation of organellar resident proteins is poorly characterized

Trafficking of proteins in the secretory pathway has been extensively studied. It was even awarded by the 2013 Nobel Prize of Physiology and Medicine to J. Rothman, R. Schekman and T. Südhof for "their discoveries of machinery regulating vesicle traffic". However, most of the discoveries about the secretory pathway operations relate the trafficking of proteins that only transit through the secretory pathway.

Trafficking routes responsible for the degradation of organellar resident proteins are less known, even though few examples popped up in the literature in last years. For examples, the degradation of proteins from the inner nuclear membrane implies an ubiquitylation step before degradation (324, 325), the ERAD pathway is also involved in the degradation of correctly folded and active ER resident proteins (326) and there are vacuolar membrane proteins that undergo vacuolar degradation when required (327, 328). Regarding Golgi localized proteins, the ubiquitin ligase Tul1p is putatively implicated in the proteostasis of this organelle (276, 295) but its exact role is not clear. Besides, some Golgi proteins enter the proteasomal degradation pathway (275). Overall, there is no canonical degradation process for Golgi proteins to date.

In this study, we aimed at identifying actors involved in Gdt1p degradation process. As a matter of fact, Gdt1p is degraded at the vacuole in a *TUL1*-independent manner. Its degradation implies trafficking via the MVB *en route* to the vacuole and is slightly slowdowned in *rsp5* depleted cells. Except for those observations, little has been uncovered regarding the degradation route of Gdt1p. Notwithstanding, the fast and efficient degradation of Gdt1p upon Mn^{2+} addition still suggests that an active degradation process is triggering Gdt1p depletion.

PART V

CONCLUSION AND PERSPECTIVES

Conclusion

In this study, we investigated two important aspects of Gdt1p physiological function, its transport activity and its regulatory mechanisms.

The initial assumption being that Gdt1p exchanges cations against H^+ across the Golgi membrane, we developed several measurement strategies to study it. Thanks to its heterologous expression in *L. lactis*, we could emphasize that Gdt1p is actually able to convey H^+ ions across biological membranes. Furthermore, we endorsed that Gdt1p operates as a Ca^{2+}-Mn^{2+}/H^+ exchanger.

To get more clues about the physiological role of Gdt1p, we developed a Golgi-localized pH sensor for *S. cerevisiae* based on the genetically encoded pHluorin (234). Its fluorescence level had to be increased by means of some specific mutations to become suitable for measurements in the tiny Golgi organelle. By fusing the probe to the transmembrane span of a Golgi-resident glycosylation enzyme, we could target the chimeric protein to the *cis*- and *medial*-Golgi lumen.

However, *in vivo* pH measurements could not completely unravel the role of Gdt1p at the Golgi membrane. We presume that Gdt1p plays subtle roles for Golgi pH, [Ca^{2+}] and [Mn^{2+}] homeostasis, whether in terms of timing of activation or because of putative reversible transport activity, according to the relative transmembrane concentration gradients.

Anyway, our results shed light on the mechanism of transport of *GDT1* family members. It emphasizes the roles of Golgi localized yeast Gdt1p, human TMEM165 and plant PML3 for Golgi homeostasis, and bring clues to deeper characterize the function and the transport parameters of plasma membrane localized or chloroplast localized *GDT1* orthologs, in bacteria, archaea or plants.

Eventually, Gdt1p degradation represents a very nice case study to get more understanding about Golgi proteostasis. Indeed, the rapid and efficient depletion of Gdt1p upon extracellular Mn^{2+} addition suggests that active and accurate degradation processes are present at the Golgi. While secretory pathway resident proteins are usually tightly maintained at their proper localization, equally strong catching mechanisms seem implicated in the retrieval of Golgi proteins when it is requested by the cell. Hence, Gdt1p degradation process could be representative for widespread organellar proteostasis mechanisms.

Perspectives

During this research project, significant advances were achieved regarding Gdt1p physiological functions elucidation. Nevertheless, much remains to be uncovered to completely understand the roles of Gdt1p, TMEM165 and other *GDT1* orthologs in various organisms. If this protein family has been so widely conserved, it is because *GDT1* family members confer a real evolutive advantage to their host organisms. Hence, many questions could be addressed in the future.

To have a better comprehension of Gdt1p transport mechanism, it would be extremely valuable to make use of *in vitro* analytical methods. For this purpose, Gdt1p should be overexpressed, purified and reconstituted into model membranes. In our laboratory, several researchers are currently working on this objective with Gdt1p and TMEM165 proteins. Sometimes, the use of thermophilic orthologs has also proven to be beneficial because their inherent thermostability eases the segregation of exogenous from endogenous proteins during the purification process.

Once proteins are integrated into liposomes, it allows the completion of direct transport assays. The heterologous expression system we used in this thesis, *i.e.* the use of *L. lactis* bacteria, was already convenient, but has some drawbacks such as the impossibility to control the chemical composition at both sides of the lipid bilayer or the presence of endogenous membrane proteins. Hence, it is quite difficult to determine several transport characteristics such as the stoichiometry, the pH optimum or some kinetic parameters. *In vitro* transport assays can overtake most of those obstacles. As an alternative to protein overexpression and purification, cell-free protein translation could also be a good way to obtain pure protein preparations for transport assays (329, 330).

The preparation of purified protein samples is also a prerequisite for structural analysis. If some tridimensional data could be obtained, it would gain substantial insights into *GDT1* family members function. Next to the achievement of a complete tridimensional Gdt1p structure, other analytical methods, such as circular dichroism, Fourier-transform infrared spectroscopy, isothermal titration calorimetry, could already bring valuable information regarding the secondary structure modifications or the binding properties of our protein of interest. If set against the tridimensional Gdt1p structure prediction generated by the AlphaFold tool (177) or by using the Rosetta algorithm (331), those data could maybe bring clues to understand how Gdt1p/TMEM165 mutations affect protein functionality.

Nevertheless, *in vitro* measurements cannot completely elucidate the *in vivo* physiological function of any protein. All the regulatory and signaling processes are usually lost during *in vitro* assays. Among Gdt1p substrates, the Ca^{2+} cation is a well-known secondary signaling transducer (332, 333) and pH fluctuations occur as a response to metabolic changes (250, 334, 335). Furthermore, Ca^{2+} and pH signaling seem coordinated in yeast intracellular signaling (207). Hence, additional cytosolic Ca^{2+} and pH measurements, for example [Ca^{2+}] monitoring during glucose deprivation / re-addition or pH recordings in cells depleted for various Ca^{2+} extruders, would probably add new hints in Gdt1p comprehension. Also, we could perform additional Golgi pH measurements with our new probe in various physiological circumstances. Hence, the modulation of Ca^{2+} and Mn^{2+} Golgi loading when *PMR1* selective mutants are expressed could maybe modify Gdt1p activity, leading to Golgi pH adjustments. Besides, V-ATPase activity can be annihilated by concanamycin A treatment. In this situation, the role of Gdt1p for H^+ influx or efflux from Golgi compartments could be disclosed (161). Finally, several Gdt1p mutants affected for Ca^{2+} and Mn^{2+} transport have been previously identified in our laboratory (206, 208). It would be pertinent to test their ability to convey H^+ ions.

Conjointly, the setting of *in vivo* Golgi [Ca^{2+}] measurement is still under investigation. Thanks to the experience we acquired during the development of the Golgi pH sensor, some work is undergoing to adapt available Ca^{2+} sensors for the Golgi lumen of *S. cerevisiae*. Three interesting candidates are the CEPIA probe, a CaM based fluorescent sensor composed of circularly permutated GFP, CaM and M13 peptide (336), the D4ER sensor, a FRET-based Cameleon derivative (337), or the GCamP-R family, tandem constructs of calcium-dependent GCamP and calcium-independent mCherry (338). Besides, the evaluation of Mn^{2+} loading within the Golgi lumen would be extremely appreciated. We already assessed whether Golgi vesicles purification coupled to ICP-AES or ICP-MS analysis could be a feasible strategy. Harder work seems necessary to set up this experimental procedure. As an alternative, nanosynchrotron X-ray fluorescence and nanoscale secondary ion mass spectrometry (339, 340) are attractive methods for Mn^{2+} quantification in subcellular compartments.

Eventually, Gdt1p degradation process is quite intriguing. As the most obvious Golgi to prevacuolar compartments trafficking pathways are not implied, we should look at other candidates. To do so, the implementation of a screening strategy is under preparation. Based on a screening methodology settled to study vacuolar membrane protein degradation process (328), we are working on the development of two complementary tools. Both implicate the fusion of a reporter gene to the cytosolic side of Gdt1p. Either a pH-

sensitive fluorescent sensor, like the pHluorin we used earlier in this study, or an auxotrophic marker, like the Ura3p or His3p metabolic enzymes. Since Gdt1p is normally embedded in the Golgi membrane, the reporter proteins would fluoresce or would enable growth on selective medium. If Mn^{2+} induces the relocalization of the chimeric Gdt1-reporter protein into the vacuole lumen, those abilities would be lost. Then, by selecting or screening for mutants able to grow or to fluoresce upon Mn^{2+} exposure, the actors involved in Gdt1p degradation process would likely be identified.

Altogether, the road to *GDT1* family elucidation is still long, but it represents a fascinating journey with multiple outstanding points of view on the extremely sophisticated cellular harmony.

PART VI

MATERIAL AND METHODS

1. Methods regarding experiments performed with *S. cerevisiae*

1.1 Plasmids

Plasmids were obtained according to standard molecular biology protocols and were validated by sequencing. They are listed in Table 1.

Table 1. Plasmids used for yeast transformation in this study.

Plasmid	Abbreviate construct name	Source
pRS315-pTPI-USER-tCYC1	Empty vector	Our laboratory
pRS315-pGDT1-MNN2(1-36)-Gly_3-HA-Gly_3-AEQ-tCYC1	Mnn2-HA-aequorin	Our laboratory (Guillaume Poncelet Master thesis)
pRS315-pGDT1-MNN2(1-36)-Gly_3-HA-Gly_3-GAP1-tCYC1	Mnn2-HA-GAP1	This study (Sophie Sluysmans Master thesis)
pRS315-pSNA2-MNN2(1-36)-Gly_3-HA-Gly_3-pHluorin-tCYC1	Mnn2-HA-pHluorin	This study
pRS315-pSNA2-MNN2(1-36)-Gly_3-HA-Gly_3-pHluorin(F64L)-tCYC1	Mnn2-HA-pHluorin*	This study
pRS315-pSNA2-MNN2(1-36)-Gly_3-HA-Gly_3-pHluorin(F64L; M153R)-tCYC1	Mnn2-HA-pHluorin**	This study
pRS315-pTPI-MNN2(1-36)-Gly_3-HA-Gly_3-pHluorin(F64L; M153R)-tCYC1	Mnn2-HA-pHluorin**	This study
pRS416-pTPI-GDT1(1-29)-GFP-$Gly_2SerGly_4SerGly_2$-(30-280)GDT1-tCYC1	Gdt1(1-29)-GFP-(30-280)Gdt1	This study
pRS316-mRFP-Sed5	mRFP-Sed5	Matsuura-Tokita *et al.*(4)
pRS316-mRFP-Gos1	mRFP-Gos1	Matsuura-Tokita *et al.*(4)
pRS316-Sec7-mRFP	Sec7-mRFP	Matsuura-Tokita *et al.*(4)
pZR4.1-pTEF1-pHluorin-tCYC1	pHluorin	R. Rao, Baltimore, MD, USA (239)
pRS41N-PMR1	Pmr1	F. Foulquier
pRS41N-PMR1(D53A)	Pmr1(D53A)	F. Foulquier
pRS41N-PMR1(D778A)	Pmr1(D778A)	F. Foulquier
pRS41N-PMR1(Q783A)	Pmr1(Q783A)	F. Foulquier

Plasmids constructed in this study for yeast transformation were mostly prepared in the pRS315 scaffold. The promoter was cloned in between SacI and NotI restriction sites, the MNN2(1-36)-Gly_3-HA-Gly_3-pHluorin chimeric sequence was obtained by triple PCR and bounded by NotI and SpeI restriction sites, and the tCYC1 (cytochrome C) terminator was cloned in between SpeI and HindIII restriction sites. Two punctual mutations (F64L and M153R) within the pHluorin were inserted sequentially by QuickChange

PCR. For GFP insertion in between amino acids 29 and 30 of *GDT1*, the construct was obtained by Gibson assembly methodology (NEB Gibson Assembly Protocol E5510) and cloned in pRS416 backbone. A Glycine-Serine linker was inserted in between the GFP C-ter and (30-280)GDT1, to move the GFP away from the lipid bilayer. All the primers are listed in Table 2.

Table 2. Primers used in this study.

Primer name	Primer sequence
NotI-MNN2_Fw	5'-CATGCGGCCGCATGCTGCTTACCAAAAGG-3'
MNN2-HA_Rv	5'-ACCTCCGCCGGCGTAGTCTGGGACATCGTATGGGTAACCGCC TCCCGACGTGTTCTCATCCAT-3'
HA-pHluorin_Fw	5'-GGAGGCGGTTACCCATACGATGTCCCAGACTACGCCGGCGGA GGTAGTAAAGGAGAACTTTTCACT-3'
pHluorin-SpeI_Rv	5'-CGGACTAGTTTATTTGTATAGTTCATCCAT-3'
pHluorin-F64L_Fw	5'-GGCCAACACTTGTCACTACTTTATCTTATGGTGTTCAATG-3'
pHluorin-F64L_Rv	5'-CATTGAACACCATAAGATAAAGTAGTGACAAGTGTTGGCC-3'
pHluorin-M153R_Fw	5'-TAACGAGCACTTGGTGTACATCAGGGCAGACAAACA-3'
pHluorin-M153R_Rv	5'- TGTTTGTCTGCCCTGATGTACACCAAGTGCTCGTTA-3'
IntLocHis3LEU2_Fw	5'-GCAGAAAGCCCTAGTAAAGCGTATTACAAATGAAACCAAGC CTTATCACGTTGAGCCATTAG-3'
IntLocHis3HindIII_Rv	5'-CCATTGGGCGAGGTGGCTTCTCTTATGGCAACCGCAAGAGGG TCGACGGTATCGATAAGCTT-3'
GDT1(Thr29)-GFP_ Rv	5'-GAAAAGTTCTTCTCCTTTACTTGTCTCCGCATCAGTAGCTG-3'
GDT1(Thr29)-GFP_ Fw	5'-CAGCTACTGATGCGGAGACAAGTAAAGGAGAAGAACTTTTC-3'
GFP-Linker*_Rv	5'-CGCTACCTCCGCCACCGCTGCCTCCTTTGTATAGTTCATCCA TGC-3'
Linker*-GDT1(Ser30)_Fw	5'-TAGCGGTGGCGGAGGTAGCGGTGGATCTATGGAATCTGGGA GTTC-3'

1.2 Strains

For genomic integration of the Golgi targeted pH sensor gene, a DNA product of approximately 4.2 kb containing two coding sequences and their related promoter and terminator, pTPI-Mnn2-HA-pHluorin**-tCYC1 and pLEU2-LEU2, was amplified by PCR from the pRS315-pTPI-MNN2(1-36)-Gly_3-HA-Gly_3-pHluorin**-tCYC1 plasmid. Primers used for amplification were containing flanking sequences corresponding to the *his3* locus (primers IntLocHis3LEU2_Fw and IntLocHis3HindIII_Rv) (Table 2). The PCR product was purified on agarose gel and used for classical yeast transformation according to previously described method (341), with the addition of 10% DMSO before transferring the cells at 42 °C. After colonies selection on the appropriate synthetic selection medium and to discard non transformed cells, colonies were picked up and plated a second time on the same selection medium, and a single colony was finally plated and maintained on YD plates.

Genomic integrations were verified by PCR. As a blank for background fluorescence measurements, the *wild type* strain was also transformed with the pLEU2-LEU2 selection marker only, amplified from pRS315-pTPI-USER-tCYC1 plasmid with the same primers.

All *S. cerevisiae* strains used for pH monitoring are listed in Table 3, while strains used in the study of Gdt1p degradation are listed in Table 4.

Table 3. Yeast strains used for pH monitoring experiments.

***S. cerevisiae* strain**	**Description**	**Source**
Wild type BY4742	*BY4742 Matα his3Δ1 leu2Δ0 lys2Δ0 ura3Δ0*	Euroscarf
gdt1Δ	*BY4742 Matα his3Δ1 leu2Δ0 lys2Δ0 ura3Δ0 gdt1::KanMX4*	Euroscarf
vma13Δ	*BY4742 Matα his3Δ1 leu2Δ0 lys2Δ0 ura3Δ0 vma13::KanMX4*	Euroscarf
vma13Δgdt1Δ	*BY Mata his3Δ1 leu2Δ0 lys2Δ0 ura3Δ0 vma13::KanMX4 gdt1::KanMX4*	Our laboratory
Wild type Mnn2-HA-pHluorin**	*BY4742 Matα leu2Δ0 lys2Δ0 ura3Δ0 his3Δ1::LEU2-pTPI-MNN2-HA-pHluorin**-tCYC1*	This study
Wild type + integrated selection marker	*BY4742 Matα leu2Δ0 lys2Δ0 ura3Δ0 his3Δ1::LEU2*	This study
gdt1Δ Mnn2-HA-pHluorin**	*BY4742 Matα leu2Δ0 lys2Δ0 ura3Δ0 his3Δ1::LEU2-pTPI-MNN2-HA-pHluorin**-tCYC1 gdt1::KanMX4*	This study
vma13Δ Mnn2-HA-pHluorin**	*BY4742 Matα leu2Δ0 lys2Δ0 ura3Δ0 his3Δ1::LEU2-pTPI-MNN2-HA-pHluorin**-tCYC1 vma13::KanMX4*	This study
vma13Δgdt1Δ Mnn2-HA-pHluorin**	*BY Mata leu2Δ0 lys2Δ0 ura3Δ0 his3Δ1::LEU2-pTPI-MNN2-HA-pHluorin**-tCYC1 vma13::KanMX4 gdt1::KanMX4*	This study
vph1Δ Mnn2-HA-pHluorin**	*BY4742 Matα leu2Δ0 lys2Δ0 ura3Δ0 his3Δ1::LEU2-pTPI-MNN2-HA-pHluorin**-tCYC1 vph1::KanMX4*	This study
vph1Δgdt1Δ Mnn2-HA-pHluorin**	*BY Matα leu2Δ0 lys2Δ0 ura3Δ0 his3Δ1::LEU2-pTPI-MNN2-HA-pHluorin**-tCYC1 vph1::KanMX4 gdt1::KanMX4*	This study
stv1Δ Mnn2-HA-pHluorin**	*BY4742 Matα leu2Δ0 lys2Δ0 ura3Δ0 his3Δ1::LEU2-pTPI-MNN2-HA-pHluorin**-tCYC1 stv1::KanMX4*	This study

stv1Δgdt1Δ Mnn2-HA-pHluorin**	*BY Mata leu2Δ0 lys2Δ0 ura3Δ0 his3Δ1::LEU2-pTPI-MNN2-HA-pHluorin**-tCYC1 stv13::KanMX4 gdt1::KanMX4*	This study
kha1Δ Mnn2-HA-pHluorin**	*BY4742 Matα leu2Δ0 lys2Δ0 ura3Δ0 his3Δ1::LEU2-pTPI-MNN2-HA-pHluorin**-tCYC1 kha1::KanMX4*	This study
pmr1Δ Mnn2-HA-pHluorin**	*BY4742 Matα leu2Δ0 lys2Δ0 ura3Δ0 his3Δ1::LEU2-pTPI-MNN2-HA-pHluorin**-tCYC1 pmr1::KanMX4*	This study
pmr1Δgdt1Δ Mnn2-HA-pHluorin**	*BY Mata leu2Δ0 lys2Δ0 met15Δ0 ura3Δ0 his3Δ1::LEU2-pTPI-MNN2-HA-pHluorin**-tCYC1 pmr1::KanMX4 gdt1::KanMX4*	This study
vcx1Δ Mnn2-HA-pHluorin**	*BY4742 Matα leu2Δ0 lys2Δ0 ura3Δ0 his3Δ1::LEU2-pTPI-MNN2-HA-pHluorin**-tCYC1 vcx1::KanMX4*	This study
vcx1Δ/gdt1Δ Mnn2-HA-pHluorin**	*BY Matα leu2Δ0 lys2Δ0 ura3Δ0 his3Δ1::LEU2-pTPI-MNN2-HA-pHluorin**-tCYC1 vcx1::KanMX4 gdt1::KanMX4*	This study

Table 4. Yeast strains used for Gdt1p degradation experiments.

***S. cerevisiae* strain**	**Description**	**Source**
Wild type BY4741	*BY4741 Mata his3Δ1 leu2Δ0 met15Δ0 ura3Δ0*	Euroscarf
gdt1Δ	*BY4741 Mata his3Δ1 leu2Δ0 met15Δ0 ura3Δ0 gdt1::KanMX4*	Euroscarf
pmr1Δ	*BY4741 Mata his3Δ1 leu2Δ0 met15Δ0 ura3Δ0 pmr1::KanMX4*	Euroscarf
pmr1Δgdt1Δ	*BY Matα his3Δ1 leu2Δ0 met15Δ0 ura3Δ0 pmr1::KanMX4 gdt1::KanMX4*	Our laboratory
smf2Δ	*BY4741 Mata his3Δ1 leu2Δ0 met15Δ0 ura3Δ0 smf2::KanMX4*	Euroscarf
smf2Δpmr1Δ	*BY Matα his3Δ1 leu2Δ0 ura3Δ0 smf2::KanMX4 pmr1::KanMX4*	Our laboratory
apm1Δ	*BY4742 Matα his3Δ1 leu2Δ0 lys2Δ0 ura3Δ0 apm1::KanMX4*	Euroscarf
apm3Δ	*BY4741 Mata his3Δ1 leu2Δ0 met15Δ0 ura3Δ0 apm3::KanMX4*	Euroscarf
apm1Δapm3Δ	*BY Mata his3Δ1 leu2Δ0 met15Δ0 lys2Δ0 ura3Δ0 apm1::KanMX4 apm3::KanMX4*	Our laboratory
pep12Δ	*BY4742 Matα his3Δ1 leu2Δ0 lys2Δ0 ura3Δ0 pep12::KanMX4*	Euroscarf
pep4Δ	*BY4741 Mata his3Δ1 leu2Δ0 met15Δ0 ura3Δ0 pep4::KanMX4*	Euroscarf
atg1Δ	*BY4742 Matα his3Δ1 leu2Δ0 lys2Δ0 ura3Δ0 atg1::KanMX4*	Euroscarf

atg2Δ	*BY4742 Matα his3Δ1 leu2Δ0 lys2Δ0 ura3Δ0 atg2::KanMX4*	Euroscarf
npi1-1 (rsp5)	*BY4741 Mata his3Δ1 leu2Δ0 met15Δ0 ura3Δ0 Promoter$_{RSP5}$::KanMX*	B. André, ULB, Belgium
bul1Δbul2Δ	*BY Mata his3Δ1 leu2Δ0 met15Δ0 ura3Δ0 bul1::KanMX4 bul2::KanMX4*	Our laboratory
bul1Δbul2Δpep4Δ	*BY Mata his3Δ1 leu2Δ0 met15Δ0 ura3Δ0 bul1::KanMX4 bul2::KanMX4 pep4::KanMX4*	Our laboratory
bsd2Δ	*BY4741 Mata his3Δ1 leu2Δ0 met15Δ0 ura3Δ0 bsd2::KanMX4*	Euroscarf
tul1Δ	*BY4741 Mata his3Δ1 leu2Δ0 met15Δ0 ura3Δ0 tul1::KanMX4*	Euroscarf
EN60	*BY4742 Matα hi3Δ1 leu2Δ0 ura3Δ0 ecm21::G418 bsd2 rog3::NatMX rod1 ygr068c aly2 aly1 ldb19 ylr395c::SpHIS5*	H. Pelham, MRC, UK
gga1Δ	*BY4741 Mata his3Δ1 leu2Δ0 met15Δ0 ura3Δ0 gga1::KanMX4*	Euroscarf
gga2Δ	*BY4741 Mata his3Δ1 leu2Δ0 met15Δ0 ura3Δ0 gga2::KanMX4*	Euroscarf
gga1Δgga2Δ	*Σ1278b ura3Δ0 gga1::KanMX gga2::KanMX*	B. André, ULB, Belgium
gga1Δgga2Δapm1Δ	*Σ1278b ura3Δ0 gga1::KanMX gga2::KanMX apm1::HygroR*	B. André, ULB, Belgium
doa4Δ	*BY4741 Mata his3Δ1 leu2Δ0 met15Δ0 ura3Δ0 doa4::KanMX4*	Euroscarf
vps27Δ	*BY4741 Mata his3Δ1 leu2Δ0 met15Δ0 ura3Δ0 vps27::KanMX4*	Euroscarf
hse1Δ	*BY4741 Mata his3Δ1 leu2Δ0 met15Δ0 ura3Δ0 hse1::KanMX4*	Euroscarf
vps23Δ	*BY4741 Mata his3Δ1 leu2Δ0 met15Δ0 ura3Δ0 vps23::KanMX4*	Euroscarf
vps36Δ	*BY4741 Mata his3Δ1 leu2Δ0 met15Δ0 ura3Δ0 vps36::KanMX4*	Euroscarf
vps24Δ	*BY4741 Mata his3Δ1 leu2Δ0 met15Δ0 ura3Δ0 vps24::KanMX4*	Euroscarf
ear1Δ	*BY4741 Mata his3Δ1 leu2Δ0 met15Δ0 ura3Δ0 ear1::KanMX4*	Euroscarf
rcr1Δ	*BY4741 Mata his3Δ1 leu2Δ0 met15Δ0 ura3Δ0 rcr1::KanMX4*	Euroscarf
rcr2Δ	*BY4741 Mata his3Δ1 leu2Δ0 met15Δ0 ura3Δ0 rcr2::KanMX4*	Euroscarf
arf2Δ	*BY4741 Mata his3Δ1 leu2Δ0 met15Δ0 ura3Δ0 arf2::KanMX4*	Euroscarf
ssh4Δ	*BY4741 Mata his3Δ1 leu2Δ0 met15Δ0 ura3Δ0 ssh4::KanMX4*	Euroscarf
end3Δ	*BY4741 Mata his3Δ1 leu2Δ0 met15Δ0 ura3Δ0 end3::KanMX4*	Euroscarf
sna1Δsna2Δsna3Δsna4Δ	*BY Matα his3Δ1 leu2Δ0 met15Δ0 ura3Δ0 sna1::URA3 sna2::HIS3 sna3::KanMX4 sna4::KanMX4*	Our laboratory

1.3 Growing conditions

Non-transformed yeast cells were routinely cultured at 28 °C in YD medium (2% yeast extract KAT, 2% glucose) under agitation. Cells transformed with plasmids were grown at 28 °C in SD (Synthetic defined) minimal medium (0.7% yeast nitrogen base without amino acids (Difco), 2% glucose, supplemented with all amino acids except the ones used as selection marker for plasmid maintenance) with agitation. For pRS41N plasmid maintenance, Nourseothricin was added at 100 µg/ml (Jena Bioscience 96736-11-7). Solid media were produced by addition of 2% agar to the mixture. For fluorimeter measurements, cells were grown in Low Fluorescence SD minimal medium (0.7% yeast nitrogen base without amino acids, riboflavin, and folic acid (ForMedium, Ref CYN65), 2% glucose, all amino acids except for those used as selection marker, 50 mM MES pH 5.0, filter-sterilized).

1.4 Fluorescence microscopy and co-localization measurements

Pictures were obtained using a Zeiss Axio Observer 7 inverted epifluorescence microscope with a 100x oil immersion objective (Alpha Plan-Apochromat 100x/1.46 Oil) and were taken with Hamamatsu ORCA-Flash 4.0 LT sCMOS camera driven by Zen2.3 Pro software. Pictures were analyzed with Fiji/ImageJ 2.0.0-rc-69. Yeast cells were grown in synthetic medium and imaged in mid-log phase (OD_{600} = 2.0 - 4.0; an OD_{600} of 1.0 corresponds approximately to 10^7 cells/ml). For imaging, they were directly mounted on a glass slide coated with a thin layer of agarose 1.5%.

For co-localization measurements with Golgi markers, cells were fixed with a solution of 4% paraformaldehyde in PBS during 20 min at 28 °C, then washed twice with 100 µl of PBS and mounted for imaging. Only cells expressing sufficiently the Golgi markers were considered for colocalization quantification.

For endosomes detection, FM4-64 was used (342). To do so, 1 ml of culture was collected by centrifugation and resuspended in 100 µl of fresh YD and 1 µl of 16 mM FM4-64 was added to the cell suspension. Cells were incubated during 20 minutes at 28°C, then mounted for immediate imaging. Alternatively, cells stained with FM4-64 were fixed with paraformaldehyde prior to imaging to be consistent with the quantification performed with Golgi markers. In this case, 1 ml of culture collected by centrifugation was resuspended in 100 µl of YD at 4 °C and 2 µl of 16 mM FM4-64 was added to the cell suspension. Cells were then incubated for 20 min on ice to allow FM4-64 to accumulate in the plasma membrane. They were then collected by centrifugation, resuspended in 100 µl of PBS and incubated for 5 min at 30 °C for FM4-64 to be internalized in endosomes. Cells were collected again and

washed with 100 µl of PBS at 4 °C. Finally, cells were fixed with a solution of 4% paraformaldehyde in PBS during 20 min on ice, then washed twice with 50 µl of PBS at 4 °C and mounted for imaging, which was performed in the following hour.

For vacuolar membrane staining, FM4-64 was pulse-chased. Briefly, 5 ml of cell culture was collected by centrifugation. Cells were resuspended in 100 µl of fresh medium and 1 µl 16 mM FM4-64 was added. Cells were incubated during 15 minutes at 30 °C with mild agitation (pulse), then centrifuged and washed twice with 1 ml of fresh medium. Finally, cells were again incubated for 30 to 45 minutes at 30 °C with mild agitation (chase), and then prepared for imaging.

To quantify the co-localization, an object-based method based on the centers of mass – particle coincidence was performed using the JACoP plugin (343). Prior to the plugin application, images were treated to identify the vesicles via the "Find maxima" tool, with the prominence value being manually adjusted for each picture, in order to get most of the visible vesicles and to avoid false positive dots. All the maxima were then resized to have a radius of 4 pixels and images generated in this way were then analyzed with the JACoP plugin. Representative images were background-subtracted with a rolling ball radius of 10-20 pixels and smoothed.

1.5 Yeast subcellular fractionation

Subcellular fractionation was performed as in Demaegd *et al.* (90), with slight modifications. The discontinuous sucrose gradient was prepared with 9 layers of 1.2 ml ranging from 22 to 54%, and 2.4 ml of the cell lysate was loaded at the top of the gradient. After ultracentrifugation, fractions of 1.2 ml were collected from the top of the gradient, were gently mixed with 300 µl of 50% glycerol, and were analyzed by immunoblotting or used for subsequent topology assay.

1.6 Golgi protein topology assay

Golgi enriched fractions obtained by subcellular fractionation were submitted to trypsin or proteinase K digestion, with two similar protocols.

When trypsin was used, 35 µl of Golgi-enriched fractions were incubated for 1 hour at 25°C in a final volume of 50 µl containing 0.1 mg/ml of trypsin. When needed, Triton X-100 was added to a 1% (v/v) final concentration. For the negative control, the Golgi-enriched fractions were pre-incubated for 10 min at room temperature with a trypsin inhibitor mixture (10 mM PMSF, 0.05 mg/ml trypsin inhibitor (Type I-S; Sigma) and a protease inhibitor cocktail (PIC; Sigma) containing a final concentration of 8 µg/ml leupeptin,

aprotinin, antipain, pepstatin, and chymostatin). At the end of all the experiments, trypsin digestion was stopped by addition of the trypsin inhibitor mixture for 10 min, followed by addition of Triton X-100 to a 1% (v/v) final concentration. The resulting samples were analyzed by SDS-PAGE and *western blotting*.

When proteinase K was used, 15 µl of sample were incubated for 1 hour at 30 °C in a final volume of 40 µl containing 1 µg/ml of proteinase K, 1 mM $CaCl_2$, 50 mM Tris pH 7.6. When needed for the negative control, Triton X-100 was added to a 1% (v/v) final concentration. For the control with inhibitors, the Golgi enriched fractions were pre-incubated for 10 min at room temperature with a protease inhibitor mixture (2.5 mM PMSF and a protease inhibitor cocktail with 16 µg/ml leupeptin, aprotinin, antipain, pepstatin, and chymostatin, final concentrations). At the end of the experiment, digestion was stopped by the addition of the protease inhibitor mixture to all the samples, then incubated for 10 min at room temperature, followed by the addition of 15 µl of sample buffer 4x concentrated preheated at 85 °C and incubated for an additional 10 min at 85 °C with mixing. The resulting samples were analyzed by SDS-PAGE and *western blotting*.

1.7 Fluorimeter and in vivo pH calibration in yeast

Data were recorded using a JASCO FP8500 fluorimeter controlled by the Spectra Manager software. To convert the fluorescence measurements into pH values, *in vivo* calibration of the probe was performed. For this purpose, 100 ml of cell culture were grown in Low Fluorescence synthetic medium until OD_{600} = 3.0. Cells were collected by 3 min centrifugation at 1,800 x *g*, were washed twice with 50 ml PBS and finally resuspended in 10 ml PBS supplemented with 0.16% digitonin. Cells were then incubated for 8 min at room temperature with mild agitation on a rocking table. Cells were collected again by 3 min centrifugation at 1,800 x *g*, were resuspended in 10 ml PBS pre-cooled at 4 °C and were aliquoted into 1 ml fractions in 2-ml microtubes. Aliquots were centrifuged during 3 min at 4,000 x *g* at 4 °C and cells were resuspended in 2 ml of the appropriate pH buffer (mix of citric acid 0.1 M – Na_2HPO_4 0.2 M in adequate proportion). They were incubated for 10 min at room temperature, before being transferred into cuvettes for excitation spectra measurement. Emission intensity was measured at 507 nm during excitation from 360 to 490 nm (5 nm bandwidths, scan speed: 200 nm/min). The background fluorescence of cells transformed with an empty plasmid and treated in an identical way was subtracted from all these spectra, and the ratio of fluorescence emitted during excitation at 400 and 480 nm was plotted against pH value. Finally, a sigmoidal four-parameter logistical curve was drawn through the experimental dots and used for subsequent determination of Golgi pH. For cytosolic pHluorin calibration, the protocol is

slightly different, as described in (133), because digitonin is added at 0.01% final concentration to permeabilize the plasma membrane.

1.8 Golgi and cytosol pH measurements at steady-state or during glucose pulse

Yeast cells expressing the Mnn2-HA-pHluorin** protein for Golgi pH measurements or the native pHluorin adapted to cytosolic pH measurements (239) were grown at 28 °C in Low Fluorescence synthetic medium. For Golgi pH measurements, 12 ml of cells were grown. When the OD_{600} reached 2.8 - 3.2, the appropriate volume to get 30 OD_{600} equivalent was collected by 5 min centrifugation at 1,500 x *g* (swinging rotor). For steady-state pH measurements, cells were immediately resuspended in 2 ml of fresh medium pre-warmed at 28 °C, the cell suspension was then transferred into a cuvette with a magnetic stirrer rotating at 300 rpm and fluorescence was measured in the fluorimeter set at 28 °C. The signal was recorded at 507 nm during excitation from 360 to 490 nm (5 nm bandwidths, scan speed: 200 nm/min). For glucose pulse measurements, the protocol is based on the procedure described by Tarsio *et al.* (39). Cells collected were washed twice with 10 ml of Low Fluorescence synthetic medium without glucose pre-cooled at 4 °C, and finally resuspended in 10 ml of the same medium. Cells were then incubated on ice during 30 min to starve them from glucose. Alternatively, cells were deprived of glucose during 60 min at 28 °C (233, 249). After this starvation period, they were collected by centrifugation, resuspended in 2 ml of Low Fluorescence synthetic medium without glucose pre-warmed at 28 °C and incubated during 5 min in a water-bath at 28 °C. Then, 1.8 ml was transferred into a cuvette with a magnetic stirrer rotating at 300 rpm and fluorescence was measured in the fluorimeter set at 28 °C. The signal was recorded at 507 nm during alternate excitation at 400 and 480 nm. After 120 sec of baseline recording, 200 µl of 20% glucose was added in the cuvette and the measurement was continued up to 10 min. For cytosolic pH measurements, the same protocol was used, except that 5 ml of cells were grown and collected by centrifugation, and that cells were resuspended every time in 5 ml of fresh medium. For all experiments, background fluorescence of cells transformed with an empty vector and treated similarly was also measured and subtracted as a blank from raw data. The 400/480 nm excitation ratio was finally converted into pH value.

1.9 Total protein extraction

For total protein extraction from yeast cells, two distinct protocols were used. Commonly, cells grown to mid-log exponential phase ($OD_{600} \approx 3.0$) were collected by centrifugation. Then, they were washed with 1 ml ice-cold

water and finally resuspended in 250 µl MBS breaking buffer (250 mM sorbitol, 0.2 g/L $MgCl_2.6H_20$, 50 mM imidazole pH 7.5, 1 mM PMSF freshly prepared, protease inhibitor cocktail 1:2000) in 2-ml microtubes. Two hundred milligrams of acid-washed glass beads (425-600 µm) were added and cells were strongly mixed by vortexing for 8 x 30 sec (15 sec on ice in between vortexing periods). Then, cells were centrifuged again for 20 sec at 5,000 rpm in a benchtop centrifuge set at 4 °C. The supernatant (150 µl) was collected and used for subsequent protein quantification, SDS-PAGE, and *western blotting*.

Alternatively, protein extraction from cells exposed to high Mn^{2+} was performed in a different manner, as the classical "MBS" extraction protocol could not completely avoid protein degradation in those protein extracts. To do so, proteins were rapidly precipitated by the addition of trichloroacetic acid (TCA) during cell lysis. Again, cells were collected in mid-log exponential phase and washed with 2 ml ice-cold water. Then, cells were resuspended in 2-ml microtubes with 300 µl TCA buffer (25 mM NH_4Ac, 1 mM Na_2EDTA, 10 mM Tris-HCl (pH 8.0), 10% trichloroacetic acid). Two hundred milligrams of acid-washed glass beads (425-600 µm) were added, and cells were submitted to 5 x 1 min vortexing (with 2 min breaks on ice). The cell lysate was then transferred in a new microtube and centrifugation was performed for 10 min at 16,000 x *g* at 4 °C. The supernatant was throwed away and the pellet was resuspended with 200 µl resuspension buffer (3% SDS, 0.1 M Tris-HCl pH 11.0). Samples were heated for 5 min at 65 °C, then centrifuged for 30 sec at 16,000 x *g* and 150 µl of supernatant was collected in a new microtube for subsequent protein quantification, SDS-PAGE, and *western blotting*.

1.10 *GDT1* mRNA level measurement by RT-qPCR

Total RNA extraction was performed from about 1.5 x 10^8 cells with the RNeasy Mini Kit (Qiagen, Ref. 74104). Then, cDNA were produced from RNA samples using a M-MLV Reverse Transcriptase (Promega, Ref. M1701). To do so, 100 ng to 2 µg total RNA are mixed with 2 µl oligo dT 50 µM, heated for 5 min at 70 °C and then cool downed for 5 min on ice. The samples were then mixed with 8 µl of a reverse transcriptase mix (5 µl M-MLV buffer, 1.25 µl 10 mM dNTPs, 0.625 µl Recombinant RNasin Ribonuclease inhibitor, 1 µl M-MLV reverse transcriptase), heated for 5 min at 25 °C, then heated for 60 min at 45 °C and finally heated for 56 min at 80 °C to inactivate the enzyme. Next, cDNA were purified with a PCR CleanUp kit (Macherey-Nagel, Ref. 740609.250) with elution performed twice with 25 µl of nuclease-free water at 65 °C.

For the qPCR analysis, two pairs of primers were used to quantify *GDT1* mRNA and two reference genes were used, *TAF10* and *FPR2*. Primers sequences are given in Table 5. The ΔΔCt methodology was used for relative quantification of *GDT1* expression at different time points after Mn^{2+} addition, compared to the condition without Mn^{2+}. Practically, 5 µl of primers premix at 1.2 µM were mixed with 5 µl of cDNA (commonly diluted 25x) and 10 µl of SYBR Green 2x Master Mix (Eurogentec), with technical triplicates. A StepOnePlus thermocycler (Applied Biosystems, ThermoFisher Scientific) was used with the following program: 10 min at 95 °C, 40x [15 sec at 95 °C, 1 min at 60 °C]. The threshold cycle (Ct) was arbitrarily measured when ΔRn equal 0.1. At the end of every experiment, melting curves were measured to check primers specificity (heating from 60 to 95 °C at a speed of 0.3 °C/sec).

Table 5. Primers used for qPCR.

Primer identity	Primer length	Sequence (5' → 3')
GDT1-Fw2	20	TTCAGCCGTTGCTTTTCTTT
GDT1-Rv2	20	AGTGTCGCCTCCTTTTTCAA
GDT1-Fw6	22	GGCGACACTGCGTATGATAAAC
GDT1-Rv6	22	TAGCTCGCCTAGGAAAACCATC
TAF10-Fw	22	AGCAGATGTACGAGTGAAACGA
TAF10-Rv	20	CGCCTGACTGTTGTTAGCAT
FPR2-Fw2	20	AGGCAATGCCAGGTGATAAA
FPR2-Rv2	20	AATTACTCTGCCAACGCCAA

2. Methods regarding experiments performed with *L. lactis*

2.1 Strain and plasmids

For expression of the sfpHluorin (38) in DML1 *L. lactis* cells (344) (gift from B. Poolman, Groningen, Netherlands), the gene was cloned in between NcoI and HindIII restriction sites of the pNZ8048 plasmid, with addition of one extra glycine after the Start codon standing within the NcoI restriction site. Therefore, the gene is under the control of pNisA promoter. For concomitant expression of *GDT1* and sfpHluorin, both genes were inserted in the same plasmid in an operon-like manner with an intergenic sequence in between the two coding sequences (intergenic sequence: AAAAATAAAGAGAGGAAAA AAAAC). Note that a NcoI restriction site initially present in the original *GDT1* sequence was removed by silent mutation. To express *GDT1* alone, it was cloned in between SphI and HindIII restriction sites.

2.2 *L. lactis* cultivation and *GDT1* and sfpHluorin induction

L. lactis cells were usually cultivated in anaerobic conditions, except if otherwise stated. They were grown at 28 °C in M17 broth according to

Terzaghi (Merck Millipore) supplemented with 1 % glucose and with 10 µg/ml chloramphenicol for pNZ8048 plasmid maintenance. Expression of genes under the control of the pNisA promoter was induced by 2.5 µg/liter nisin addition during log growth phase (OD_{600} = 0.4–0.5) and the culture was extended for two additional hours before harvesting cells. For anaerobic growth, fully filled closed tubes were used, with no agitation. In case the sfpHluorin was produced, cell cultivation was performed in aerobic condition during the induction period. There, half-filled slightly open tubes were used, with agitation, to ease sfpHluorin folding and expression.

Table 6. Plasmids used for *L. lactis* transformation in this study.

Plasmid	Abbreviate construct name	Source
pNZ8048-pNisA-empty	C-	B. Poolman, Groningen, Netherlands
pNZ8048-pNisA-GDT1	GDT1	Our laboratory
pNZ8048-pNisA-sfpHluorin	sfpHluorin	This study
pNZ8048-pNisA-GDT1-intergenic sequence-sfpHluorin	GDT1 + sfpHluorin	This study

2.3 *In vivo* sfpHluorin calibration

For *in vivo* calibration of the sfpHluorin in *L. lactis*, 200 ml of cell suspension were harvested by 5 min centrifugation at 1,500 x *g* at 28 °C. Cells were washed twice with 15 ml of washing buffer (100 mM KCl, 1 mM EGTA, 1 mM $MgCl_2$, 20 mM MOPS pH 7.2) and resuspended again in the same buffer in an appropriate volume to reach OD_{600} = 5.0. Cell suspension was distributed in 2 ml fractions in microtubes. After 1 min centrifugation at 5,000 x *g*, the cell pellets were resuspended in buffer solutions at different pH. Those buffers have the same chemical composition than the washing buffer, except the buffering compound that is MES (pH 5.5, 6.0, or 6.5), MOPS (pH 7.0 or 7.2), TRIS (pH 7.5, 8.0, 8.5, or 9.0) or CAPS (pH 9.0) and that nigericin K^+/H^+ ionophore was added at 0.5 µg/ml. Excitation spectra were measured from 340 to 490 nm, with emission recorded at 507 nm, with a JASCO FP8500 fluorimeter controlled by the Spectra Manager Software. After blank subtraction, a four-parameters sigmoidal curve was drawn through the 390/470 nm excitation ratio versus pH graph.

2.4 Intracellular pH measurements in *L. lactis*

For intracellular pH measurements, 50 ml of induced cells expressing the sfpHluorin were collected by 3 min centrifugation at 1,500 x *g* at 28 °C, washed twice with 15 ml washing buffer (100 mM KCl, 1 mM EGTA, 1 mM $MgCl_2$, 20 mM MOPS pH 7.4) and resuspended again in the same buffer to get

OD_{600} = 10.0. Two millilitres of cell suspension were then used for fluorescence measurement with alternate excitation at 390 and 470 nm (emission at 507 nm) during 5 to 10 minutes. Cells were maintained at 28 °C and continuously stirred (300 rpm) during the measurement. After baseline recording for 60 sec, different compounds were added to generate transmembrane pH gradients. At the end of every measurement, nigericin was added at 0.5 µg/ml to observe pH shift and hence make sure cells were not leaky earlier in the experiment. Finally, blank subtracted data were converted into intracellular pH values thanks to the calibration curve.

2.5 Extracellular pH measurements with *L. lactis*

Extracellular pH measurements were performed using a classical pH-meter. Basically, cells were grown similarly as for intracellular pH measurements, except that the strains used were expressing only GDT1, or no exogenous protein for the negative control. One hundred milliliters of cell suspension were collected and washed twice with 50 ml washing buffer (100 mM KCl, 1 mM EGTA, 1 mM $MgCl_2$, 50 mM Tris pH 7.0). Then, a third washing was performed with weakly buffered solution (100 mM KCl, 1 mM EGTA, 1 mM $MgCl_2$, 1 mM Tris pH 7.0). A last resuspension was performed in the same weakly buffered solution with a volume appropriate to get OD_{600} = 5.0, and 20 ml of the cell suspension were transferred into a small beaker for extracellular pH measurement. During pH recording, continuous stirring was performed, and $CaCl_2$, $MnCl_2$ or $MgCl_2$ was added at indicated time point. For data analysis, measurements were normalized to the initial pH value.

2.6 Ca^{2+} and Mn^{2+} transport measurements in *L. lactis* at different extracellular pH

The *in vivo* Ca^{2+} and Mn^{2+} transport measurements were carried out using the fluorescent dye Fura-2/AM according to the method previously described by (92) with slight modifications. Briefly, *L. lactis* DML1 cells expressing *GDT1* or transformed with an empty plasmid were collected, washed 3 times, and incubated with 10 µM Fura-2/AM and 1.7 mM probenecid for 2 hours at 28 °C with agitation. Then, cells were washed twice with the appropriate washing buffer solution (100 mM KCl, 1 mM $MgCl_2$, 1 mM EGTA, 50 mM Tris-HCl, pH 6.8, 7.5 or 8.0). The final pellet was resuspended in the corresponding buffer devoid of EGTA but previously passed through a calcium sponge resin (BAPTA chelator coupled to a polymer matrix ; Invitrogen) in order to decrease as much as possible the free Ca^{2+} concentration. For Ca^{2+} measurement, two excitation wavelengths of 340 and 380 nm were used and the excitation ratio is plotted as an estimation of [Ca^{2+}] (ratiometric measurement), while for Mn^{2+} measurement the excitation is performed at 360 nm and the quenching of

fluorescence is used as a read-out for [Mn^{2+}]. In both cases, fluorescence emission was recorded at 510 nm by a JASCO FP8500 fluorimeter controlled by the Spectra Manager software.

2.7 Protein extraction from *L. lactis* cells

To extract proteins from *L. lactis* cells, 50 ml of cell culture was centrifuged during 12 min at 1,700 x *g* g at 4 °C. The pellet was resuspended in 25 ml of ice-cold washing buffer (300 mM NaCl, 10% glycerol, 50 mM Tris-HCl pH 8.0). Cells were pelleted identically and resuspended in 1.5 ml of lysis buffer (300 mM NaCl, 10% glycerol, 1 mM PMSF, 1/2000 protease inhibitor cocktail, 2 mg/ml lysozyme, 50 mM Tris-HCl, pH 8.0). Eight hundred microliters of cell suspension were mixed with 800 mg of glass beads (0.17-0.18 mm) and cell lysis was performed with Precellys apparatus, 5 x 30 sec at 5,000 rpm. Centrifugation was performed for 12 min at 5000 rpm at 4 °C to remove cell debris and 500 µl of supernatant was collected for further protein quantification, SDS-PAGE, and *western blotting*.

3 Other methodologies

3.1 Protein quantification

Proteins were quantified with the bicinchoninic acid (BCA) method. Basically, 20 µl of 5 to 20 times diluted total protein extract were mixed with 200 µl of reactive (50:1 – BCA : $CuSO_4.5H_2O$ 4%). In parallel, a standard curve was prepared with 20 µl of bovine serum albumin (BSA) at 0 – 2,000 µg/ml. All samples were incubated for 30 min at 37 °C with mild agitation and the absorbance was measured at 562 nm.

3.2 *Western blotting* and antibodies

Routinely, protein samples were mixed with four-time concentrated sample buffer (0.32 M Tris-HCl pH 6.8, 8% SDS, 40% glycerol, 0.02% bromophenol blue, 1% DTT). Samples from *L. lactis* protein extraction were heated for 5 min at 65 °C to facilitate protein solubilization. Then, 20 µg of proteins were separated on a 10% or 4-20% SDS-PAGE and *western blotting* analysis was carried out. Primary antibodies used in this study are listed in Table 7. Secondary antibodies were horseradish peroxidase-coupled anti-rabbit IgG and anti-rat IgG secondary antibodies (1:10,000 dilution) and Lumi-Light *Western Blotting* Substrate was used (Roche Diagnostics). Chemiluminescence was captured using an Amersham Imager 600 (GE Healthcare) with automatic exposure time for high dynamic range.

For *western blot* signal quantification, the Fiji/ImageJ 2.0.0-rc-69 software was used. Briefly, rectangles of identical size and shape were drawn around the band of interest. Then, the *Gel Plot lanes* tool was used, and the surface of each peak was measured. Finally, data were normalized to the signal of the loading control, and represented as the ratio of the strain of interest compared to the reference strain.

Table 7. Primary antibodies used in this study.

Antibody target	Details	Dilution	Source
α-Gdt1p	Polyclonal rabbit	1:150 to 1:700	Our laboratory (90)
α-Sec22p	Rabbit	1:2,000	Gift from C. Barlowe, Hanover, New Hampshire
α-Prc1p (α-CPY)	Rabbit	1:2,000	Gift from H. Riezman, Geneva, Switzerland
α-Pma1p	Rabbit	1:2,000	Our laboratory (345)
α-Emp47p	Rabbit	1:2,000	Gift from H. Riezman, Geneva, Switzerland
α-Pmr1p	Polyclonal rabbit	1:125	Our laboratory (91)
α-Cdc48p	Rabbit	1:2,000	Gift from M. Ghislain, UCLouvain, Belgium
α-Ubx4p	Rabbit, Ref. UC254	1:1,000	Gift from M. Ghislain, UCLouvain, Belgium
α-GFP	Polyclonal rabbit, Ref. PABG1	1:1,000	Chromotek
α-Aeq	Polyclonal rabbit, Ref. ab9096	1:4,000	Abcam
α-HA	Monoclonal rat, Ref. 3F10	1:1,000	Roche

3.3 Statistical analysis

All statistical analyses were performed using GraphPad Prism version 9.2.0. Except if otherwise stated, the number of replicates (N) refers to independent biological replicates. When possible, data sets were tested for Gaussian distribution with Kolmogorov–Smirnov test ($\alpha = 0.05$). All data sets analyzed successfully passed normality test. When Gaussian distribution could not be tested, Geisser-Greenhouse correction was applied. According to the experiment, two-tailed unpaired t-test was used to compare two conditions, parametric one-way ANOVA with a multiple comparison Tukey test was used for more than two data sets and a single variable, and two-ways ANOVA or mixed-effects model including interaction term was used when several variables are compared completed by a multiple comparison Bonferroni test. Significance of means comparison is represented on the graphs with asterisks: * : $p < 0.05$; ** : $p < 0.01$; *** : $p < 0.001$.

REFERENCES

1. Foulquier F, Amyere M, Jaeken J, Zeevaert R, Schollen E, Race V, et al. TMEM165 deficiency causes a congenital disorder of glycosylation. American journal of human genetics. 2012;91(1):15-26.
2. Demaegd D, Colinet AS, Deschamps A, Morsomme P. Molecular evolution of a novel family of putative calcium transporters. PloS one. 2014;9(6):e100851.
3. Golgi C. On the structure of nerve cells. 1898. Journal of microscopy. 1989;155(Pt 1):3-7.
4. Matsuura-Tokita K, Takeuchi M, Ichihara A, Mikuriya K, Nakano A. Live imaging of yeast Golgi cisternal maturation. Nature. 2006;441(7096):1007-10.
5. Day KJ, Casler JC, Glick BS. Budding Yeast Has a Minimal Endomembrane System. Developmental cell. 2018;44(1):56-72 e4.
6. Grissom JH, Segarra VA, Chi RJ. New Perspectives on SNARE Function in the Yeast Minimal Endomembrane System. Genes (Basel). 2020;11(8).
7. Huh WK, Falvo JV, Gerke LC, Carroll AS, Howson RW, Weissman JS, et al. Global analysis of protein localization in budding yeast. Nature. 2003;425(6959):686-91.
8. Thul PJ, Akesson L, Wiking M, Mahdessian D, Geladaki A, Ait Blal H, et al. A subcellular map of the human proteome. Science. 2017;356(6340).
9. Becuwe M, Leon S. Integrated control of transporter endocytosis and recycling by the arrestin-related protein Rod1 and the ubiquitin ligase Rsp5. Elife. 2014;3.
10. Feyder S, De Craene JO, Bar S, Bertazzi DL, Friant S. Membrane trafficking in the yeast Saccharomyces cerevisiae model. Int J Mol Sci. 2015;16(1):1509-25.
11. Van Den Hazel HB, Kielland-Brandt MC, Winther JR. Review: biosynthesis and function of yeast vacuolar proteases. Yeast. 1996;12(1):1-16.
12. Hecht KA, O'Donnell AF, Brodsky JL. The proteolytic landscape of the yeast vacuole. Cell Logist. 2014;4(1):e28023.
13. Lujan P, Campelo F. Should I stay or should I go? Golgi membrane spatial organization for protein sorting and retention. Archives of biochemistry and biophysics. 2021;707:108921.
14. Luini A. A brief history of the cisternal progression-maturation model. Cell Logist. 2011;1(1):6-11.
15. Bannykh SI, Balch WE. Membrane dynamics at the endoplasmic reticulum-Golgi interface. The Journal of cell biology. 1997;138(1):1-4.
16. Emr S, Glick BS, Linstedt AD, Lippincott-Schwartz J, Luini A, Malhotra V, et al. Journeys through the Golgi--taking stock in a new era. The Journal of cell biology. 2009;187(4):449-53.
17. Papanikou E, Glick BS. Golgi compartmentation and identity. Curr Opin Cell Biol. 2014;29:74-81.
18. Losev E, Reinke CA, Jellen J, Strongin DE, Bevis BJ, Glick BS. Golgi maturation visualized in living yeast. Nature. 2006;441(7096):1002-6.
19. Suda Y, Nakano A. The yeast Golgi apparatus. Traffic. 2012;13(4):505-10.
20. Pantazopoulou A, Glick BS. A Kinetic View of Membrane Traffic Pathways Can Transcend the Classical View of Golgi Compartments. Front Cell Dev Biol. 2019;7:153.
21. Banfield DK, Lewis MJ, Pelham HR. A SNARE-like protein required for traffic through the Golgi complex. Nature. 1995;375(6534):806-9.
22. Miller VJ, Ungar D. Re'COG'nition at the Golgi. Traffic. 2012;13(7):891-7.

23. Witkos TM, Lowe M. Recognition and tethering of transport vesicles at the Golgi apparatus. Curr Opin Cell Biol. 2017;47:16-23.
24. Rothman JH, Stevens TH. Protein sorting in yeast: mutants defective in vacuole biogenesis mislocalize vacuolar proteins into the late secretory pathway. Cell. 1986;47(6):1041-51.
25. Bankaitis VA, Johnson LM, Emr SD. Isolation of yeast mutants defective in protein targeting to the vacuole. Proceedings of the National Academy of Sciences of the United States of America. 1986;83(23):9075-9.
26. Cooper AA, Stevens TH. Vps10p cycles between the late-Golgi and prevacuolar compartments in its function as the sorting receptor for multiple yeast vacuolar hydrolases. The Journal of cell biology. 1996;133(3):529-41.
27. Cowles CR, Snyder WB, Burd CG, Emr SD. Novel Golgi to vacuole delivery pathway in yeast: identification of a sorting determinant and required transport component. The EMBO journal. 1997;16(10):2769-82.
28. Cowles CR, Odorizzi G, Payne GS, Emr SD. The AP-3 adaptor complex is essential for cargo-selective transport to the yeast vacuole. Cell. 1997;91(1):109-18.
29. Stepp JD, Huang K, Lemmon SK. The yeast adaptor protein complex, AP-3, is essential for the efficient delivery of alkaline phosphatase by the alternate pathway to the vacuole. The Journal of cell biology. 1997;139(7):1761-74.
30. Llinares E, Barry AO, Andre B. The AP-3 adaptor complex mediates sorting of yeast and mammalian PQ-loop-family basic amino acid transporters to the vacuolar/lysosomal membrane. Sci Rep. 2015;5:16665.
31. Hirst J, Lui WW, Bright NA, Totty N, Seaman MN, Robinson MS. A family of proteins with gamma-adaptin and VHS domains that facilitate trafficking between the trans-Golgi network and the vacuole/lysosome. The Journal of cell biology. 2000;149(1):67-80.
32. Boman AL. GGA proteins: new players in the sorting game. Journal of cell science. 2001;114(Pt 19):3413-8.
33. Scott PM, Bilodeau PS, Zhdankina O, Winistorfer SC, Hauglund MJ, Allaman MM, et al. GGA proteins bind ubiquitin to facilitate sorting at the trans-Golgi network. Nature cell biology. 2004;6(3):252-9.
34. Pelham HR. SNAREs and the secretory pathway-lessons from yeast. Experimental cell research. 1999;247(1):1-8.
35. Leon S, Erpapazoglou Z, Haguenauer-Tsapis R. Ear1p and Ssh4p are new adaptors of the ubiquitin ligase Rsp5p for cargo ubiquitylation and sorting at multivesicular bodies. Molecular biology of the cell. 2008;19(6):2379-88.
36. Buelto D, Hung CW, Aoh QL, Lahiri S, Duncan MC. Plasma membrane to vacuole traffic induced by glucose starvation requires Gga2-dependent sorting at the trans-Golgi network. Biol Cell. 2020;112(11):349-67.
37. Diakov TT, Kane PM. Regulation of vacuolar proton-translocating ATPase activity and assembly by extracellular pH. The Journal of biological chemistry. 2010;285(31):23771-8.
38. Reifenrath M, Boles E. A superfolder variant of pH-sensitive pHluorin for in vivo pH measurements in the endoplasmic reticulum. Sci Rep. 2018;8(1):11985.
39. Tarsio M, Zheng H, Smardon AM, Martinez-Munoz GA, Kane PM. Consequences of loss of Vph1 protein-containing vacuolar ATPases (V-ATPases) for overall cellular pH homeostasis. The Journal of biological chemistry. 2011;286(32):28089-96.
40. Preston RA, Murphy RF, Jones EW. Assay of vacuolar pH in yeast and identification of acidification-defective mutants. Proceedings of the National Academy of Sciences of the United States of America. 1989;86(18):7027-31.

41. Martinez-Munoz GA, Kane P. Vacuolar and plasma membrane proton pumps collaborate to achieve cytosolic pH homeostasis in yeast. The Journal of biological chemistry. 2008;283(29):20309-19.
42. Wilson DW, Lewis MJ, Pelham HR. pH-dependent binding of KDEL to its receptor in vitro. The Journal of biological chemistry. 1993;268(10):7465-8.
43. Brauer P, Parker JL, Gerondopoulos A, Zimmermann I, Seeger MA, Barr FA, et al. Structural basis for pH-dependent retrieval of ER proteins from the Golgi by the KDEL receptor. Science. 2019;363(6431):1103-7.
44. Hassinen A, Pujol FM, Kokkonen N, Pieters C, Kihlstrom M, Korhonen K, et al. Functional organization of Golgi N- and O-glycosylation pathways involves pH-dependent complex formation that is impaired in cancer cells. The Journal of biological chemistry. 2011;286(44):38329-40.
45. Hassinen A, Kellokumpu S. Organizational interplay of Golgi N-glycosyltransferases involves organelle microenvironment-dependent transitions between enzyme homo- and heteromers. The Journal of biological chemistry. 2014;289(39):26937-48.
46. Olson LJ, Hindsgaul O, Dahms NM, Kim JJ. Structural insights into the mechanism of pH-dependent ligand binding and release by the cation-dependent mannose 6-phosphate receptor. The Journal of biological chemistry. 2008;283(15):10124-34.
47. Van Den Hazel H, Wolff AM, Kielland-Brandt MC, Winther JR. Mechanism and ion-dependence of in vitro autoactivation of yeast proteinase A: possible implications for compartmentalized activation in vivo. The Biochemical journal. 1997;326 (Pt 2):339-44.
48. Mukherjee S, Ghosh RN, Maxfield FR. Endocytosis. Physiological reviews. 1997;77(3):759-803.
49. Cagnac O, Aranda-Sicilia MN, Leterrier M, Rodriguez-Rosales MP, Venema K. Vacuolar cation/H+ antiporters of Saccharomyces cerevisiae. The Journal of biological chemistry. 2010;285(44):33914-22.
50. Paroutis P, Touret N, Grinstein S. The pH of the secretory pathway: measurement, determinants, and regulation. Physiology (Bethesda). 2004;19:207-15.
51. Kellokumpu S. Golgi pH, Ion and Redox Homeostasis: How Much Do They Really Matter? Front Cell Dev Biol. 2019;7:93.
52. Forgac M. Structure and function of vacuolar class of ATP-driven proton pumps. Physiological reviews. 1989;69(3):765-96.
53. Kane PM. Disassembly and reassembly of the yeast vacuolar H(+)-ATPase in vivo. The Journal of biological chemistry. 1995;270(28):17025-32.
54. Sautin YY, Lu M, Gaugler A, Zhang L, Gluck SL. Phosphatidylinositol 3-kinase-mediated effects of glucose on vacuolar H+-ATPase assembly, translocation, and acidification of intracellular compartments in renal epithelial cells. Molecular and cellular biology. 2005;25(2):575-89.
55. Kawasaki-Nishi S, Nishi T, Forgac M. Yeast V-ATPase complexes containing different isoforms of the 100-kDa a-subunit differ in coupling efficiency and in vivo dissociation. The Journal of biological chemistry. 2001;276(21):17941-8.
56. Qi J, Forgac M. Cellular environment is important in controlling V-ATPase dissociation and its dependence on activity. The Journal of biological chemistry. 2007;282(34):24743-51.
57. Forgac M. Vacuolar ATPases: rotary proton pumps in physiology and pathophysiology. Nature reviews Molecular cell biology. 2007;8(11):917-29.

58. Vik SB, Long JC, Wada T, Zhang D. A model for the structure of subunit a of the Escherichia coli ATP synthase and its role in proton translocation. Biochimica et biophysica acta. 2000;1458(2-3):457-66.
59. Kawasaki-Nishi S, Nishi T, Forgac M. Arg-735 of the 100-kDa subunit a of the yeast V-ATPase is essential for proton translocation. Proceedings of the National Academy of Sciences of the United States of America. 2001;98(22):12397-402.
60. Manolson MF, Proteau D, Preston RA, Stenbit A, Roberts BT, Hoyt MA, et al. The VPH1 gene encodes a 95-kDa integral membrane polypeptide required for in vivo assembly and activity of the yeast vacuolar H(+)-ATPase. The Journal of biological chemistry. 1992;267(20):14294-303.
61. Manolson MF, Wu B, Proteau D, Taillon BE, Roberts BT, Hoyt MA, et al. STV1 gene encodes functional homologue of 95-kDa yeast vacuolar H(+)-ATPase subunit Vph1p. The Journal of biological chemistry. 1994;269(19):14064-74.
62. Kawasaki-Nishi S, Bowers K, Nishi T, Forgac M, Stevens TH. The amino-terminal domain of the vacuolar proton-translocating ATPase a subunit controls targeting and in vivo dissociation, and the carboxyl-terminal domain affects coupling of proton transport and ATP hydrolysis. The Journal of biological chemistry. 2001;276(50):47411-20.
63. Toyomura T, Murata Y, Yamamoto A, Oka T, Sun-Wada GH, Wada Y, et al. From lysosomes to the plasma membrane: localization of vacuolar-type H+ -ATPase with the a3 isoform during osteoclast differentiation. The Journal of biological chemistry. 2003;278(24):22023-30.
64. Wagner CA, Finberg KE, Breton S, Marshansky V, Brown D, Geibel JP. Renal vacuolar H+-ATPase. Physiological reviews. 2004;84(4):1263-314.
65. Pietrement C, Sun-Wada GH, Silva ND, McKee M, Marshansky V, Brown D, et al. Distinct expression patterns of different subunit isoforms of the V-ATPase in the rat epididymis. Biology of reproduction. 2006;74(1):185-94.
66. Munn AL, Riezman H. Endocytosis is required for the growth of vacuolar H(+)-ATPase-defective yeast: identification of six new END genes. The Journal of cell biology. 1994;127(2):373-86.
67. Smardon AM, Kane PM. Loss of vacuolar H+-ATPase activity in organelles signals ubiquitination and endocytosis of the yeast plasma membrane proton pump Pma1p. The Journal of biological chemistry. 2014;289(46):32316-26.
68. Matamala E, Castillo C, Vivar JP, Rojas PA, Brauchi SE. Imaging the electrical activity of organelles in living cells. Commun Biol. 2021;4(1):389.
69. Maeda Y, Ide T, Koike M, Uchiyama Y, Kinoshita T. GPHR is a novel anion channel critical for acidification and functions of the Golgi apparatus. Nature cell biology. 2008;10(10):1135-45.
70. Braun NA, Morgan B, Dick TP, Schwappach B. The yeast CLC protein counteracts vesicular acidification during iron starvation. Journal of cell science. 2010;123(Pt 13):2342-50.
71. Schwappach B, Stobrawa S, Hechenberger M, Steinmeyer K, Jentsch TJ. Golgi localization and functionally important domains in the NH2 and COOH terminus of the yeast CLC putative chloride channel Gef1p. The Journal of biological chemistry. 1998;273(24):15110-8.
72. Flis K, Bednarczyk P, Hordejuk R, Szewczyk A, Berest V, Dolowy K, et al. The Gef1 protein of Saccharomyces cerevisiae is associated with chloride channel activity. Biochemical and biophysical research communications. 2002;294(5):1144-50.
73. Brett CL, Tukaye DN, Mukherjee S, Rao R. The yeast endosomal Na+K+/H+ exchanger Nhx1 regulates cellular pH to control vesicle trafficking. Molecular biology of the cell. 2005;16(3):1396-405.

74. Maresova L, Sychrova H. Physiological characterization of Saccharomyces cerevisiae kha1 deletion mutants. Molecular microbiology. 2005;55(2):588-600.
75. Flis K, Hinzpeter A, Edelman A, Kurlandzka A. The functioning of mammalian ClC-2 chloride channel in Saccharomyces cerevisiae cells requires an increased level of Kha1p. The Biochemical journal. 2005;390(Pt 3):655-64.
76. Wu MM, Grabe M, Adams S, Tsien RY, Moore HP, Machen TE. Mechanisms of pH regulation in the regulated secretory pathway. The Journal of biological chemistry. 2001;276(35):33027-35.
77. Khosrowabadi E, Rivinoja A, Risteli M, Tuomisto A, Salo T, Makinen MJ, et al. SLC4A2 anion exchanger promotes tumour cell malignancy via enhancing net acid efflux across golgi membranes. Cellular and molecular life sciences : CMLS. 2021;78(17-18):6283-304.
78. Nozawa A, Takano J, Kobayashi M, von Wiren N, Fujiwara T. Roles of BOR1, DUR3, and FPS1 in boron transport and tolerance in Saccharomyces cerevisiae. FEMS microbiology letters. 2006;262(2):216-22.
79. Hadley B, Maggioni A, Ashikov A, Day CJ, Haselhorst T, Tiralongo J. Structure and function of nucleotide sugar transporters: Current progress. Computational and structural biotechnology journal. 2014;10(16):23-32.
80. Snyder NA, Stefan CP, Soroudi CT, Kim A, Evangelista C, Cunningham KW. H+ and Pi Byproducts of Glycosylation Affect Ca2+ Homeostasis and Are Retrieved from the Golgi Complex by Homologs of TMEM165 and XPR1. G3 (Bethesda). 2017.
81. Halachmi D, Eilam Y. Elevated cytosolic free Ca2+ concentrations and massive Ca2+ accumulation within vacuoles, in yeast mutant lacking PMR1, a homolog of Ca2+ -ATPase. FEBS letters. 1996;392(2):194-200.
82. Lauer Junior CM, Bonatto D, Mielniczki-Pereira AA, Schuch AZ, Dias JF, Yoneama ML, et al. The Pmr1 protein, the major yeast Ca2+-ATPase in the Golgi, regulates intracellular levels of the cadmium ion. FEMS microbiology letters. 2008;285(1):79-88.
83. Rudolph HK, Antebi A, Fink GR, Buckley CM, Dorman TE, LeVitre J, et al. The yeast secretory pathway is perturbed by mutations in PMR1, a member of a Ca2+ ATPase family. Cell. 1989;58(1):133-45.
84. Durr G, Strayle J, Plemper R, Elbs S, Klee SK, Catty P, et al. The medial-Golgi ion pump Pmr1 supplies the yeast secretory pathway with Ca2+ and Mn2+ required for glycosylation, sorting, and endoplasmic reticulum-associated protein degradation. Molecular biology of the cell. 1998;9(5):1149-62.
85. Cronin SR, Rao R, Hampton RY. Cod1p/Spf1p is a P-type ATPase involved in ER function and Ca2+ homeostasis. The Journal of cell biology. 2002;157(6):1017-28.
86. Vashist S, Frank CG, Jakob CA, Ng DT. Two distinctly localized p-type ATPases collaborate to maintain organelle homeostasis required for glycoprotein processing and quality control. Molecular biology of the cell. 2002;13(11):3955-66.
87. D'Hooge P, Coun C, Van Eyck V, Faes L, Ghillebert R, Marien L, et al. Ca(2+) homeostasis in the budding yeast Saccharomyces cerevisiae: Impact of ER/Golgi Ca(2+) storage. Cell calcium. 2015;58(2):226-35.
88. Luk EE, Culotta VC. Manganese superoxide dismutase in Saccharomyces cerevisiae acquires its metal co-factor through a pathway involving the Nramp metal transporter, Smf2p. The Journal of biological chemistry. 2001;276(50):47556-62.
89. Garcia-Rodriguez N, Manzano-Lopez J, Munoz-Bravo M, Fernandez-Garcia E, Muniz M, Wellinger RE. Manganese redistribution by calcium-stimulated vesicle trafficking bypasses the need for P-type ATPase function. The Journal of biological chemistry. 2015;290(15):9335-47.

90. Demaegd D, Foulquier F, Colinet AS, Gremillon L, Legrand D, Mariot P, et al. Newly characterized Golgi-localized family of proteins is involved in calcium and pH homeostasis in yeast and human cells. Proceedings of the National Academy of Sciences of the United States of America. 2013;110(17):6859-64.
91. Colinet AS, Sengottaiyan P, Deschamps A, Colsoul ML, Thines L, Demaegd D, et al. Yeast Gdt1 is a Golgi-localized calcium transporter required for stress-induced calcium signaling and protein glycosylation. Sci Rep. 2016;6:24282.
92. Thines L, Deschamps A, Sengottaiyan P, Savel O, Stribny J, Morsomme P. The yeast protein Gdt1p transports Mn(2+) ions and thereby regulates manganese homeostasis in the Golgi. The Journal of biological chemistry. 2018;293(21):8048-55.
93. Cyert MS, Philpott CC. Regulation of cation balance in Saccharomyces cerevisiae. Genetics. 2013;193(3):677-713.
94. Patton JL, Lester RL. The phosphoinositol sphingolipids of Saccharomyces cerevisiae are highly localized in the plasma membrane. Journal of bacteriology. 1991;173(10):3101-8.
95. Holthuis JC, Menon AK. Lipid landscapes and pipelines in membrane homeostasis. Nature. 2014;510(7503):48-57.
96. Futerman AH, Riezman H. The ins and outs of sphingolipid synthesis. Trends in cell biology. 2005;15(6):312-8.
97. Levine TP, Wiggins CA, Munro S. Inositol phosphorylceramide synthase is located in the Golgi apparatus of Saccharomyces cerevisiae. Molecular biology of the cell. 2000;11(7):2267-81.
98. Nagiec MM, Nagiec EE, Baltisberger JA, Wells GB, Lester RL, Dickson RC. Sphingolipid synthesis as a target for antifungal drugs. Complementation of the inositol phosphorylceramide synthase defect in a mutant strain of Saccharomyces cerevisiae by the AUR1 gene. The Journal of biological chemistry. 1997;272(15):9809-17.
99. Dukhovny A, Yaffe Y, Shepshelovitch J, Hirschberg K. The length of cargo-protein transmembrane segments drives secretory transport by facilitating cargo concentration in export domains. Journal of cell science. 2009;122(Pt 11):1759-67.
100. Schmidt U, Weiss M. Hydrophobic mismatch-induced clustering as a primer for protein sorting in the secretory pathway. Biophys Chem. 2010;151(1-2):34-8.
101. Bretscher MS, Munro S. Cholesterol and the Golgi apparatus. Science. 1993;261(5126):1280-1.
102. Ronchi P, Colombo S, Francolini M, Borgese N. Transmembrane domain-dependent partitioning of membrane proteins within the endoplasmic reticulum. The Journal of cell biology. 2008;181(1):105-18.
103. Sharpe HJ, Stevens TJ, Munro S. A comprehensive comparison of transmembrane domains reveals organelle-specific properties. Cell. 2010;142(1):158-69.
104. Munro S. An investigation of the role of transmembrane domains in Golgi protein retention. The EMBO journal. 1995;14(19):4695-704.
105. Strahl T, Thorner J. Synthesis and function of membrane phosphoinositides in budding yeast, Saccharomyces cerevisiae. Biochimica et biophysica acta. 2007;1771(3):353-404.
106. Bankaitis VA, Aitken JR, Cleves AE, Dowhan W. An essential role for a phospholipid transfer protein in yeast Golgi function. Nature. 1990;347(6293):561-2.
107. Herman PK, Emr SD. Characterization of VPS34, a gene required for vacuolar protein sorting and vacuole segregation in Saccharomyces cerevisiae. Molecular and cellular biology. 1990;10(12):6742-54.

108. Schu PV, Takegawa K, Fry MJ, Stack JH, Waterfield MD, Emr SD. Phosphatidylinositol 3-kinase encoded by yeast VPS34 gene essential for protein sorting. Science. 1993;260(5104):88-91.
109. Hama H, Schnieders EA, Thorner J, Takemoto JY, DeWald DB. Direct involvement of phosphatidylinositol 4-phosphate in secretion in the yeast Saccharomyces cerevisiae. The Journal of biological chemistry. 1999;274(48):34294-300.
110. Walch-Solimena C, Novick P. The yeast phosphatidylinositol-4-OH kinase pik1 regulates secretion at the Golgi. Nature cell biology. 1999;1(8):523-5.
111. Shibuya A, Margulis N, Christiano R, Walther TC, Barlowe C. The Erv41-Erv46 complex serves as a retrograde receptor to retrieve escaped ER proteins. The Journal of cell biology. 2015;208(2):197-209.
112. Rivinoja A, Hassinen A, Kokkonen N, Kauppila A, Kellokumpu S. Elevated Golgi pH impairs terminal N-glycosylation by inducing mislocalization of Golgi glycosyltransferases. Journal of cellular physiology. 2009;220(1):144-54.
113. Huang C, Chang A. pH-dependent cargo sorting from the Golgi. The Journal of biological chemistry. 2011;286(12):10058-65.
114. Fuller RS, Brake A, Thorner J. Yeast prohormone processing enzyme (KEX2 gene product) is a Ca2+-dependent serine protease. Proceedings of the National Academy of Sciences of the United States of America. 1989;86(5):1434-8.
115. Matsumoto R, Suzuki K, Ohya Y. Organelle acidification is important for localisation of vacuolar proteins in Saccharomyces cerevisiae. Protoplasma. 2013;250(6):1283-93.
116. Brett CL, Kallay L, Hua Z, Green R, Chyou A, Zhang Y, et al. Genome-wide analysis reveals the vacuolar pH-stat of Saccharomyces cerevisiae. PloS one. 2011;6(3):e17619.
117. Banerjee S, Kane PM. Direct interaction of the Golgi V-ATPase a-subunit isoform with PI(4)P drives localization of Golgi V-ATPases in yeast. Molecular biology of the cell. 2017;28(19):2518-30.
118. Li SC, Diakov TT, Xu T, Tarsio M, Zhu W, Couoh-Cardel S, et al. The signaling lipid PI(3,5)P(2) stabilizes V(1)-V(o) sector interactions and activates the V-ATPase. Molecular biology of the cell. 2014;25(8):1251-62.
119. Banerjee S, Clapp K, Tarsio M, Kane PM. Interaction of the late endo-lysosomal lipid PI(3,5)P2 with the Vph1 isoform of yeast V-ATPase increases its activity and cellular stress tolerance. The Journal of biological chemistry. 2019;294(23):9161-71.
120. Dong XP, Shen D, Wang X, Dawson T, Li X, Zhang Q, et al. PI(3,5)P(2) controls membrane trafficking by direct activation of mucolipin Ca(2+) release channels in the endolysosome. Nature communications. 2010;1:38.
121. Hay JC. Calcium: a fundamental regulator of intracellular membrane fusion? EMBO Rep. 2007;8(3):236-40.
122. Chadwick SR, Grinstein S, Freeman SA. From the inside out: Ion fluxes at the centre of endocytic traffic. Curr Opin Cell Biol. 2021;71:77-86.
123. Wood CS, Hung CS, Huoh YS, Mousley CJ, Stefan CJ, Bankaitis V, et al. Local control of phosphatidylinositol 4-phosphate signaling in the Golgi apparatus by Vps74 and Sac1 phosphoinositide phosphatase. Molecular biology of the cell. 2012;23(13):2527-36.
124. Shin JJH, Liu P, Chan LJ, Ullah A, Pan J, Borchers CH, et al. pH Biosensing by PI4P Regulates Cargo Sorting at the TGN. Developmental cell. 2020;52(4):461-76 e4.
125. Reynders E, Foulquier F, Annaert W, Matthijs G. How Golgi glycosylation meets and needs trafficking: the case of the COG complex. Glycobiology. 2011;21(7):853-63.

126. Gosavi P, Gleeson PA. The Function of the Golgi Ribbon Structure - An Enduring Mystery Unfolds! Bioessays. 2017;39(11).
127. Paczkowski JE, Richardson BC, Fromme JC. Cargo adaptors: structures illuminate mechanisms regulating vesicle biogenesis. Trends in cell biology. 2015;25(7):408-16.
128. Banfield DK, Lewis MJ, Rabouille C, Warren G, Pelham HR. Localization of Sed5, a putative vesicle targeting molecule, to the cis-Golgi network involves both its transmembrane and cytoplasmic domains. The Journal of cell biology. 1994;127(2):357-71.
129. Gao G, Banfield DK. Multiple features within the syntaxin Sed5p mediate its Golgi localization. Traffic. 2020;21(3):274-96.
130. Wilson C, Ragnini-Wilson A. Conserved molecular mechanisms underlying homeostasis of the Golgi complex. Int J Cell Biol. 2010;2010:758230.
131. Varki A. Biological roles of oligosaccharides: all of the theories are correct. Glycobiology. 1993;3(2):97-130.
132. Kostova Z, Wolf DH. Importance of carbohydrate positioning in the recognition of mutated CPY for ER-associated degradation. Journal of cell science. 2005;118(Pt 7):1485-92.
133. Colinet AS. Yeast Gdt1 is a Golgi-localized calcium transporter required for stress-induced calcium signaling and protein glycosylation [PhD thesis]. Louvain-la-Neuve, Belgium: Université catholique de Louvain; 2016.
134. Aebi M. N-linked protein glycosylation in the ER. Biochimica et biophysica acta. 2013;1833(11):2430-7.
135. Lehle L, Strahl S, Tanner W. Protein glycosylation, conserved from yeast to man: a model organism helps elucidate congenital human diseases. Angew Chem Int Ed Engl. 2006;45(41):6802-18.
136. Neubert P, Halim A, Zauser M, Essig A, Joshi HJ, Zatorska E, et al. Mapping the O-Mannose Glycoproteome in Saccharomyces cerevisiae. Molecular & cellular proteomics : MCP. 2016;15(4):1323-37.
137. Van den Steen P, Rudd PM, Dwek RA, Opdenakker G. Concepts and principles of O-linked glycosylation. Crit Rev Biochem Mol Biol. 1998;33(3):151-208.
138. Hang I, Lin CW, Grant OC, Fleurkens S, Villiger TK, Soos M, et al. Analysis of site-specific N-glycan remodeling in the endoplasmic reticulum and the Golgi. Glycobiology. 2015;25(12):1335-49.
139. Pothukuchi P, Agliarulo I, Russo D, Rizzo R, Russo F, Parashuraman S. Translation of genome to glycome: role of the Golgi apparatus. FEBS letters. 2019;593(17):2390-411.
140. Losfeld ME, Scibona E, Lin CW, Villiger TK, Gauss R, Morbidelli M, et al. Influence of protein/glycan interaction on site-specific glycan heterogeneity. FASEB journal : official publication of the Federation of American Societies for Experimental Biology. 2017;31(10):4623-35.
141. Maeda Y. pH Control in Golgi Apparatus and Congenital Disorders of Glycosylation. Glycoscience: Biology and Medicine. 2015.
142. Frappaolo A, Karimpour-Ghahnavieh A, Sechi S, Giansanti MG. The Close Relationship between the Golgi Trafficking Machinery and Protein Glycosylation. Cells. 2020;9(12).
143. Axelsson MA, Karlsson NG, Steel DM, Ouwendijk J, Nilsson T, Hansson GC. Neutralization of pH in the Golgi apparatus causes redistribution of glycosyltransferases and changes in the O-glycosylation of mucins. Glycobiology. 2001;11(8):633-44.

144. Apweiler R, Hermjakob H, Sharon N. On the frequency of protein glycosylation, as deduced from analysis of the SWISS-PROT database. Biochimica et biophysica acta. 1999;1473(1):4-8.
145. Zafar S, Nasir A, Bokhari H. Computational analysis reveals abundance of potential glycoproteins in Archaea, Bacteria and Eukarya. Bioinformation. 2011;6(9):352-5.
146. Khoury GA, Baliban RC, Floudas CA. Proteome-wide post-translational modification statistics: frequency analysis and curation of the swiss-prot database. Sci Rep. 2011;1.
147. Wilson MP, Matthijs G. The evolving genetic landscape of congenital disorders of glycosylation. Biochim Biophys Acta Gen Subj. 2021;1865(11):129976.
148. Jaeken JV-L, M.; Casaer, P.; Snoeck, L.; Corbeel, L.; Eggermont, E.; Eeckels, R. Familial psychomotor retardation with markedly fluctuating serum prolactin, FSH and GH levels, partial TBG-deficiency, increased serum arylsulphatase A and increased CSF protein: a new syndrome? Pediatric research. 1980;14:179.
149. Van Schaftingen E, Jaeken J. Phosphomannomutase deficiency is a cause of carbohydrate-deficient glycoprotein syndrome type I. FEBS letters. 1995;377(3):318-20.
150. Freeze HH. Update and perspectives on congenital disorders of glycosylation. Glycobiology. 2001;11(12):129R-43R.
151. Ondruskova N, Cechova A, Hansikova H, Honzik T, Jaeken J. Congenital disorders of glycosylation: Still "hot" in 2020. Biochim Biophys Acta Gen Subj. 2021;1865(1):129751.
152. Breton C, Snajdrova L, Jeanneau C, Koca J, Imberty A. Structures and mechanisms of glycosyltransferases. Glycobiology. 2006;16(2):29R-37R.
153. Breton C, Fournel-Gigleux S, Palcic MM. Recent structures, evolution and mechanisms of glycosyltransferases. Current opinion in structural biology. 2012;22(5):540-9.
154. Ramakrishnan B, Ramasamy V, Qasba PK. Structural snapshots of beta-1,4-galactosyltransferase-I along the kinetic pathway. Journal of molecular biology. 2006;357(5):1619-33.
155. Beckers CJ, Balch WE. Calcium and GTP: essential components in vesicular trafficking between the endoplasmic reticulum and Golgi apparatus. The Journal of cell biology. 1989;108(4):1245-56.
156. Yoshibori M, Yorimitsu T, Sato K. Involvement of the penta-EF-hand protein Pef1p in the Ca2+-dependent regulation of COPII subunit assembly in Saccharomyces cerevisiae. PloS one. 2012;7(7):e40765.
157. Hu K, Carroll J, Fedorovich S, Rickman C, Sukhodub A, Davletov B. Vesicular restriction of synaptobrevin suggests a role for calcium in membrane fusion. Nature. 2002;415(6872):646-50.
158. Antebi A, Fink GR. The yeast Ca(2+)-ATPase homologue, PMR1, is required for normal Golgi function and localizes in a novel Golgi-like distribution. Molecular biology of the cell. 1992;3(6):633-54.
159. Kellokumpu S, Hassinen A, Glumoff T. Glycosyltransferase complexes in eukaryotes: long-known, prevalent but still unrecognized. Cellular and molecular life sciences : CMLS. 2016;73(2):305-25.
160. Nilsson T, Slusarewicz P, Hoe MH, Warren G. Kin recognition. A model for the retention of Golgi enzymes. FEBS letters. 1993;330(1):1-4.
161. Khosrowabadi E, Kellokumpu S. Golgi pH and Ion Homeostasis in Health and Disease. Rev Physiol Biochem Pharmacol. 2020.

162. Kornak U, Reynders E, Dimopoulou A, van Reeuwijk J, Fischer B, Rajab A, et al. Impaired glycosylation and cutis laxa caused by mutations in the vesicular H+-ATPase subunit ATP6V0A2. Nat Genet. 2008;40(1):32-4.
163. Guillard M, Dimopoulou A, Fischer B, Morava E, Lefeber DJ, Kornak U, et al. Vacuolar H+-ATPase meets glycosylation in patients with cutis laxa. Biochimica et biophysica acta. 2009;1792(9):903-14.
164. Corbacho I, Teixido F, Olivero I, Hernandez LM. Dependence of Saccharomyces cerevisiae Golgi functions on V-ATPase activity. FEMS yeast research. 2012;12(3):341-50.
165. Althoff SS, Gruneberg M, Reunert J, Park JH, Rust S, Muhlhausen C, et al. TMEM165 Deficiency: Postnatal Changes in Glycosylation. JIMD reports. 2015.
166. Vicogne D, Houdou M, Garat A, Climer L, Lupashin V, Morelle W, et al. Fetal bovine serum impacts the observed N-glycosylation defects in TMEM165 KO HEK cells. Journal of inherited metabolic disease. 2020;43(2):357-66.
167. Xia B, Zhang W, Li X, Jiang R, Harper T, Liu R, et al. Serum N-glycan and O-glycan analysis by mass spectrometry for diagnosis of congenital disorders of glycosylation. Analytical biochemistry. 2013;442(2):178-85.
168. Bammens R, Mehta N, Race V, Foulquier F, Jaeken J, Tiemeyer M, et al. Abnormal cartilage development and altered N-glycosylation in Tmem165-deficient zebrafish mirrors the phenotypes associated with TMEM165-CDG. Glycobiology. 2015;25(6):669-82.
169. Morelle W, Potelle S, Witters P, Wong S, Climer L, Lupashin V, et al. Galactose Supplementation in Patients With TMEM165-CDG Rescues the Glycosylation Defects. The Journal of clinical endocrinology and metabolism. 2017;102(4):1375-86.
170. Rosnoblet C, Legrand D, Demaegd D, Hacine-Gherbi H, de Bettignies G, Bammens R, et al. Impact of disease-causing mutations on TMEM165 subcellular localization, a recently identified protein involved in CDG-II. Human molecular genetics. 2013;22(14):2914-28.
171. Wang H, Yang Y, Huang F, He Z, Li P, Zhang W, et al. In Situ Fluorescent and Photoacoustic Imaging of Golgi pH to Elucidate the Function of Transmembrane Protein 165. Analytical chemistry. 2020;92(4):3103-10.
172. Potelle S, Morelle W, Dulary E, Duvet S, Vicogne D, Spriet C, et al. Glycosylation abnormalities in Gdt1p/TMEM165 deficient cells result from a defect in Golgi manganese homeostasis. Human molecular genetics. 2016;25(8):1489-500.
173. Demaegd D. Characterization of Gdt1p, a yeast protein localized in the Golgi apparatus and involved in calcium homeostasis [PhD thesis]. Louvain-la-Neuve, Belgium: Université catholique de Louvain; 2013.
174. Stribny J, Thines L, Deschamps A, Goffin P, Morsomme P. The human Golgi protein TMEM165 transports calcium and manganese in yeast and bacterial cells. The Journal of biological chemistry. 2020;295(12):3865-74.
175. Cai X, Lytton J. The cation/Ca(2+) exchanger superfamily: phylogenetic analysis and structural implications. Molecular biology and evolution. 2004;21(9):1692-703.
176. Liao J, Li H, Zeng W, Sauer DB, Belmares R, Jiang Y. Structural insight into the ion-exchange mechanism of the sodium/calcium exchanger. Science. 2012;335(6069):686-90.
177. Jumper J, Evans R, Pritzel A, Green T, Figurnov M, Ronneberger O, et al. Highly accurate protein structure prediction with AlphaFold. Nature. 2021;596(7873):583-9.

178. Nishizawa T, Kita S, Maturana AD, Furuya N, Hirata K, Kasuya G, et al. Structural basis for the counter-transport mechanism of a H+/Ca2+ exchanger. Science. 2013;341(6142):168-72.
179. Thines L, Stribny J, Morsomme P. From the Uncharacterized Protein Family 0016 to the GDT1 family: Molecular insights into a newly-characterized family of cation secondary transporters. Microb Cell. 2020;7(8):202-14.
180. Eisenhut M, Hoecker N, Schmidt SB, Basgaran RM, Flachbart S, Jahns P, et al. The plastid envelope CHLOROPLAST MANGANESE TRANSPORTER1 is essential for manganese homeostasis in Arabidopsis. Molecular plant. 2018.
181. Zhang B, Zhang C, Liu C, Jing Y, Wang Y, Jin L, et al. Inner Envelope CHLOROPLAST MANGANESE TRANSPORTER 1 Supports Manganese Homeostasis and Phototrophic Growth in Arabidopsis. Molecular plant. 2018;11(7):943-54.
182. Schneider A, Steinberger I, Herdean A, Gandini C, Eisenhut M, Kurz S, et al. The Evolutionarily Conserved Protein PHOTOSYNTHESIS AFFECTED MUTANT71 Is Required for Efficient Manganese Uptake at the Thylakoid Membrane in Arabidopsis. The Plant cell. 2016;28(4):892-910.
183. Wang C, Xu W, Jin H, Zhang T, Lai J, Zhou X, et al. A Putative Chloroplast-Localized Ca(2+)/H(+) Antiporter CCHA1 Is Involved in Calcium and pH Homeostasis and Required for PSII Function in Arabidopsis. Molecular plant. 2016;9(8):1183-96.
184. Frank J, Happeck R, Meier B, Hoang MTT, Stribny J, Hause G, et al. Chloroplast-localized BICAT proteins shape stromal calcium signals and are required for efficient photosynthesis. The New phytologist. 2019;221(2):866-80.
185. Gandini C, Schmidt SB, Husted S, Schneider A, Leister D. The transporter SynPAM71 is located in the plasma membrane and thylakoids, and mediates manganese tolerance in Synechocystis PCC6803. The New phytologist. 2017;215(1):256-68.
186. Brandenburg F, Schoffman H, Kurz S, Kramer U, Keren N, Weber AP, et al. The Synechocystis Manganese Exporter Mnx Is Essential for Manganese Homeostasis in Cyanobacteria. Plant physiology. 2017;173(3):1798-810.
187. Fisher CR, Wyckoff EE, Peng ED, Payne SM. Identification and Characterization of a Putative Manganese Export Protein in Vibrio cholerae. Journal of bacteriology. 2016.
188. Ramakrishnan S, Unger LM, Baptista RP, Cruz-Bustos T, Docampo R. Deletion of a Golgi protein in Trypanosoma cruzi reveals a critical role for Mn2+ in protein glycosylation needed for host cell invasion and intracellular replication. PLoS pathogens. 2021;17(3):e1009399.
189. Yang CH, Wang C, Singh S, Fan N, Liu S, Zhao L, et al. Golgi-localised manganese transporter PML3 regulates Arabidopsis growth through modulating Golgi glycosylation and cell wall biosynthesis. The New phytologist. 2021.
190. Reinhardt TA, Lippolis JD, Sacco RE. The Ca/H antiporter TMEM165 expression, localization in the developing, lactating and involuting mammary gland parallels the secretory pathway Ca2+ATPase (SPCA1). Biochemical and biophysical research communications. 2014.
191. Snyder NA, Palmer MV, Reinhardt TA, Cunningham KW. Milk biosynthesis requires the Golgi cation exchanger TMEM165. The Journal of biological chemistry. 2019.
192. Hoecker N, Honke A, Frey K, Leister D, Schneider A. Homologous Proteins of the Manganese Transporter PAM71 Are Localized in the Golgi Apparatus and Endoplasmic Reticulum. Plants (Basel). 2020;9(2).
193. Jiang L, Wang J, Asghar F, Snyder N, Cunningham KW. CaGdt1 plays a compensatory role for the calcium pump CaPmr1 in the regulation of calcium signaling and cell wall integrity signaling in Candida albicans. Cell communication and signaling : CCS. 2018;16(1):33.

194. Wang C, Ou D, Wang C, Lu X, Du J, Li J, et al. Functional characterization of a chloroplast-localized Mn(2+)(Ca(2+))/H(+) antiporter, ZmmCCHA1 from Zea mays ssp. mexicana L. Plant Physiol Biochem. 2020;155:396-405.
195. Dulary E, Yu SY, Houdou M, de Bettignies G, Decool V, Potelle S, et al. Investigating the function of Gdt1p in yeast Golgi glycosylation. Biochimica et biophysica acta. 2017.
196. Lebredonchel E, Houdou M, Potelle S, de Bettignies G, Schulz C, Krzewinski Recchi MA, et al. Dissection of TMEM165 function in Golgi glycosylation and its Mn(2+) sensitivity. Biochimie. 2019;165:123-30.
197. Yoshimoto H, Saltsman K, Gasch AP, Li HX, Ogawa N, Botstein D, et al. Genome-wide analysis of gene expression regulated by the calcineurin/Crz1p signaling pathway in Saccharomyces cerevisiae. The Journal of biological chemistry. 2002;277(34):31079-88.
198. Cunningham KW. Acidic calcium stores of Saccharomyces cerevisiae. Cell calcium. 2011;50(2):129-38.
199. Andreeva N, Kulakovskaya E, Zvonarev A, Penin A, Eliseeva I, Teterina A, et al. Transcriptome profile of yeast reveals the essential role of PMA2 and uncharacterized gene YBR056W-A (MNC1) in adaptation to toxic manganese concentration. Metallomics. 2017;9(2):175-82.
200. Clapham DE. Calcium signaling. Cell. 2007;131(6):1047-58.
201. Cui J, Kaandorp JA, Sloot PM, Lloyd CM, Filatov MV. Calcium homeostasis and signaling in yeast cells and cardiac myocytes. FEMS yeast research. 2009;9(8):1137-47.
202. Strayle J, Pozzan T, Rudolph HK. Steady-state free Ca(2+) in the yeast endoplasmic reticulum reaches only 10 microM and is mainly controlled by the secretory pathway pump pmr1. The EMBO journal. 1999;18(17):4733-43.
203. Dunn T, Gable K, Beeler T. Regulation of cellular Ca2+ by yeast vacuoles. The Journal of biological chemistry. 1994;269(10):7273-8.
204. Aulestia FJ, Alonso MT, Garcia-Sancho J. Differential calcium handling by the cis and trans regions of the Golgi apparatus. The Biochemical journal. 2015;466(3):455-65.
205. Denis V, Cyert MS. Internal Ca(2+) release in yeast is triggered by hypertonic shock and mediated by a TRP channel homologue. The Journal of cell biology. 2002;156(1):29-34.
206. Colinet AS, Thines L, Deschamps A, Flemal G, Demaegd D, Morsomme P. Acidic and uncharged polar residues in the consensus motifs of the yeast Ca2+ transporter Gdt1p are required for calcium transport. Cellular microbiology. 2017;19(7).
207. Ma TY, Deprez MA, Callewaert G, Winderickx J. Coordinated glucose-induced Ca(2+) and pH responses in yeast Saccharomyces cerevisiae. Cell calcium. 2021;100:102479.
208. Thines L. The yeast protein Gdt1 is a newly-identified actor in manganese homeostasis at the Golgi [PhD thesis]. Louvain-la-Neuve, Belgium: UCLouvain; 2019.
209. Lebredonchel E, Houdou M, Hoffmann HH, Kondratska K, Krzewinski MA, Vicogne D, et al. Investigating the functional link between TMEM165 and SPCA1. The Biochemical journal. 2019;476(21):3281-93.
210. Potelle S, Dulary E, Climer L, Duvet S, Morelle W, Vicogne D, et al. Manganese-induced turnover of TMEM165. The Biochemical journal. 2017;474(9):1481-93.
211. Winzeler EA, Shoemaker DD, Astromoff A, Liang H, Anderson K, Andre B, et al. Functional characterization of the S. cerevisiae genome by gene deletion and parallel analysis. Science. 1999;285(5429):901-6.

212. Alonso MT, Rojo-Ruiz J, Navas-Navarro P, Rodriguez-Prados M, Garcia-Sancho J. Measuring Ca2+ inside intracellular organelles with luminescent and fluorescent aequorin-based sensors. Biochimica et biophysica acta. 2017;1864(6):894-9.
213. Whitaker M. Genetically encoded probes for measurement of intracellular calcium. Methods in cell biology. 2010;99:153-82.
214. Perez Koldenkova V, Nagai T. Genetically encoded Ca(2+) indicators: properties and evaluation. Biochimica et biophysica acta. 2013;1833(7):1787-97.
215. Bootman MD, Rietdorf K, Collins T, Walker S, Sanderson M. Ca2+-sensitive fluorescent dyes and intracellular Ca2+ imaging. Cold Spring Harbor protocols. 2013;2013(2):83-99.
216. Taylor CW, Prole DL. Ca(2+) signalling by IP(3) receptors. Subcell Biochem. 2012;59:1-34.
217. Yanez M, Gil-Longo J, Campos-Toimil M. Calcium binding proteins. Advances in experimental medicine and biology. 2012;740:461-82.
218. Shimomura O, Johnson FH, Saiga Y. Extraction, purification and properties of aequorin, a bioluminescent protein from the luminous hydromedusan, Aequorea. Journal of cellular and comparative physiology. 1962;59:223-39.
219. Shimomura O, Johnson FH, Saiga Y. Microdetermination of Calcium by Aequorin Luminescence. Science. 1963;140(3573):1339-40.
220. Allen DG, Blinks JR, Prendergast FG. Aequorin luminescence: relation of light emission to calcium concentration--a calcium-independent component. Science. 1977;195(4282):996-8.
221. Webb SE, Karplus E, Miller AL. Retrospective on the development of aequorin and aequorin-based imaging to visualize changes in intracellular free [Ca]. Molecular reproduction and development. 2013.
222. Zhang M, Abrams C, Wang L, Gizzi A, He L, Lin R, et al. Structural basis for calmodulin as a dynamic calcium sensor. Structure. 2012;20(5):911-23.
223. Miyawaki A, Llopis J, Heim R, McCaffery JM, Adams JA, Ikura M, et al. Fluorescent indicators for Ca2+ based on green fluorescent proteins and calmodulin. Nature. 1997;388(6645):882-7.
224. Ikura M, Clore GM, Gronenborn AM, Zhu G, Klee CB, Bax A. Solution structure of a calmodulin-target peptide complex by multidimensional NMR. Science. 1992;256(5057):632-8.
225. Baird GS, Zacharias DA, Tsien RY. Circular permutation and receptor insertion within green fluorescent proteins. Proceedings of the National Academy of Sciences of the United States of America. 1999;96(20):11241-6.
226. Rodriguez-Garcia A, Rojo-Ruiz J, Navas-Navarro P, Aulestia FJ, Gallego-Sandin S, Garcia-Sancho J, et al. GAP, an aequorin-based fluorescent indicator for imaging Ca2+ in organelles. Proceedings of the National Academy of Sciences of the United States of America. 2014.
227. Rayner JC, Munro S. Identification of the MNN2 and MNN5 mannosyltransferases required for forming and extending the mannose branches of the outer chain mannans of Saccharomyces cerevisiae. The Journal of biological chemistry. 1998;273(41):26836-43.
228. Nett JH, Stadheim TA, Li H, Bobrowicz P, Hamilton SR, Davidson RC, et al. A combinatorial genetic library approach to target heterologous glycosylation enzymes to the endoplasmic reticulum or the Golgi apparatus of Pichia pastoris. Yeast. 2011;28(3):237-52.

229. Pinton P, Pozzan T, Rizzuto R. The Golgi apparatus is an inositol 1,4,5-trisphosphate-sensitive Ca2+ store, with functional properties distinct from those of the endoplasmic reticulum. The EMBO journal. 1998;17(18):5298-308.
230. Kendall JM, Sala-Newby G, Ghalaut V, Dormer RL, Campbell AK. Engineering the CA(2+)-activated photoprotein aequorin with reduced affinity for calcium. Biochemical and biophysical research communications. 1992;187(2):1091-7.
231. de la Fuente S, Fonteriz RI, de la Cruz PJ, Montero M, Alvarez J. Mitochondrial free [Ca(2+)] dynamics measured with a novel low-Ca(2+) affinity aequorin probe. The Biochemical journal. 2012;445(3):371-6.
232. Casey JR, Grinstein S, Orlowski J. Sensors and regulators of intracellular pH. Nature reviews Molecular cell biology. 2010;11(1):50-61.
233. Diakov TT, Tarsio M, Kane PM. Measurement of vacuolar and cytosolic pH in vivo in yeast cell suspensions. Journal of visualized experiments : JoVE. 2013(74).
234. Miesenbock G, De Angelis DA, Rothman JE. Visualizing secretion and synaptic transmission with pH-sensitive green fluorescent proteins. Nature. 1998;394(6689):192-5.
235. Renard HF, Demaegd D, Guerriat B, Morsomme P. Efficient ER exit and vacuole targeting of yeast Sna2p require two tyrosine-based sorting motifs. Traffic. 2010;11(7):931-46.
236. Mahon MJ. pHluorin2: an enhanced, ratiometric, pH-sensitive green florescent protein. Adv Biosci Biotechnol. 2011;2(3):132-7.
237. Morimoto YV, Kojima S, Namba K, Minamino T. M153R mutation in a pH-sensitive green fluorescent protein stabilizes its fusion proteins. PloS one. 2011;6(5):e19598.
238. Zimmermannova O, Salazar A, Sychrova H, Ramos J. Zygosaccharomyces rouxii Trk1 is an efficient potassium transporter providing yeast cells with high lithium tolerance. FEMS yeast research. 2015;15(4):fov029.
239. Zhang YQ, Gamarra S, Garcia-Effron G, Park S, Perlin DS, Rao R. Requirement for ergosterol in V-ATPase function underlies antifungal activity of azole drugs. PLoS pathogens. 2010;6(6):e1000939.
240. Kane PM. Proton Transport and pH Control in Fungi. Advances in experimental medicine and biology. 2016;892:33-68.
241. Martiniere A, Bassil E, Jublanc E, Alcon C, Reguera M, Sentenac H, et al. In vivo intracellular pH measurements in tobacco and Arabidopsis reveal an unexpected pH gradient in the endomembrane system. The Plant cell. 2013;25(10):4028-43.
242. Reguera M, Bassil E, Tajima H, Wimmer M, Chanoca A, Otegui MS, et al. pH Regulation by NHX-Type Antiporters Is Required for Receptor-Mediated Protein Trafficking to the Vacuole in Arabidopsis. The Plant cell. 2015;27(4):1200-17.
243. Wu MM, Llopis J, Adams S, McCaffery JM, Kulomaa MS, Machen TE, et al. Organelle pH studies using targeted avidin and fluorescein-biotin. Chemistry & biology. 2000;7(3):197-209.
244. Lee JH, Kim J, Park JH, Heo WD, Lee GM. Analysis of Golgi pH in Chinese hamster ovary cells using ratiometric pH-sensitive fluorescent proteins. Biotechnology and bioengineering. 2019.
245. Ho MN, Hirata R, Umemoto N, Ohya Y, Takatsuki A, Stevens TH, et al. VMA13 encodes a 54-kDa vacuolar H(+)-ATPase subunit required for activity but not assembly of the enzyme complex in Saccharomyces cerevisiae. The Journal of biological chemistry. 1993;268(24):18286-92.
246. Stevens TH, Forgac M. Structure, function and regulation of the vacuolar (H+)-ATPase. Annu Rev Cell Dev Biol. 1997;13:779-808.

247. Perzov N, Padler-Karavani V, Nelson H, Nelson N. Characterization of yeast V-ATPase mutants lacking Vph1p or Stv1p and the effect on endocytosis. The Journal of experimental biology. 2002;205(Pt 9):1209-19.
248. Dechant R, Saad S, Ibanez AJ, Peter M. Cytosolic pH regulates cell growth through distinct GTPases, Arf1 and Gtr1, to promote Ras/PKA and TORC1 activity. Mol Cell. 2014;55(3):409-21.
249. Wilms T, Swinnen E, Eskes E, Dolz-Edo L, Uwineza A, Van Essche R, et al. The yeast protein kinase Sch9 adjusts V-ATPase assembly/disassembly to control pH homeostasis and longevity in response to glucose availability. PLoS genetics. 2017;13(6):e1006835.
250. Isom DG, Page SC, Collins LB, Kapolka NJ, Taghon GJ, Dohlman HG. Coordinated regulation of intracellular pH by two glucose-sensing pathways in yeast. The Journal of biological chemistry. 2018;293(7):2318-29.
251. Serrano R. In vivo glucose activation of the yeast plasma membrane ATPase. FEBS letters. 1983;156(1):11-4.
252. Germond A, Fujita H, Ichimura T, Watanabe TM. Design and development of genetically encoded fluorescent sensors to monitor intracellular chemical and physical parameters. Biophysical Reviews. 2016;8(2):121-38.
253. Martiniere A, Desbrosses G, Sentenac H, Paris N. Development and properties of genetically encoded pH sensors in plants. Frontiers in plant science. 2013;4:523.
254. Llopis J, McCaffery JM, Miyawaki A, Farquhar MG, Tsien RY. Measurement of cytosolic, mitochondrial, and Golgi pH in single living cells with green fluorescent proteins. Proceedings of the National Academy of Sciences of the United States of America. 1998;95(12):6803-8.
255. Kokkonen N, Khosrowabadi E, Hassinen A, Harrus D, Glumoff T, Kietzmann T, et al. Abnormal Golgi pH Homeostasis in Cancer Cells Impairs Apical Targeting of Carcinoembryonic Antigen by Inhibiting Its Glycosyl-Phosphatidylinositol Anchor-Mediated Association with Lipid Rafts. Antioxidants & redox signaling. 2019;30(1):5-21.
256. Powell JT, Brew K. Metal ion activation of galactosyltransferase. The Journal of biological chemistry. 1976;251(12):3645-52.
257. Culotta VC, Daly MJ. Manganese complexes: diverse metabolic routes to oxidative stress resistance in prokaryotes and yeast. Antioxidants & redox signaling. 2013;19(9):933-44.
258. Pedelacq JD, Cabantous S, Tran T, Terwilliger TC, Waldo GS. Engineering and characterization of a superfolder green fluorescent protein. Nature biotechnology. 2006;24(1):79-88.
259. Siegumfeldt H, Bjorn Rechinger K, Jakobsen M. Dynamic changes of intracellular pH in individual lactic acid bacterium cells in response to a rapid drop in extracellular pH. Applied and environmental microbiology. 2000;66(6):2330-5.
260. Olsen KN, Budde BB, Siegumfeldt H, Rechinger KB, Jakobsen M, Ingmer H. Noninvasive measurement of bacterial intracellular pH on a single-cell level with green fluorescent protein and fluorescence ratio imaging microscopy. Applied and environmental microbiology. 2002;68(8):4145-7.
261. Jones HE, Holland IB, Baker HL, Campbell AK. Slow changes in cytosolic free Ca2+ in Escherichia coli highlight two putative influx mechanisms in response to changes in extracellular calcium. Cell calcium. 1999;25(3):265-74.
262. Dominguez DC. Calcium signalling in bacteria. Molecular microbiology. 2004;54(2):291-7.

263. Waight AB, Pedersen BP, Schlessinger A, Bonomi M, Chau BH, Roe-Zurz Z, et al. Structural basis for alternating access of a eukaryotic calcium/proton exchanger. Nature. 2013;499(7456):107-10.
264. Poznanski J, Szczesny P, Ruszczynska K, Zielenkiewicz P, Paczek L. Proteins contribute insignificantly to the intrinsic buffering capacity of yeast cytoplasm. Biochemical and biophysical research communications. 2013;430(2):741-4.
265. Miseta A, Kellermayer R, Aiello DP, Fu L, Bedwell DM. The vacuolar Ca2+/H+ exchanger Vcx1p/Hum1p tightly controls cytosolic Ca2+ levels in S. cerevisiae. FEBS letters. 1999;451(2):132-6.
266. Tisi R, Baldassa S, Belotti F, Martegani E. Phospholipase C is required for glucose-induced calcium influx in budding yeast. FEBS letters. 2002;520(1-3):133-8.
267. Kellermayer R, Szigeti R, Kellermayer M, Miseta A. The intracellular dissipation of cytosolic calcium following glucose re-addition to carbohydrate depleted Saccharomyces cerevisiae. FEBS letters. 2004;571(1-3):55-60.
268. Marchi V, Sorin A, Wei Y, Rao R. Induction of vacuolar Ca2+-ATPase and H+/Ca2+ exchange activity in yeast mutants lacking Pmr1, the Golgi Ca2+-ATPase. FEBS letters. 1999;454(3):181-6.
269. von Heijne G. Control of topology and mode of assembly of a polytopic membrane protein by positively charged residues. Nature. 1989;341(6241):456-8.
270. Kane PM. The where, when, and how of organelle acidification by the yeast vacuolar H+-ATPase. Microbiology and molecular biology reviews : MMBR. 2006;70(1):177-91.
271. Yamaguchi H, Arakawa S, Kanaseki T, Miyatsuka T, Fujitani Y, Watada H, et al. Golgi membrane-associated degradation pathway in yeast and mammals. The EMBO journal. 2016;35(18):1991-2007.
272. Tewari R, Bachert C, Linstedt AD. Induced oligomerization targets Golgi proteins for degradation in lysosomes. Molecular biology of the cell. 2015;26(24):4427-37.
273. Hellerschmied D, Serebrenik YV, Shao L, Burslem GM, Crews CM. Protein folding state-dependent sorting at the Golgi apparatus. Molecular biology of the cell. 2019;30(17):2296-308.
274. Schmidt O, Weyer Y, Baumann V, Widerin MA, Eising S, Angelova M, et al. Endosome and Golgi-associated degradation (EGAD) of membrane proteins regulates sphingolipid metabolism. The EMBO journal. 2019;38(15):e101433.
275. Eisenberg-Lerner A, Benyair R, Hizkiahou N, Nudel N, Maor R, Kramer MP, et al. Golgi organization is regulated by proteasomal degradation. Nature communications. 2020;11(1):409.
276. Reggiori F, Pelham HR. A transmembrane ubiquitin ligase required to sort membrane proteins into multivesicular bodies. Nature cell biology. 2002;4(2):117-23.
277. Daboussi L, Costaguta G, Ghukasyan R, Payne GS. Conserved role for Gga proteins in phosphatidylinositol 4-kinase localization to the trans-Golgi network. Proceedings of the National Academy of Sciences of the United States of America. 2017;114(13):3433-8.
278. Wei Y, Chen J, Rosas G, Tompkins DA, Holt PA, Rao R. Phenotypic screening of mutations in Pmr1, the yeast secretory pathway Ca2+/Mn2+-ATPase, reveals residues critical for ion selectivity and transport. The Journal of biological chemistry. 2000;275(31):23927-32.
279. Wei Y, Marchi V, Wang R, Rao R. An N-terminal EF hand-like motif modulates ion transport by Pmr1, the yeast Golgi Ca(2+)/Mn(2+)-ATPase. Biochemistry. 1999;38(44):14534-41.

280. Mandal D, Woolf TB, Rao R. Manganese selectivity of pmr1, the yeast secretory pathway ion pump, is defined by residue gln783 in transmembrane segment 6. Residue Asp778 is essential for cation transport. The Journal of biological chemistry. 2000;275(31):23933-8.
281. Lapinskas PJ, Lin SJ, Culotta VC. The role of the Saccharomyces cerevisiae CCC1 gene in the homeostasis of manganese ions. Molecular microbiology. 1996;21(3):519-28.
282. Li L, Chen OS, McVey Ward D, Kaplan J. CCC1 is a transporter that mediates vacuolar iron storage in yeast. The Journal of biological chemistry. 2001;276(31):29515-9.
283. Christiano R, Nagaraj N, Frohlich F, Walther TC. Global proteome turnover analyses of the Yeasts S. cerevisiae and S. pombe. Cell reports. 2014;9(5):1959-65.
284. Mauthe M, Orhon I, Rocchi C, Zhou X, Luhr M, Hijlkema KJ, et al. Chloroquine inhibits autophagic flux by decreasing autophagosome-lysosome fusion. Autophagy. 2018;14(8):1435-55.
285. Gerrard SR, Levi BP, Stevens TH. Pep12p is a multifunctional yeast syntaxin that controls entry of biosynthetic, endocytic and retrograde traffic into the prevacuolar compartment. Traffic. 2000;1(3):259-69.
286. Becherer KA, Rieder SE, Emr SD, Jones EW. Novel syntaxin homologue, Pep12p, required for the sorting of lumenal hydrolases to the lysosome-like vacuole in yeast. Molecular biology of the cell. 1996;7(4):579-94.
287. Henne WM, Buchkovich NJ, Emr SD. The ESCRT pathway. Developmental cell. 2011;21(1):77-91.
288. Raymond CK, Howald-Stevenson I, Vater CA, Stevens TH. Morphological classification of the yeast vacuolar protein sorting mutants: evidence for a prevacuolar compartment in class E vps mutants. Molecular biology of the cell. 1992;3(12):1389-402.
289. Katzmann DJ, Odorizzi G, Emr SD. Receptor downregulation and multivesicular-body sorting. Nature reviews Molecular cell biology. 2002;3(12):893-905.
290. Coonrod EM, Stevens TH. The yeast vps class E mutants: the beginning of the molecular genetic analysis of multivesicular body biogenesis. Molecular biology of the cell. 2010;21(23):4057-60.
291. Foot N, Henshall T, Kumar S. Ubiquitination and the Regulation of Membrane Proteins. Physiological reviews. 2017;97(1):253-81.
292. Rotin D, Staub O, Haguenauer-Tsapis R. Ubiquitination and endocytosis of plasma membrane proteins: role of Nedd4/Rsp5p family of ubiquitin-protein ligases. The Journal of membrane biology. 2000;176(1):1-17.
293. Gupta R, Kus B, Fladd C, Wasmuth J, Tonikian R, Sidhu S, et al. Ubiquitination screen using protein microarrays for comprehensive identification of Rsp5 substrates in yeast. Mol Syst Biol. 2007;3:116.
294. Belgareh-Touze N, Leon S, Erpapazoglou Z, Stawiecka-Mirota M, Urban-Grimal D, Haguenauer-Tsapis R. Versatile role of the yeast ubiquitin ligase Rsp5p in intracellular trafficking. Biochemical Society transactions. 2008;36(Pt 5):791-6.
295. Tong Z, Kim MS, Pandey A, Espenshade PJ. Identification of candidate substrates for the Golgi Tul1 E3 ligase using quantitative diGly proteomics in yeast. Molecular & cellular proteomics : MCP. 2014;13(11):2871-82.
296. Yang X, Arines FM, Zhang W, Li M. Sorting of a multi-subunit ubiquitin ligase complex in the endolysosome system. Elife. 2018;7.
297. Springael JY, Andre B. Nitrogen-regulated ubiquitination of the Gap1 permease of Saccharomyces cerevisiae. Molecular biology of the cell. 1998;9(6):1253-63.

298. Savocco J, Nootens S, Afokpa W, Bausart M, Chen X, Villers J, et al. Yeast alpha-arrestin Art2 is the key regulator of ubiquitylation-dependent endocytosis of plasma membrane vitamin B1 transporters. PLoS biology. 2019;17(10):e3000512.
299. Hein C, Springael JY, Volland C, Haguenauer-Tsapis R, Andre B. NPl1, an essential yeast gene involved in induced degradation of Gap1 and Fur4 permeases, encodes the Rsp5 ubiquitin-protein ligase. Molecular microbiology. 1995;18(1):77-87.
300. Portnoy ME, Liu XF, Culotta VC. Saccharomyces cerevisiae expresses three functionally distinct homologues of the nramp family of metal transporters. Molecular and cellular biology. 2000;20(21):7893-902.
301. Jensen LT, Carroll MC, Hall MD, Harvey CJ, Beese SE, Culotta VC. Down-regulation of a manganese transporter in the face of metal toxicity. Molecular biology of the cell. 2009;20(12):2810-9.
302. Stimpson HE, Lewis MJ, Pelham HR. Transferrin receptor-like proteins control the degradation of a yeast metal transporter. The EMBO journal. 2006;25(4):662-72.
303. Zhu L, Sardana R, Jin DK, Emr SD. Calcineurin-dependent regulation of endocytosis by a plasma membrane ubiquitin ligase adaptor, Rcr1. The Journal of cell biology. 2020;219(8).
304. Liu XF, Culotta VC. Post-translation control of Nramp metal transport in yeast. Role of metal ions and the BSD2 gene. The Journal of biological chemistry. 1999;274(8):4863-8.
305. Katzmann DJ, Babst M, Emr SD. Ubiquitin-dependent sorting into the multivesicular body pathway requires the function of a conserved endosomal protein sorting complex, ESCRT-I. Cell. 2001;106(2):145-55.
306. Swaney DL, Beltrao P, Starita L, Guo A, Rush J, Fields S, et al. Global analysis of phosphorylation and ubiquitylation cross-talk in protein degradation. Nature methods. 2013;10(7):676-82.
307. Kolawa N, Sweredoski MJ, Graham RL, Oania R, Hess S, Deshaies RJ. Perturbations to the ubiquitin conjugate proteome in yeast deltaubx mutants identify Ubx2 as a regulator of membrane lipid composition. Molecular & cellular proteomics : MCP. 2013;12(10):2791-803.
308. Finnigan GC, Hanson-Smith V, Houser BD, Park HJ, Stevens TH. The reconstructed ancestral subunit a functions as both V-ATPase isoforms Vph1p and Stv1p in Saccharomyces cerevisiae. Molecular biology of the cell. 2011;22(17):3176-91.
309. Chavez C, Bowman EJ, Reidling JC, Haw KH, Bowman BJ. Analysis of strains with mutations in six genes encoding subunits of the V-ATPase: eukaryotes differ in the composition of the V0 sector of the enzyme. The Journal of biological chemistry. 2006;281(37):27052-62.
310. Marshansky V. The V-ATPase a2-subunit as a putative endosomal pH-sensor. Biochemical Society transactions. 2007;35(Pt 5):1092-9.
311. Baars TL, Petri S, Peters C, Mayer A. Role of the V-ATPase in regulation of the vacuolar fission-fusion equilibrium. Molecular biology of the cell. 2007;18(10):3873-82.
312. Gabba M, Frallicciardi J, van 't Klooster J, Henderson R, Syga L, Mans R, et al. Weak Acid Permeation in Synthetic Lipid Vesicles and Across the Yeast Plasma Membrane. Biophysical journal. 2020;118(2):422-34.
313. Sorin A, Rosas G, Rao R. PMR1, a Ca2+-ATPase in yeast Golgi, has properties distinct from sarco/endoplasmic reticulum and plasma membrane calcium pumps. The Journal of biological chemistry. 1997;272(15):9895-901.

314. Chen JL, Ahluwalia JP, Stamnes M. Selective effects of calcium chelators on anterograde and retrograde protein transport in the cell. The Journal of biological chemistry. 2002;277(38):35682-7.
315. Porat A, Elazar Z. Regulation of intra-Golgi membrane transport by calcium. The Journal of biological chemistry. 2000;275(38):29233-7.
316. Adamany AM, Spiro RG. Glycoprotein biosynthesis: studies on thyroid mannosyltransferases. I. Action on glycopeptides and simple glycosides. The Journal of biological chemistry. 1975;250(8):2830-41.
317. Boeggeman E, Qasba PK. Studies on the metal binding sites in the catalytic domain of beta1,4-galactosyltransferase. Glycobiology. 2002;12(7):395-407.
318. Palma AS, Morais VA, Coelho AV, Costa J. Effect of the manganese ion on human alpha3/4 fucosyltransferase III activity. Biometals. 2004;17(1):35-43.
319. Culotta VC, Yang M, Hall MD. Manganese transport and trafficking: lessons learned from Saccharomyces cerevisiae. Eukaryotic cell. 2005;4(7):1159-65.
320. Rivinoja A, Pujol FM, Hassinen A, Kellokumpu S. Golgi pH, its regulation and roles in human disease. Annals of medicine. 2012;44(6):542-54.
321. Chen P, Bornhorst J, Aschner M. Manganese metabolism in humans. Front Biosci (Landmark Ed). 2018;23:1655-79.
322. Yang M, Jensen LT, Gardner AJ, Culotta VC. Manganese toxicity and Saccharomyces cerevisiae Mam3p, a member of the ACDP (ancient conserved domain protein) family. The Biochemical journal. 2005;386(Pt 3):479-87.
323. Thines L, Deschamps A, Stribny J, Morsomme P. Yeast as a Tool for Deeper Understanding of Human Manganese-Related Diseases. Genes (Basel). 2019;10(7).
324. Foresti O, Rodriguez-Vaello V, Funaya C, Carvalho P. Quality control of inner nuclear membrane proteins by the Asi complex. Science. 2014;346(6210):751-5.
325. Khmelinskii A, Blaszczak E, Pantazopoulou M, Fischer B, Omnus DJ, Le Dez G, et al. Protein quality control at the inner nuclear membrane. Nature. 2014;516(7531):410-3.
326. Ruggiano A, Foresti O, Carvalho P. Quality control: ER-associated degradation: protein quality control and beyond. The Journal of cell biology. 2014;204(6):869-79.
327. Li M, Rong Y, Chuang YS, Peng D, Emr SD. Ubiquitin-dependent lysosomal membrane protein sorting and degradation. Mol Cell. 2015;57(3):467-78.
328. Zhu L, Jorgensen JR, Li M, Chuang YS, Emr SD. ESCRTs function directly on the lysosome membrane to downregulate ubiquitinated lysosomal membrane proteins. Elife. 2017;6.
329. Schneider B, Junge F, Shirokov VA, Durst F, Schwarz D, Dotsch V, et al. Membrane protein expression in cell-free systems. Methods Mol Biol. 2010;601:165-86.
330. Kuruma Y, Ueda T. The PURE system for the cell-free synthesis of membrane proteins. Nature protocols. 2015;10(9):1328-44.
331. Rohl CA, Strauss CE, Misura KM, Baker D. Protein structure prediction using Rosetta. Methods in enzymology. 2004;383:66-93.
332. Berridge MJ, Lipp P, Bootman MD. The versatility and universality of calcium signalling. Nature reviews Molecular cell biology. 2000;1(1):11-21.
333. Carafoli E, Krebs J. Why Calcium? How Calcium became the best communicator. The Journal of biological chemistry. 2016.
334. Dechant R, Binda M, Lee SS, Pelet S, Winderickx J, Peter M. Cytosolic pH is a second messenger for glucose and regulates the PKA pathway through V-ATPase. The EMBO journal. 2010;29(15):2515-26.

335. Deprez MA, Eskes E, Wilms T, Ludovico P, Winderickx J. pH homeostasis links the nutrient sensing PKA/TORC1/Sch9 menage-a-trois to stress tolerance and longevity. Microb Cell. 2018;5(3):119-36.
336. Suzuki J, Kanemaru K, Ishii K, Ohkura M, Okubo Y, Iino M. Imaging intraorganellar Ca(2+) at subcellular resolution using CEPIA. Nature communications. 2014;5:4153.
337. Greotti E, Wong A, Pozzan T, Pendin D, Pizzo P. Characterization of the ER-Targeted Low Affinity Ca(2+) Probe D4ER. Sensors (Basel). 2016;16(9).
338. Cho JH, Swanson CJ, Chen J, Li A, Lippert LG, Boye SE, et al. The GCaMP-R Family of Genetically Encoded Ratiometric Calcium Indicators. ACS chemical biology. 2017;12(4):1066-74.
339. Das S, Carmona A, Khatua K, Porcaro F, Somogyi A, Ortega R, et al. Manganese Mapping Using a Fluorescent Mn(2+) Sensor and Nanosynchrotron X-ray Fluorescence Reveals the Role of the Golgi Apparatus as a Manganese Storage Site. Inorganic chemistry. 2019;58(20):13724-32.
340. Tsednee M, Castruita M, Salome PA, Sharma A, Lewis BE, Schmollinger SR, et al. Manganese co-localizes with calcium and phosphorus in Chlamydomonas acidocalcisomes and is mobilized in manganese-deficient conditions. The Journal of biological chemistry. 2019;294(46):17626-41.
341. Guldener U, Heck S, Fielder T, Beinhauer J, Hegemann JH. A new efficient gene disruption cassette for repeated use in budding yeast. Nucleic acids research. 1996;24(13):2519-24.
342. Vida TA, Emr SD. A new vital stain for visualizing vacuolar membrane dynamics and endocytosis in yeast. The Journal of cell biology. 1995;128(5):779-92.
343. Bolte S, Cordelieres FP. A guided tour into subcellular colocalization analysis in light microscopy. Journal of microscopy. 2006;224(Pt 3):213-32.
344. Linares DM, Geertsma ER, Poolman B. Evolved Lactococcus lactis strains for enhanced expression of recombinant membrane proteins. Journal of molecular biology. 2010;401(1):45-55.
345. Szopinska A, Degand H, Hochstenbach JF, Nader J, Morsomme P. Rapid response of the yeast plasma membrane proteome to salt stress. Molecular & cellular proteomics : MCP. 2011;10(11):M111 009589.

ANNEXES

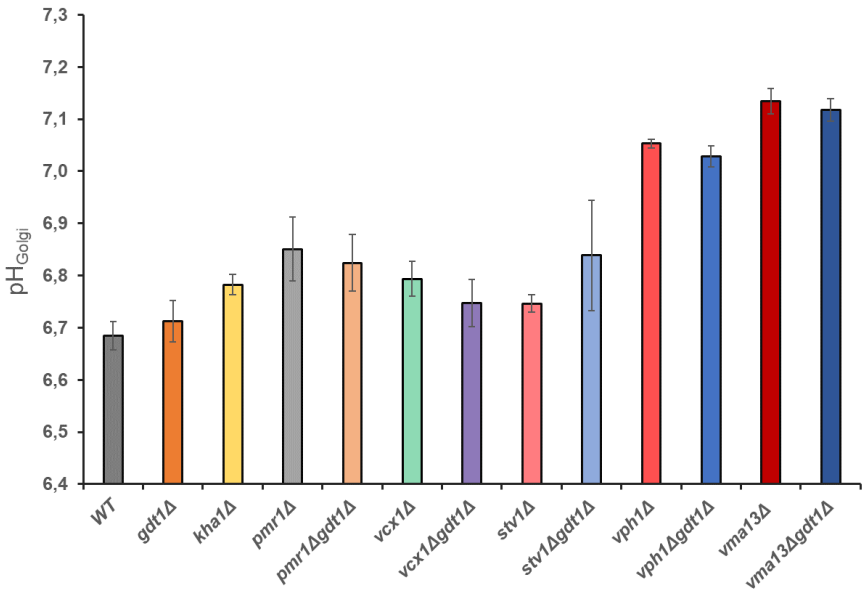

Annex 1 – *Cis/medial*-Golgi pH at steady-state, in various strains. Golgi pH measurements were performed as in Figure 26B. N = 3 to 14, error bars represent SD.

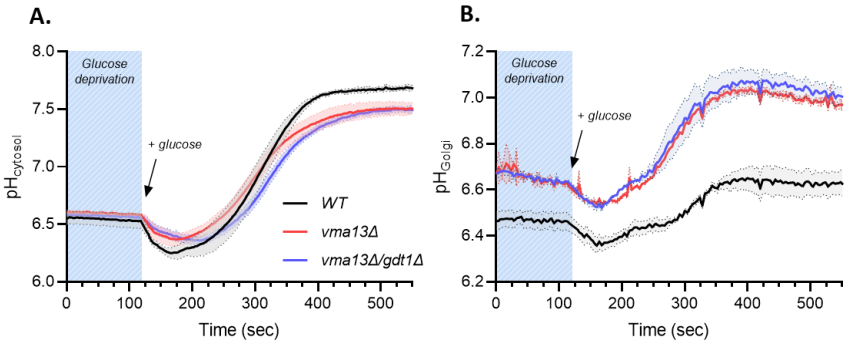

Annex 2 – Cytosol and Golgi pH during glucose deprivation / re-addition in V-ATPase deficient strains. (A) Cytosol pH measurements and (B) Golgi pH measurement performed as in Figure 26C *and* E. N = 2 - 3, means and SD are represented.

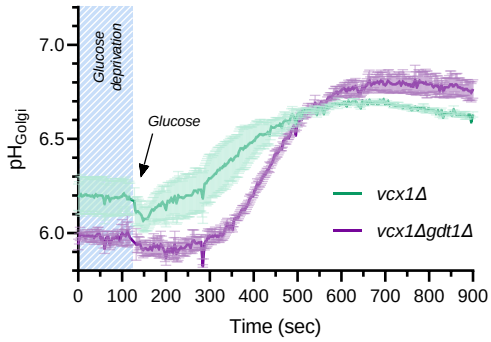

Annex 3 – Golgi pH in the *vcx1Δ* and *vcx1Δgdt1Δ* strains during glucose deprivation/re-addition procedure. Measurement were performed as in Figure 26C *and* E, except that cells were deprived of glucose during 60 min at 28 °C and that the pH recordings were extended up to 900 sec. N = 2, means and SD are represented.

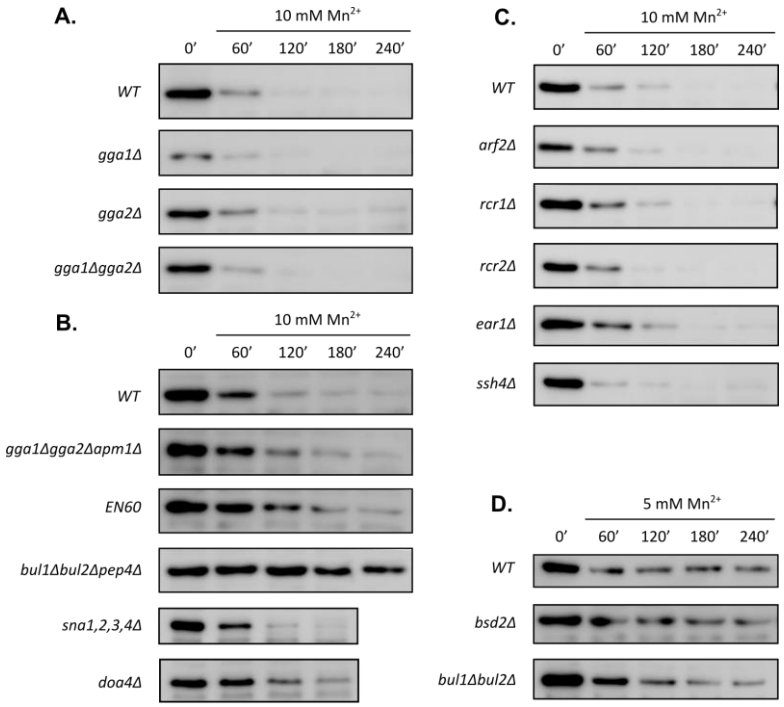

Annex 4 – Gdt1p degradation upon Mn^{2+} addition in various strains deleted for possible Golgi to vacuole trafficking players.
Four independent experimental data sets are presented. Abundance of endogenous Gdt1p is analyzed by *western blotting* from protein extracts of cells collected before and after addition of **D.** 5 mM Mn^{2+} or **A.**, **B.** *and* **C.** 10 mM Mn^{2+}. The *WT* strain is compared as a control for each data set. The *bul1Δbul2Δpep4Δ* strain serves as a negative degradation control, as *PEP4* was shown to be essential for Gdt1p degradation.